Cosmic Microwave Background (WMAP experiment)

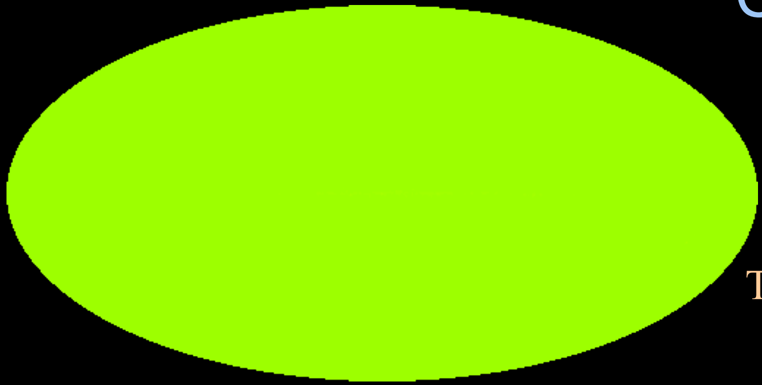

Temperature = 2.72 Kelvin

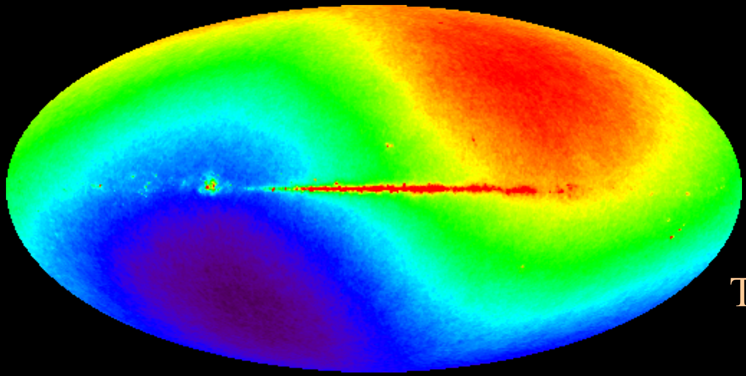

Temperature = 2.721 – 2.729 Kelvin

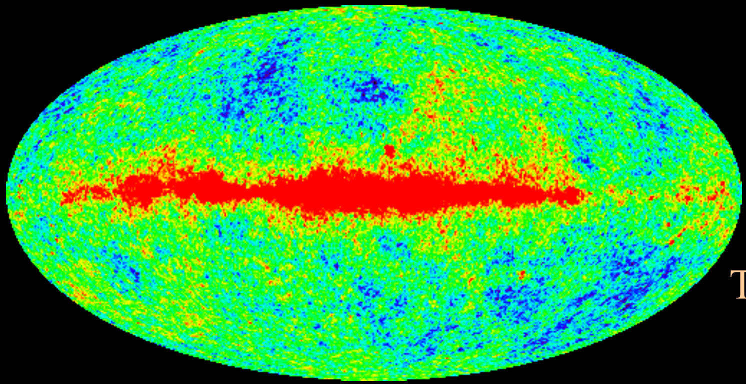

Temperature = 2.7249 – 2.7251 Kelvin

But the universe today (13.7 billion years old) doesn't look like that at all!

It contains all sorts of structure on all scales.

- Small scales: people, planets, stars, solar systems…
  (less than one light year)

- Intermediate scales: galaxies
  (1 – million light years)

- Large scales: clusters of galaxies, super-clusters…
  (million – billion light years)

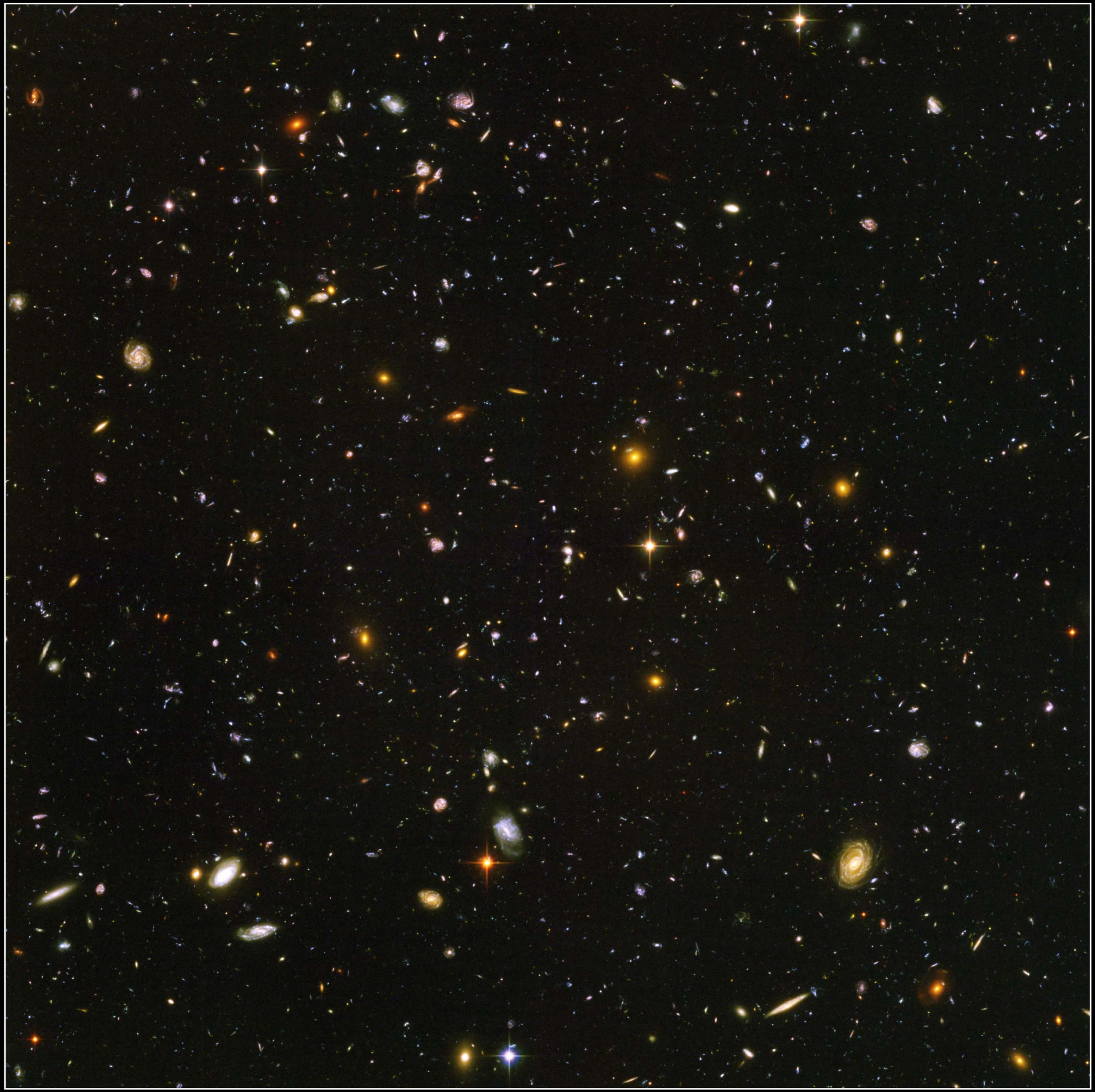

Hubble Ultra Deep Field

Hubble Space Telescope • Advanced Camera for Surveys

NASA, ESA, S. Beckwith (STScI) and the HUDF Team

STScI-PRC04-07a


Galaxies

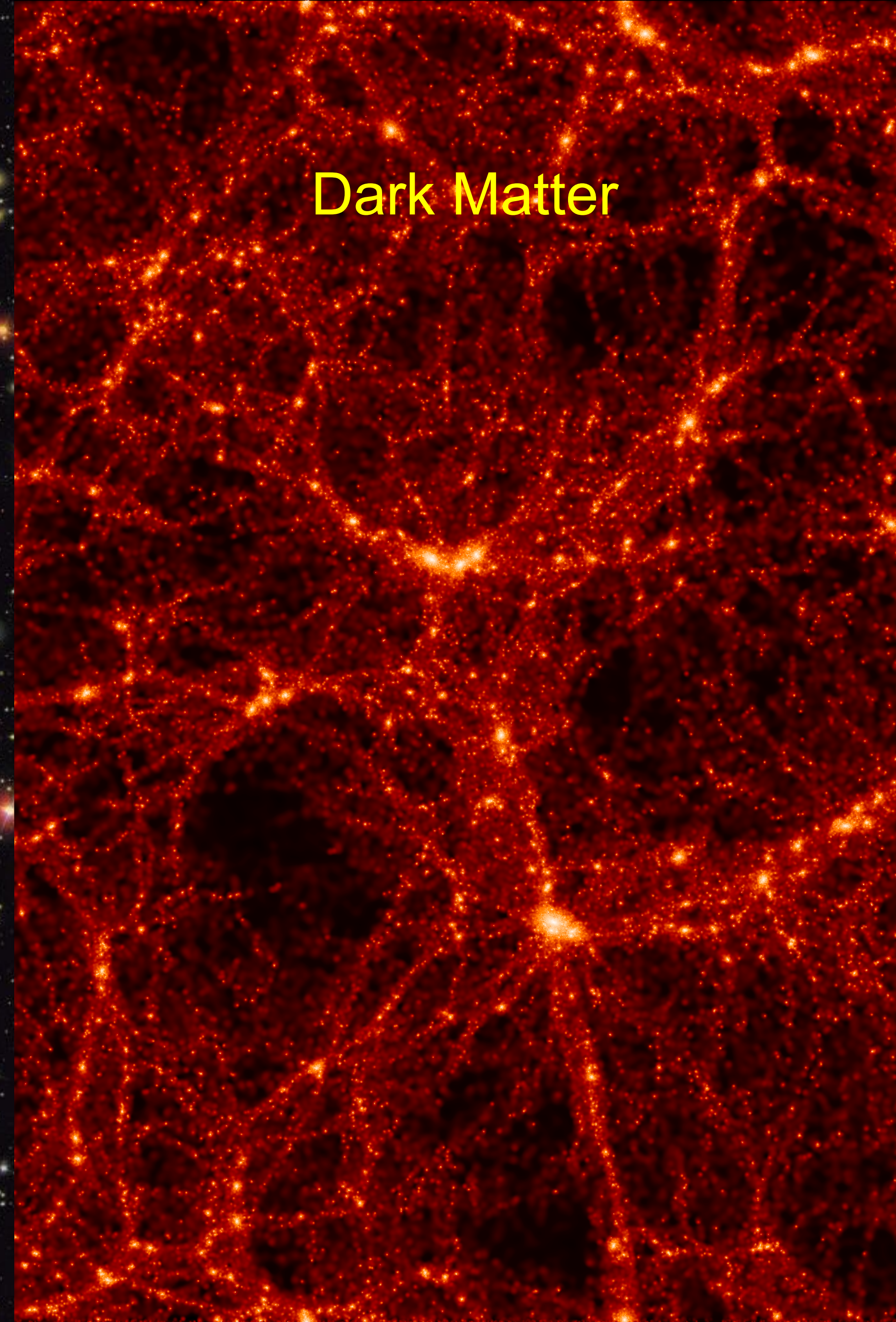
Dark Matter

How did structure in the universe grow?

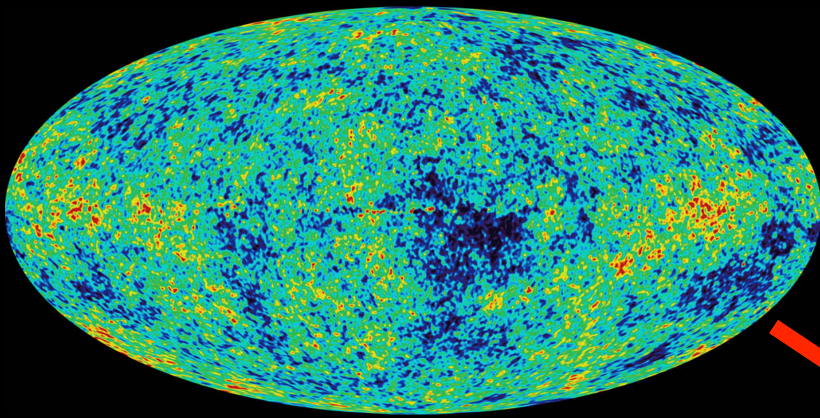

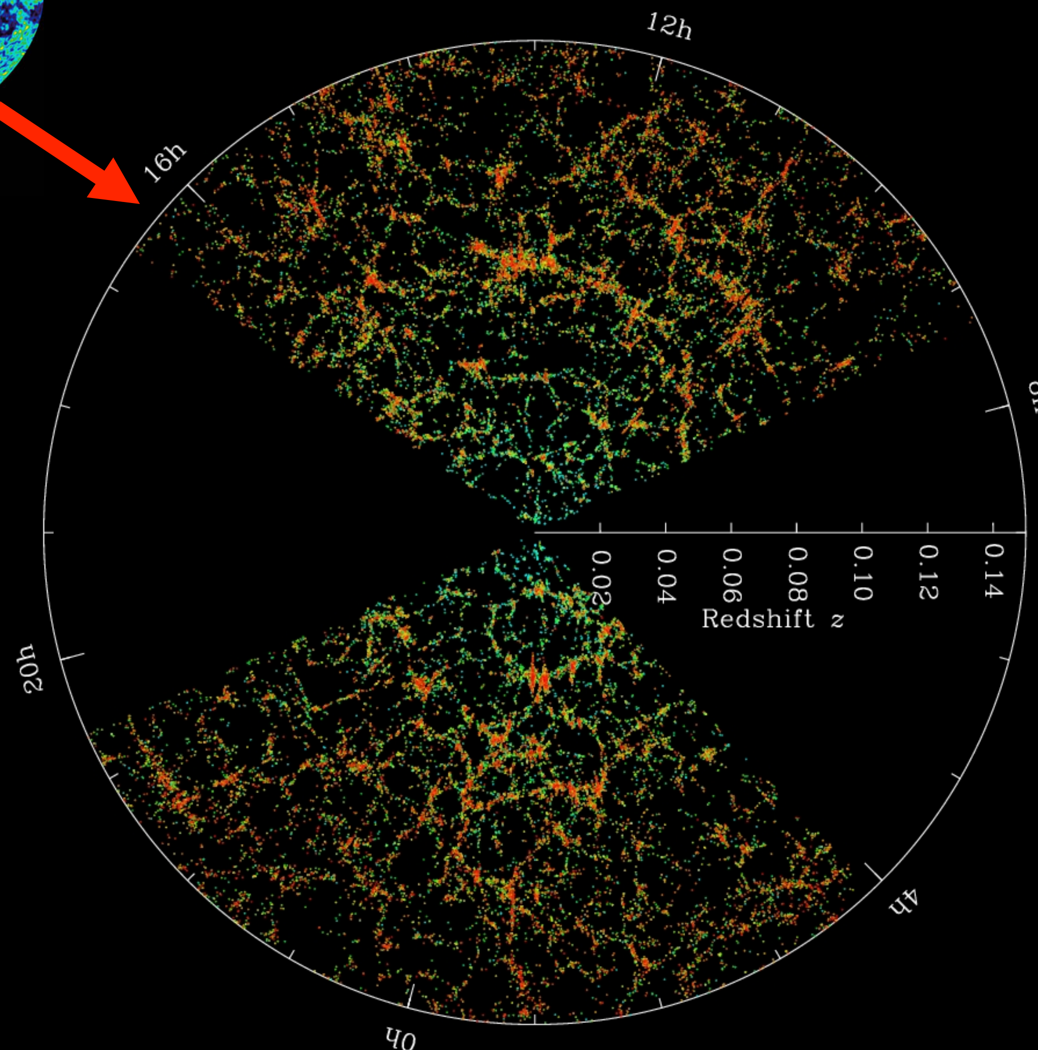

Aims of the course

- How do we measure galaxy properties?
- Galaxy surveys
- What statistics are used to quantify structure and how are they measured?
- Brief review of homogeneous universe
- How did the universe form structure on all scales?
- What models are used to connect observations to theory?
- What observational probes are used to constrain cosmology?
- How do galaxies form?

Radio Sky

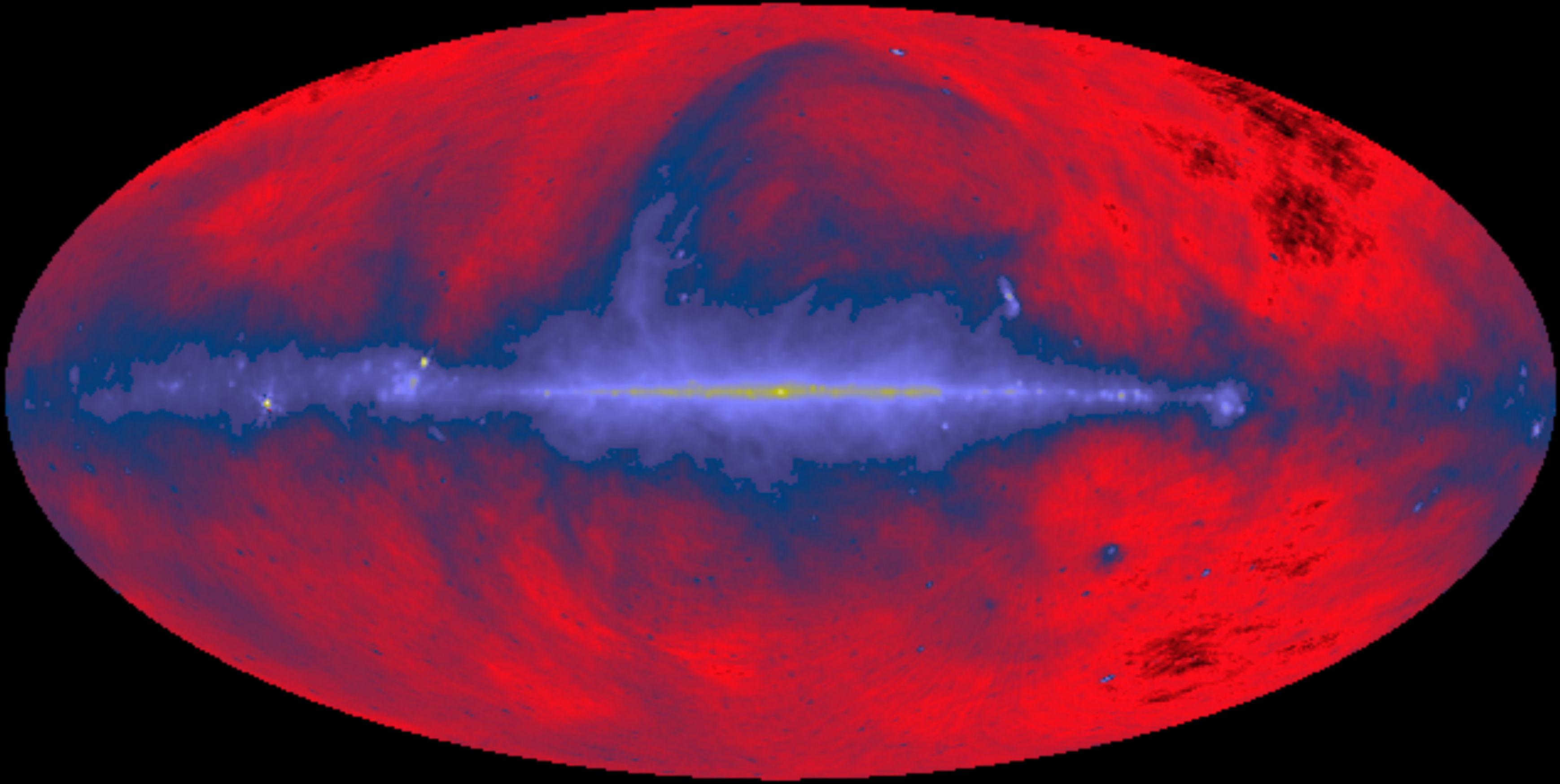

Microwave Sky

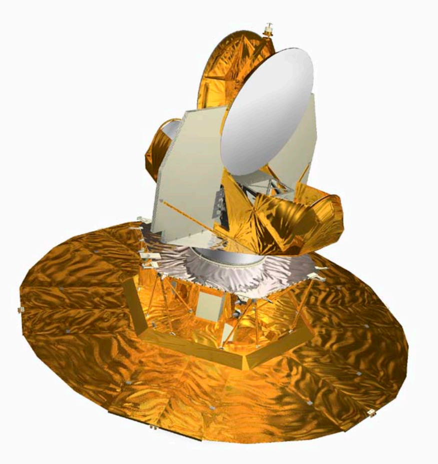

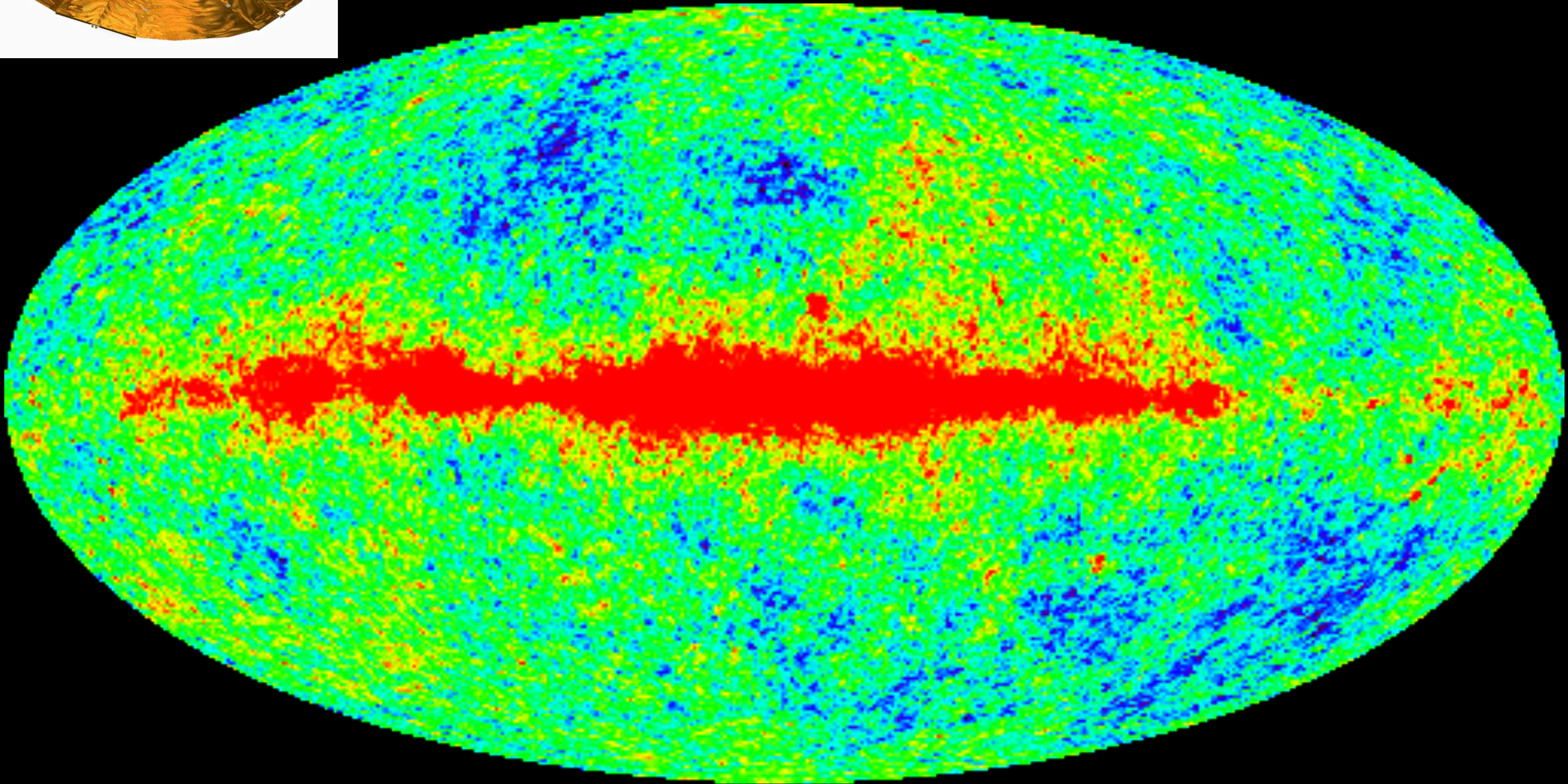

WMAP

Infrared Sky

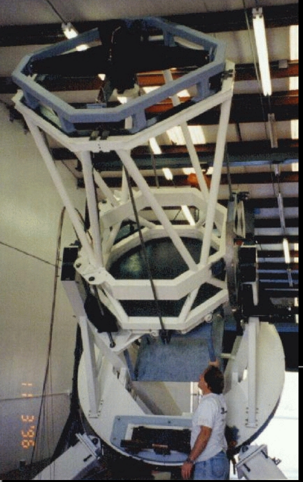

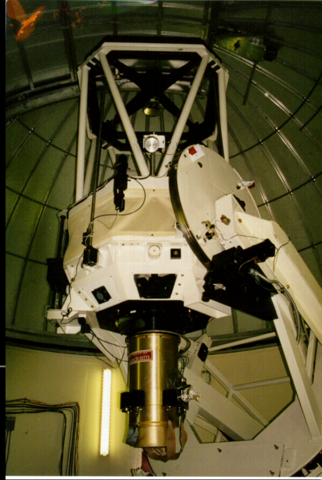

2MASS

Optical Sky

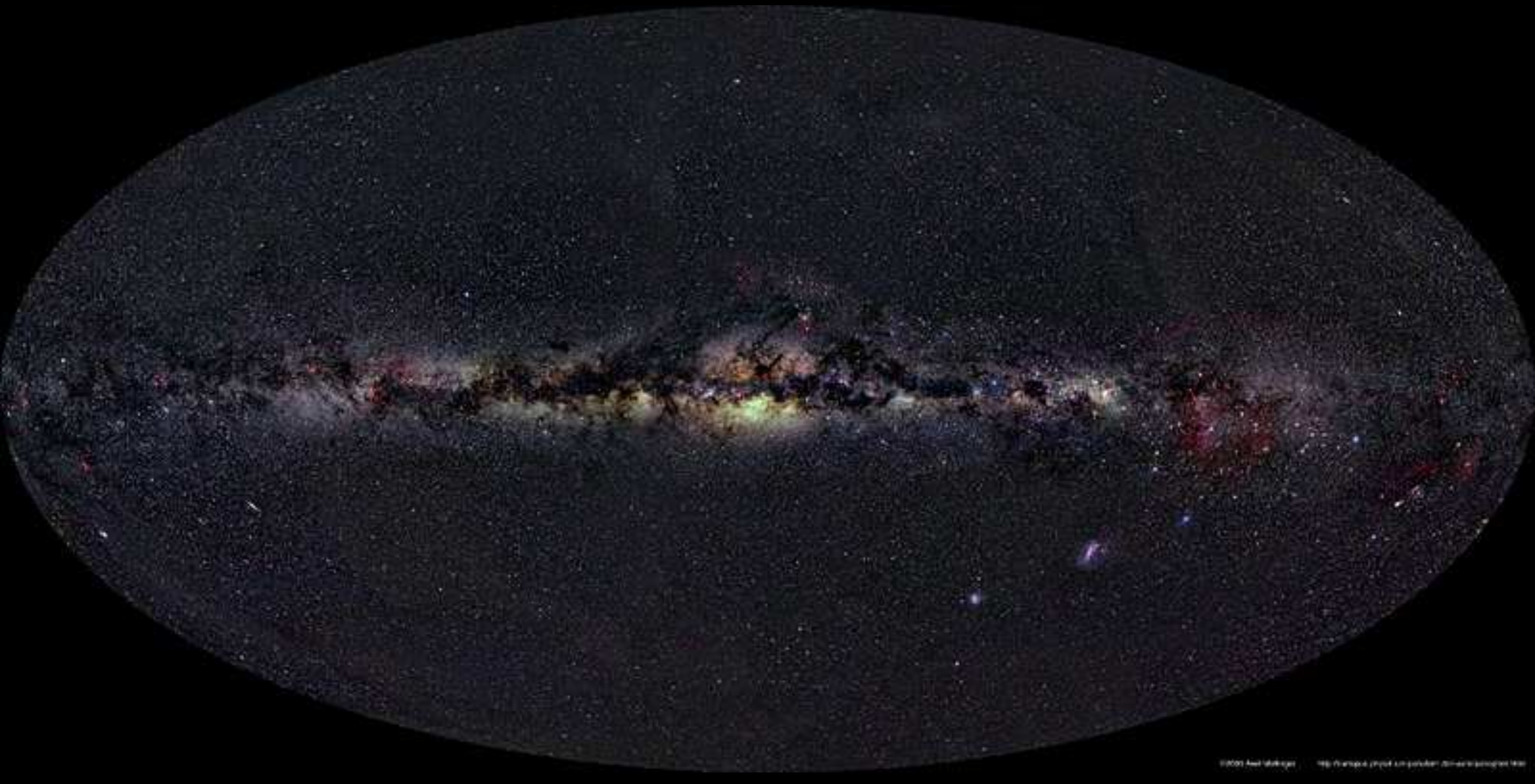

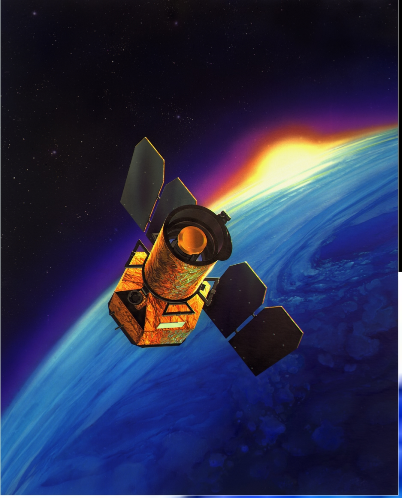

Ultraviolet Sky

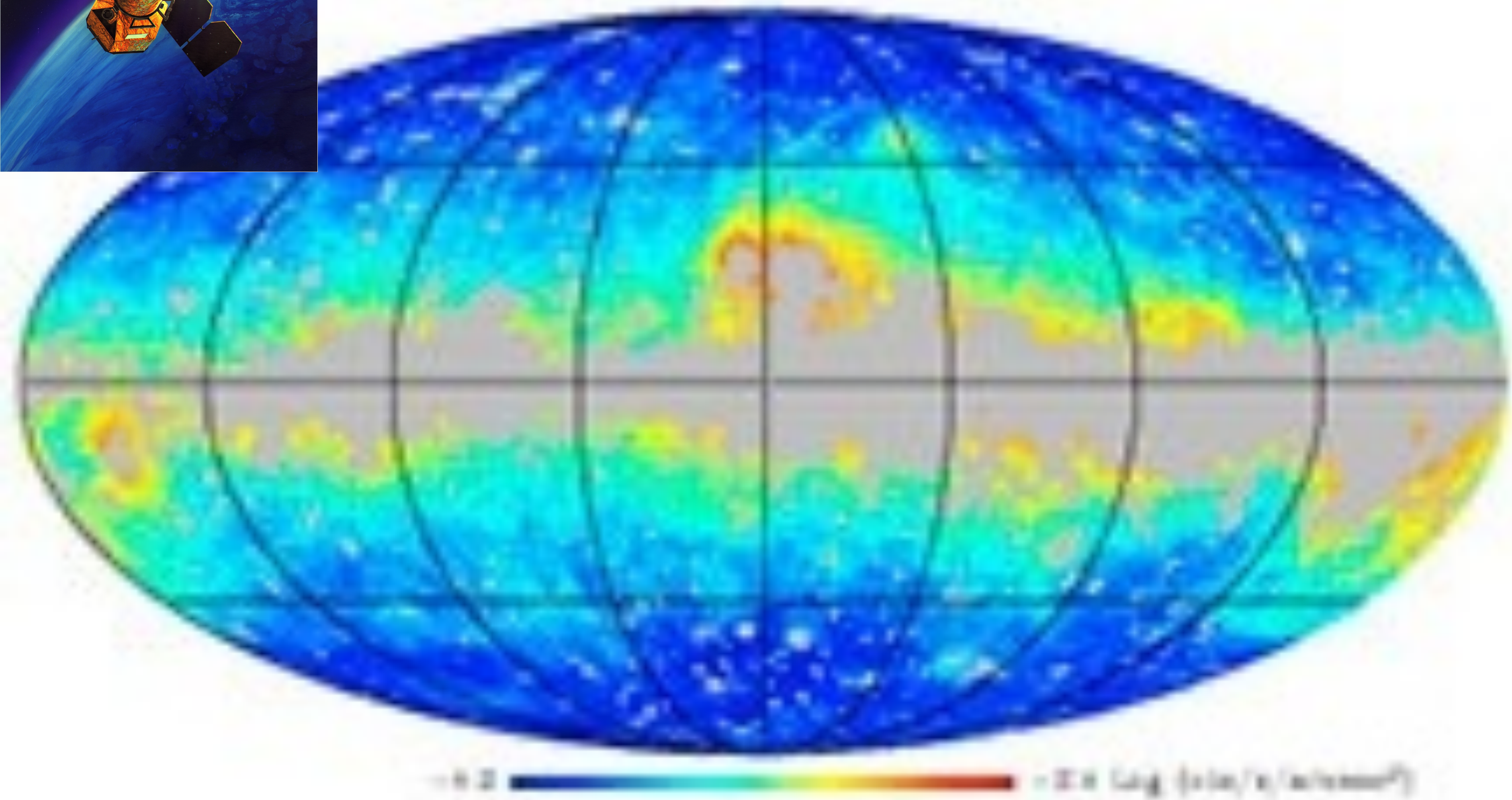

GALEX

X-ray Sky

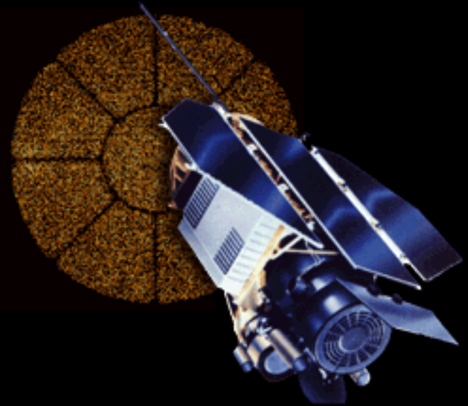

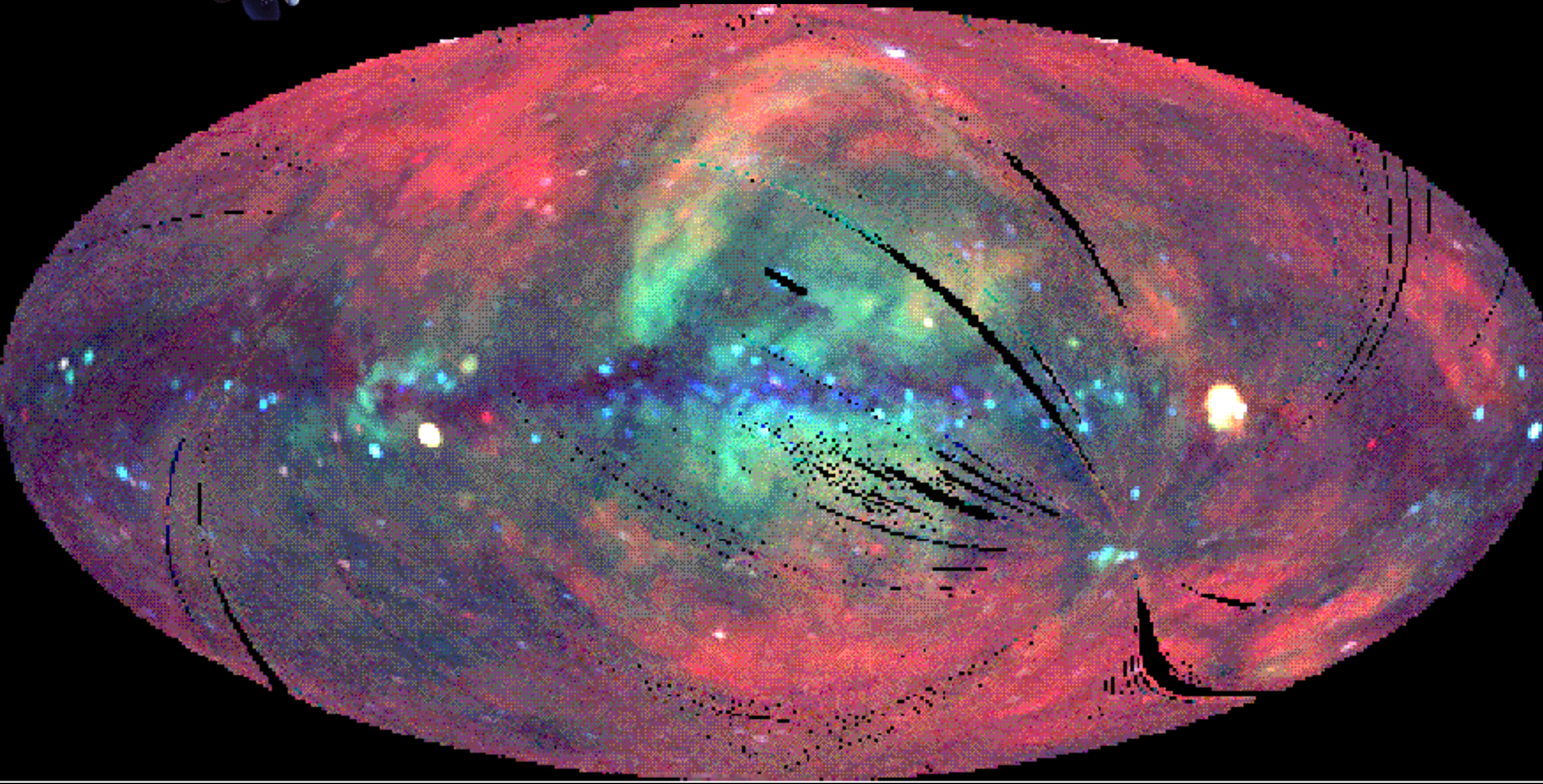

ROSAT

γ-ray Sky

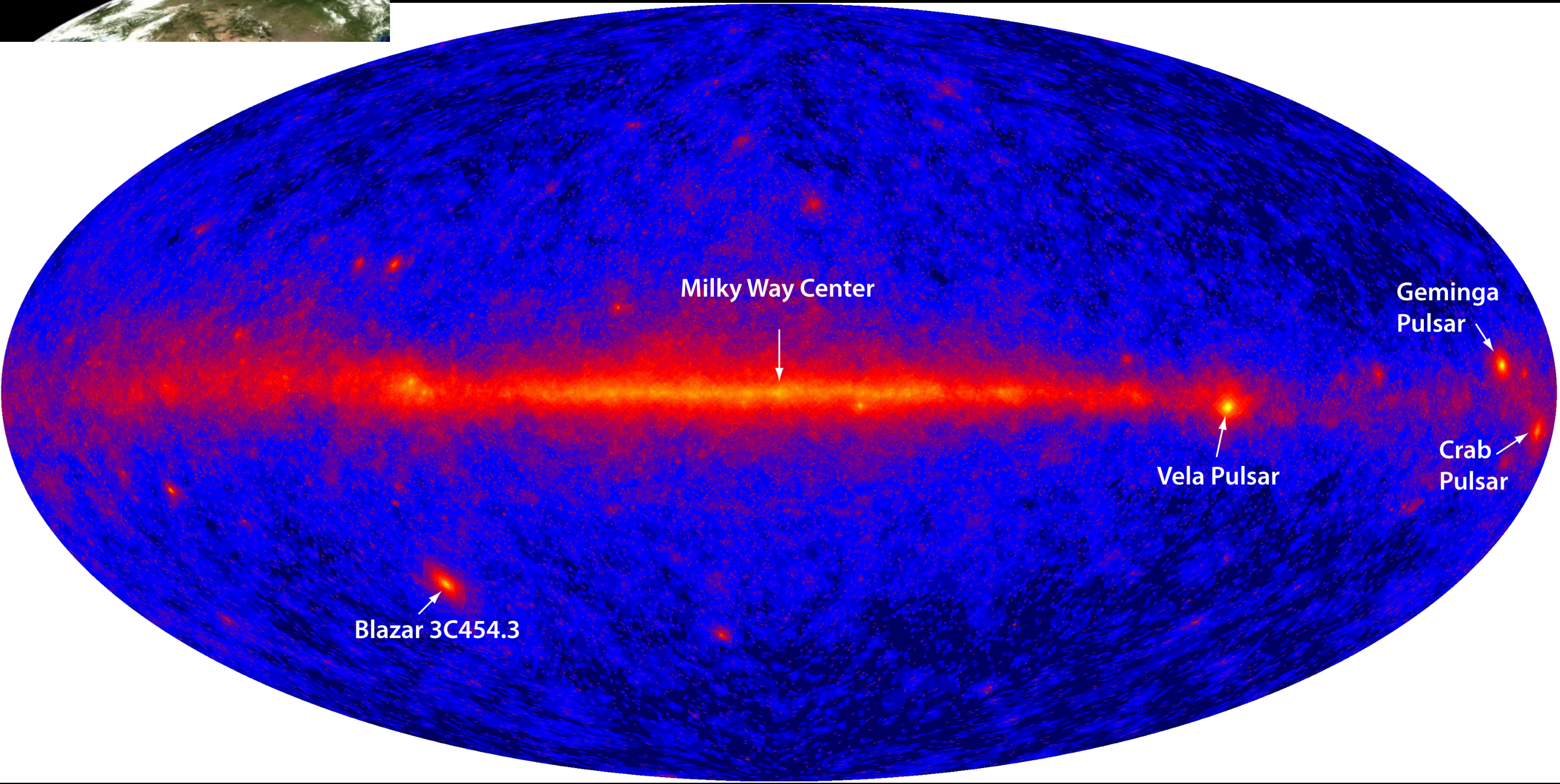

Fermi

Milky Way

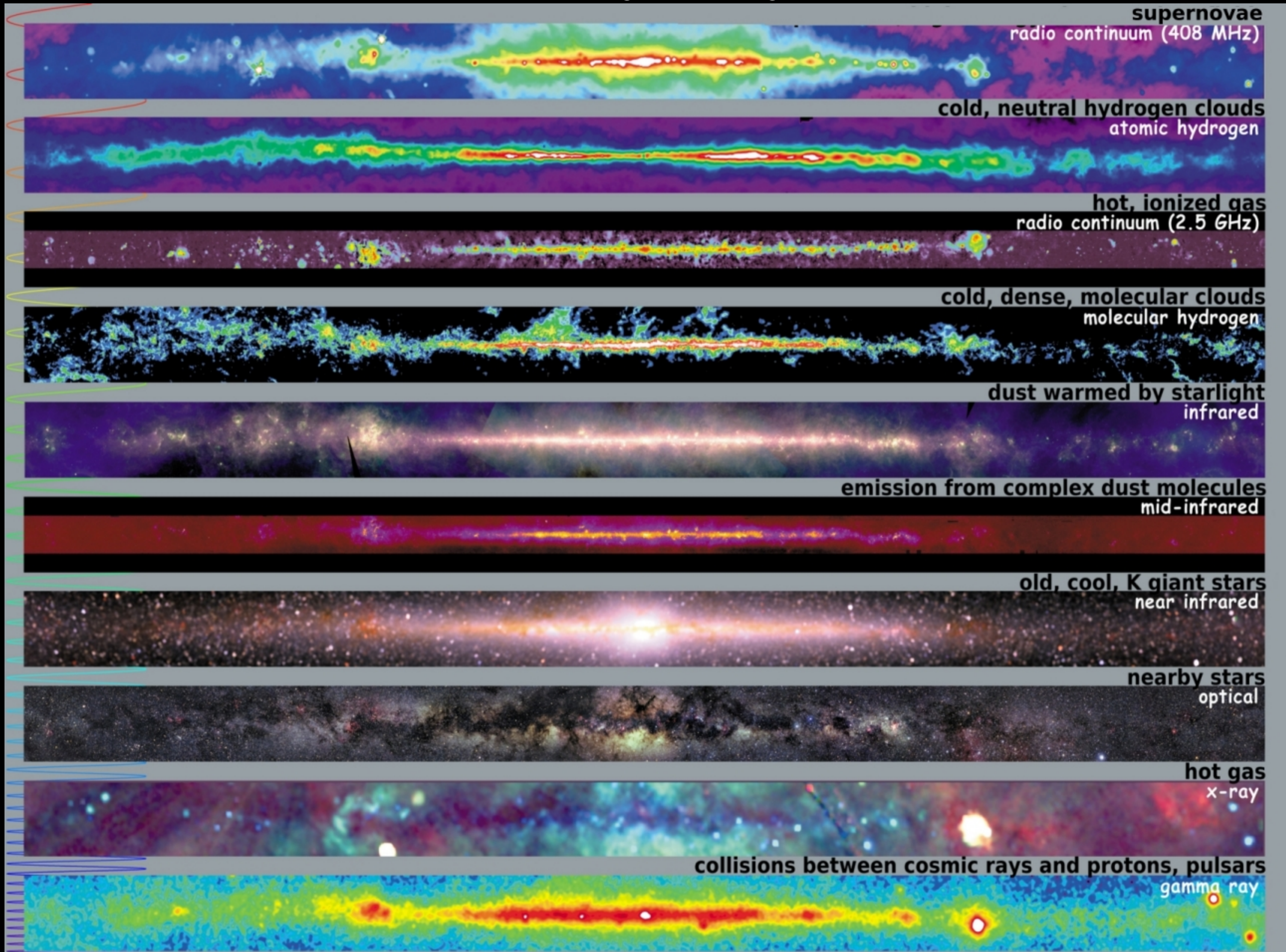

supernovae
radio continuum (408 MHz)
cold, neutral hydrogen clouds
atomic hydrogen
hot, ionized gas
radio continuum (2.5 GHz)
cold, dense, molecular clouds
molecular hydrogen
dust warmed by starlight
infrared
emission from complex dust molecules
mid-infrared
old, cool, K giant stars
near infrared
nearby stars
optical
hot gas
x-ray
collisions between cosmic rays and protons, pulsars
gamma ray

The Cosmic Microwave Background

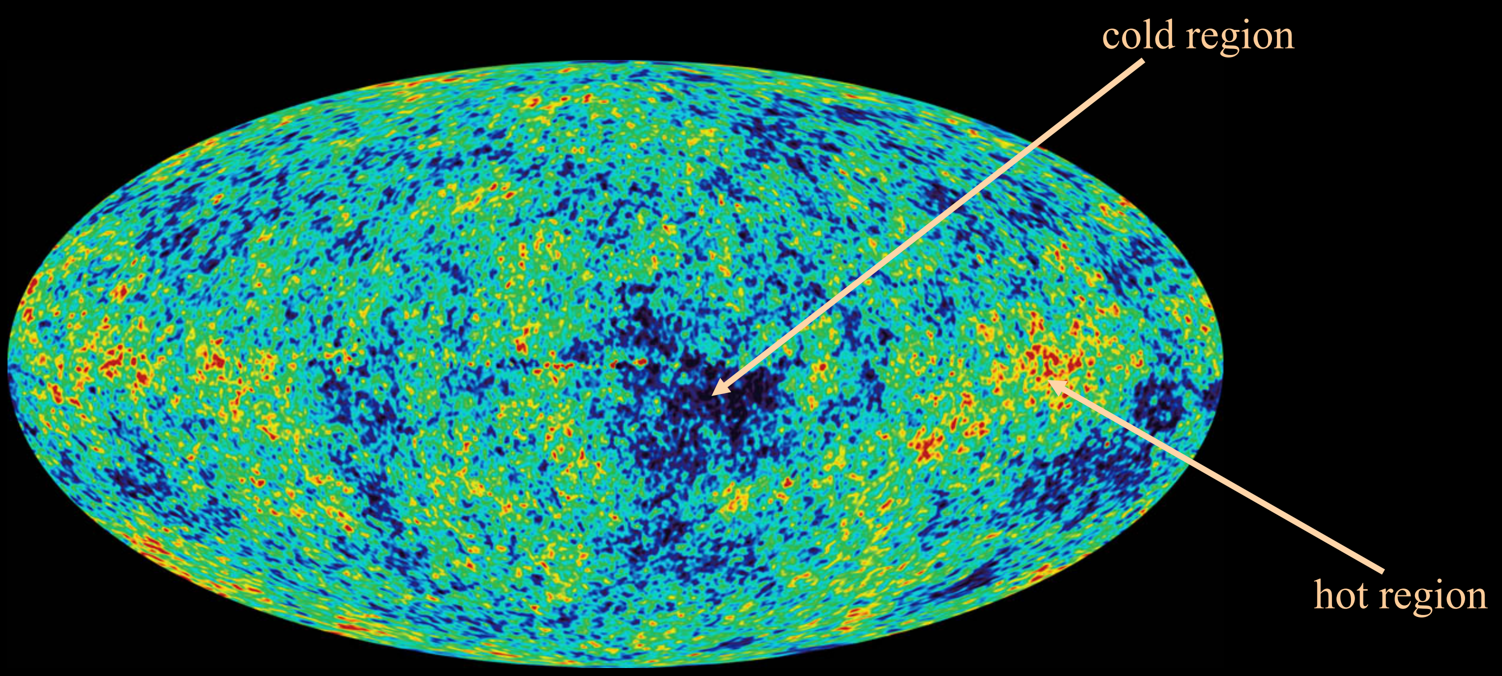

The Cosmic Microwave Background

The CMB temperature map corresponds to a density map at the epoch of recombination: 300,000 years after the Big Bang

But the exact physics is complicated!

Basic picture:

- As the universe expands, the photon-baryon plasma in it cools.
- When the temperature drops below about 3000^{o}K, electrons recombine with protons and photons can move freely.
- In overdense regions of the universe, the photon-baryon plasma is compressed and slightly hotter than average.

The Cosmic Microwave Background

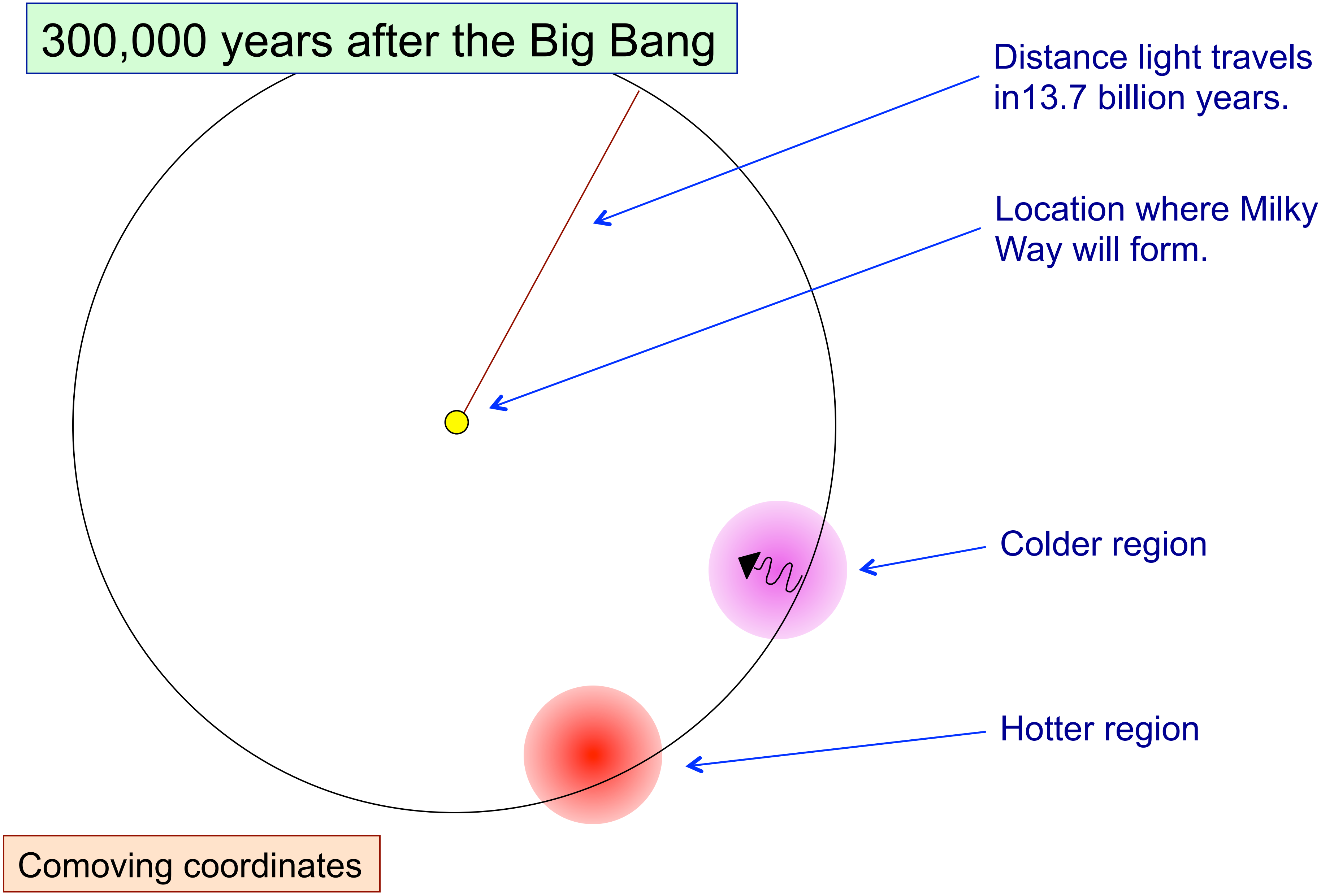

The Cosmic Microwave Background

A little bit later…

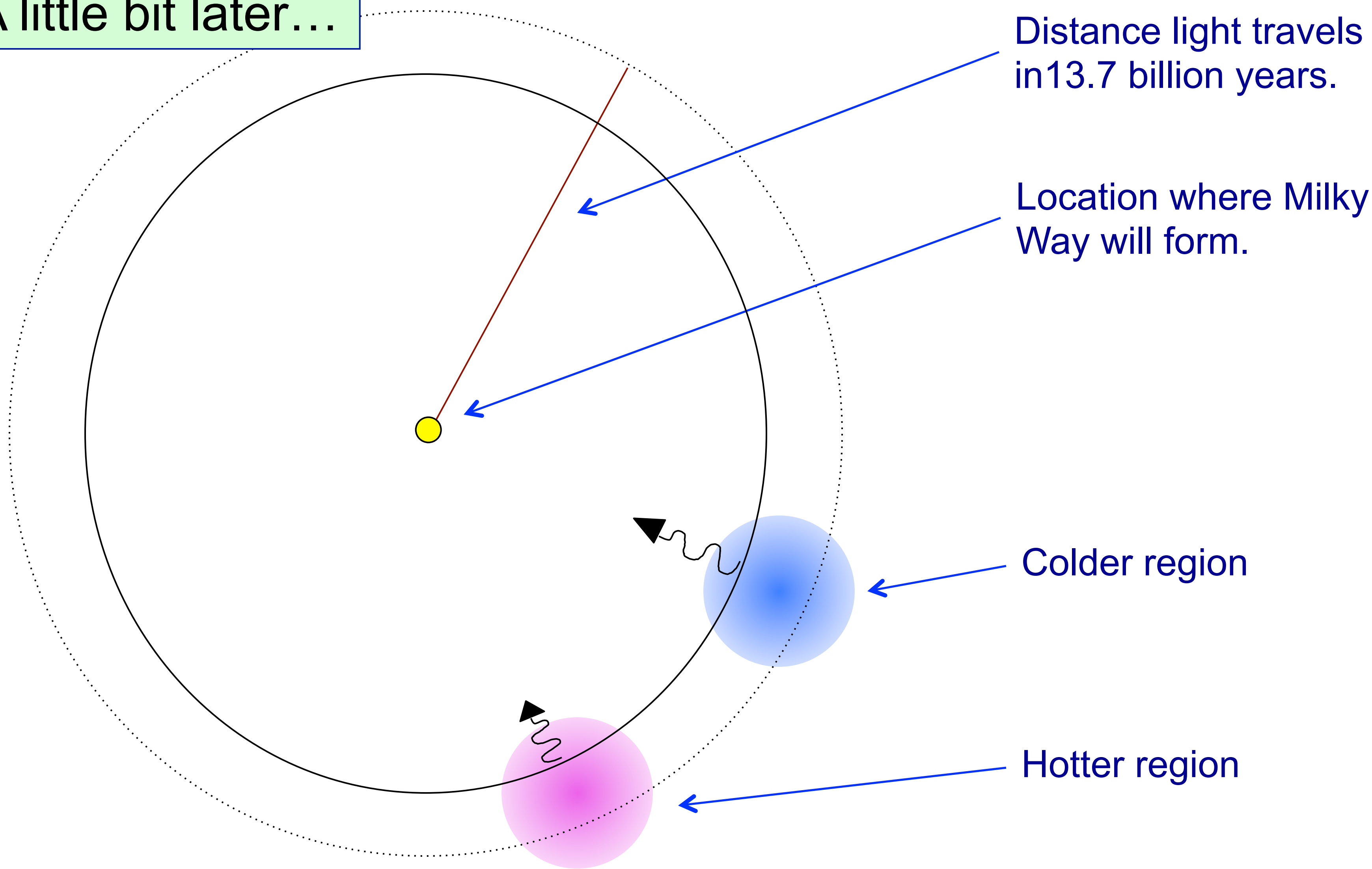

Comoving coordinates

The Cosmic Microwave Background

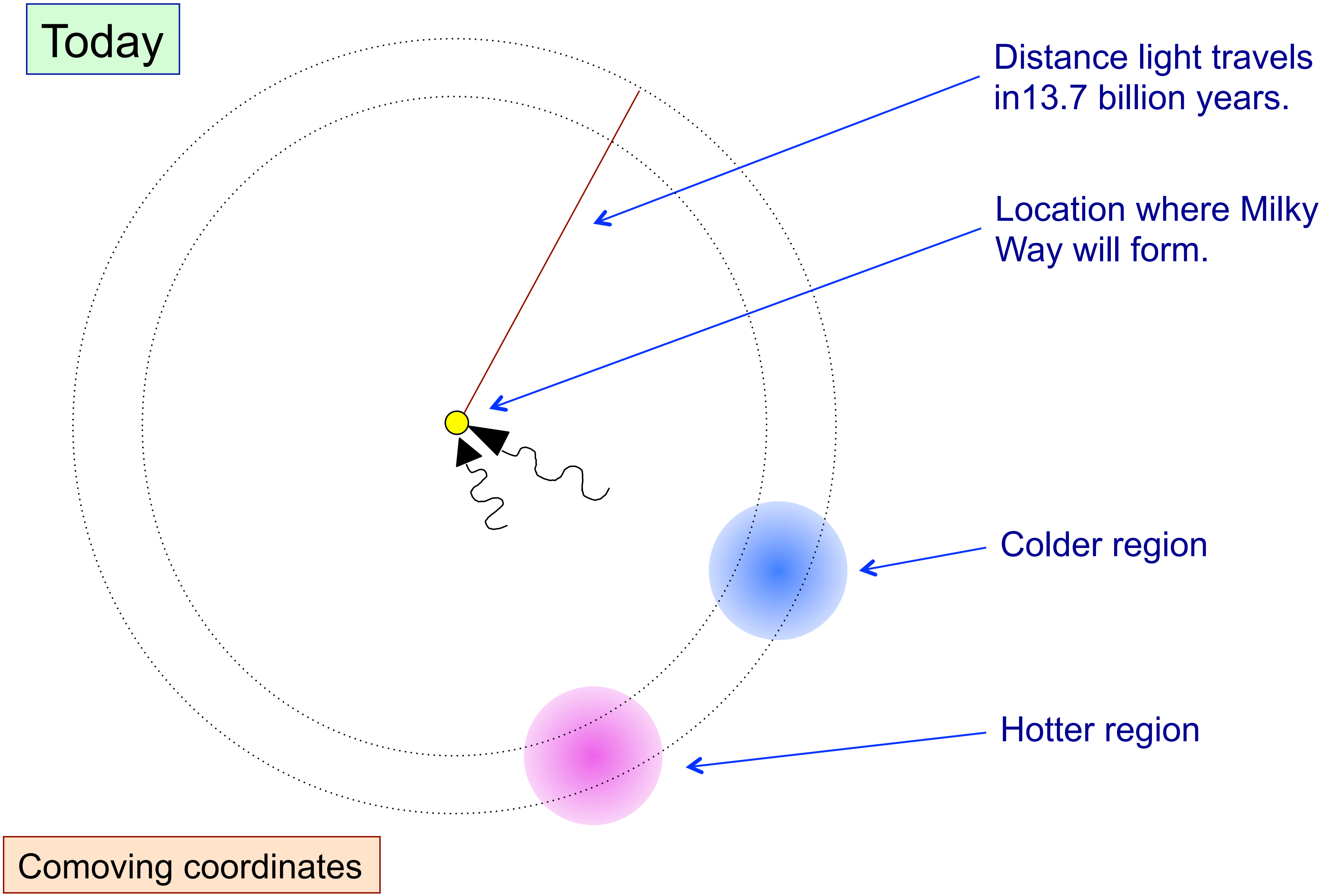

The Cosmic Microwave Background

Primary fluctuations (at origin):

- Adiabatic fluctuations: high density regions appear hot
- Gravitational redshift: high density regions appear cold
    - Time dilation: high density regions appear hot
- Doppler effect: photons scattered by moving plasma
- Acoustic oscillations of baryon-photon plasma

Secondary fluctuations (along path to us):

- CMB photons traverse changing gravitational field
- CMB photons scatter off hot plasma in clusters
- CMB photons are gravitationally lensed
- + many more effects

The CMB: COBE (1989-1993)

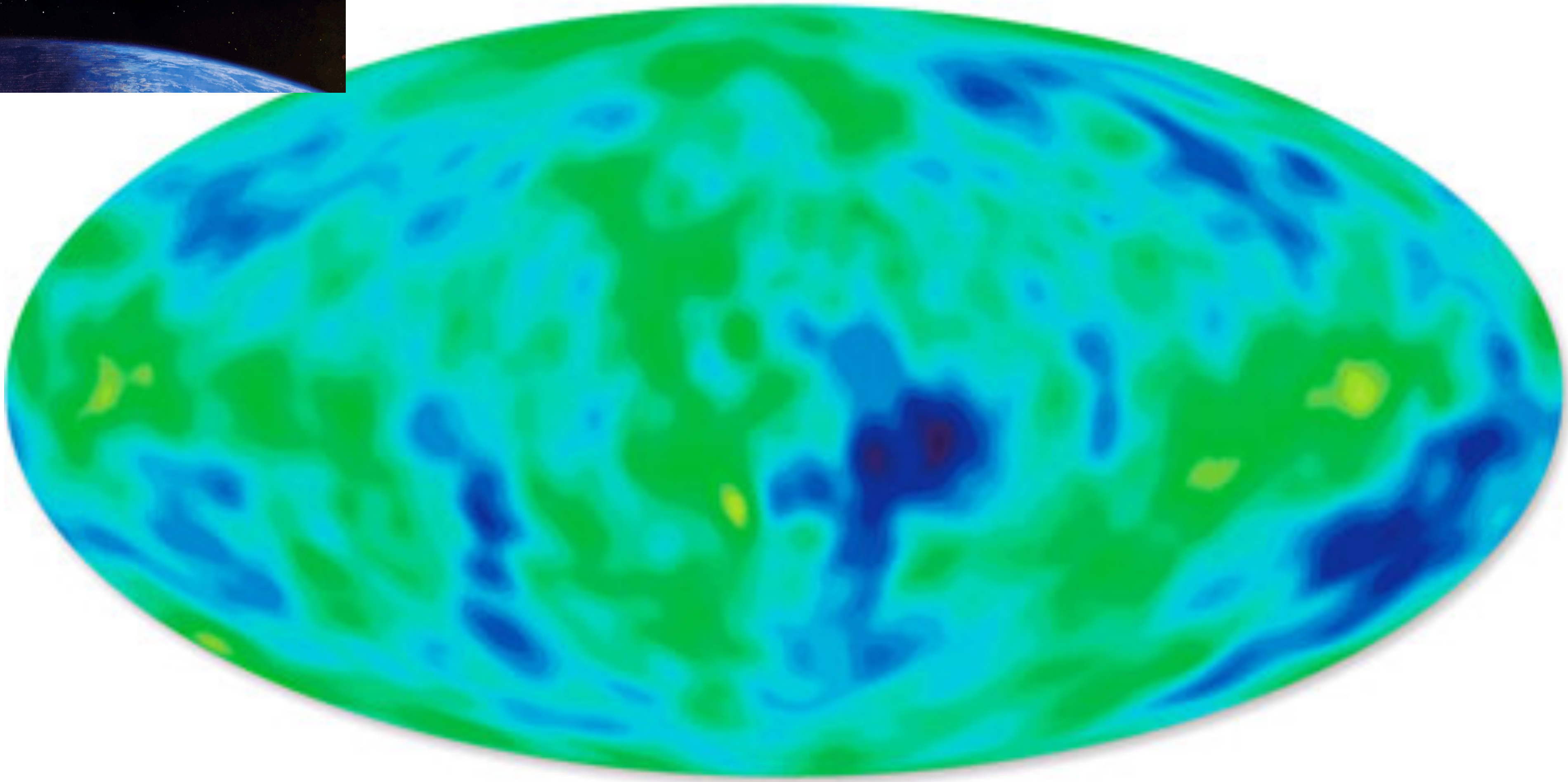

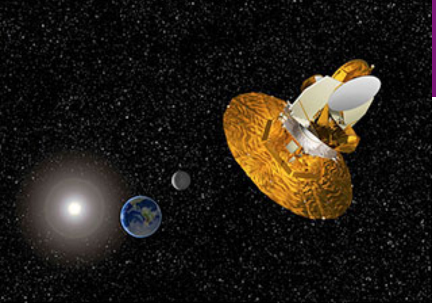

The CMB: WMAP (2001-2010)

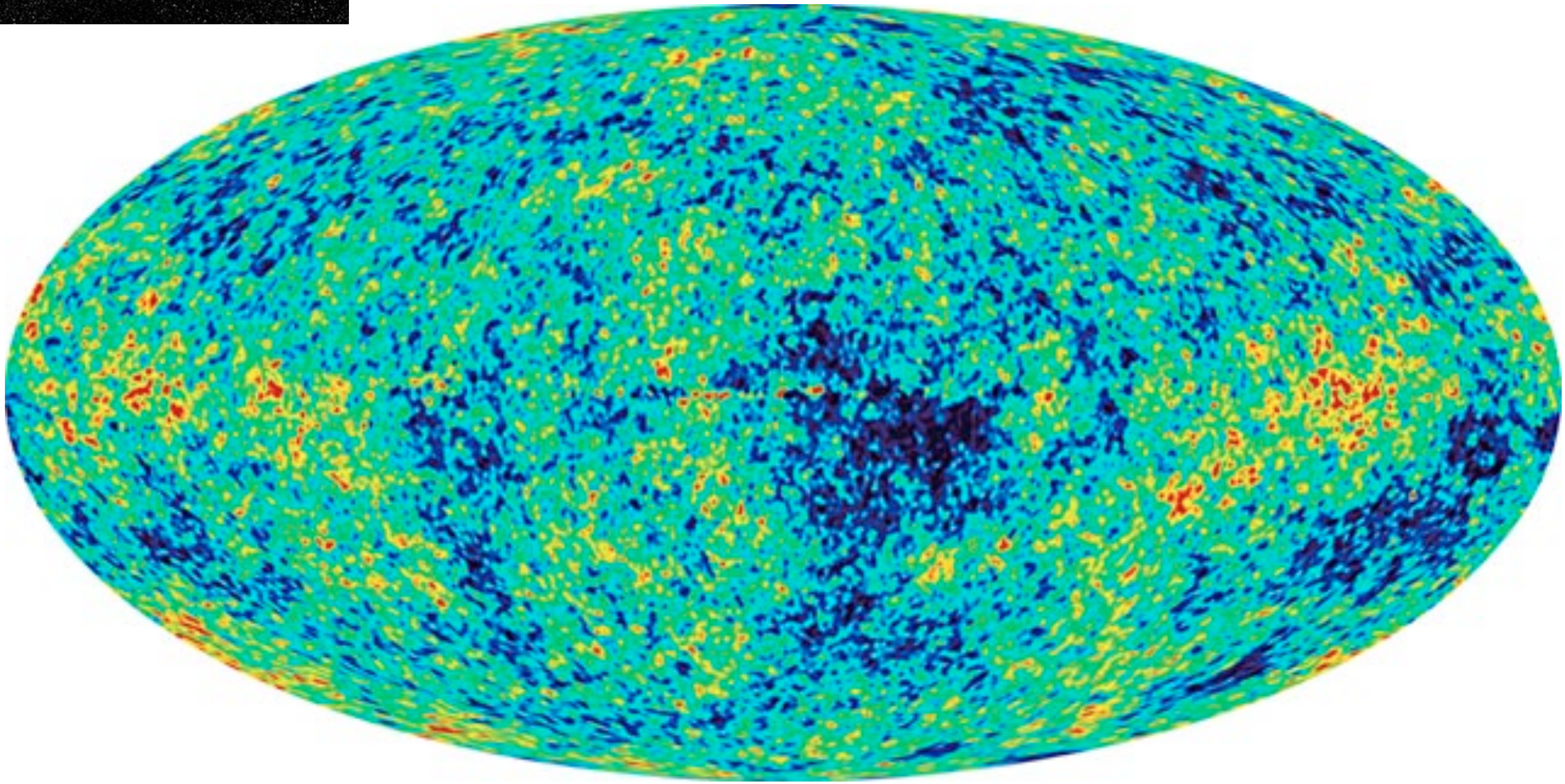

The CMB: Planck (2009-2013)

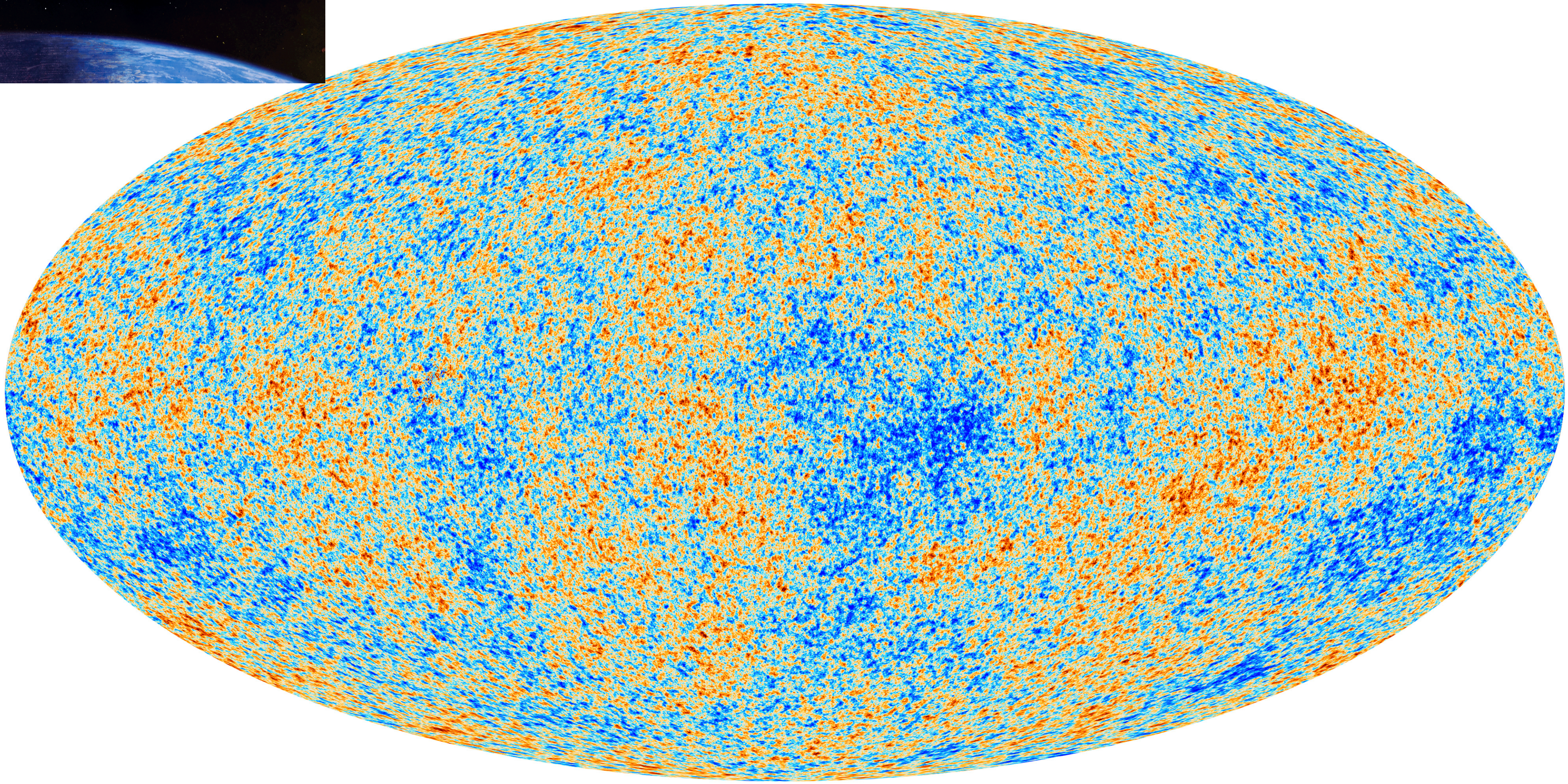

The Cosmic Microwave Background

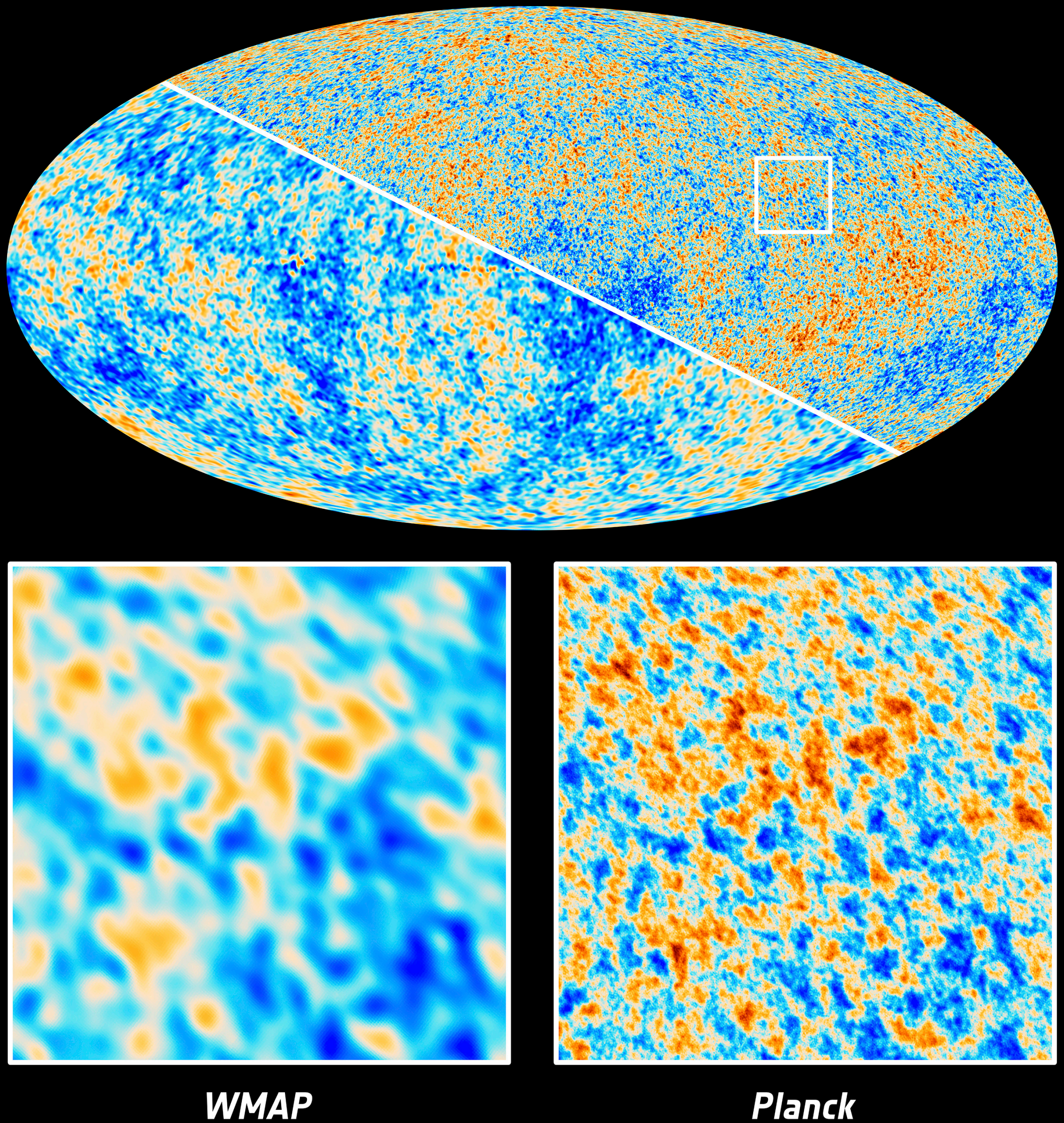

The Cosmic Microwave Background

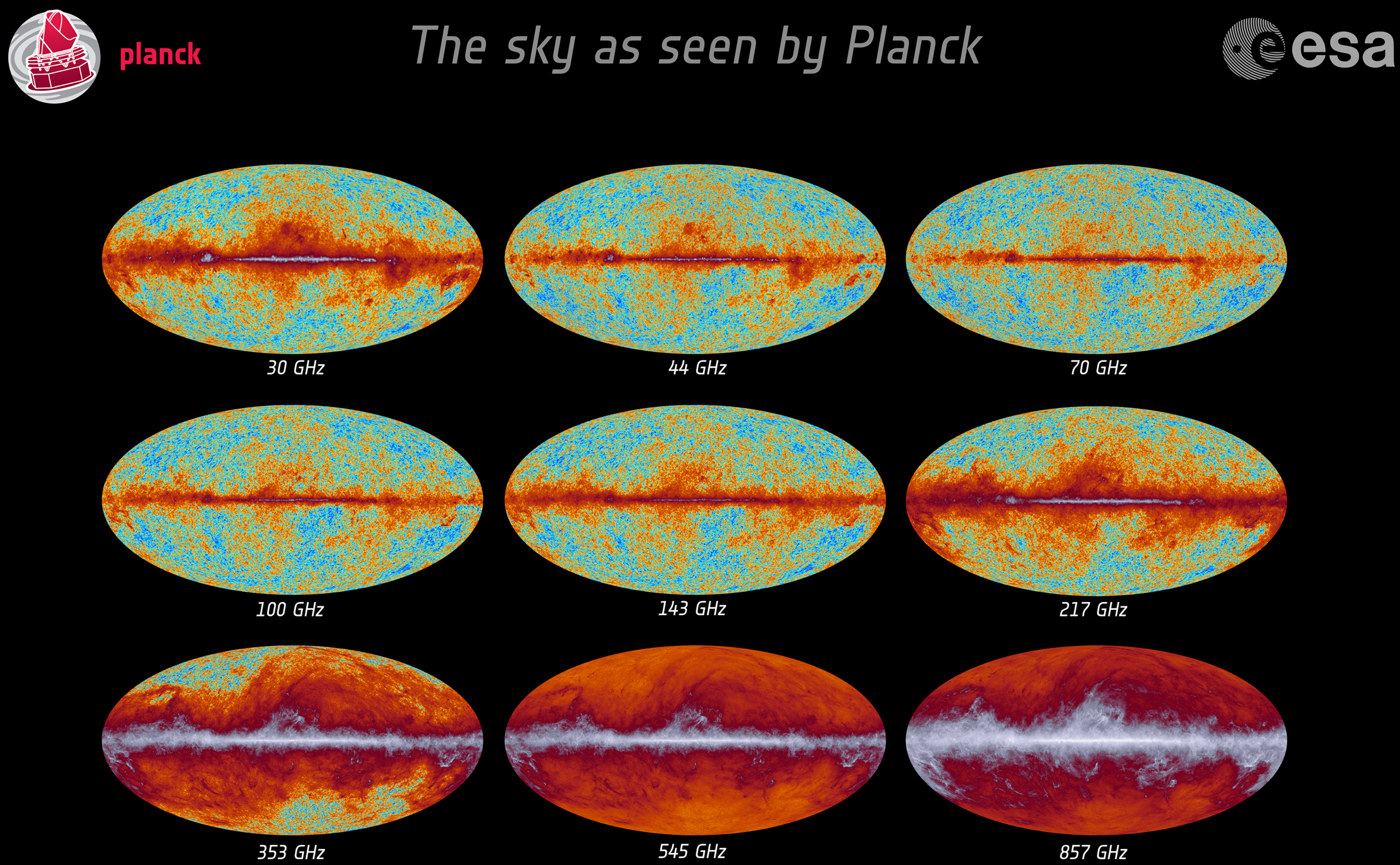

The CMB: How the Planck map is made

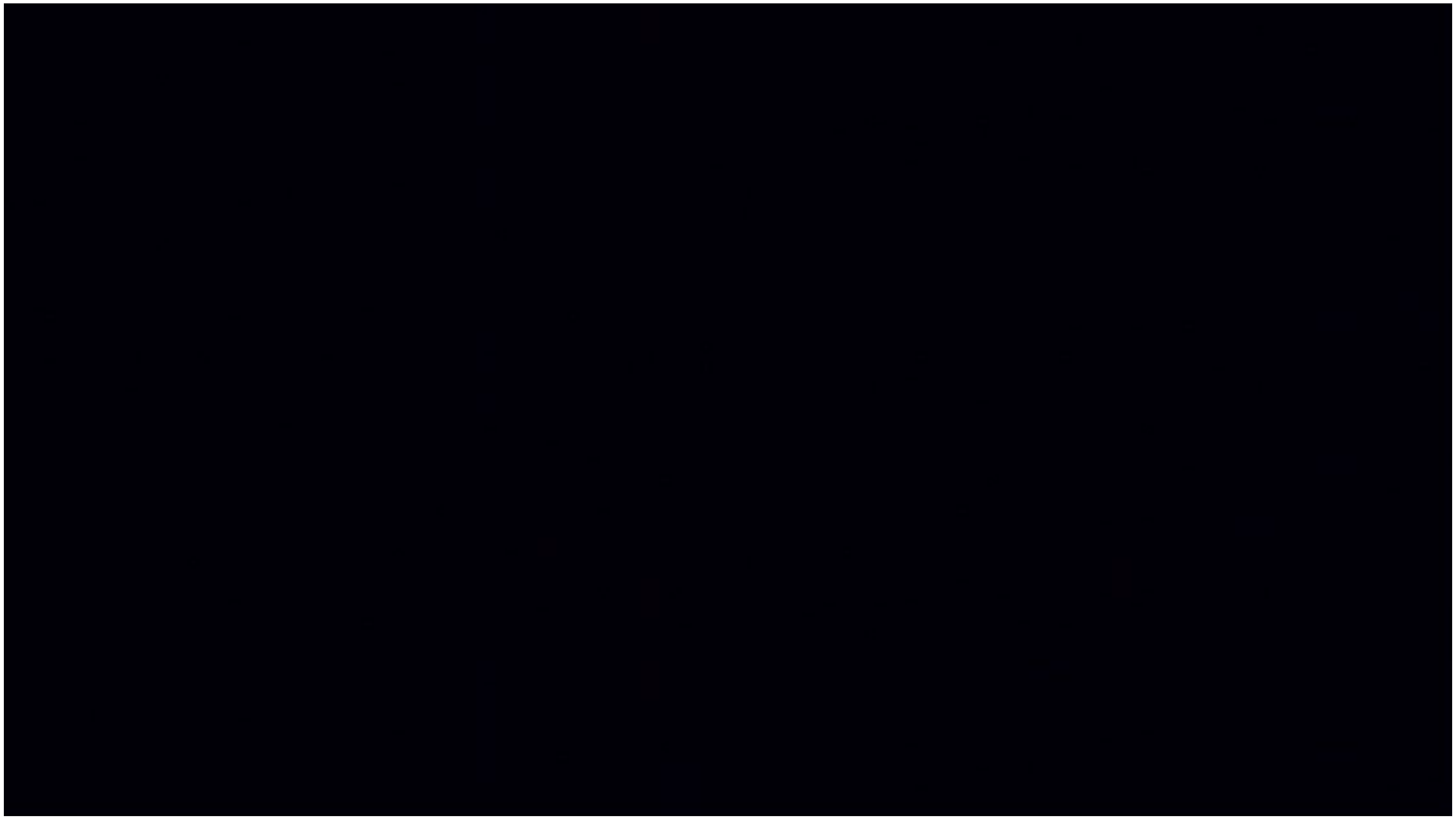

The CMB: How the Planck power spectrum is made

The CMB power spectrum: WMAP

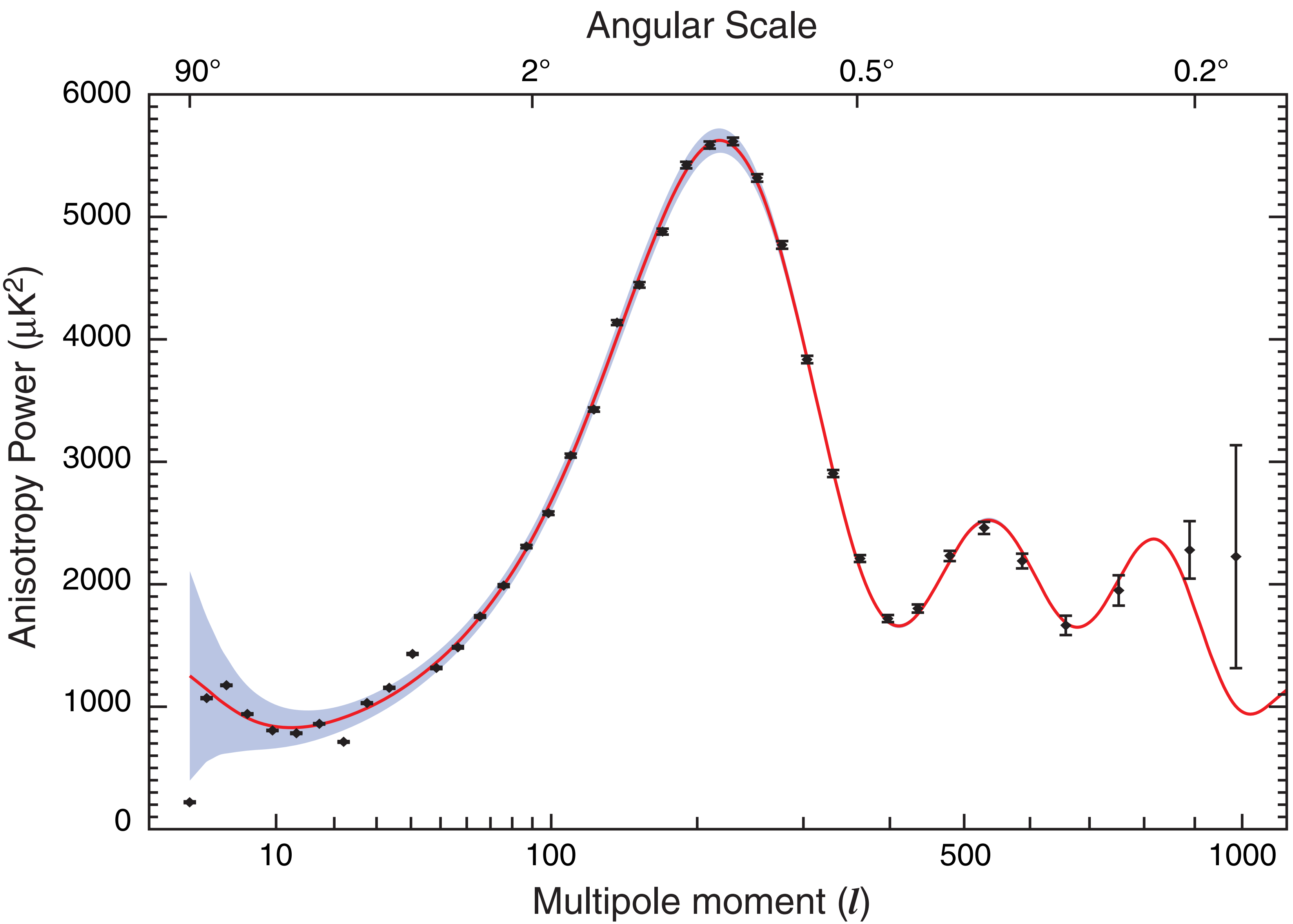

The CMB power spectrum: Planck

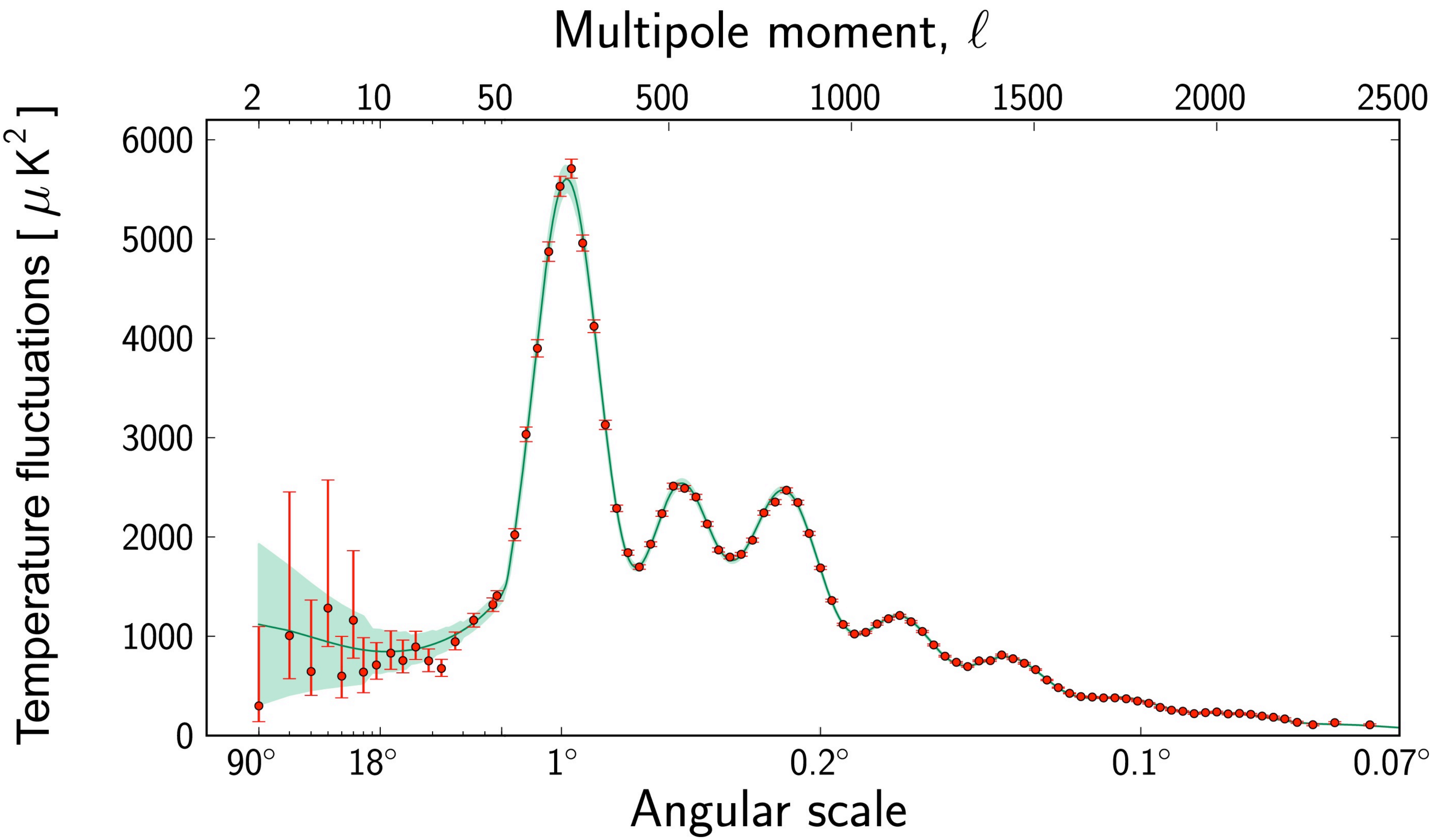

The CMB tells us what the universe is made of

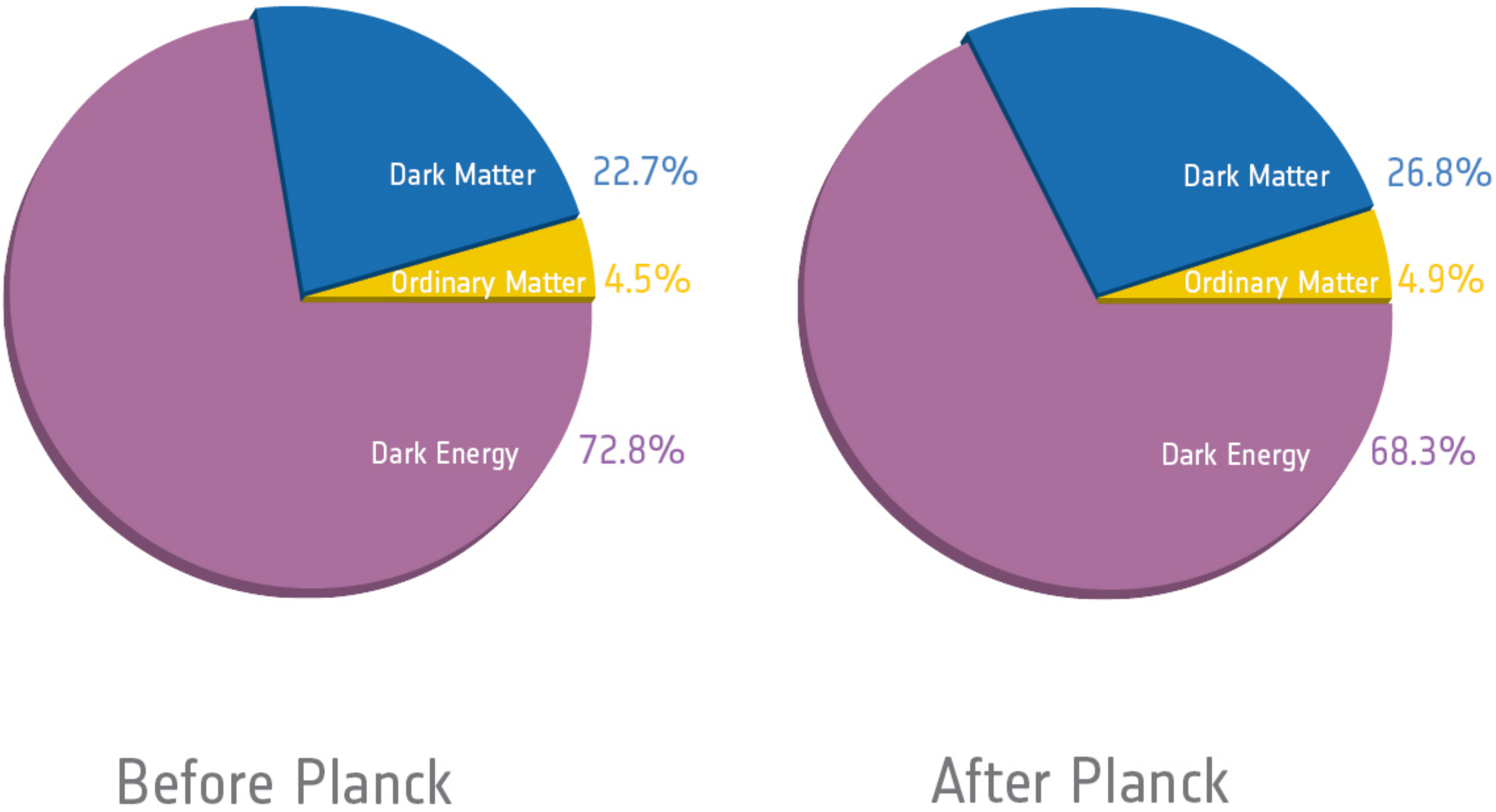

Hubble Ultra Deep Field
Hubble Space Telescope • Advanced Camera for Surveys

NASA, ESA, S. Beckwith (STScI) and the HUDF Team   STScI-PRC04-07a

- 11 days total exposure time

  10,000 galaxies

  3 arcminutes size
  (0.1 x diameter of moon)

Galaxies with disks

Spiral Galaxy M64

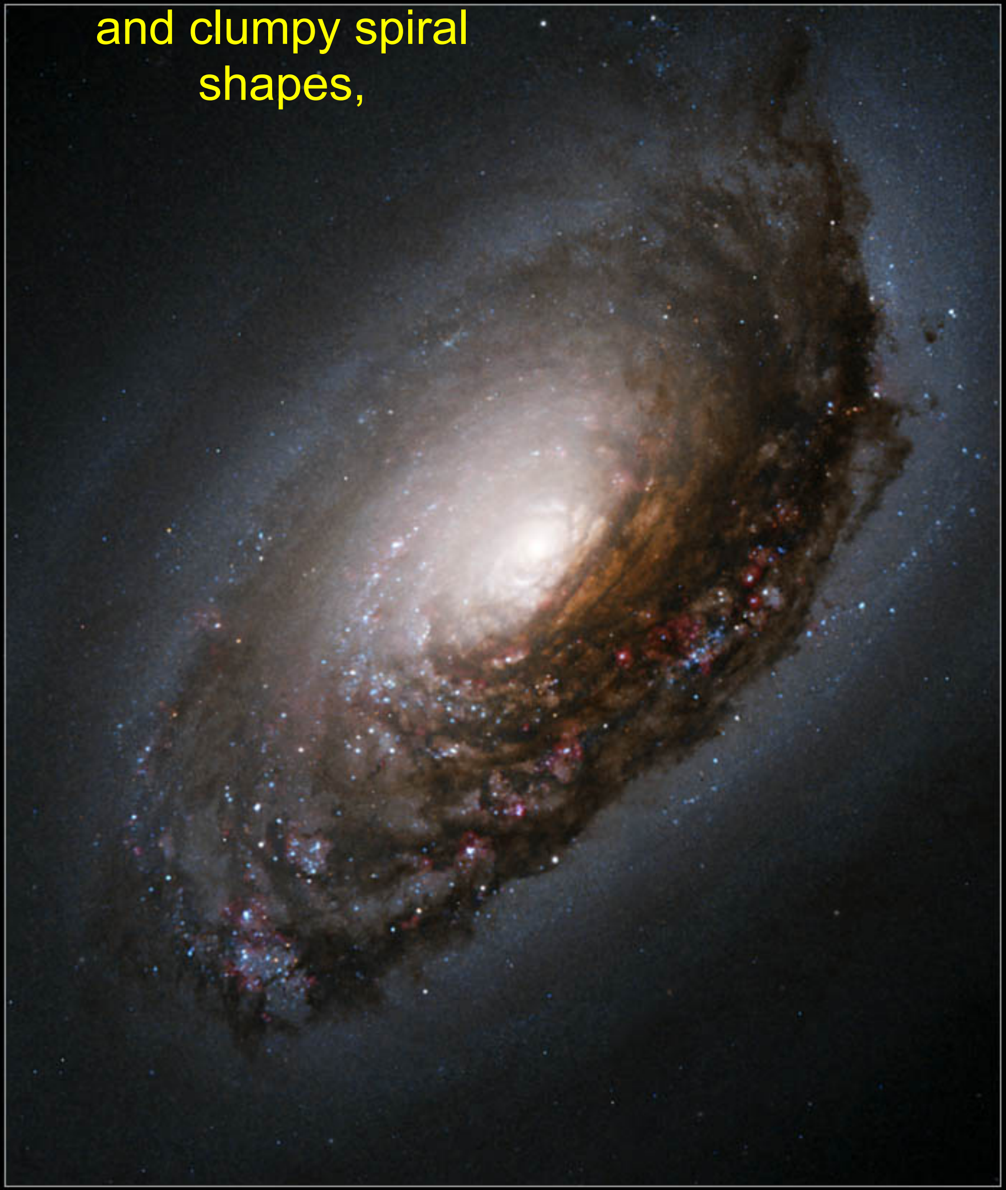

NASA and The Hubble Heritage Team (STScI/AURA) • Hubble Space Telescope WFPC2 • STScI-PRC04-04 and smooth elliptical galaxies.

M87 © Anglo-Australian Observatory
Photo by David Malin

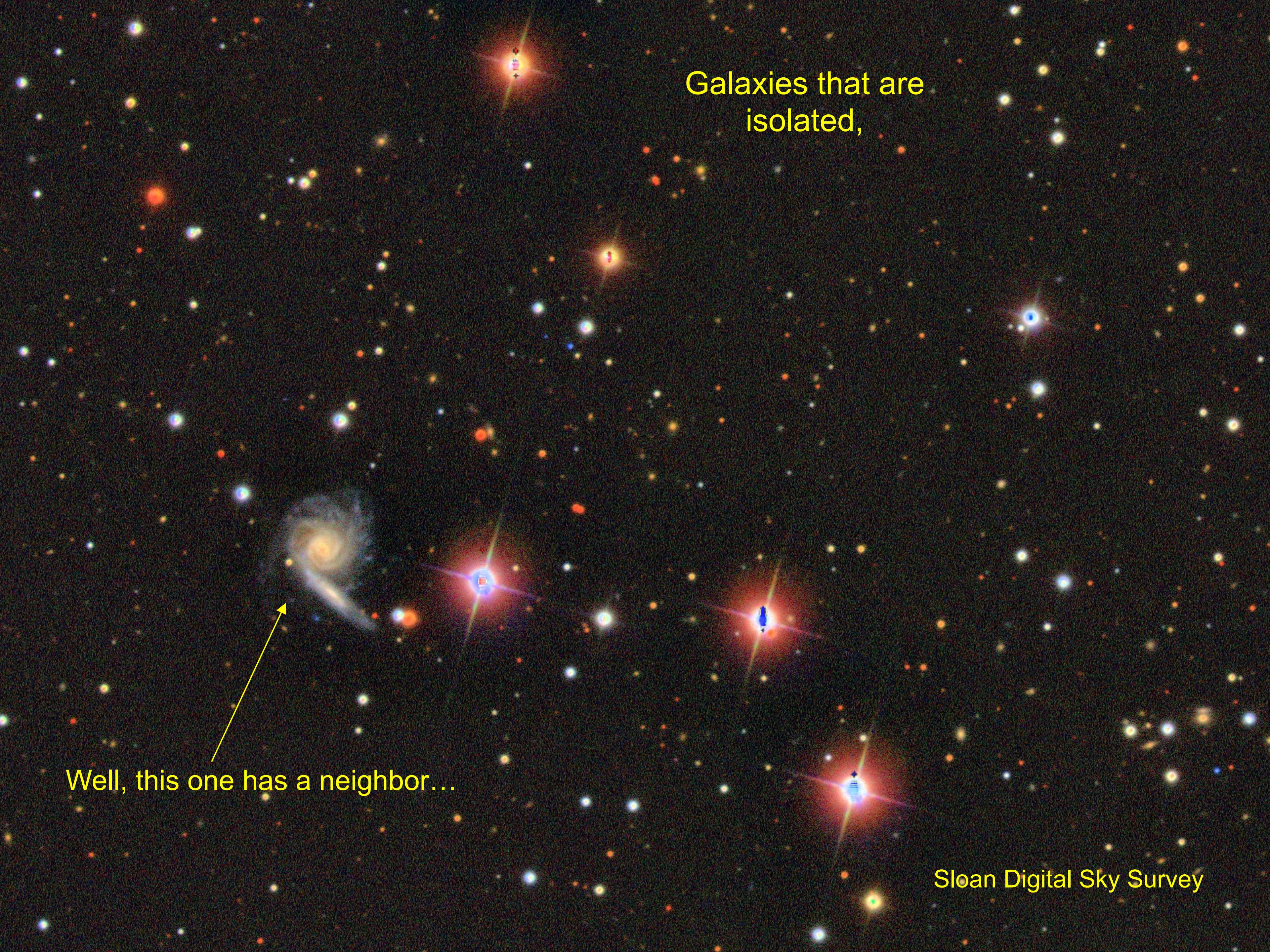
Galaxies that are isolated,
Well, this one has a neighbor…
Sloan Digital Sky Survey

Perseus cluster - Sloan Digital Sky Survey

Antennae galaxies – OSU Bright galaxy survey

Anatomy of a galaxy

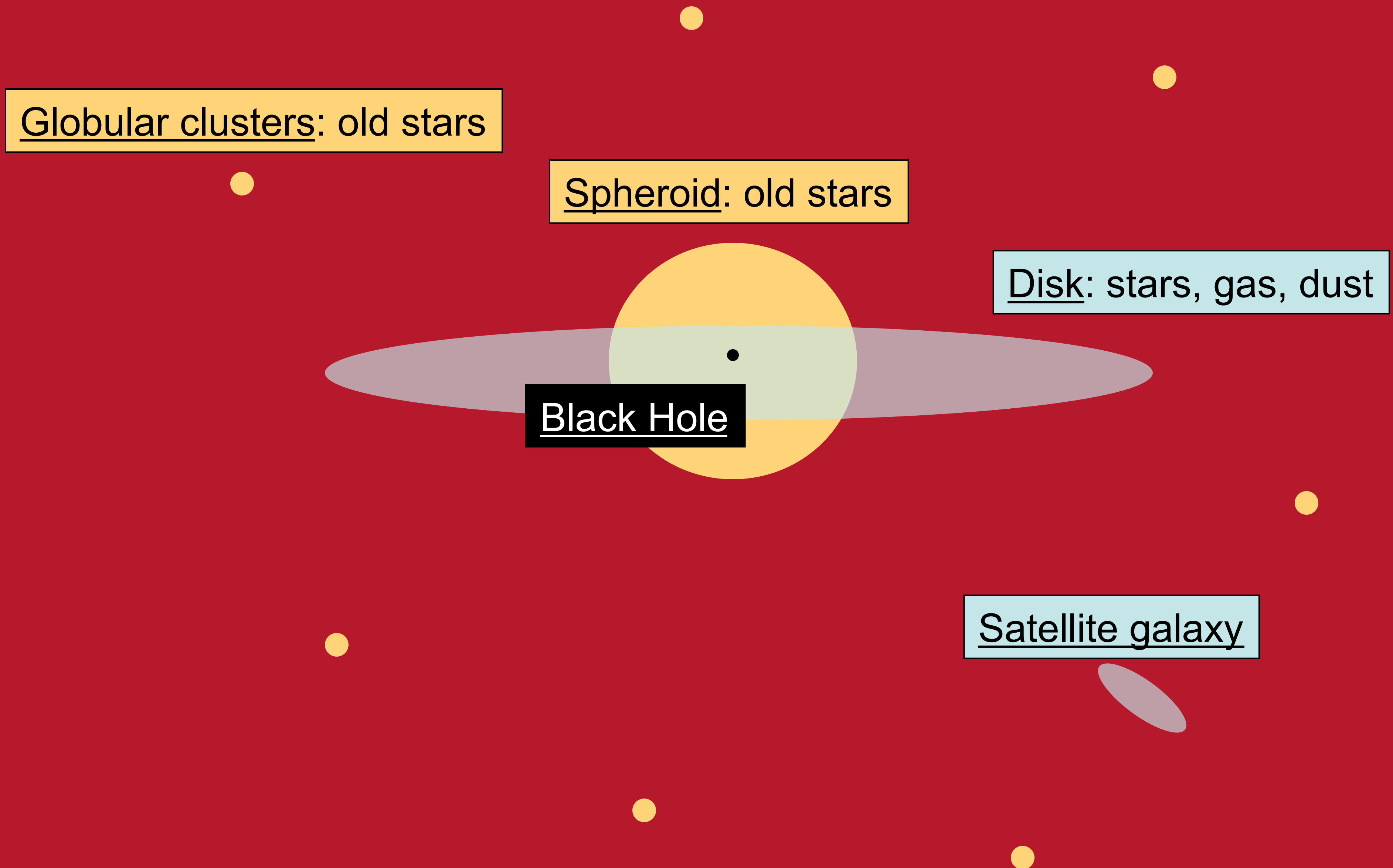

Anatomy of a galaxy

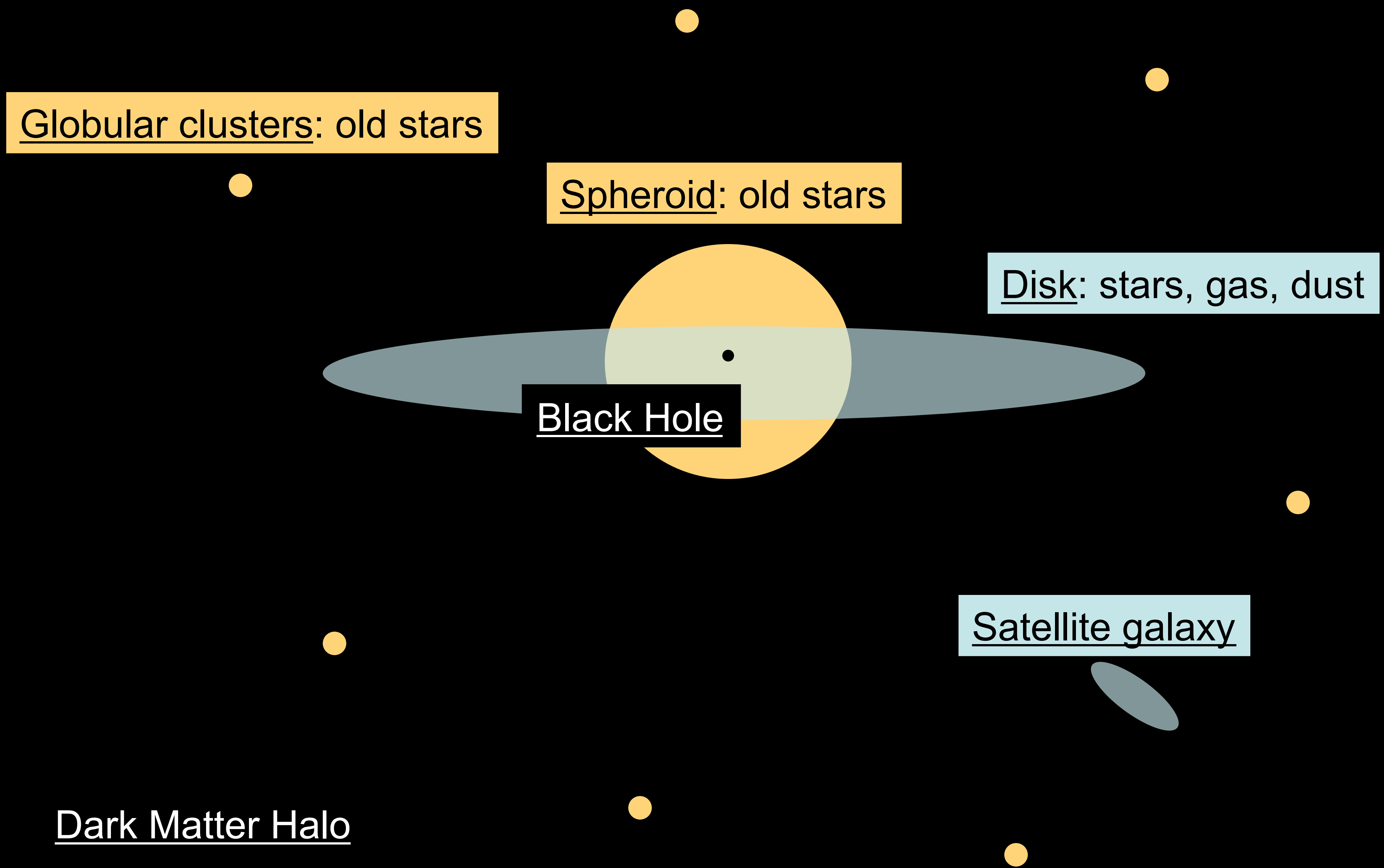

Very generally, there are two types of galaxies that we see:

Spiral/disk galaxies:
- have a disk-like structure
- are blue-ish in color
- tend to be isolated

Elliptical galaxies:
- have no disk
- are red-ish in color
- tend to be located in clusters

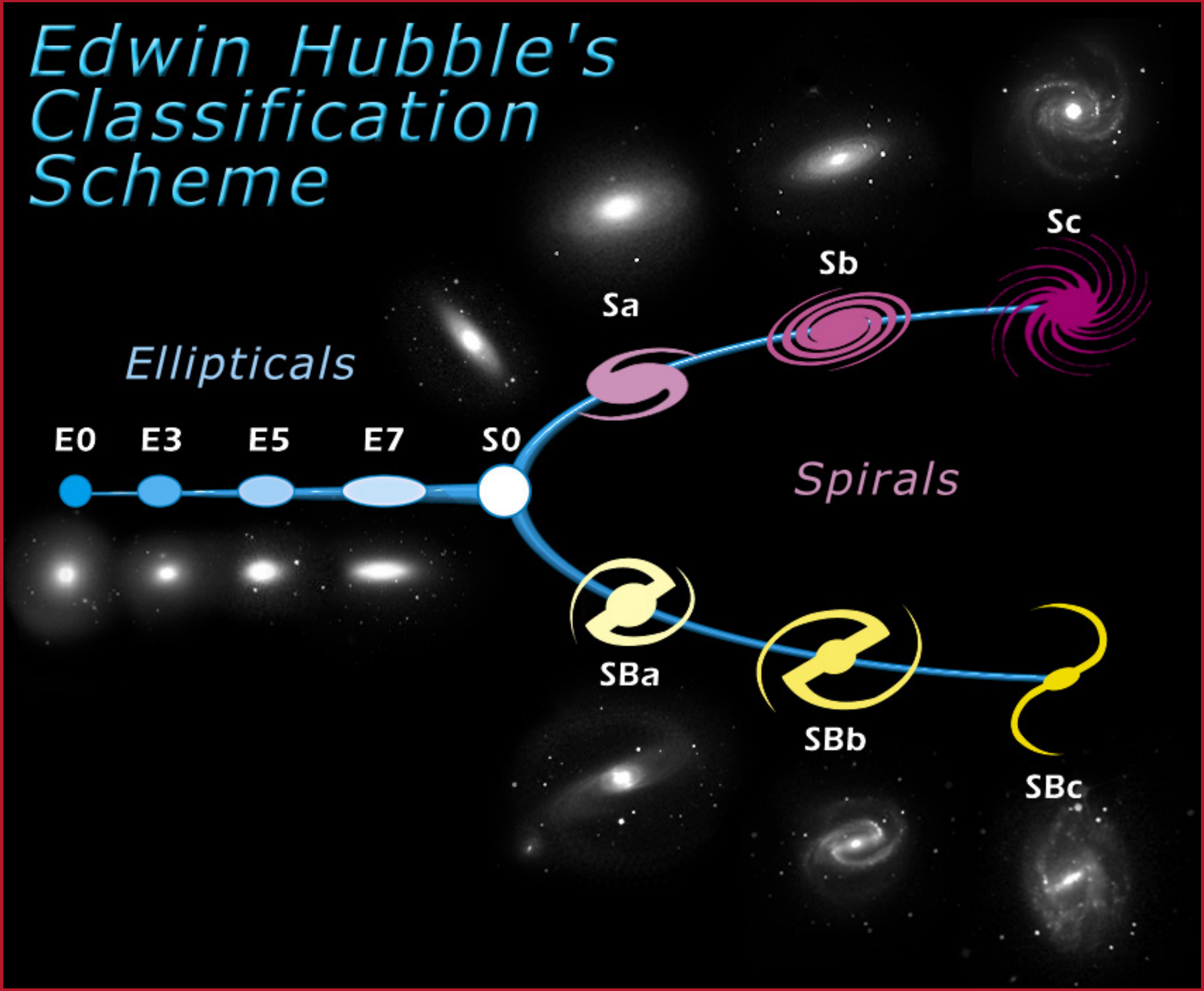
Edwin Hubble's Classification Scheme
Ellipticals
E0
E3
E5
E7
S0
Sa
Sb
Sc
Spirals
SBa
SBb
SBc

M87 : E0

ESO325 : E3

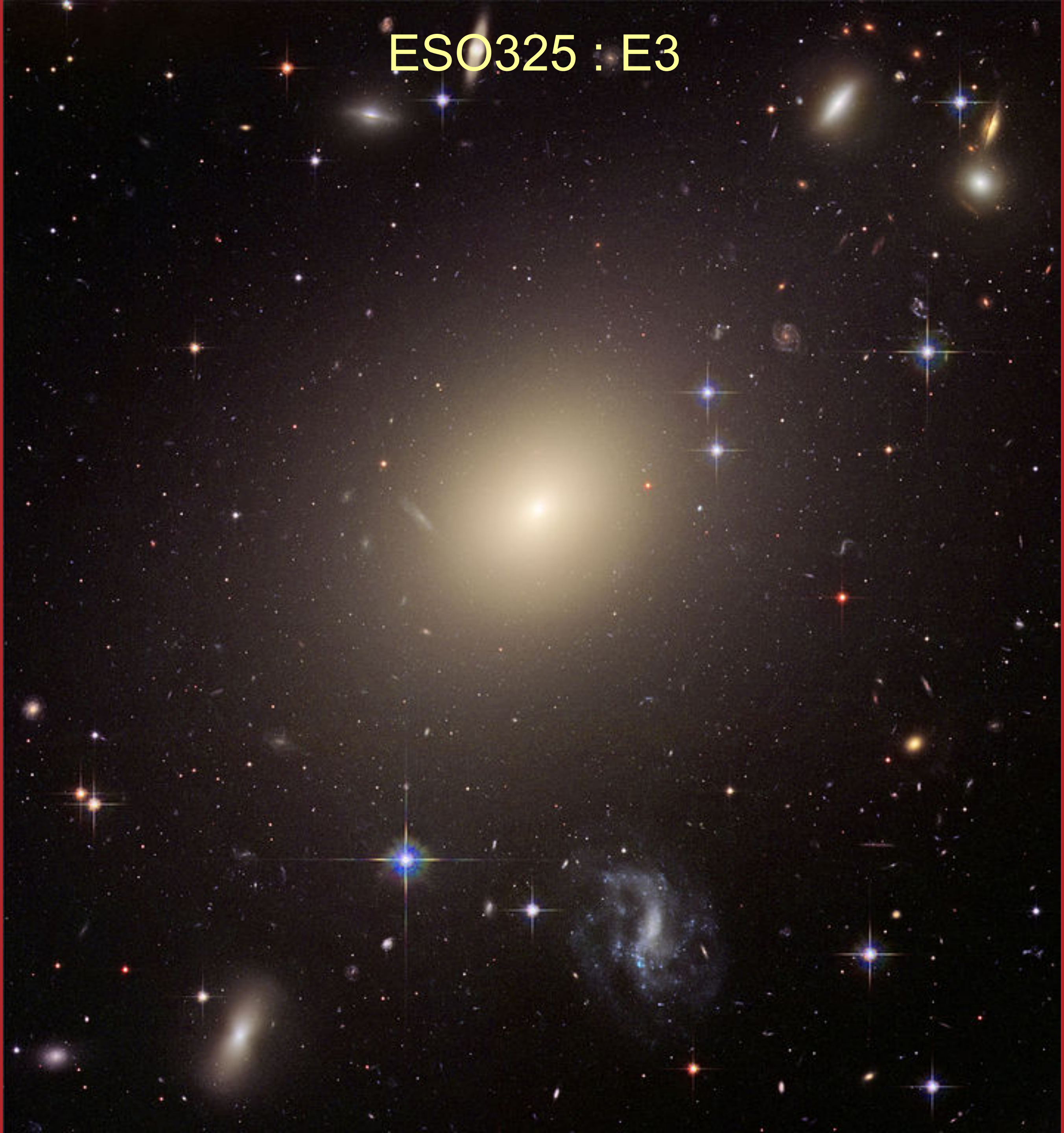

NGC5866 : S0

M81 : Sab

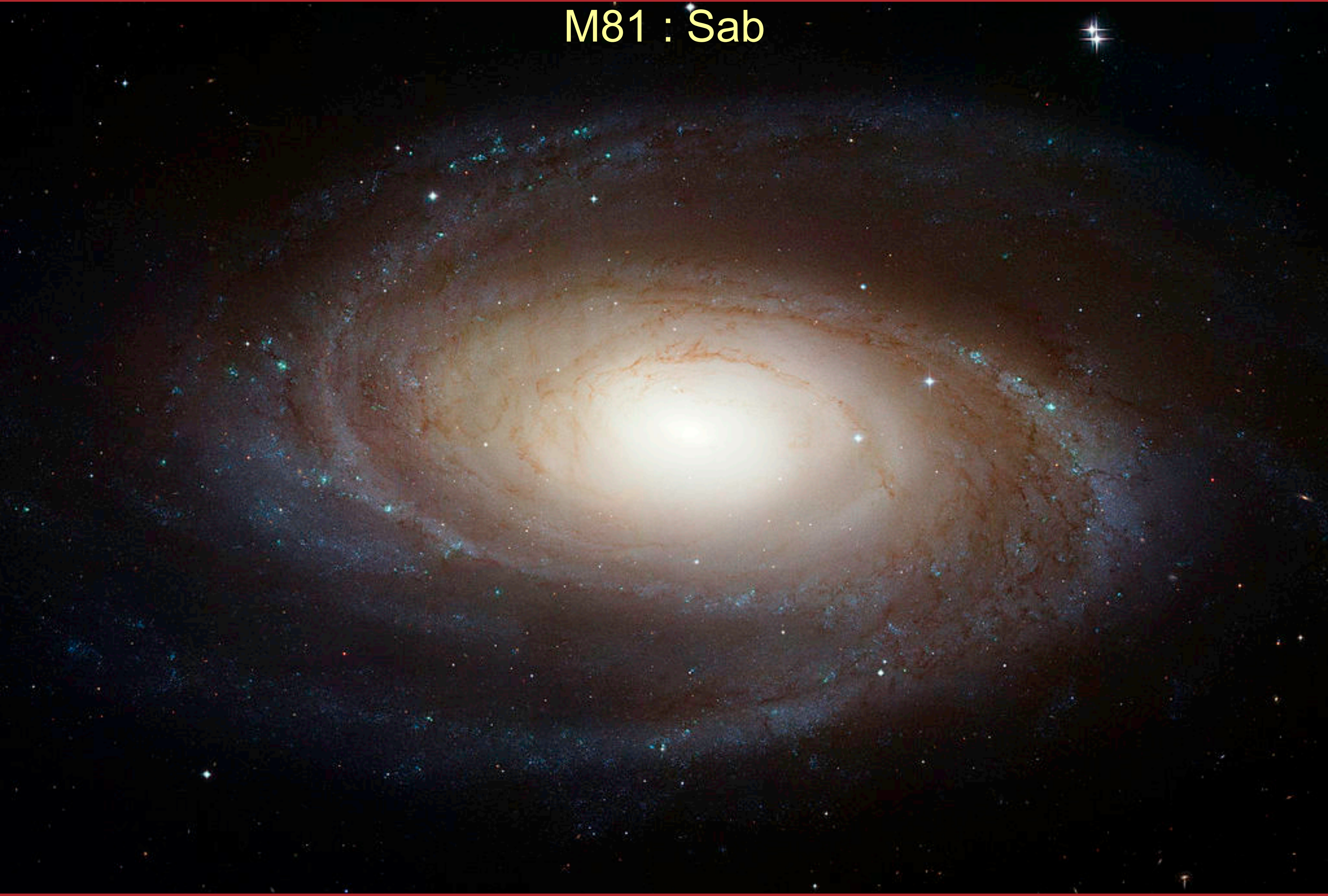


M101 : Scd

NGC1300 : SBbc

The Spitzer Infrared Nearby Galaxies Survey (SINGS) Hubble Tuning-Fork

The Spitzer Space Telescope observed 75 galaxies as part of its SINGS (Spitzer Infrared Nearby Galaxies Survey) Legacy Program. The galaxies are presented here in a Hubble Tuning-Fork diagram, which groups galaxies according to the morphology of their nuclei and spiral arms. The designation of these galaxies and their placement in the diagram is based on their visible-light appearance. The main goal of the SINGS program is to characterize the infrared properties of a wide range of galaxy types. The images of the galaxies are composites created from data taken by IRAC (the Infrared Array Camera) at 3.6 and 8.0 µm, and MIPS (the Multiband Imaging Photometer for Spitzer) at 24 µm.

The infrared range probed by these and other observations taken for the SINGS project allows for the detailed study of star formation, dust emission, and the distribution of stars in each galaxy. Light from old stars appears as blue in the images, while the lumpy knots of green and red light are produced by dust clouds surrounding newly born stars. The elliptical galaxies on the left are almost entirely made of old stars, while spiral galaxies like our own Milky Way are rich in young stars and the raw materials for future star formation.

More information can be found at:
http://sings.stsci.edu/

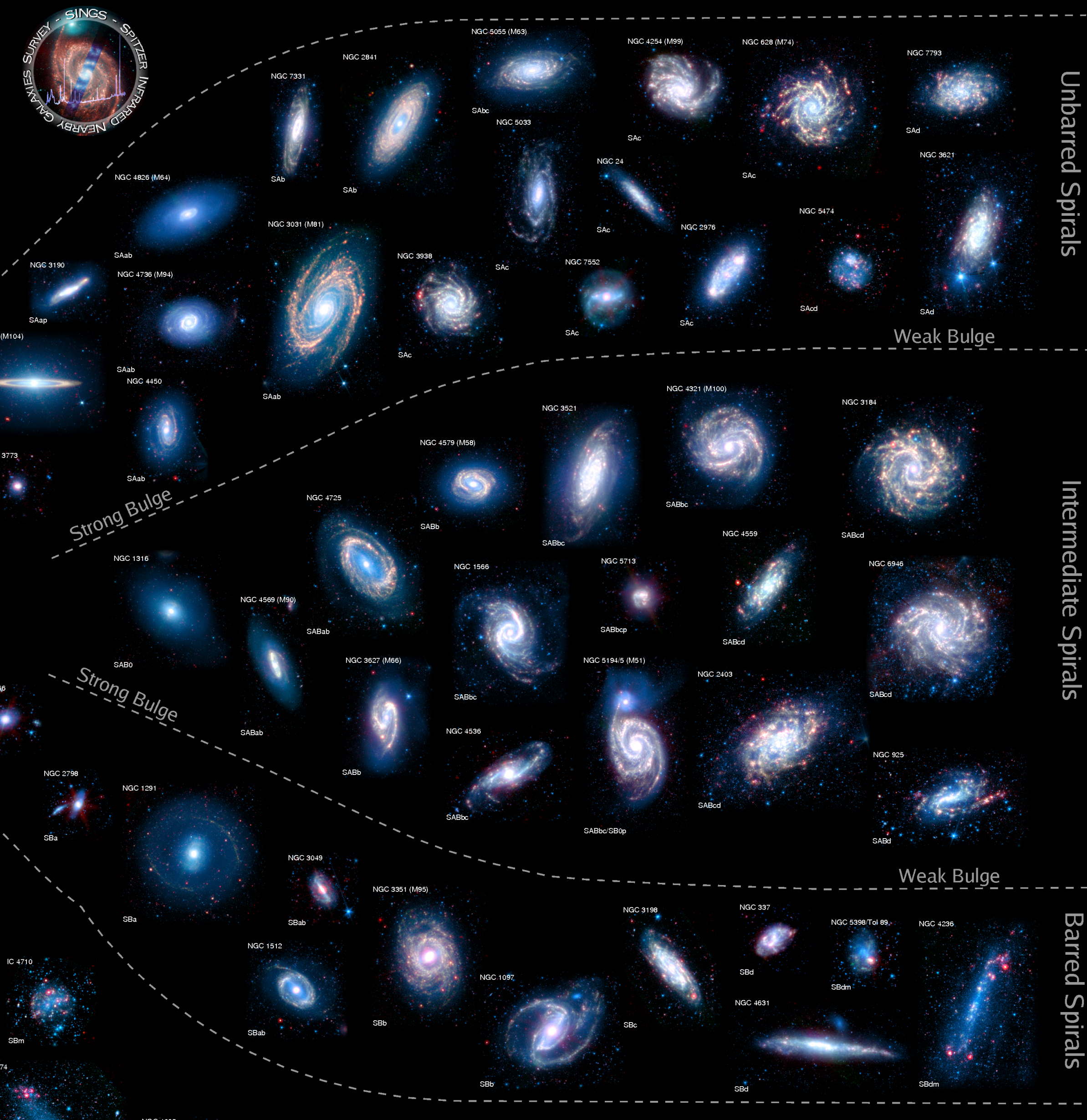

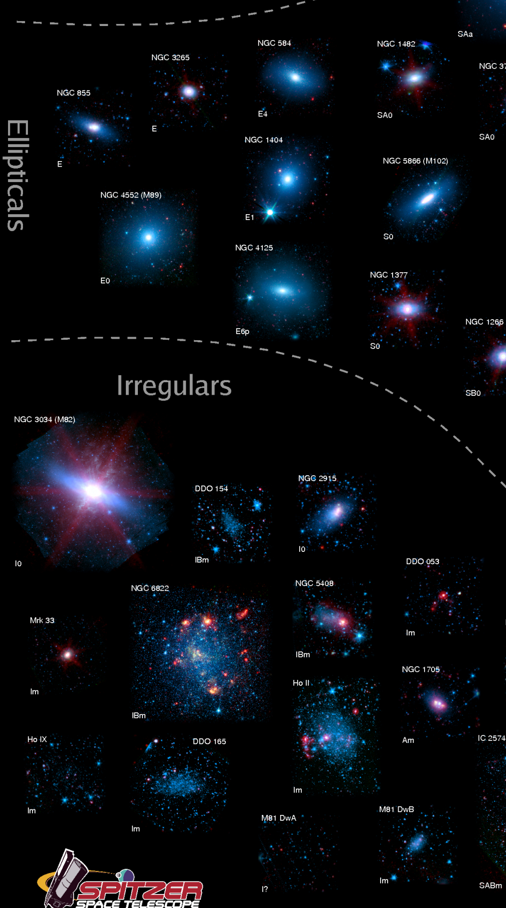

Poster and composite images created from SINGS observations by Karl D. Gordon (Oct 2007)
Blue=IRAC 3.6µm (stars)
Green=IRAC 8µm
(aromatic features from dust grains/molecules)
Red=MIPS 24µm (warm dust)

SINGS Team

Robert Kennicutt, Jr. (Principle Investigator), Daniela Calzetti (Deputy Principle Investigator), Charles Engelbracht (Technical Contact), Lee Armus, George Bendo, Caroline Bot, Brent Buckalew, John Cannon, Daniel Dale, Bruce Draine, Karl Gordon, Albert Grauer, David Hollenbach, Tom Jarrett, Lisa Kewley, Claus Leitherer, Aigen Li, Sangeeta Malhotra, Martin Meyer, John Moustakas, Eric Murphy, Michael Regan, George Rieke, Marcia Rieke, Helene Roussel, Kartik Sheth, J.D. Smith, Michele Thornley, Fabian Walter & George Helou

Luminosity and flux

Luminosity	L : energy/time (erg/s)
Flux	f : luminosity/area (erg/s/cm^2)

Inverse square law: $$f = \frac{L}{4\pi d^2}$$

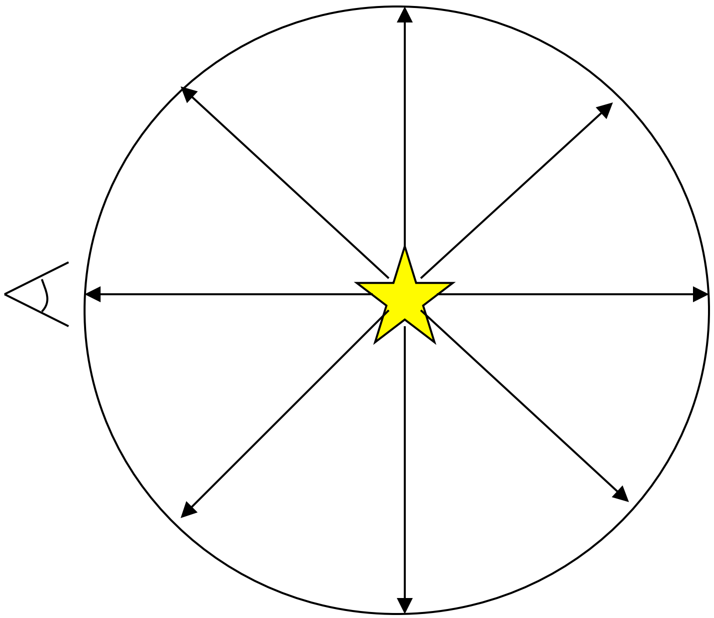

Surface brightness

Surface brightness $\quad I$: flux/solid angle (erg/s/cm^2/st)

(4π steradians on the sky $\quad$ 1 steradian = 3282.8 deg^2)

At twice the distance:

- flux from each star is 4x fainter
- area covered by solid angle is 4x larger (i.e., 4x more stars)

Surface brightness is distance-independent

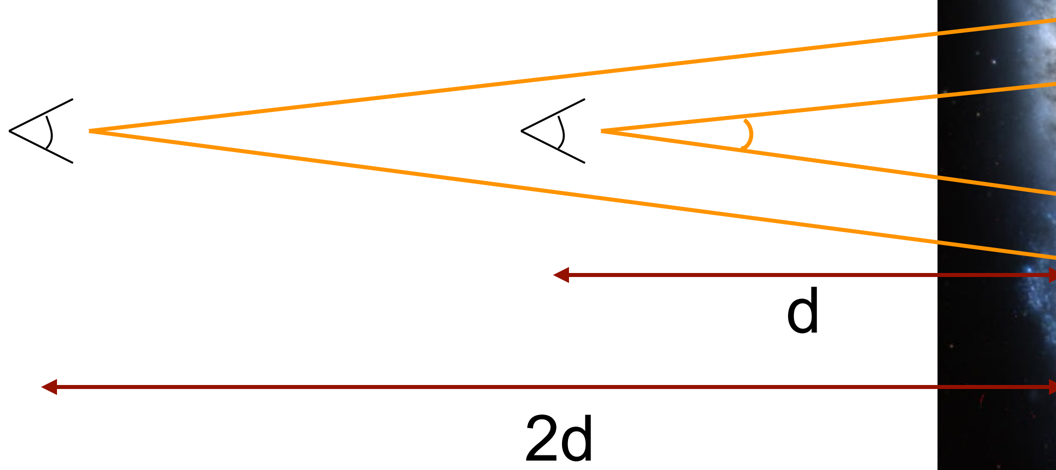

Apparent magnitude

$$m = -2.5\log f + const$$

A star that is 5 magnitudes brighter (smaller m) has 100x the flux.

$$m_1 - m_2 = -2.5\log\left(f_1/f_2\right)$$

$$\frac{f_1}{f_2} = 10^{\left(m_2 - m_1\right)/2.5}$$

Photometric filters

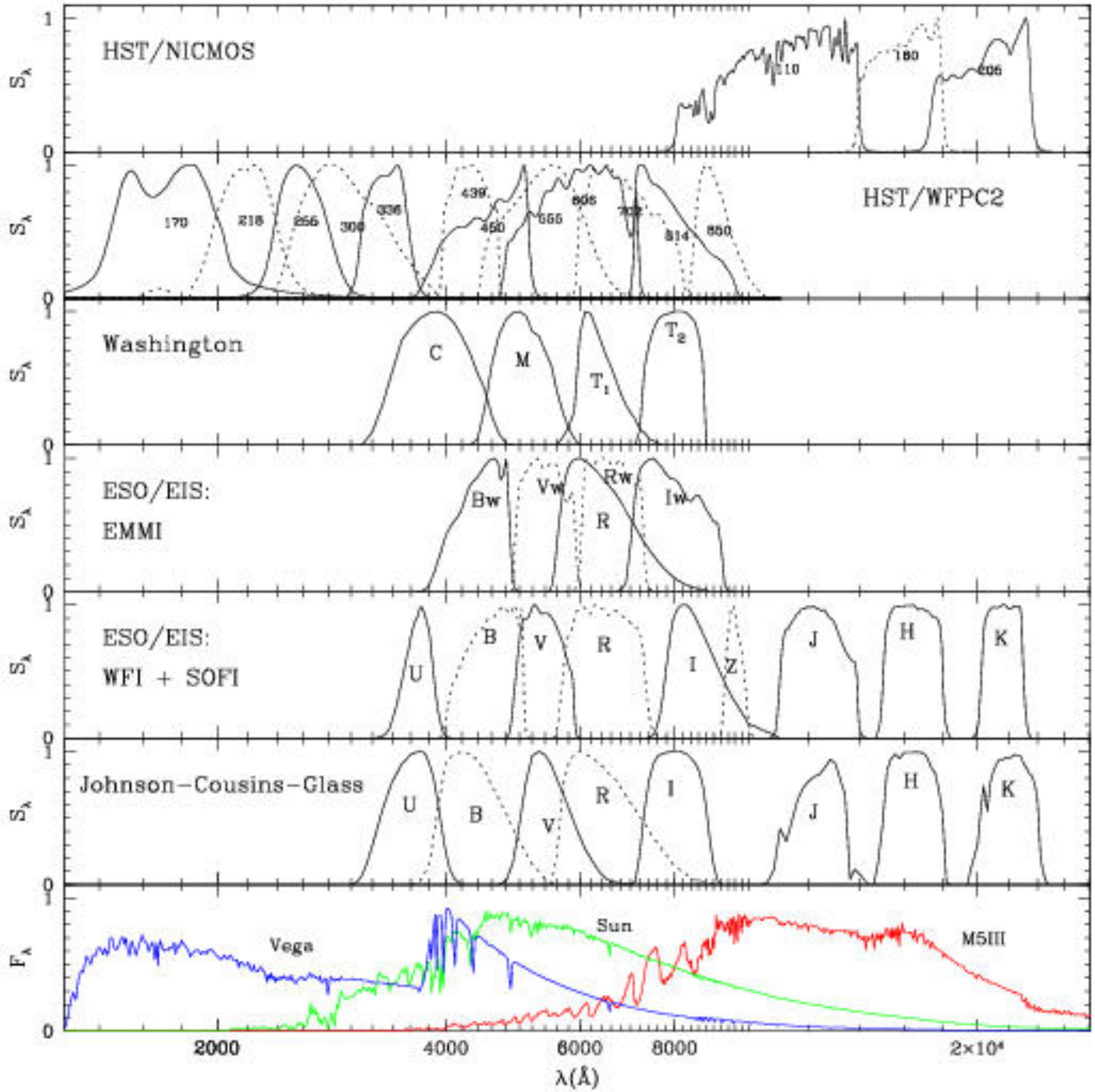

SDSS filters

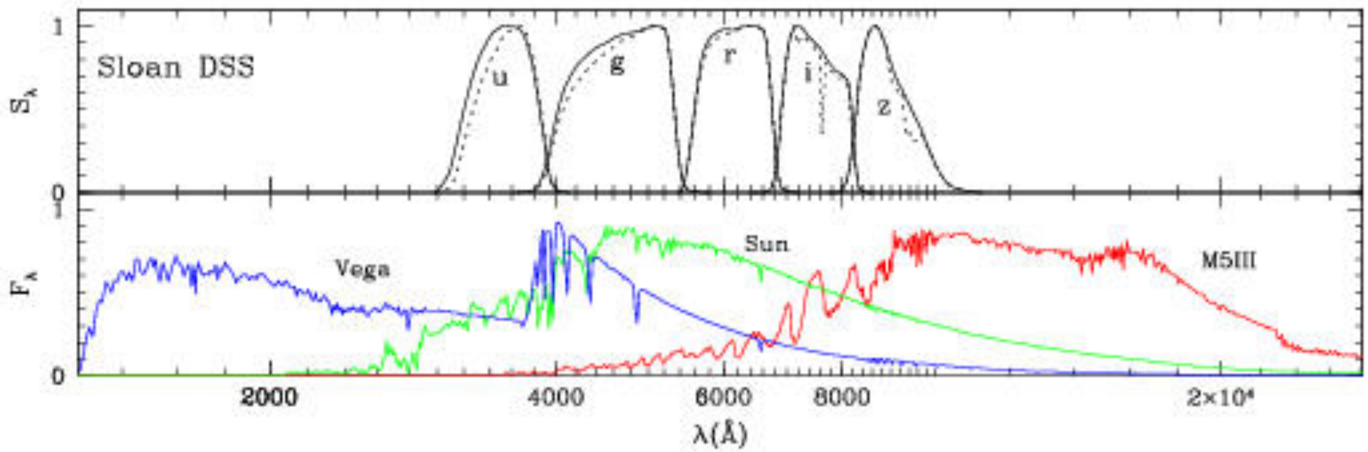

Absolute magnitude

M = apparent magnitude the star would have if it were 10pc away.

$$f = \frac{L}{4\pi d^2}$$

$$f_{10} = \frac{L}{4\pi (10\,pc)^2}$$

$$m - M = 5\log\left(\frac{d}{10\,pc}\right)$$

distance modulus

For example, the distance modulus for M31 is about 24.5

Color

Color = crude, low resolution, estimate of spectral shape

$$B - V = m_B - m_V = M_B - M_V = -2.5 \log\left(\frac{f_B}{f_V}\right)$$

- distance independent
- indicator of surface temperature
- by definition, B-V=0 for Vega (T~9500K)

Color

- Measure a star's brightness through two different filters

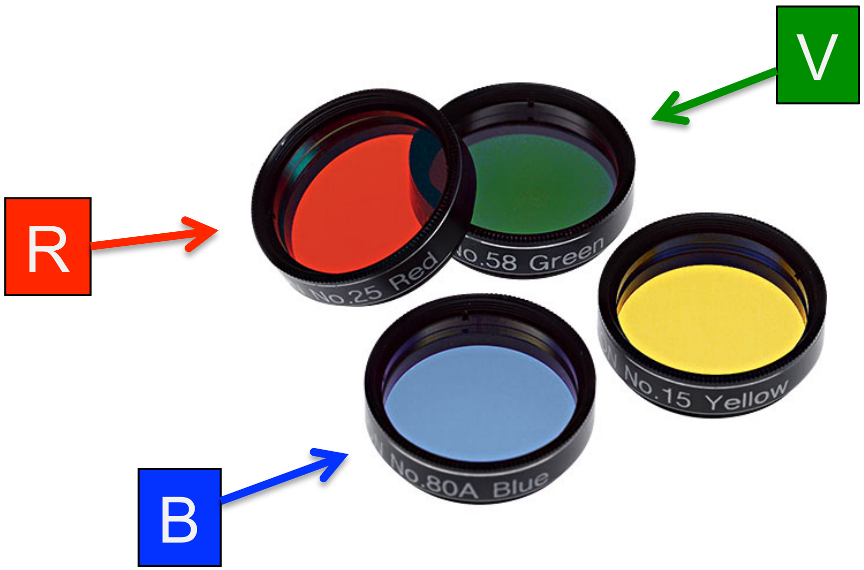

- Take the ratio of brightness: (redder filter)/(bluer filter)

  if ratio is large → red star

  if ratio is small → blue star

e.g., **V**/**B**

Color

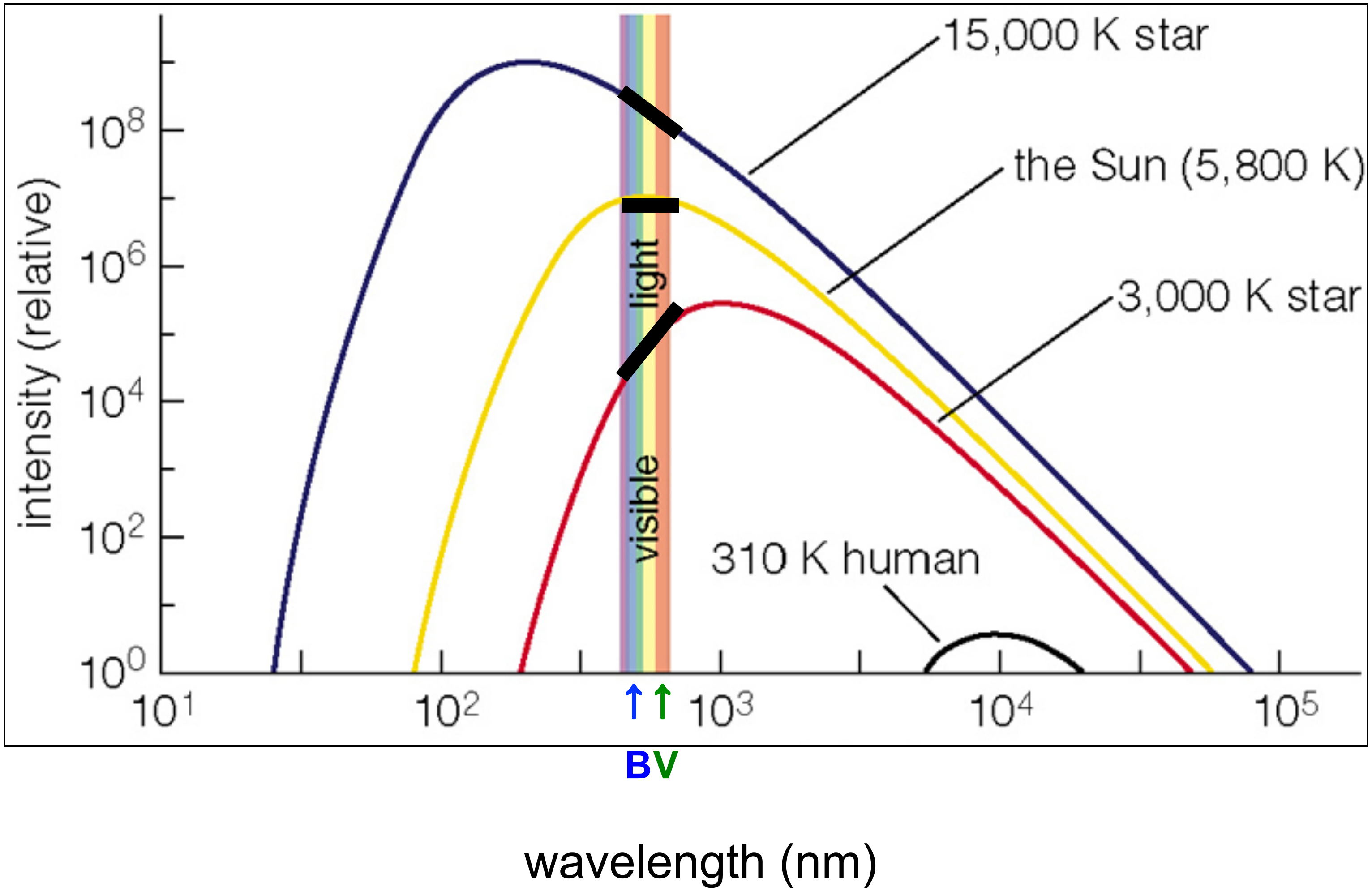

The color of a star measured like this tells us its temperature!

Stellar spectra

The solar spectrum can be approximated as

- a blackbody

  +

- absorption lines (looking at hotter layers through cooler outer layers)

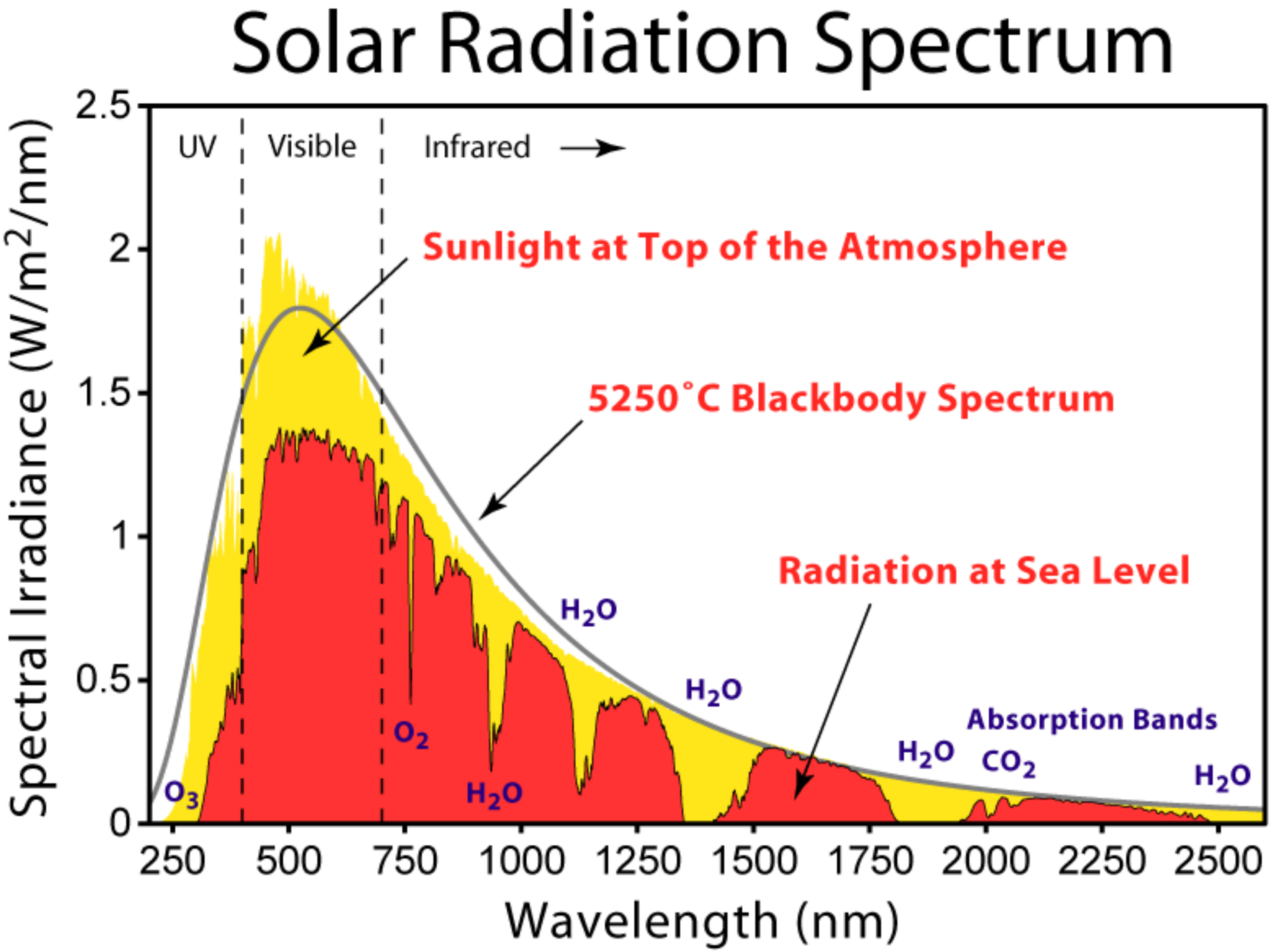

Solar Radiation Spectrum
Spectral Irradiance (W/m²/nm)
2.5
2
1.5
1
0.5
0
UV
Visible
Infrared
Sunlight at Top of the Atmosphere
5250°C Blackbody Spectrum
Radiation at Sea Level
H_2O
H_2O
O_2
H_2O
O_3
H_2O
Absorption Bands
CO_2
H_2O
250
500
750
1000
1250
1500
1750
2000
2250
2500
Wavelength (nm)

Stellar Spectra

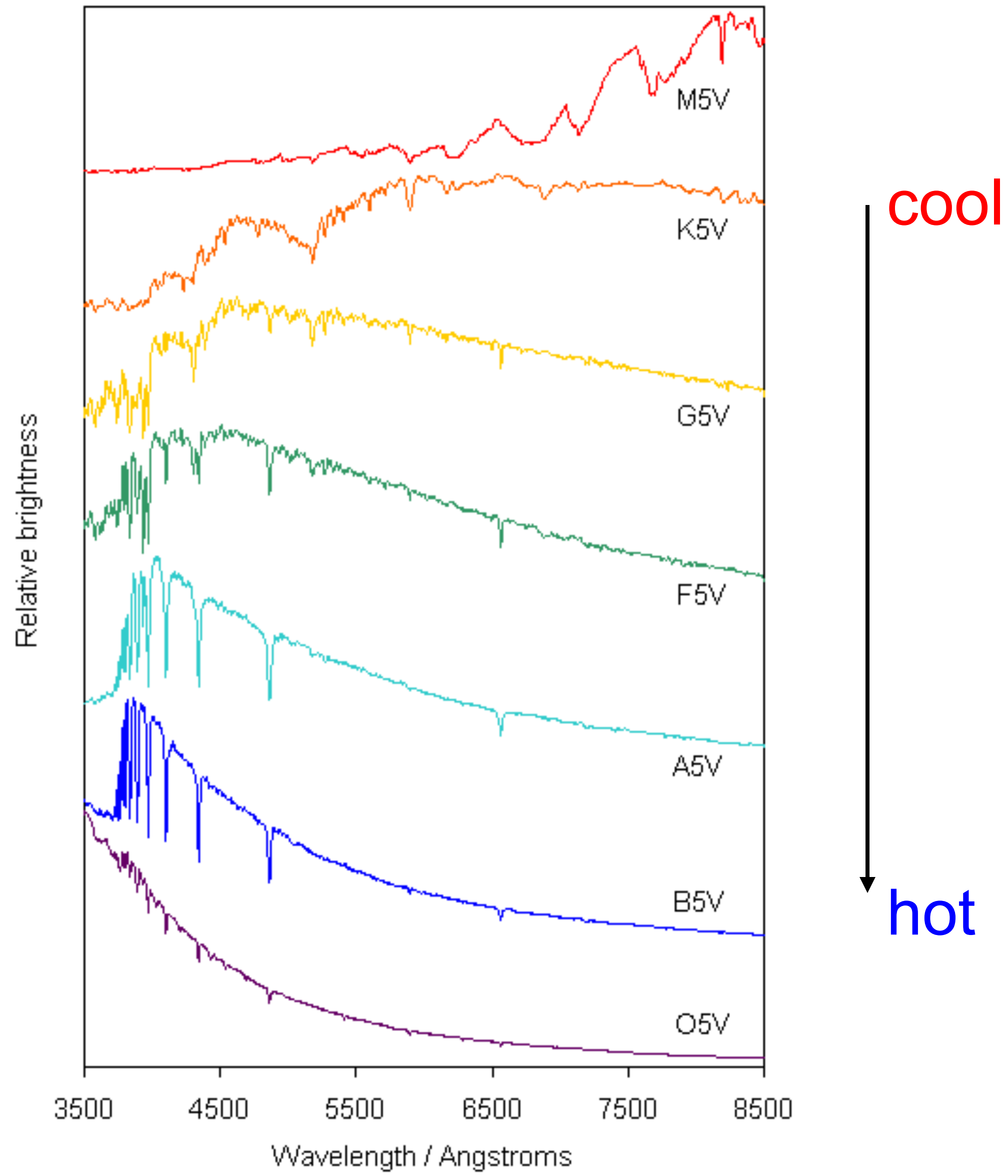

Galaxy Spectra

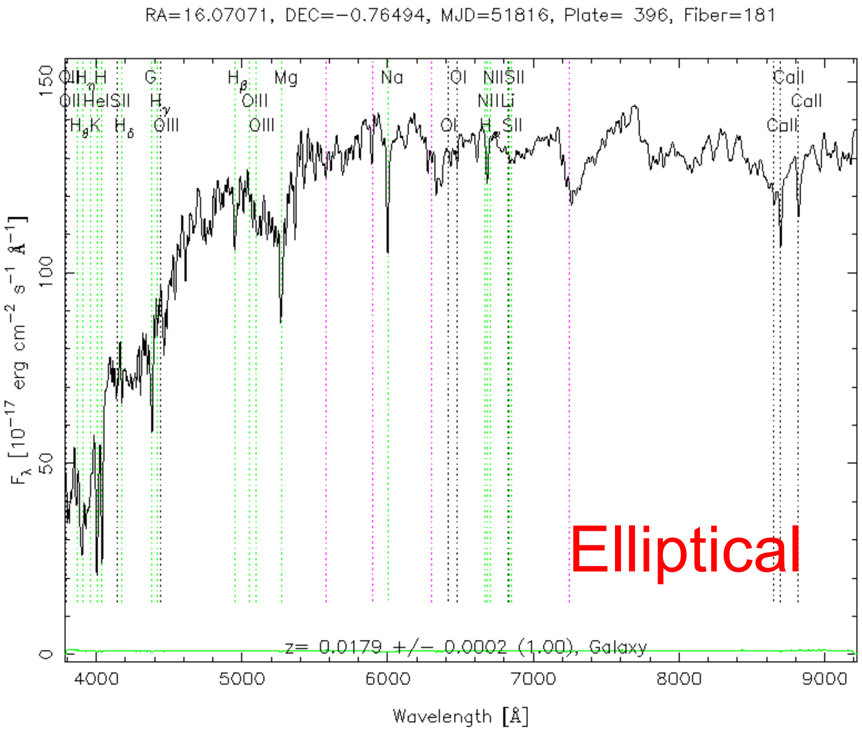

Which one is an Elliptical and which is a Spiral?

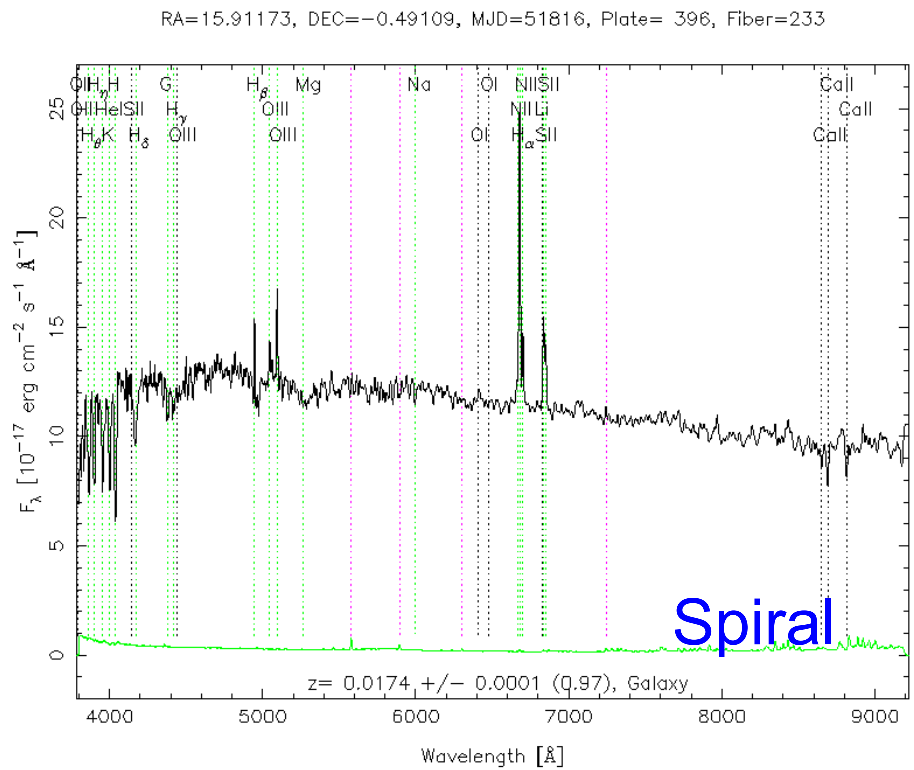

Hertzsprung - Russell Diagram

B stars:

$M \sim 6\ M_{sun}$

$L \sim 1000\ L_{sun}$

$t \sim 0.1$ Gyr

A stars:

$M \sim 2\ M_{sun}$

$L \sim 10\ L_{sun}$

$t \sim 1$ Gyr

G stars:

$M \sim 1\ M_{sun}$

$L \sim L_{sun}$

$t \sim 10$ Gyr

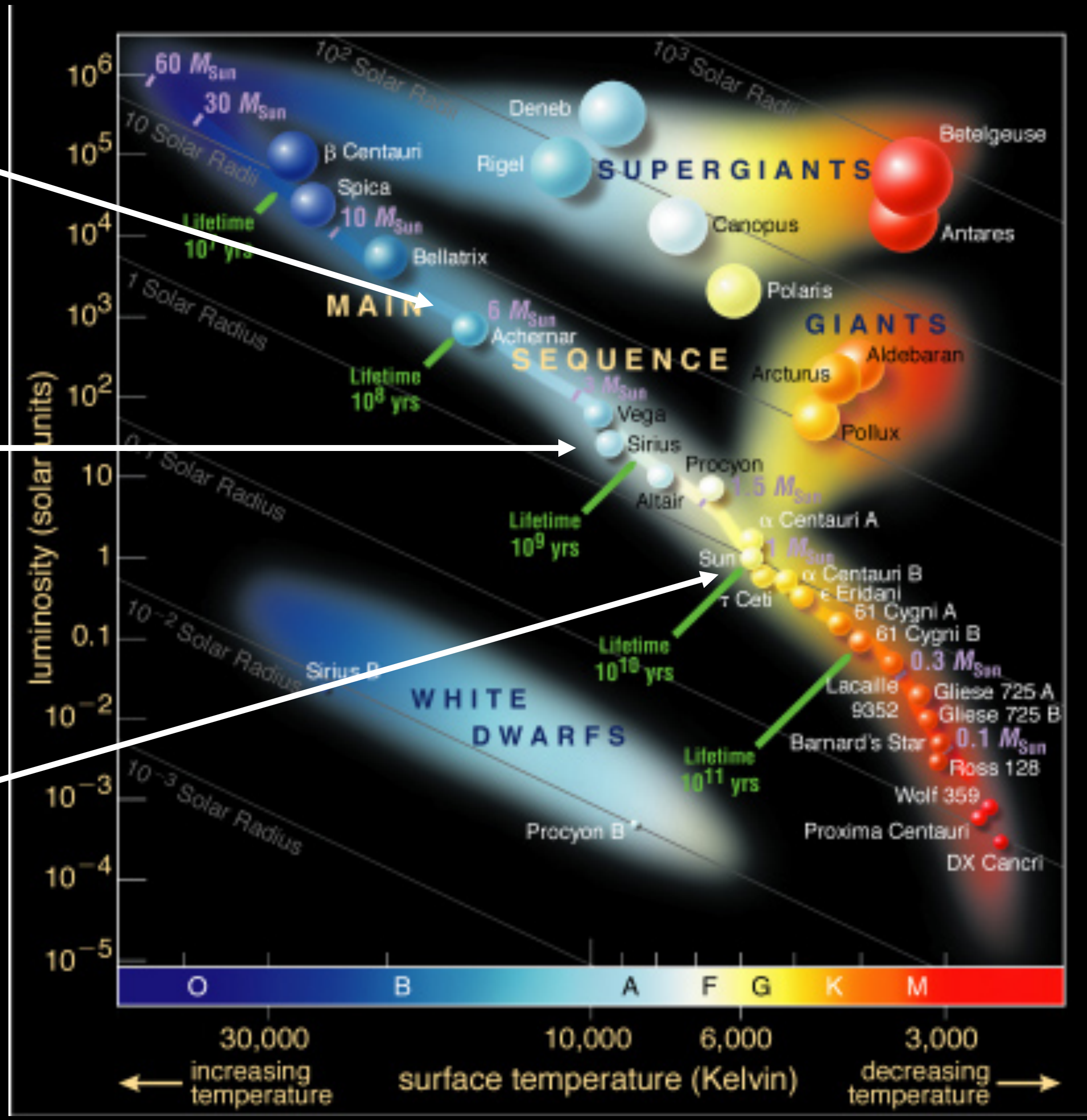

Stellar populations

- Luminosity-mass relation

$$L \approx L_\odot \left(\frac{M}{M_\odot} \right)^{3.5}$$

- Lifetime on the Main Sequence

$$t \approx \frac{f \varepsilon M c^2}{L}$$

$\varepsilon = 0.07\%$ 4H → He

$f \sim 0.1$ Fraction of total mass in core

$$t \approx 10\mathrm{Gyr} \left(\frac{M}{M_\odot} \right)^{-2.5}$$

10Gyr	$1 M_\odot$
1Gyr	$2.5 M_\odot$
0.1Gyr	$6.3 M_\odot$

Stellar populations

- Initial mass function

$$\frac{dN}{dM} = \text{const} \times M^{-\alpha}$$

Salpeter: α=2.35

Scalo , Kroupa: flattens below $1M_{sun}$

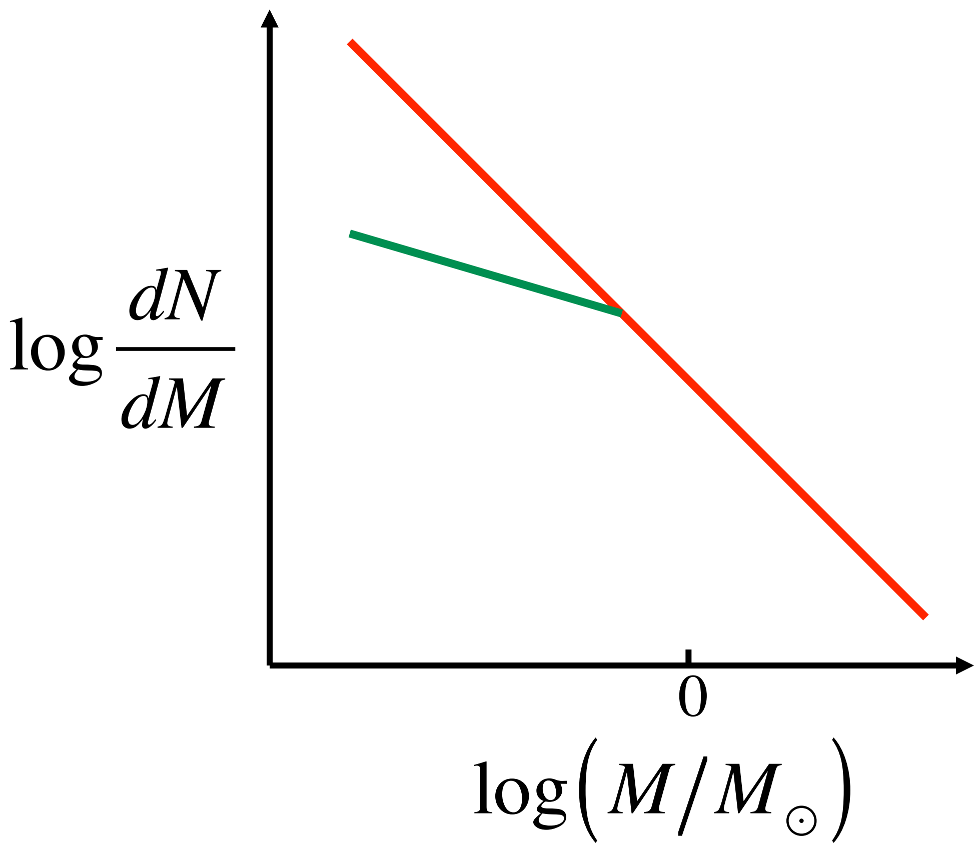

Stellar populations

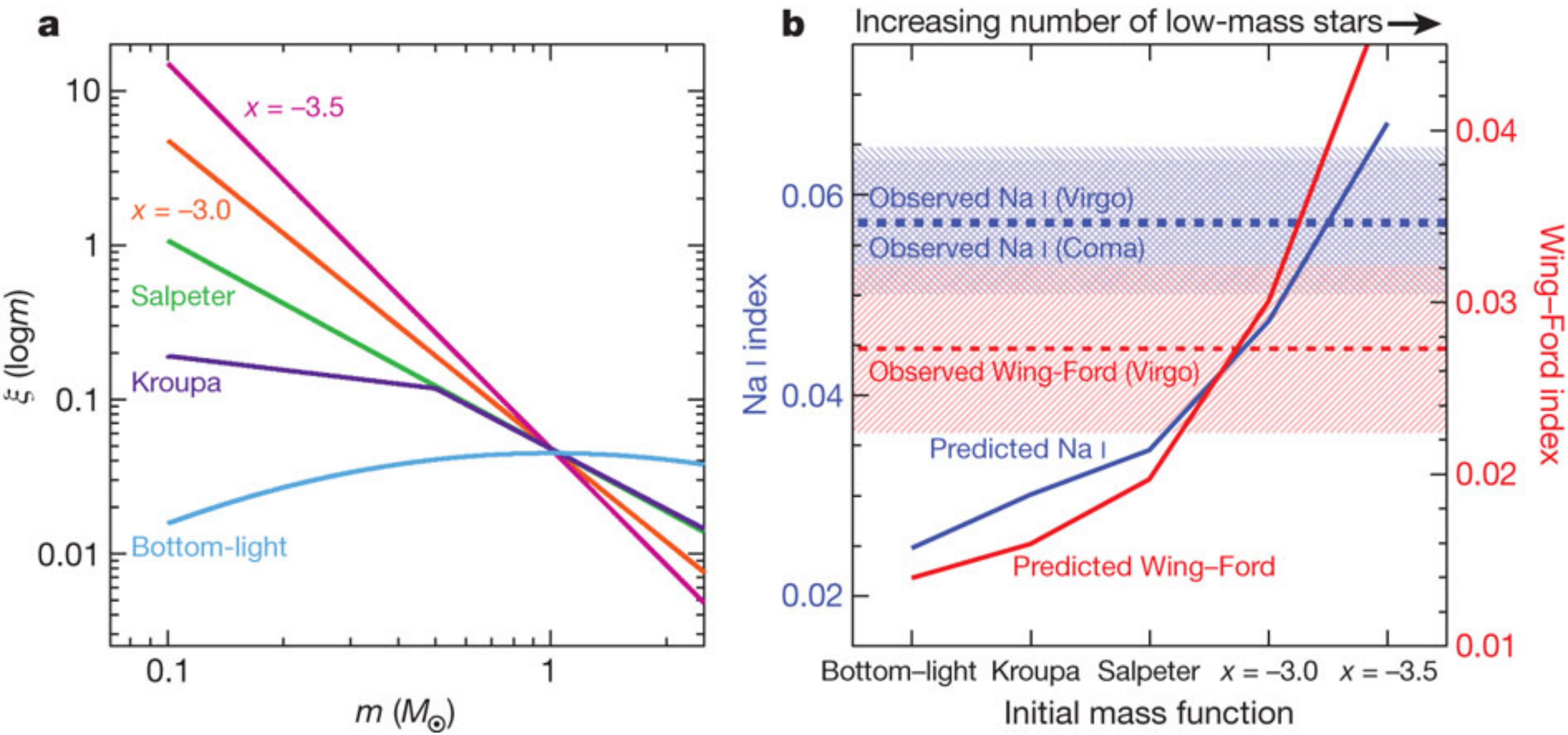

Van Dokkum & Conroy (2010)

Stellar populations

- Fraction of **number** of stars of different masses

$$N_{\text{tot}}\left(M : M_1 \rightarrow M_2\right) = \int_{M_1}^{M_2} \frac{dN}{dM}\, dM$$

$$= \text{const} \times \int_{M_1}^{M_2} M^{-2.35}\, dM$$

$$= \text{const} \times \left(M_2^{-1.35} - M_1^{-1.35}\right)$$

Number of stars that live <0.1Gyr:	0.27%
Number of stars that live <1Gyr:	0.95%
Number of stars that live <10Gyr:	3.30%

Stellar populations

- **Fraction of light from stars of different masses**

$$L_{\text{tot}}\left(M : M_1 \rightarrow M_2\right) = \int_{M_1}^{M_2} L\left(M\right)\frac{dN}{dM}dM$$

$$= \text{const} \times \int_{M_1}^{M_2} M^{3.5} M^{-2.35}\, dM$$

$$= \text{const} \times \int_{M_1}^{M_2} M^{1.15}\, dM = \text{const} \times \left(M_2^{2.15} - M_1^{2.15}\right)$$

Luminosity of stars that live <0.1Gyr:	99.74%
Luminosity of stars that live <1Gyr:	99.96%
Luminosity of stars that live <10Gyr:	99.99%

Stellar populations

- Fraction of **mass** from stars of different masses

$$M_{\text{tot}}\left(M : M_1 \rightarrow M_2\right) = \int_{M_1}^{M_2} M \frac{dN}{dM} dM$$

$$= \text{const} \times \int_{M_1}^{M_2} M \cdot M^{-2.35} \, dM$$

$$= \text{const} \times \int_{M_1}^{M_2} M^{-1.35} \, dM = \text{const} \times \left(M_2^{-0.35} - M_1^{-0.35}\right)$$

Mass of stars that live <0.1Gyr:	14.66%
Mass of stars that live <1Gyr:	23.69%
Mass of stars that live <10Gyr:	36.04%

The evolution of a stellar population

At $t = t_0$, a new stellar population is formed

The evolution of a stellar population

100 Myr later

The evolution of a stellar population

At t = t_1, star formation shuts off

100 Myr later

The evolution of a stellar population

100 Myr later

The evolution of a stellar population

1 Gyr later

The evolution of a stellar population

Once star formation turns off in a galaxy:

- Its luminosity decreases with time
- Its color gets redder with time
- It's spectrum looks more like that of low mass stars

This is called "Passive Evolution", i.e., involves no new star formation.

The evolution of a stellar population

Galaxy luminosity also depends on the total mass of the galaxy (i.e., total number of stars)

Color, however, does not

Galaxy color is thus an age indicator
Red galaxies are old
Blue galaxies are young

Color changes fast at first, and not much past 1Gyr
It is thus not a very *good* age indicator.

It is a much better star formation history indicator:
Red galaxies haven't formed new stars in the past Gyr
Blue galaxies are still forming stars

Determining distance

<u>Standard candle</u>

$$d = \left(\frac{L}{4\pi f} \right)^{\frac{1}{2}}$$

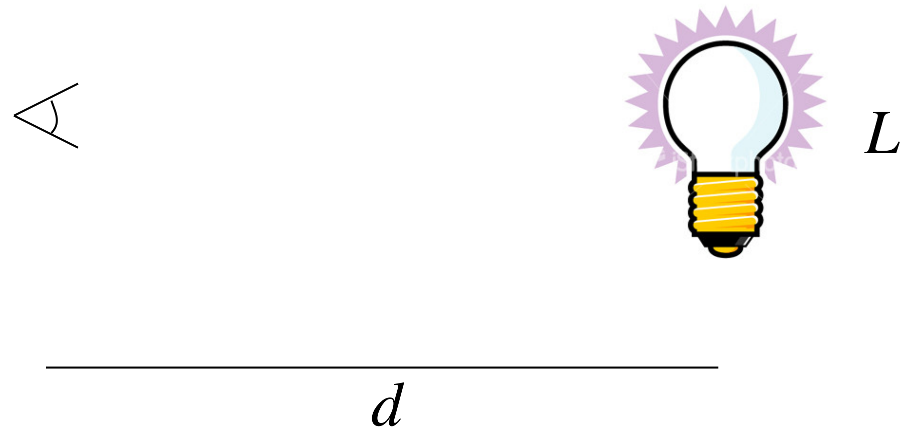

<u>Standard ruler</u>

$$d = \frac{R}{\theta}$$

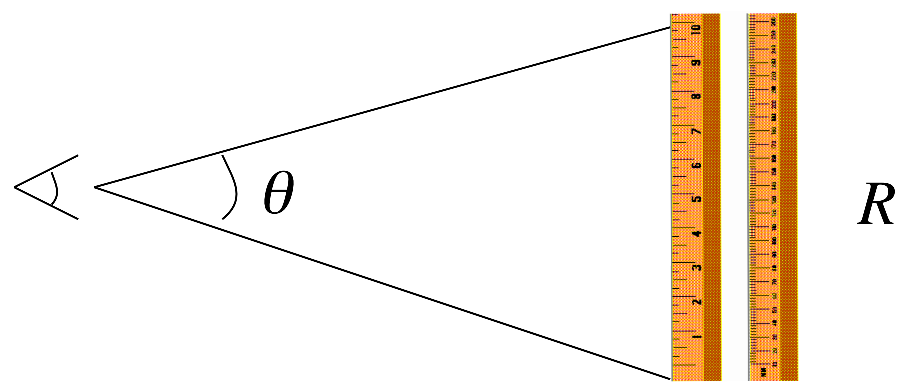

Determining distance: Parallax

RULER

$$\tan\pi = \frac{R}{d} \approx \pi$$

$$R = 1AU = 1.5\times10^{13}\,cm$$

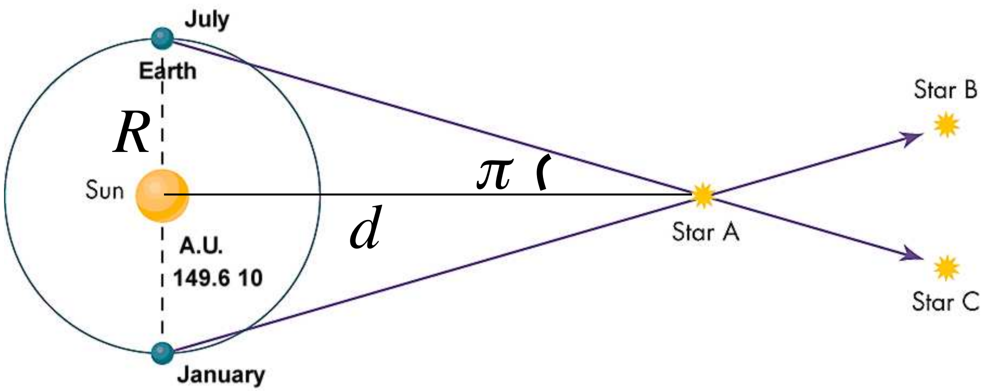

Define new distance unit: parsec (**par**allax-**sec**ond)

$$1pc = \frac{1AU}{\tan(1'')} = 206{,}265AU = 3.26ly$$

$$\left(\frac{d}{1pc}\right) = \frac{1}{\pi''}$$

Determining distance: Parallax

Determining distance: Parallax

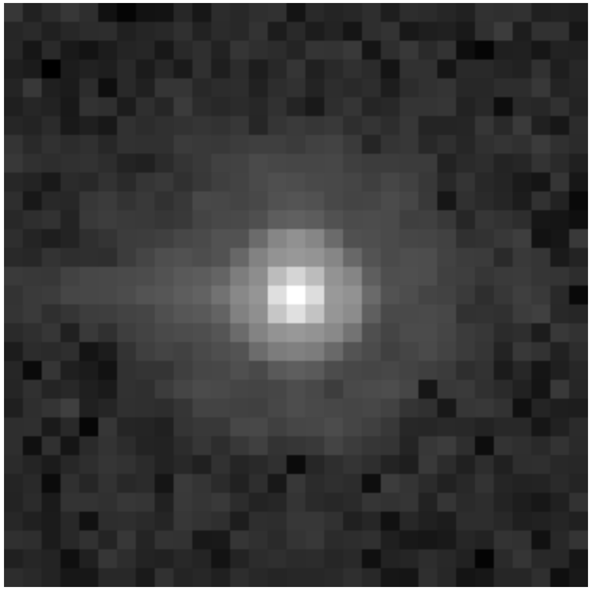

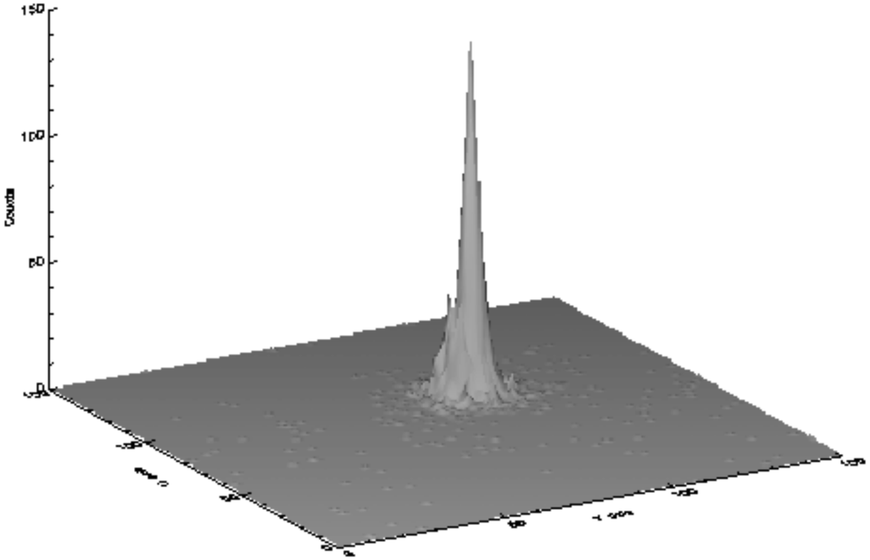

Point spread function (PSF)

Determining distance: Parallax

Need high angular precision to probe far away stars.

$$\frac{\sigma_d}{d} = \frac{\sigma_\pi}{\pi} = d\sigma_\pi \rightarrow d = \left(\frac{\sigma_d}{d}\right)\frac{1}{\sigma_\pi}$$

e.g., to get 10% distance errors

$$d_{\max} = \frac{0.1}{\sigma_\pi}$$

Mission	Dates	σ_π	d_{max}
Earth telescope		~ 0.1 as	1 pc
Hipparcos	1989-1993	~ 1 mas	100 pc
Gaia	2013-2018	~ 20 μas	5 Kpc
SIM	cancelled	~ 4 μas	25 Kpc

Astrometry Missions

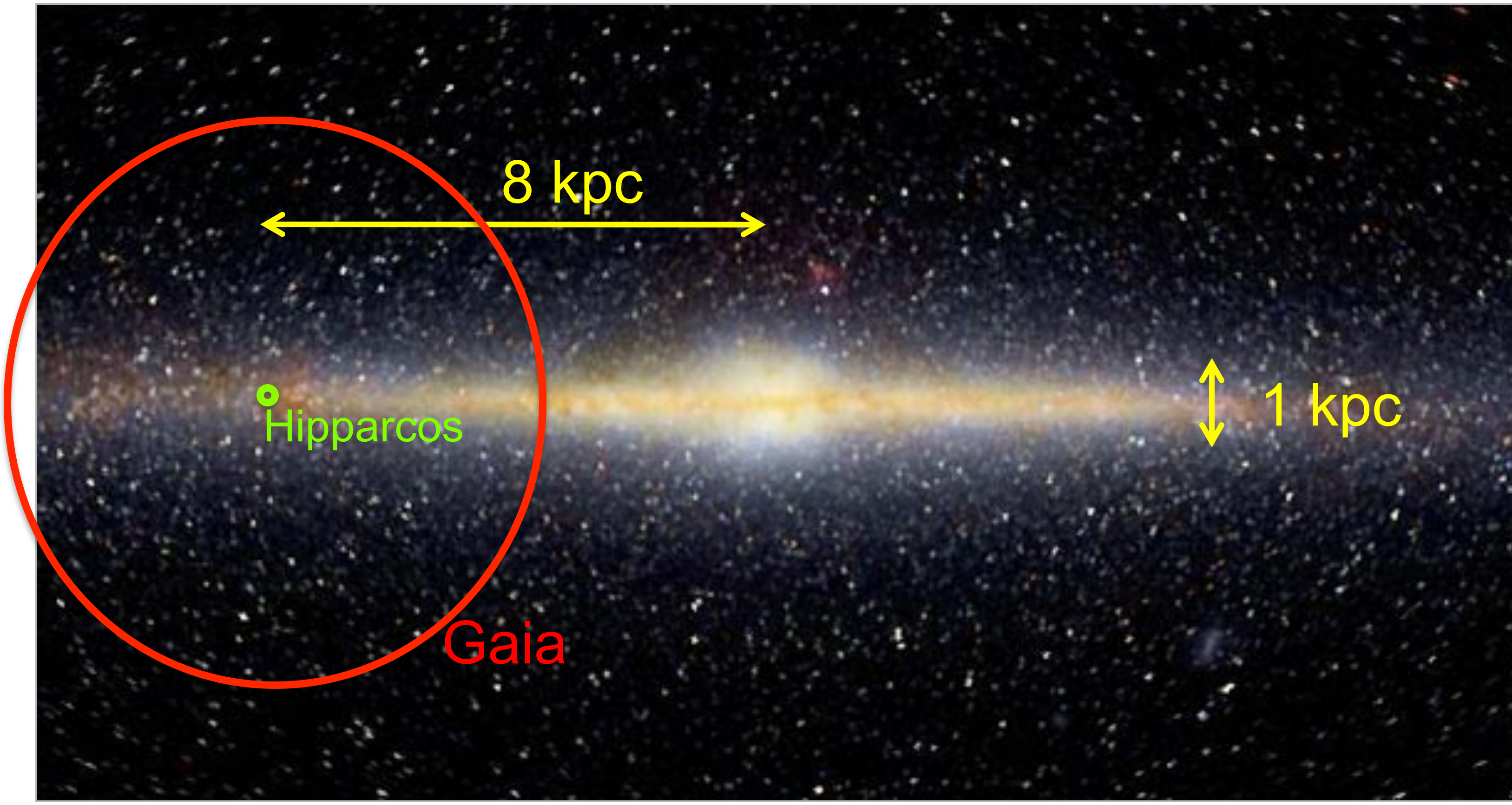

Determining distance: variable stars

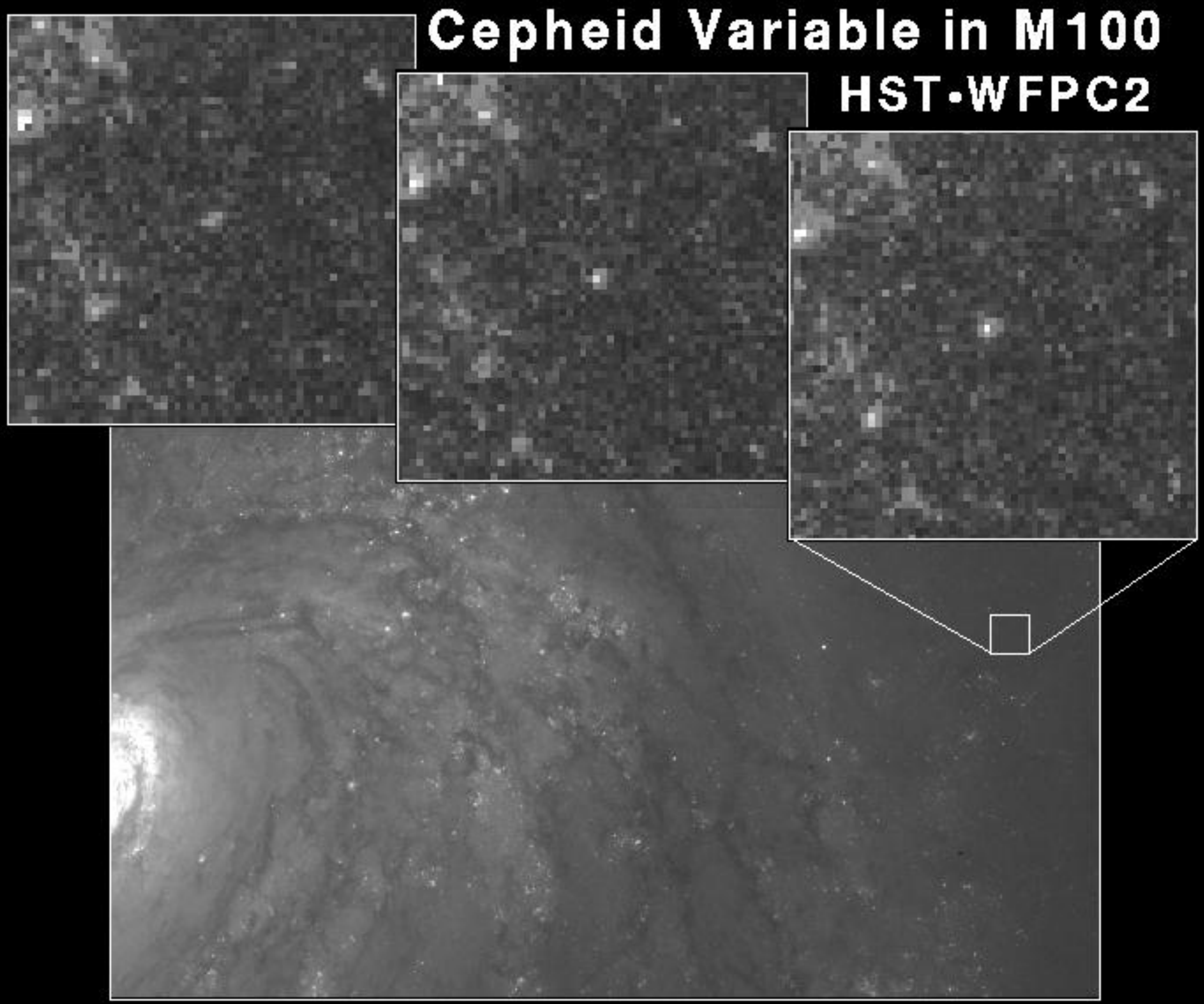

Determining distance: variable stars

<u>Cepheid variables</u>:
Pop I giants, M ~ 5-20 M_{sun}

Pulsation due to feedback loop:

An increase in T
➔ HeIII (doubly ionized He)
➔ high opacity
➔ radiation can't escape
➔ even higher T and P
➔ atmosphere expands
➔ low T
➔ HeII (singly ionized He)
➔ low opacity
➔ atmosphere contracts
➔ rinse and repeat…

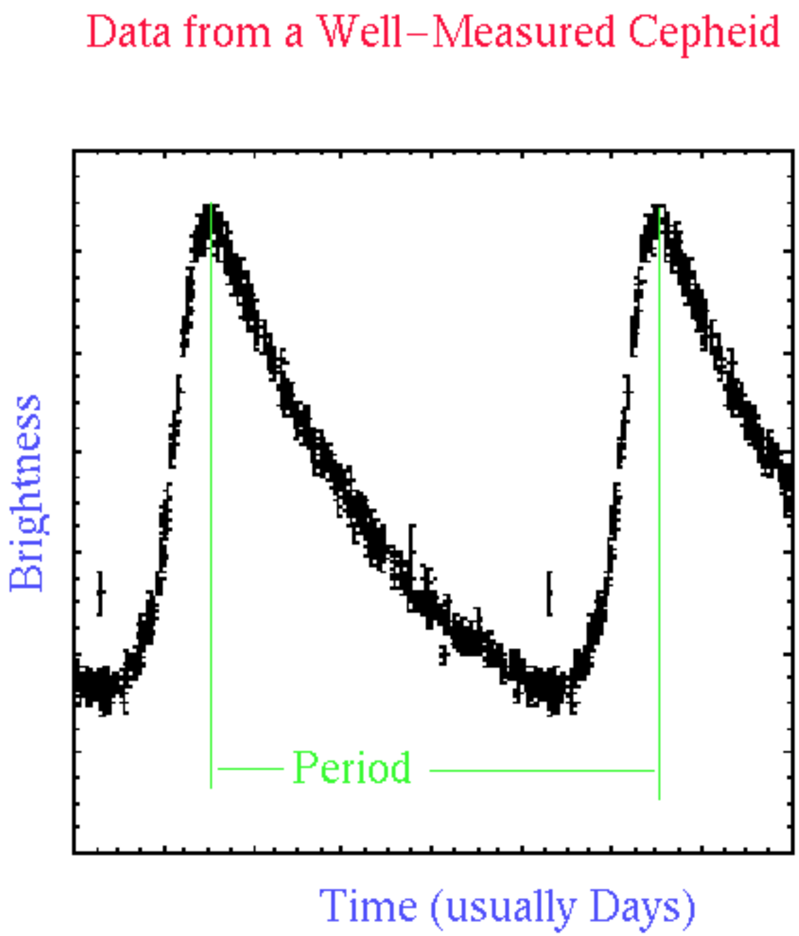

Determining distance: variable stars

RR-Lyrae variables:

Pop II dwarfs, $M \sim 0.5\ M_{sun}$

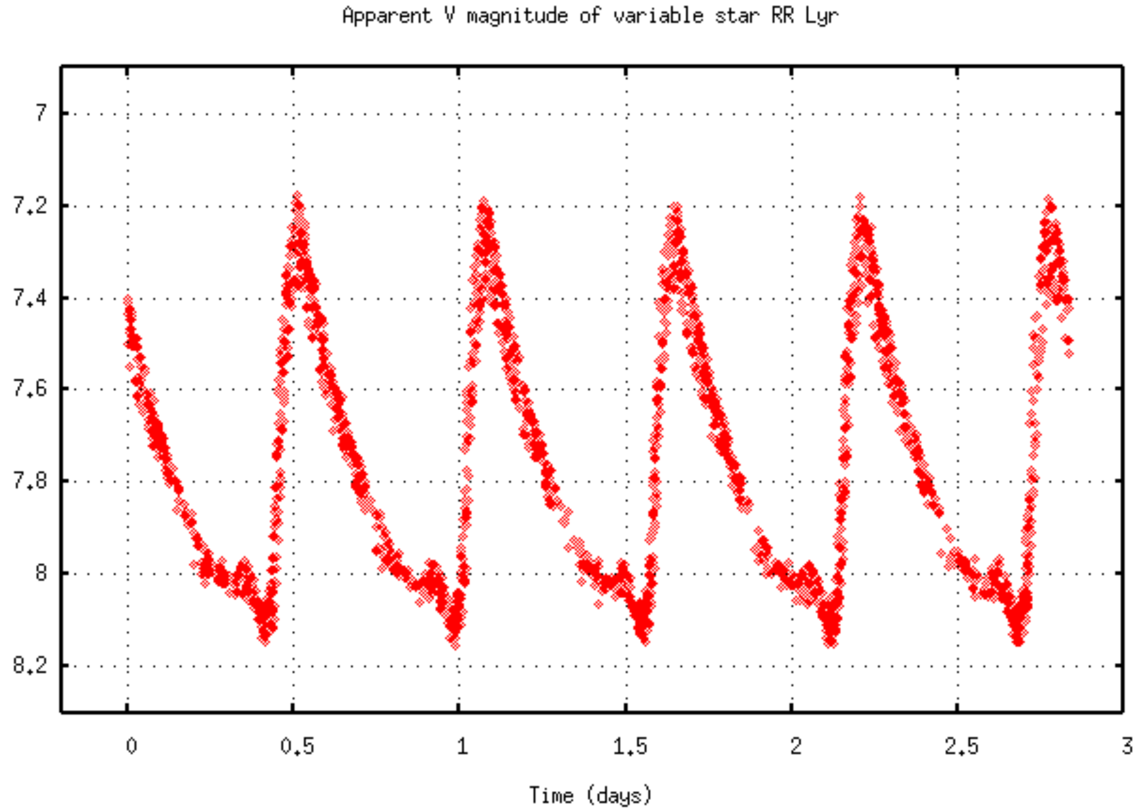

Determining distance: variable stars

CANDLE

Variable stars have a tight period-luminosity relation

- Measure lightcurves: flux(t)
- Get period P
- From P-L relation, get L
- Use L to get distance

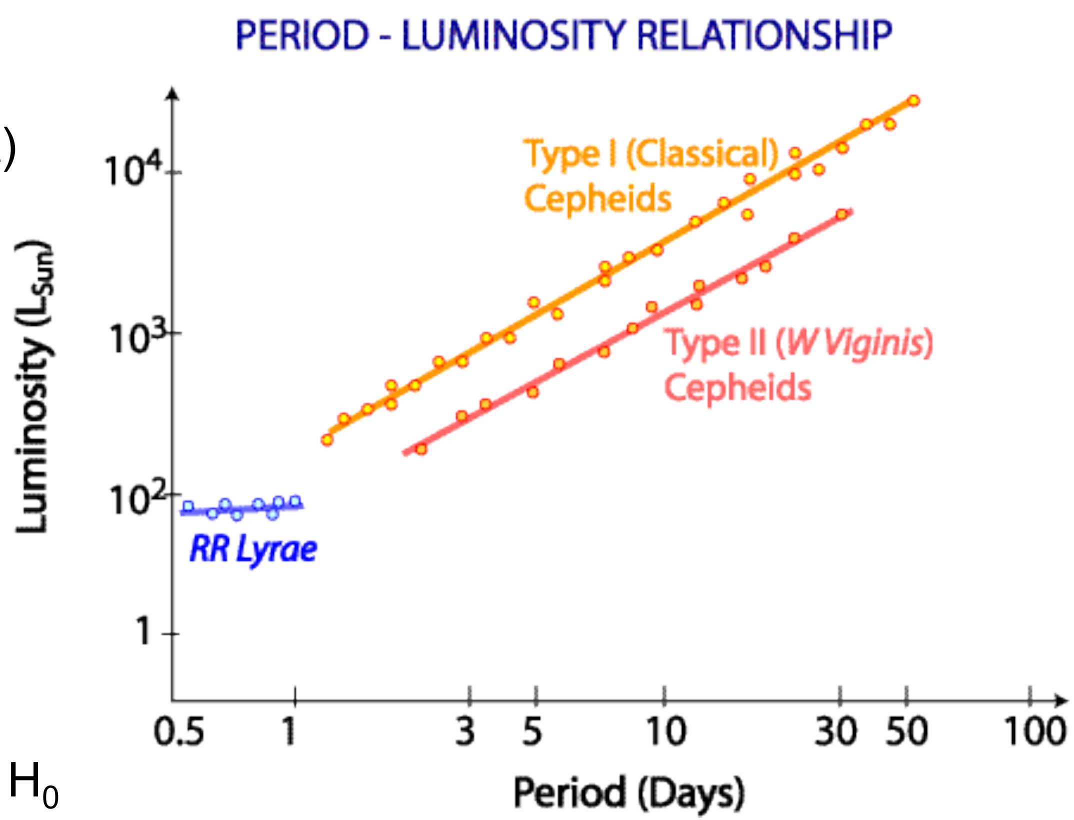

Very powerful method. Cepheids can be seen very far away. Used to measure H_0

P-L relation is calibrated on local variables with parallax measurements

Determining distance: Tully-Fisher

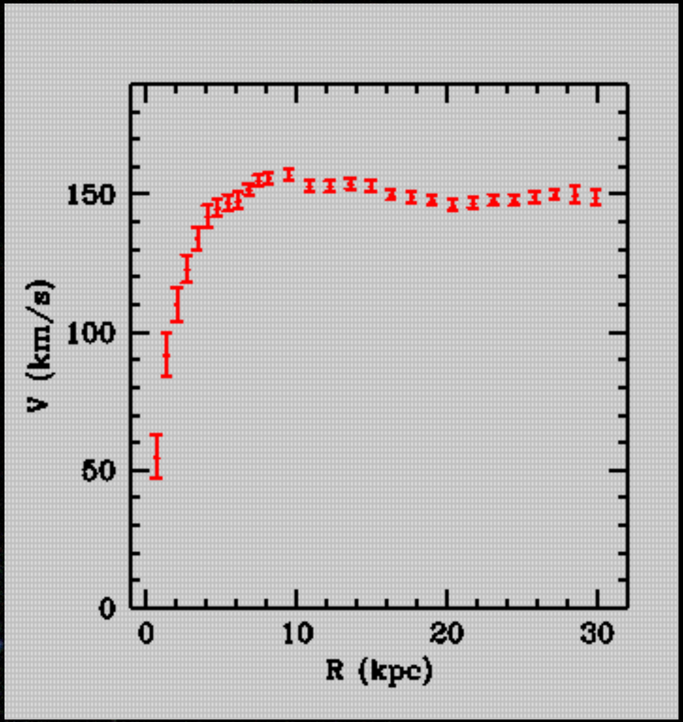

NGC 3198 rotation curve

Determining distance: Tully-Fisher

$$v_{\rm rot}^2 = \frac{Gm(<r)}{r}$$

$$m(<r) = \int_0^r \rho(r) 4\pi r^2 \, dr$$

Flat rotation curve ➔ density profile is a singular isothermal sphere (SIS)

$$\rho(r) = \frac{C}{r^2}$$

$$m(<r) = \int_0^r \frac{C}{r^2} 4\pi r^2 \, dr = 4\pi C r$$

$$v_{\rm rot}^2 = \frac{G 4\pi C r}{r} = 4\pi G C$$

Determining distance: Tully-Fisher

Dark matter halo definition:

$$M = \frac{4}{3}\pi R^3 \rho(<R)$$
$$= \frac{4}{3}\pi R^3 \Delta_{\rm crit}\bar{\rho}_0$$

$$\Delta_{\rm crit} \approx 200$$

For a SIS density profile:

$$M = 4\pi C R$$

$$4\pi C = \left(\frac{4\pi\Delta_{\rm crit}\bar{\rho}_0}{3}\right)^{1/3} M^{2/3}$$

$$v_{\rm rot}^2 = G\left(\frac{4\pi\Delta_{\rm crit}\bar{\rho}_0}{3}\right)^{1/3} M^{2/3} \rightarrow$$

$$M = \left(\frac{3}{4\pi G^3 \Delta_{\rm crit}\bar{\rho}_0}\right)^{1/2} v_{\rm rot}^3$$

Determining distance: Tully-Fisher

A New Method of Determining Distances to Galaxies

R. Brent Tully[1*] and J. Richard Fisher[2]

[1] Observatoire de Marseille, France

[2] National Radio Astronomy Observatory**, P.O. Box 2, Green Bank, W. Va. 24944, USA

Received July 15, 1975, revised April 26, 1976

Summary. A good correlation between a distance-independent observable, global galaxian H I profile widths, and absolute magnitudes or diameters of galaxies offers a new extragalactic distance tool, as well as potentially being fundamental to an understanding of galactic structure. The relationships are calibrated with members of the Local Group, the M81 group, and the M101 group and have been used to derive distances to the Virgo cluster ($\mu_0 = 30\overset{m}{.}6 \pm 0\overset{m}{.}2$) and the Ursa Major cluster ($\mu_0 = 30\overset{m}{.}5 \pm 0\overset{m}{.}35$). A preliminary estimate of the Hubble constant is $H_0 = 80$ km/s/Mpc.

Key words: galaxies — distances — neutral hydrogen

total mass and t
correlation is prim
systems that have
than later systems
with luminosity, v
This point is im
structure of galax
for the measurem
The basic diff
and presumably th
notice, is that if
extremely well kn
observational sca
tion of little use.
effect in two ways

Determining distance: Tully-Fisher

CANDLE

$$L = C v_{rot}^{\alpha}$$

R. B. Tully and J. R. Fisher: Distances to Galaxies

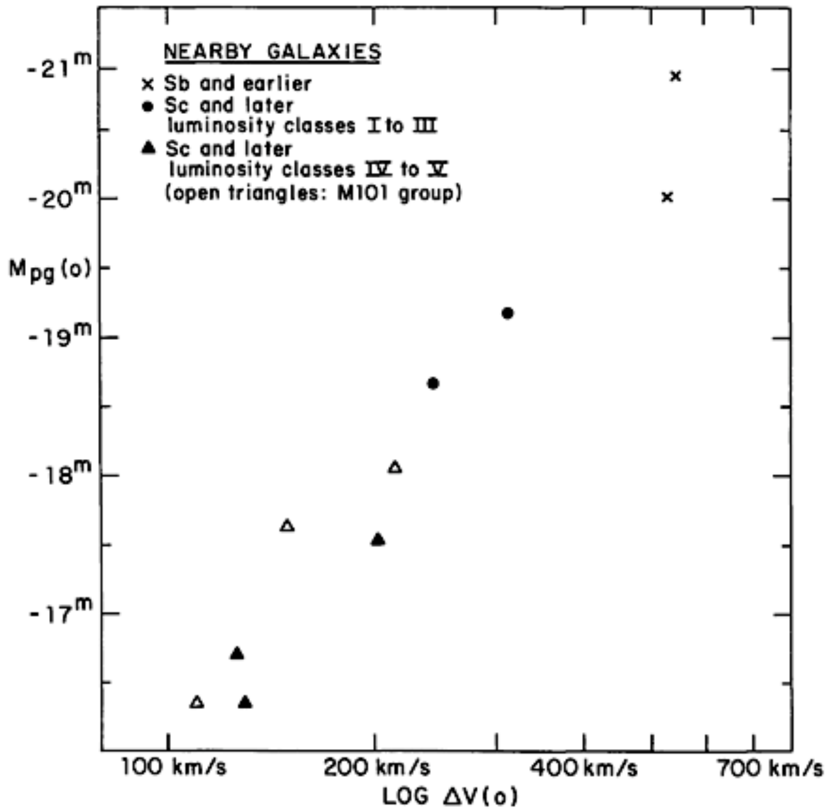

Fig. 1. Absolute magnitude – global profile width relation for nearby galaxies with previously well-determined distances. Crosses are M31 and M81, dots are M33 and NGC 2403, filled triangles are smaller systems in the M81 group and open triangles are smaller systems in the M101 group

Determining distance: Tully-Fisher

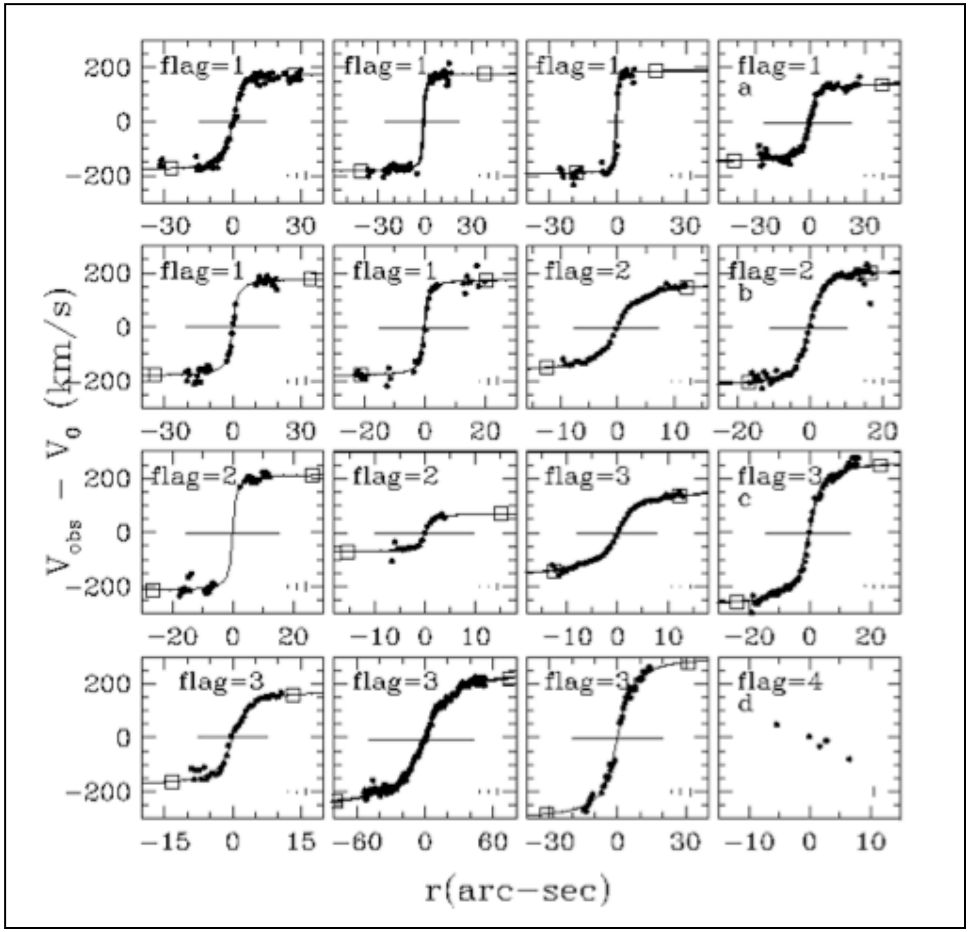

Pizagno et al. (2007)

Determining distance: Tully-Fisher

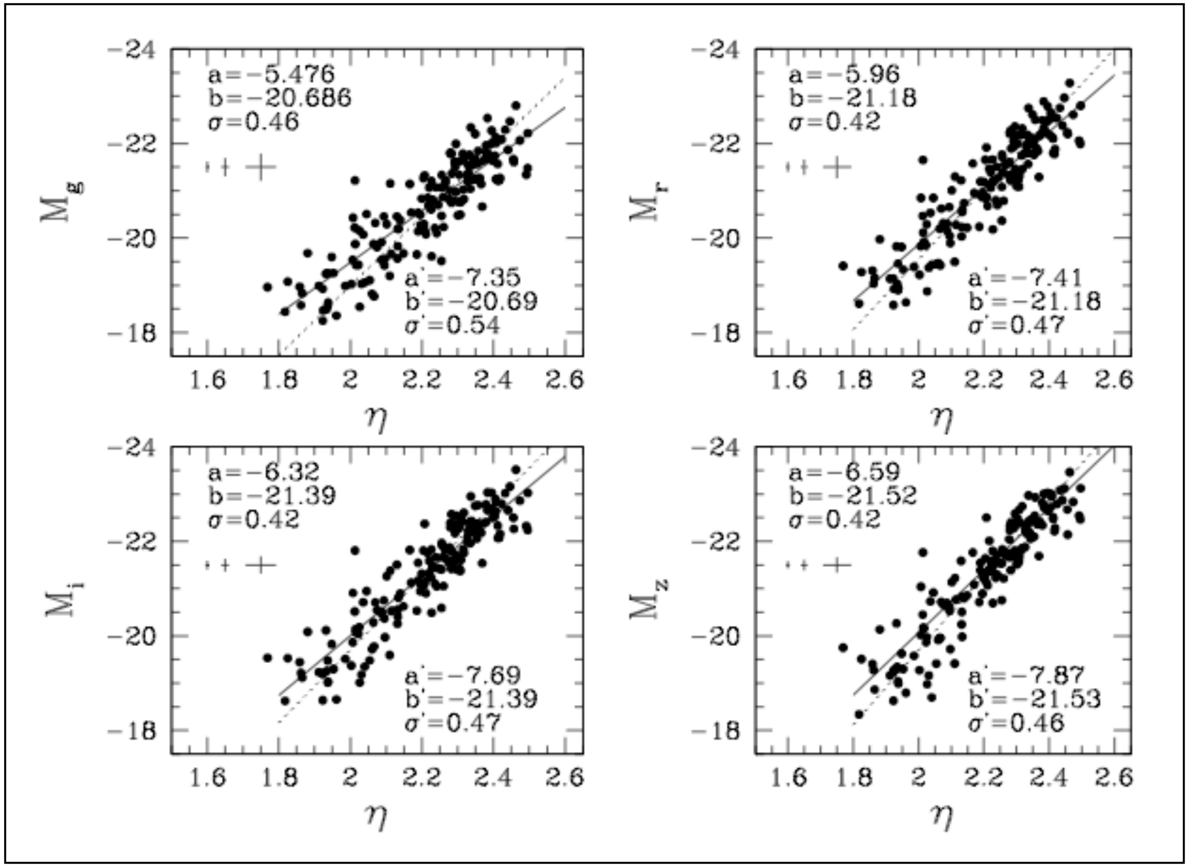

Pizagno et al. (2007)

$$L = C v_{rot}^{\alpha} \rightarrow M_i = a \log v_{rot} + b$$

Determining distance: Faber-Jackson

Determining distance: Faber-Jackson

VELOCITY DISPERSIONS AND MASS-TO-LIGHT RATIOS FOR ELLIPTICAL GALAXIES*

S. M. Faber and Robert E. Jackson
Lick Observatory and Board of Studies in Astronomy and Astrophysics, University of California, Santa Cruz
Received 1975 June 30; revised 1975 August 28

ABSTRACT

Velocity dispersions for 25 galaxies have been measured using conventional and Fourier techniques. The resultant velocity system is probably accurate to 10–15 percent. Internal rms errors are on the order of 10 percent. Using unpublished data of King, we have computed core values of M/L_B. For luminous ellipticals with $M_B < -20$, M/L_B averages $7(H/50\ \mathrm{km\ s^{-1}\ Mpc^{-1}})$, considerably smaller than previous estimates. This value agrees well with M/L_B for early-type spirals, indicating that there is no large discontinuity in M/L_B between ellipticals and early-type spirals. This result is consistent with the observed small color differences between ellipticals and Sa's.

Velocity dispersions increase with luminosity for normal elliptical galaxies of moderate ellipticity. The data also suggest that M/L_B generally increases with luminosity. This conclusion is consistent with predictions based on King's data on core radii and central surface brightness (to be discussed fully in a separate paper). This increase in M/L_B might be due at least in part to the known increase in metal abundance with luminosity for normal elliptical galaxies.

The close correlation between luminosity and dynamical properties for normal ellipticals is further evidence that the ellipticals are very nearly a one-parameter family with total mass as the most important independent variable.

Subject headings: galaxies: internal motions — galaxies: stellar content

Determining distance: Faber-Jackson

CANDLE

$$L = C\sigma_v^{\alpha}$$

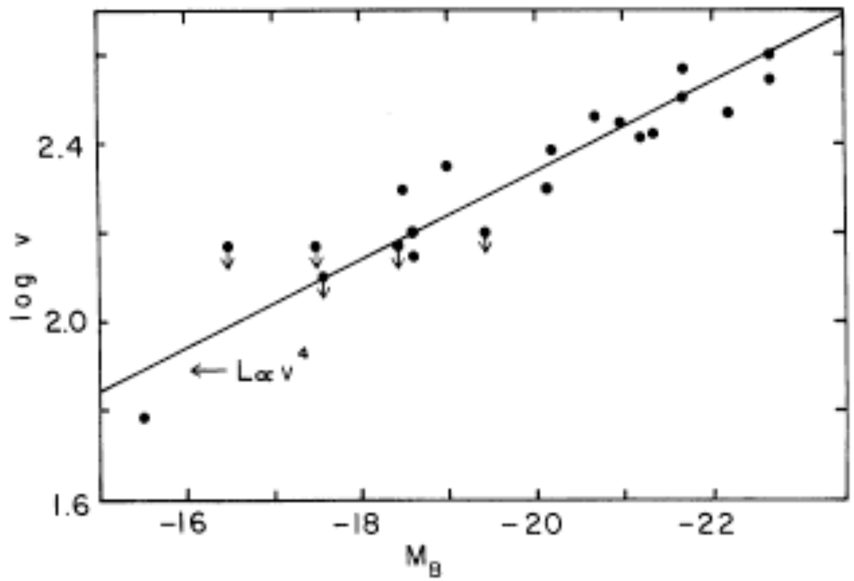

FIG. 16.—Line-of-sight velocity dispersions versus absolute magnitude from Table 1. The point with smallest velocity corresponds to M32, for which the velocity dispersion (60 km s^{-1}) was taken from Richstone and Sargent (1972).

Determining distance: Fundamental Plane

SPECTROSCOPY AND PHOTOMETRY OF ELLIPTICAL GALAXIES. I. A NEW DISTANCE ESTIMATOR[1]

ALAN DRESSLER
Mount Wilson and Las Campanas Observatories of the Carnegie Institution of Washington

DONALD LYNDEN-BELL
Institute of Astronomy, The Observatories, Cambridge

DAVID BURSTEIN
Physics Department, Arizona State University

ROGER L. DAVIES
Kitt Peak National Observatory, National Optical Astronomy Observatories

S. M. FABER
Lick Observatory and Board of Studies in Astronomy and Astrophysics, University of California, Santa Cruz

R. J. TERLEVICH
Royal Greenwich Observatory

AND

GARY WEGNER
Department of Physics and Astronomy, Dartmouth College

Received 1986 May 7; accepted 1986 July 24

ABSTRACT

Kinematic and photometric data have been obtained for 97 elliptical galaxies in six rich clusters. These data show that ellipticals describe a plane in three dimensions which, when viewed edge-on, projects a smaller scatter than the Faber-Jackson relationship between luminosity and velocity dispersion σ. This plane is approximately given by $L \propto \sigma^{8/3}\Sigma_e^{-3/5}$, where Σ_e is the surface brightness within the effective radius A_e, or equivalently $A_e \propto \sigma^{1.325}\Sigma_e^{-0.825}$.

We present a new photometric parameter D_n, the diameter which encloses an integrated surface brightness Σ, that correlates as well with σ as any linear combination of L (or A_e) and Σ. Thus, D_n effectively replaces two parameters with one. We show that the D_n-σ relation can be used to find relative distances of ellipticals with rms errors of $\lesssim 25\%$ for a single galaxy and $\lesssim 10\%$ for rich clusters. This accuracy is comparable to that of the infrared Tully-Fisher method used to find distances to spiral galaxies.

Determining distance: Fundamental Plane

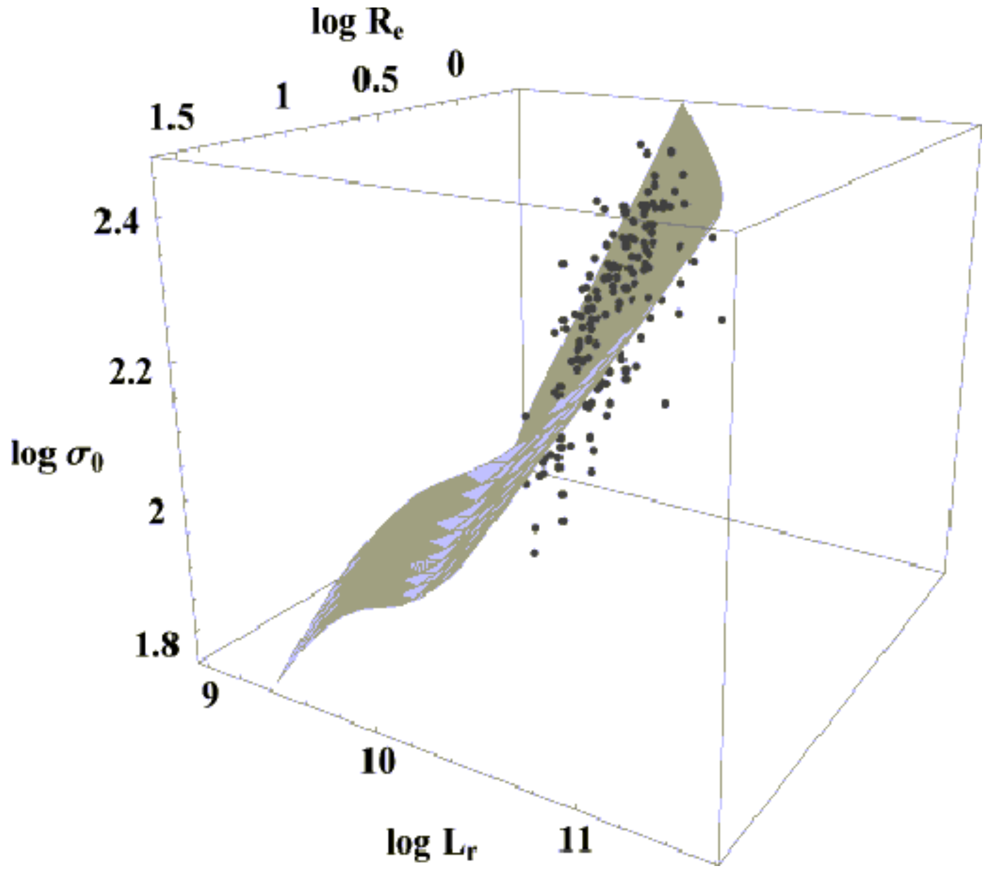

Determining distance: Fundamental Plane

RULER

$$L = C\sigma_v^{\alpha} I^{\beta}$$

$$R = S\sigma_v^{\gamma} \times I^{\delta}$$

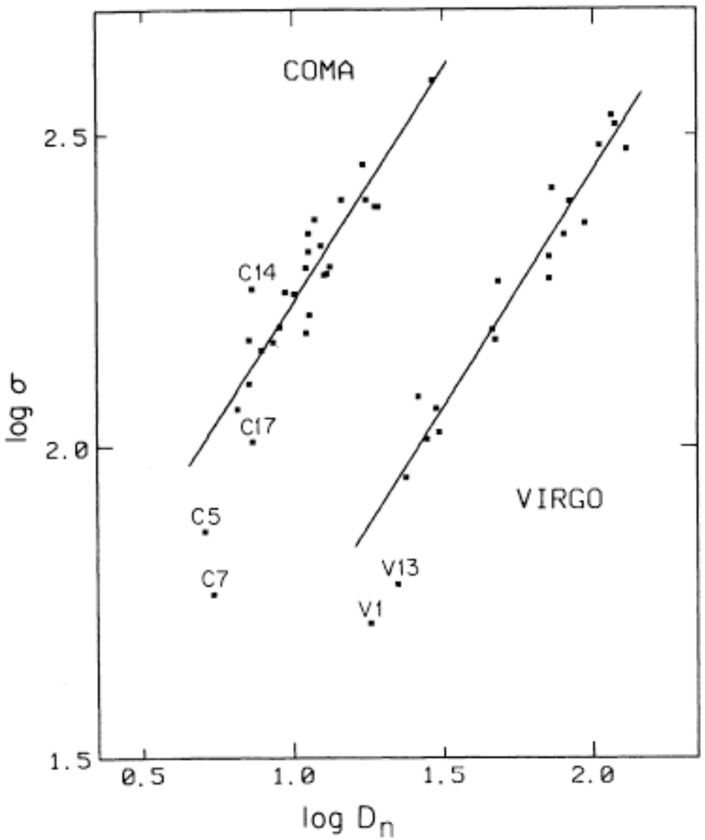

FIG. 1b

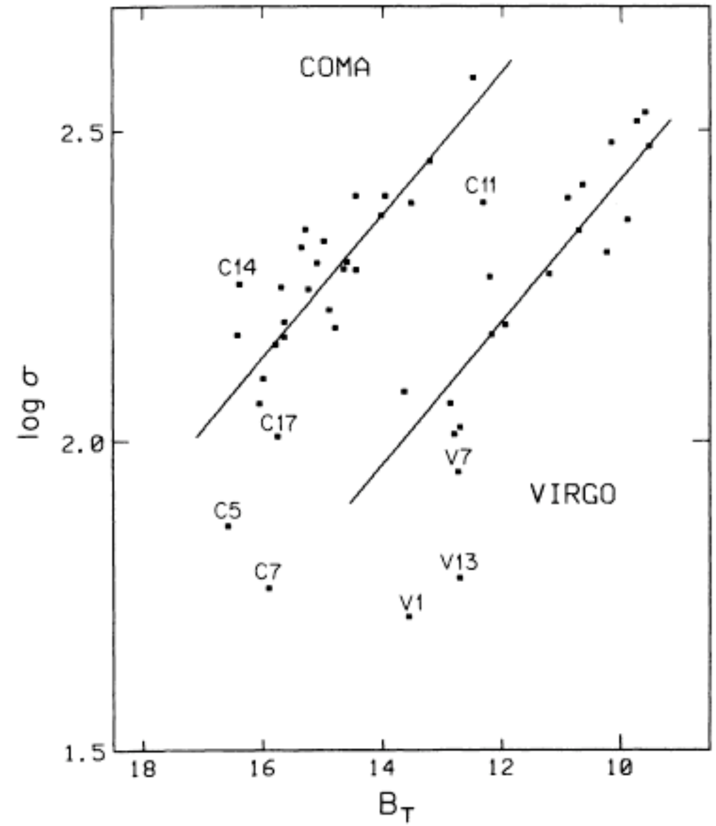

FIG. 1a

FIG. 1.—(a) B_T, the total blue magnitude, vs. log σ, the central velocity dispersion, for ellipticals in the Coma and Virgo clusters. These are the variables of the Faber-Jackson relationship. The lines log $\sigma = -0.114B_T + C$, where $C = 3.561$ for Virgo and $C = 3.960$ for Coma, are best median fits, as described in the text. The rms scatters in B_T from these lines are 0.57 mag for Virgo and 0.69 mag for Coma. (b) log D_n, the diameter within which the integrated blue surface brightness is 20.75 B mag arcsec^{-2}, vs. log σ for the same galaxies. The horizontal scales correspond to a factor of 10 in distance in both figures. The lines log $\sigma = 0.750$ log $D_n + C$, where $C = 0.934$ for Virgo and $C = 1.475$ for Coma, are best median fits. The rms scatter in log D_n is 0.059 for Virgo and 0.072 for Coma, a factor of 2 smaller scatter than with the Faber-Jackson relationship.

Determining distance: Fundamental Plane

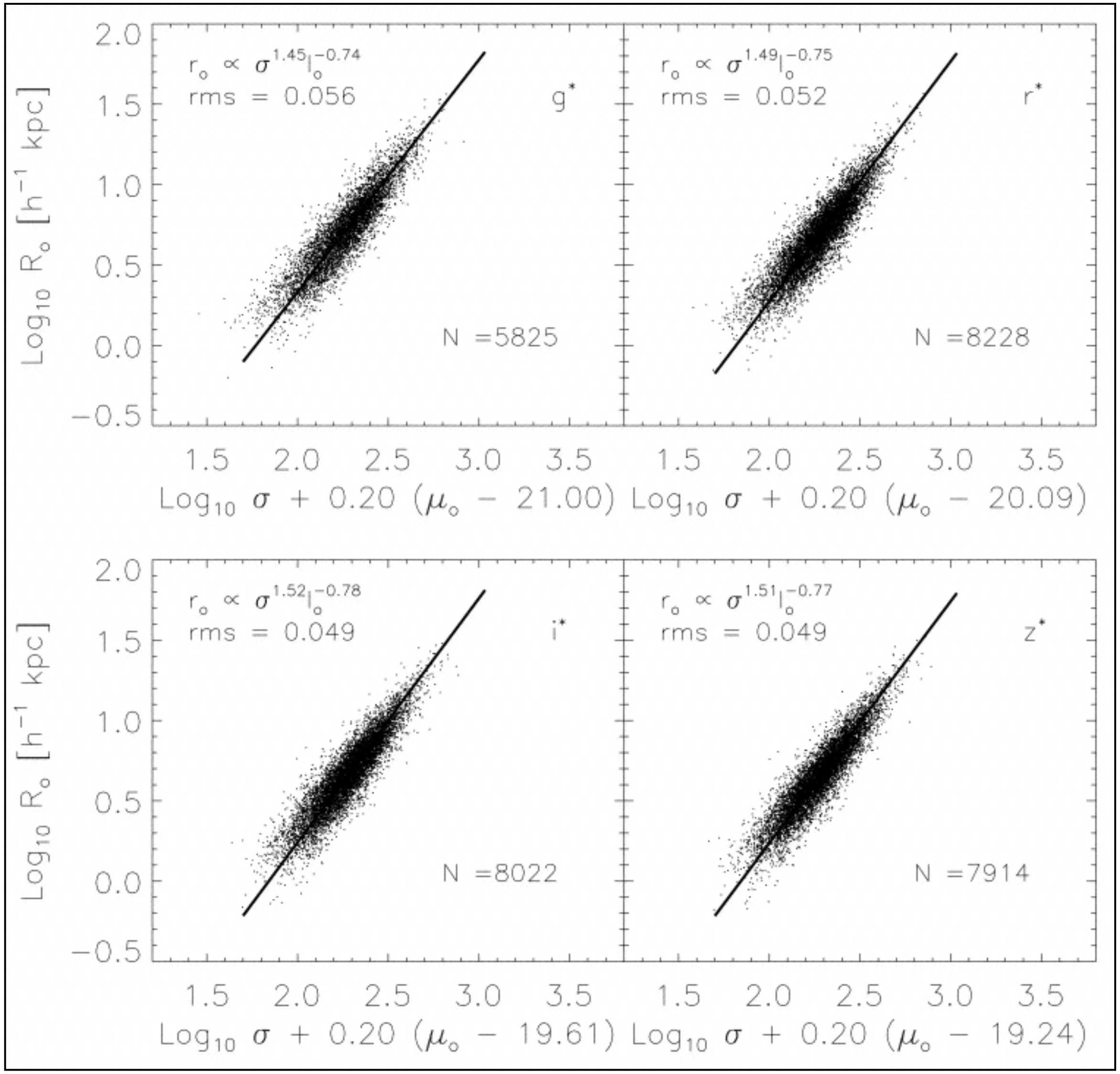

Bernardi et al. (2007)

Determining distance: Surface Brightness Fluctuations

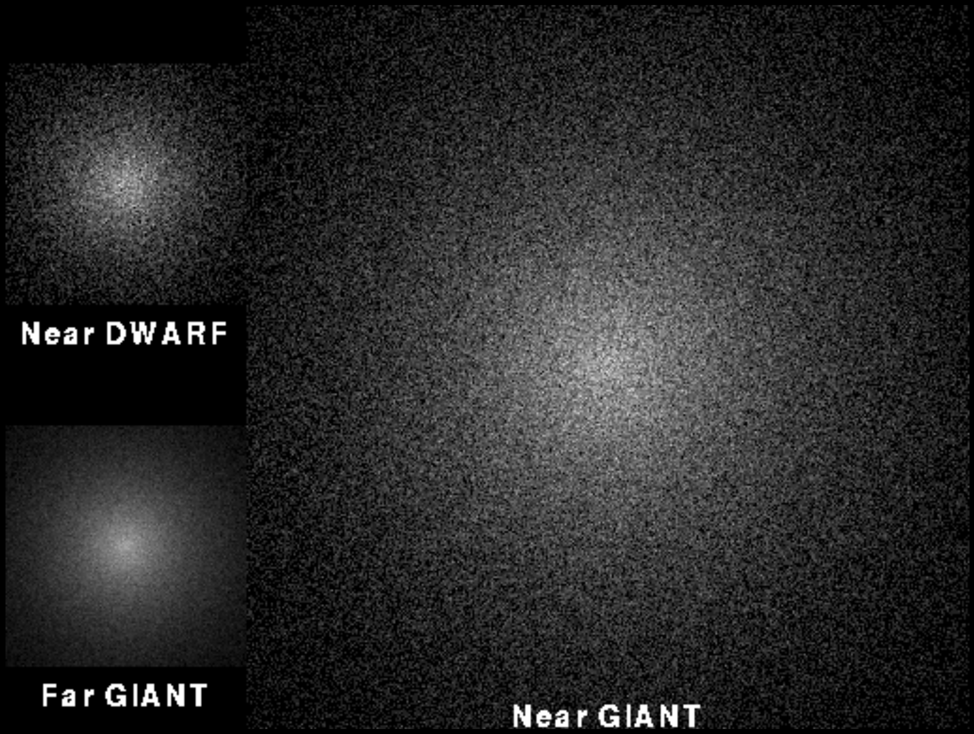

Determining distance: Surface Brightness Fluctuations

THE ASTRONOMICAL JOURNAL VOLUME 96, NUMBER 3 SEPTEMBER 1988

A NEW TECHNIQUE FOR MEASURING EXTRAGALACTIC DISTANCES[a]

JOHN TONRY[b]
Physics Department, Massachusetts Institute of Technology, Cambridge, Massachusetts 02139

DONALD P. SCHNEIDER
Institute for Advanced Study, Princeton, New Jersey 08540
Received 26 April 1988

ABSTRACT

We describe a relatively direct technique of determining extragalactic distances. The method relies on measuring the luminosity fluctuations that arise from the counting statistics of the stars contributing the flux in each pixel of a high-signal-to-noise CCD image of a galaxy. The amplitude of these fluctuations is inversely proportional to the distance of the galaxy. This approach bypasses most of the successive stages of calibration required in the traditional extragalactic distance ladder; the only serious drawback to this method is that it requires an accurate knowledge of the bright end ($M_V \leqslant 3$) of the luminosity function. Potentially, this method can produce accurate distances of elliptical galaxies and spiral bulges at distances out to about 20 Mpc. In this paper, we explain how to calculate the value of the fluctuations, taking into account various sources of contamination and the effects of finite spatial resolution, and we demonstrate, via simulations and CCD images of M32 and N3379, the feasibility and limitations of this technique.

Determining distance: Surface Brightness Fluctuations

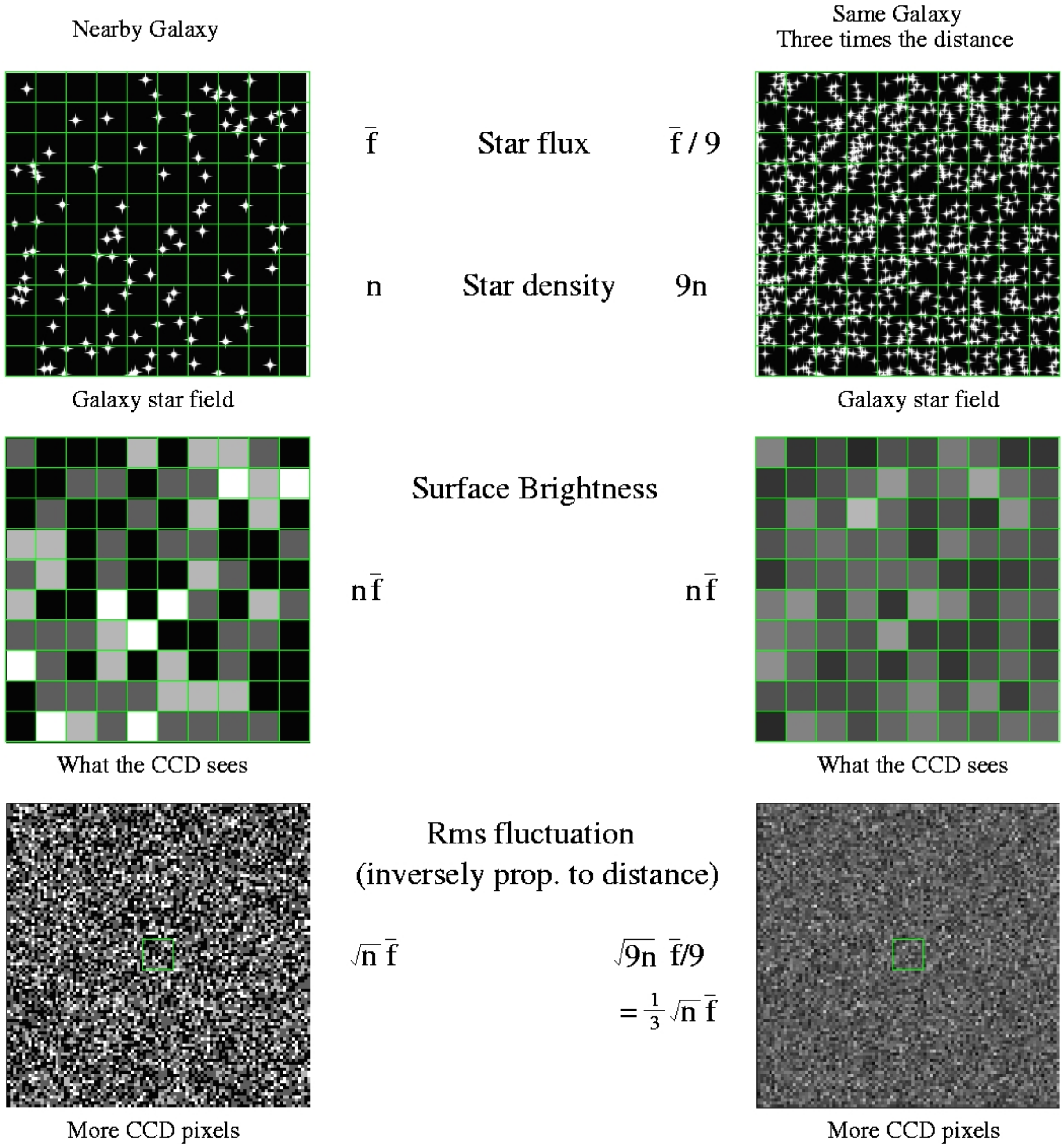

Determining distance: Surface Brightness Fluctuations

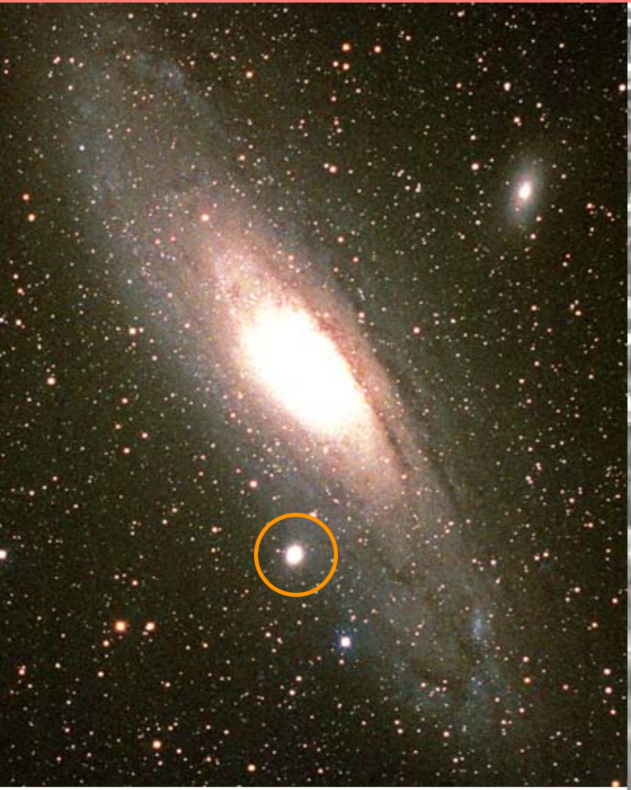

M32

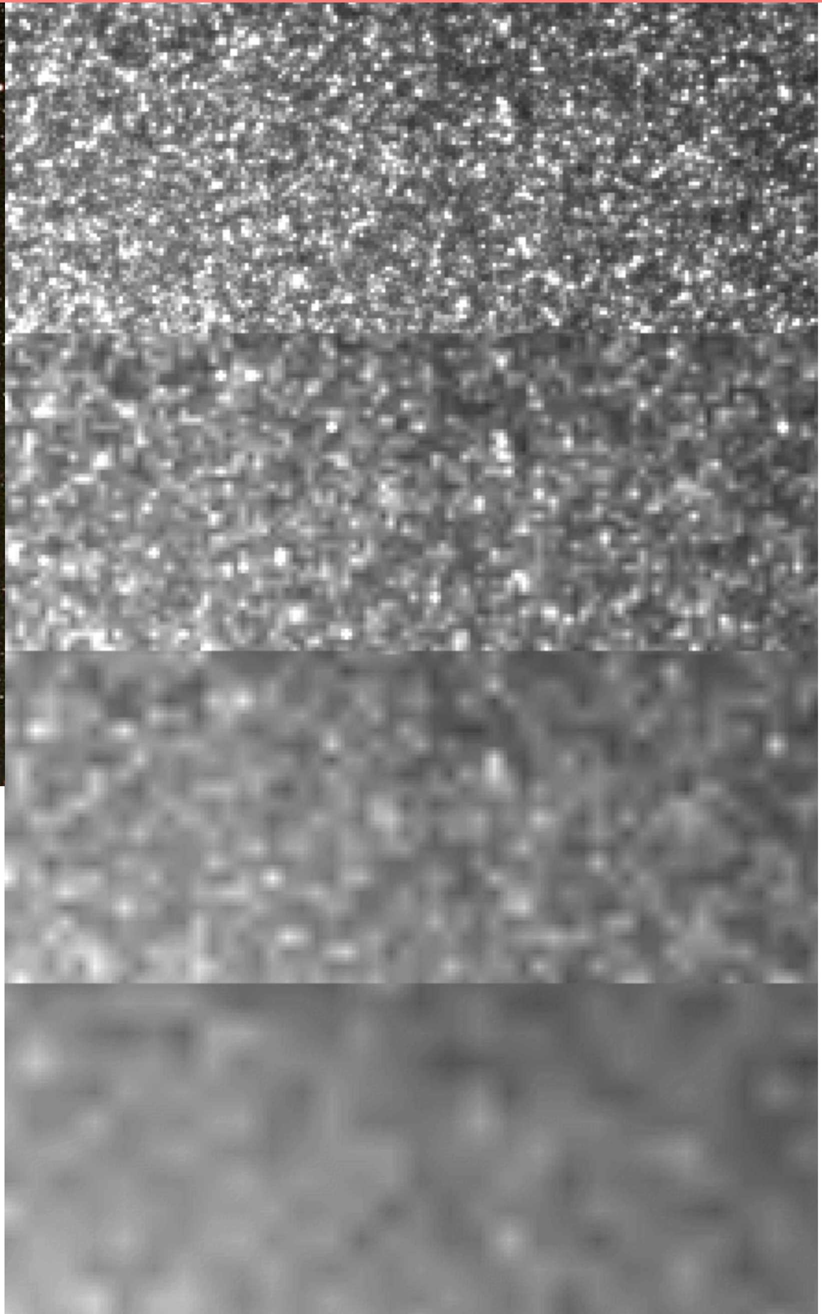

d=0.76 Mpc

x2

x4

x8

Determining distance: Supernovae type Ia

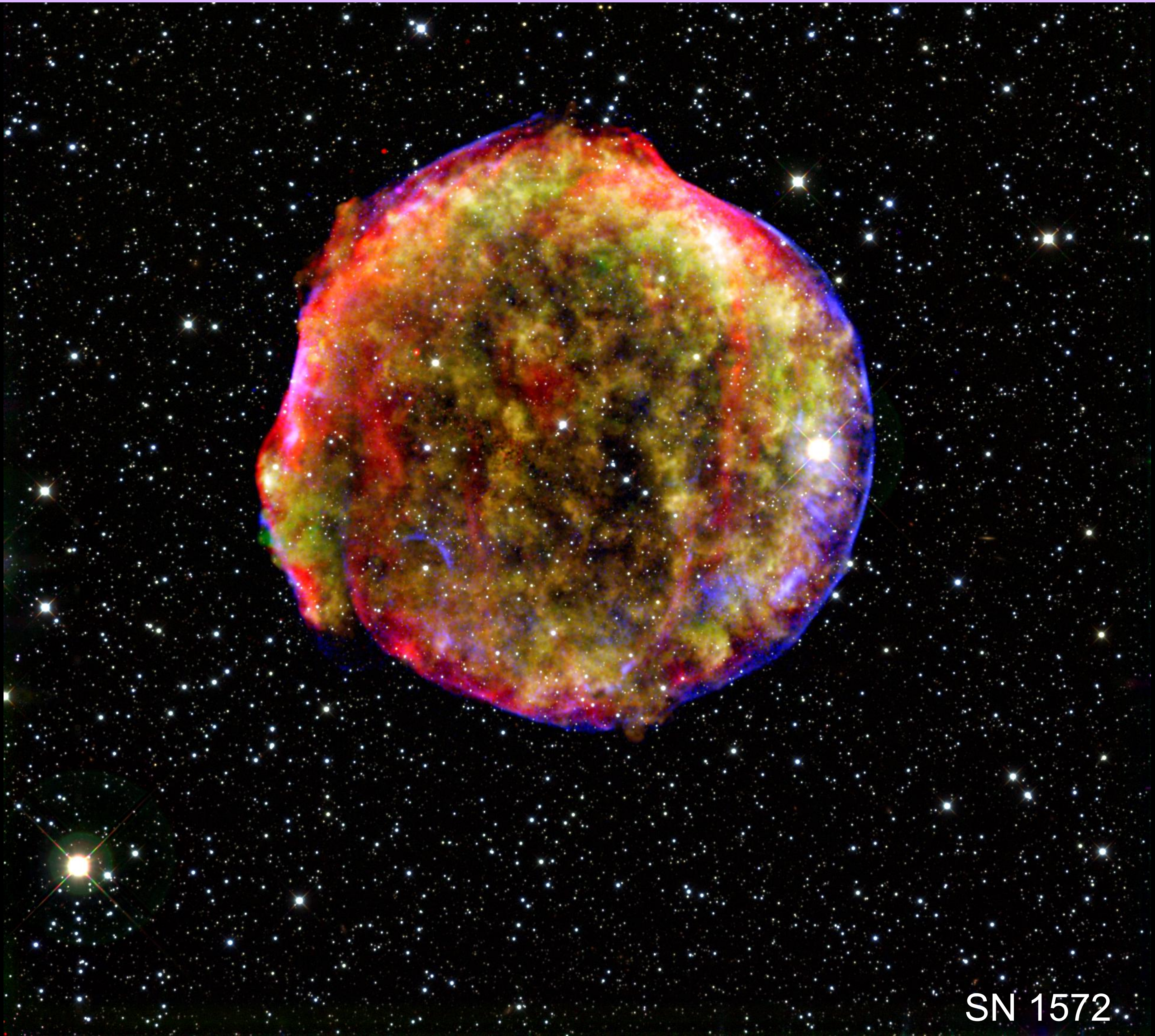

Determining distance: Supernovae type Ia

White dwarfs are made of a C/O core that is supported by electron degeneracy pressure.

WD masses cannot exceed 1.4 M_{sun} (Chandrasekhar limit) because then gravity wins.

WD that accretes enough mass to surpass this limit, collapses, heats up, and fuses all its C/O in a fast runaway reaction.

The energy released unbinds the star. SN Ia

SNIa have similar peak luminosities because they come from the same mass star.

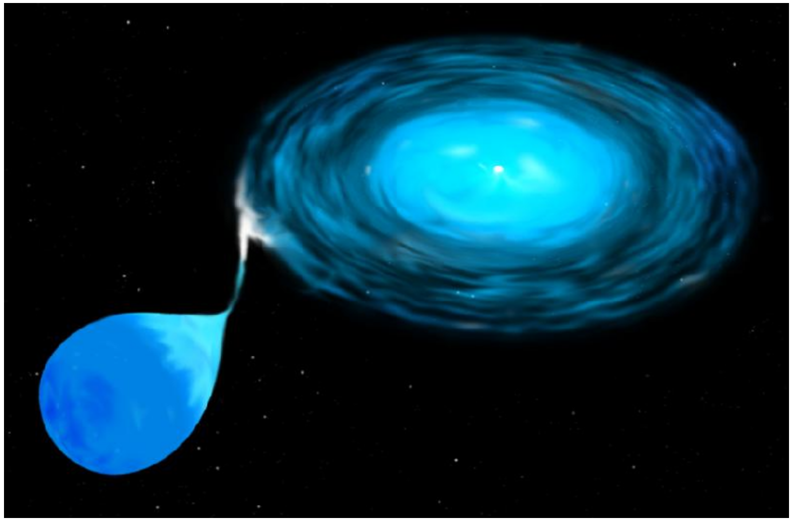

Determining distance: Supernovae type Ia

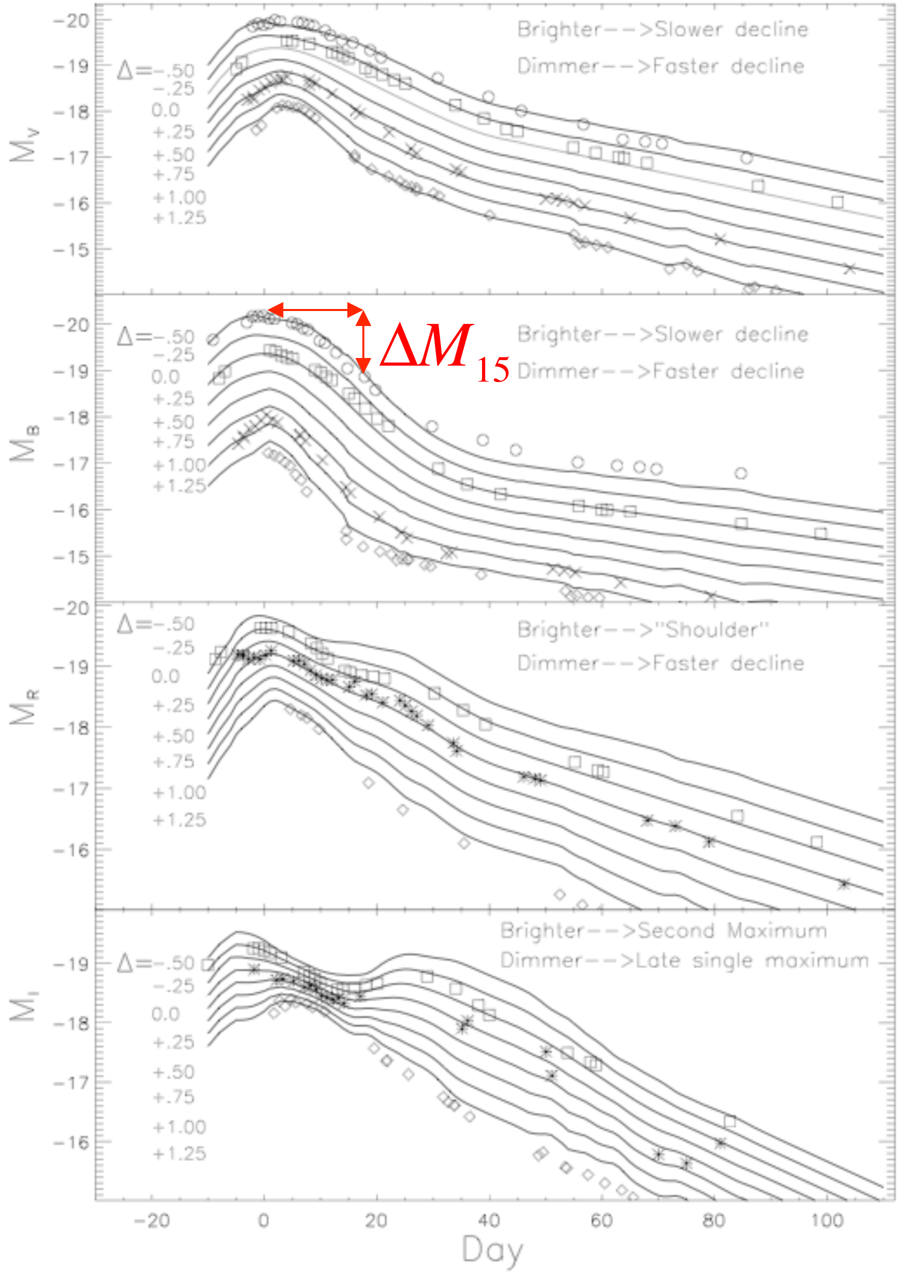

Riess et al. (2006)

Determining distance: Supernovae type Ia

CANDLE

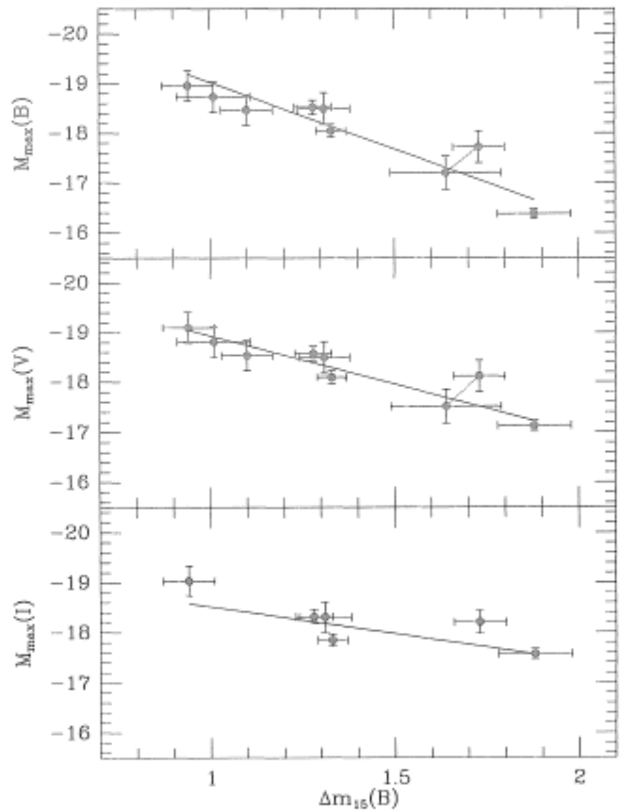

FIG. 1.—Decline rate–peak luminosity relation for the nine best-observed SN Ia's. Absolute magnitudes in *B*, *V*, and *I* are plotted vs. $\Delta m_{15}(B)$, which measures the amount in magnitudes that the *B* light curve drops during the first 15 days following maximum.

Phillips (1993)

The Distance Ladder

Method	Scatter	Reach	Systematics
Parallax	~d	<1 kpc	
Cepheids	5-10%	30 Mpc	Metallicity
SBF	5-10%	50 Mpc	Stellar LF
Tully-Fisher	10-20%	>100 Mpc	Mass-to-light
FP/D_n-sigma	10-20%	>100 Mpc	Kinematics
SN Ia	5-10%	>1000 Mpc	Dust

The Distance Ladder

SN Ia

Tully-Fisher/D_n-sigma

Cepheids/RR Lyrae

parallax

Redshift

We can measure galaxies' radial velocity using the Doppler effect.

Doppler effect: when an object is moving away from (or toward) us, the frequency of light that we see from it is shifted.

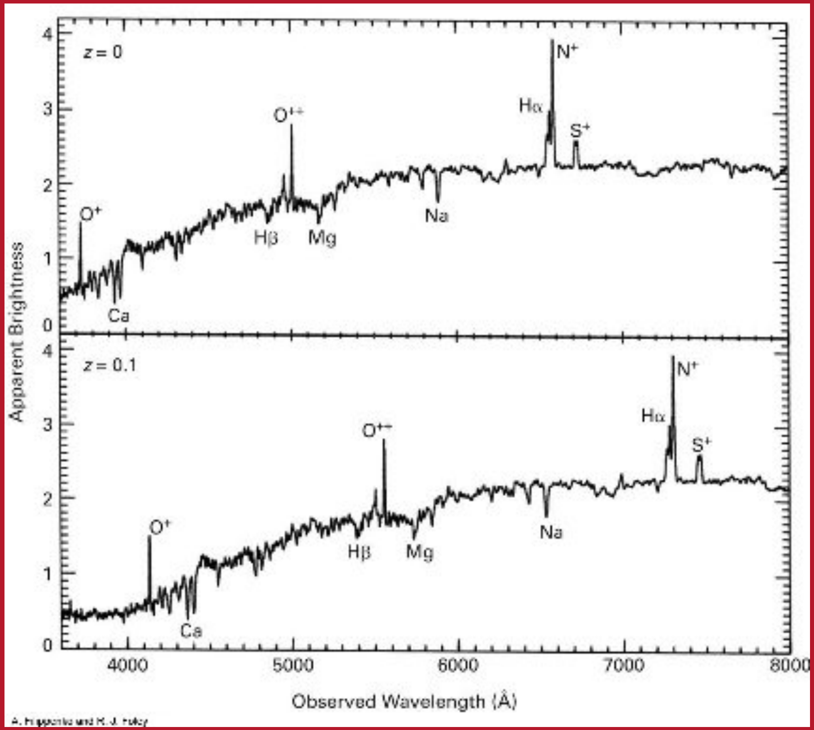

galaxy spectrum ➔ Doppler shift (redshift) ➔ radial velocity

Redshift

$$z = \frac{\lambda_{\text{obs}} - \lambda_{\text{emit}}}{\lambda_{\text{emit}}}$$

Relativistic Doppler Effect

$$1 + z = \sqrt{\frac{1 + v_r / c}{1 - v_r / c}}$$

$$z \simeq \frac{v_r}{c}$$

Hubble Law

corrected for solar motion. The result, 745 km./sec. for a distance of 1.4×10^6 parsecs, falls between the two previous solutions and indicates a value for K of 530 as against the proposed value, 500 km./sec.

Secondly, the scatter of the individual nebulae can be examined by assuming the relation between distances and velocities as previously determined. Distances can then be calculated from the velocities corrected for solar motion, and absolute magnitudes can be derived from the apparent magnitudes. The results are given in table 2 and may be compared with the distribution of absolute magnitudes among the nebulae in table 1, whose distances are derived from other criteria. N. G. C. 404

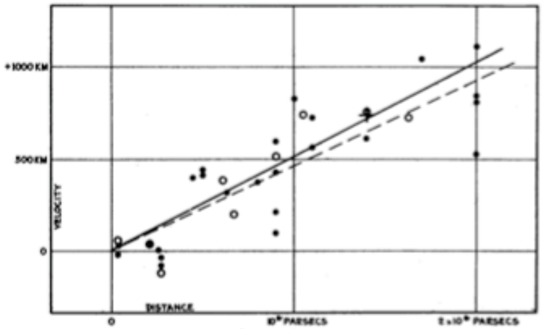

FIGURE 1

Velocity-Distance Relation among Extra-Galactic Nebulae.

Radial velocities, corrected for solar motion, are plotted against distances estimated from involved stars and mean luminosities of nebulae in a cluster. The black discs and full line represent the solution for solar motion using the nebulae individually; the circles and broken line represent the solution combining the nebulae into groups; the cross represents the mean velocity corresponding to the mean distance of 22 nebulae whose distances could not be estimated individually.

can be excluded, since the observed velocity is so small that the peculiar motion must be large in comparison with the distance effect. The object is not necessarily an exception, however, since a distance can be assigned for which the peculiar motion and the absolute magnitude are both within the range previously determined. The two mean magnitudes, -15.3 and -15.5, the ranges, 4.9 and 5.0 mag., and the frequency distributions are closely similar for these two entirely independent sets of data; and even the slight difference in mean magnitudes can be attributed to the selected, very bright, nebulae in the Virgo Cluster. This entirely unforced agreement supports the validity of the velocity-distance relation in a very

evident matter. Finally, it is worth recording that the frequency distribution of absolute magnitudes in the two tables combined is comparable with those found in the various clusters of nebulae.

The results establish a roughly linear relation between velocities and distances among nebulae for which velocities have been previously published, and the relation appears to dominate the distribution of velocities. In order to investigate the matter on a much larger scale, Mr. Humason at Mount Wilson has initiated a program of determining velocities of the most distant nebulae that can be observed with confidence. These, naturally, are the brightest nebulae in clusters of nebulae. The first definite result,[4] $v = +3779$ km./sec. for N. G. C. 7619, is thoroughly consistent with the present conclusions. Corrected for the solar motion, this velocity is $+3910$, which, with $K = 500$, corresponds to a distance of 7.8×10^6 parsecs. Since the apparent magnitude is 11.8, the absolute magnitude at such a distance is -17.65, which is of the right order for the brightest nebulae in a cluster. A preliminary distance, derived independently from the cluster of which this nebula appears to be a member, is of the order of 7×10^6 parsecs.

New data to be expected in the near future may modify the significance of the present investigation or, if confirmatory, will lead to a solution having many times the weight. For this reason it is thought premature to discuss in detail the obvious consequences of the present results. For example, if the solar motion with respect to the clusters represents the rotation of the galactic system, this motion could be subtracted from the results for the nebulae and the remainder would represent the motion of the galactic system with respect to the extra-galactic nebulae.

The outstanding feature, however, is the possibility that the velocity-distance relation may represent the de Sitter effect, and hence that numerical data may be introduced into discussions of the general curvature of space. In the de Sitter cosmology, displacements of the spectra arise from two sources, an apparent slowing down of atomic vibrations and a general tendency of material particles to scatter. The latter involves an acceleration and hence introduces the element of time. The relative importance of these two effects should determine the form of the relation between distances and observed velocities; and in this connection it may be emphasized that the linear relation found in the present discussion is a first approximation representing a restricted range in distance.

[1] *Mt. Wilson Contr.*, No. 324; *Astroph. J., Chicago, Ill.*, **64**, 1926 (321).
[2] *Harvard Coll. Obs. Circ.*, 294, 1926.
[3] *Mon. Not. R. Astr. Soc.*, **85**, 1925 (865–894).
[4] These PROCEEDINGS, **15**, 1929 (167).

Hubble Law

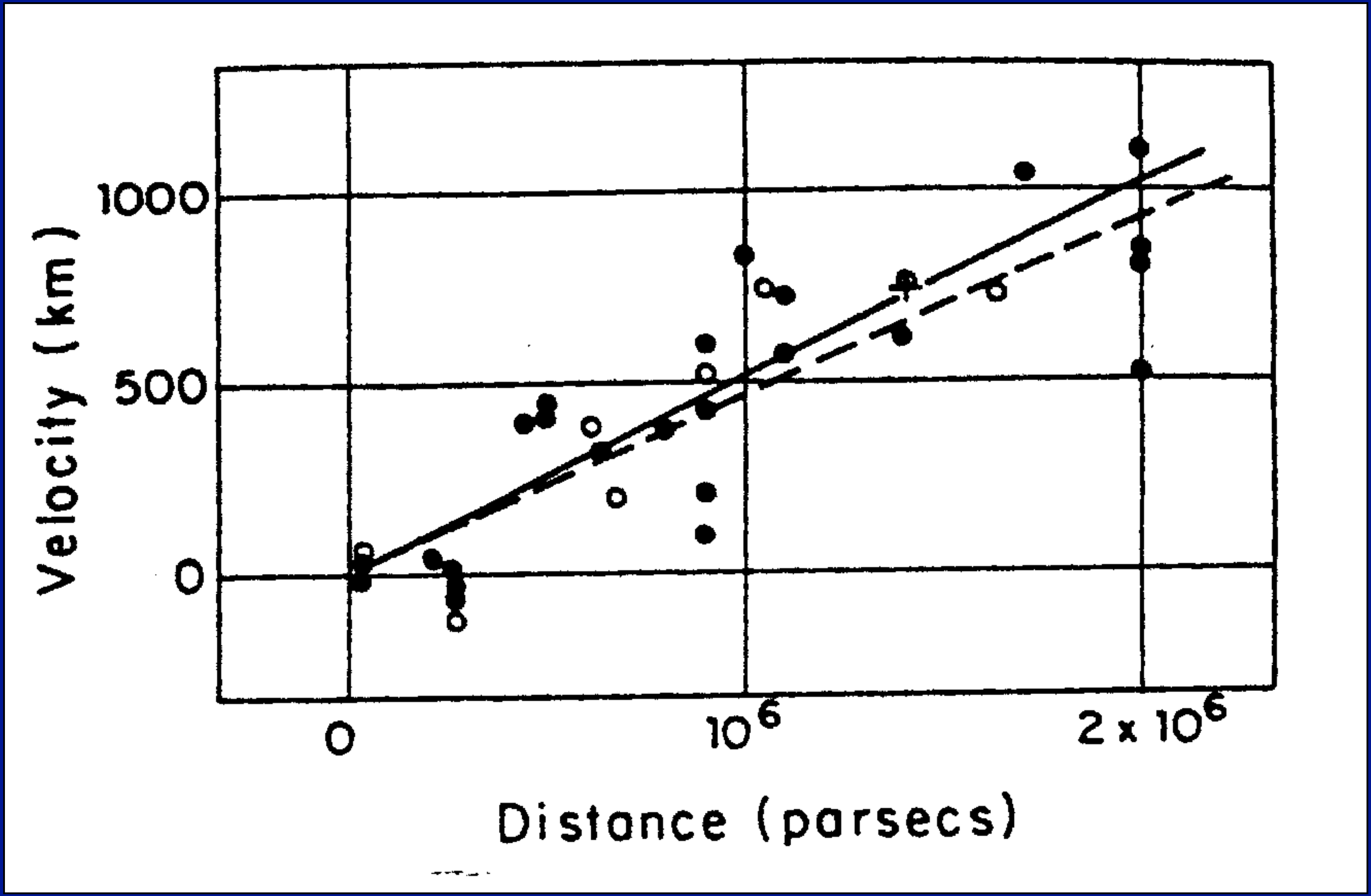

$$v_r = H_0 \times d$$

$$\left(H_0 \approx 500 \frac{km}{s} Mpc^{-1} \right)$$

Hubble Law

The expansion of the universe is such that galaxies' recessional speeds are proportional to their distance.

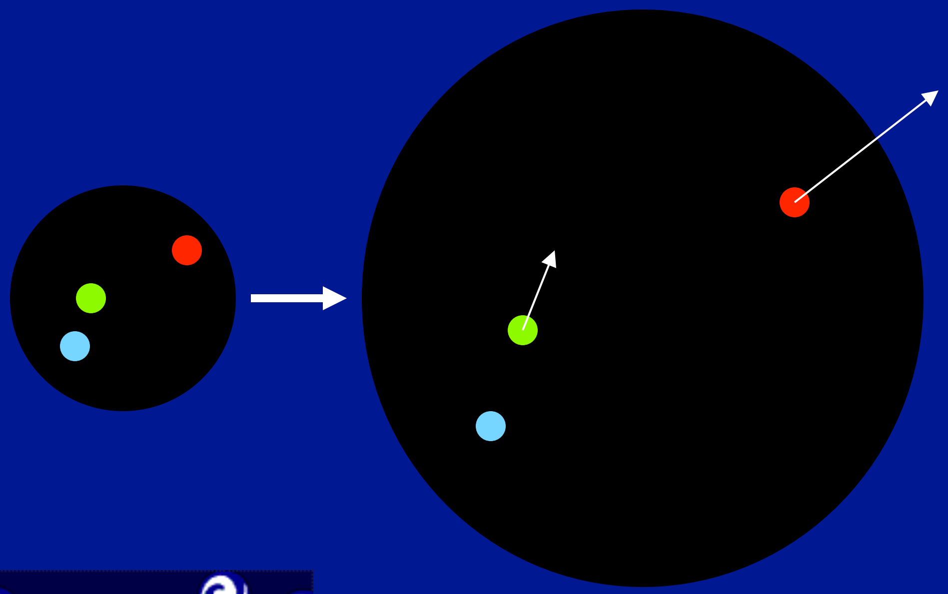

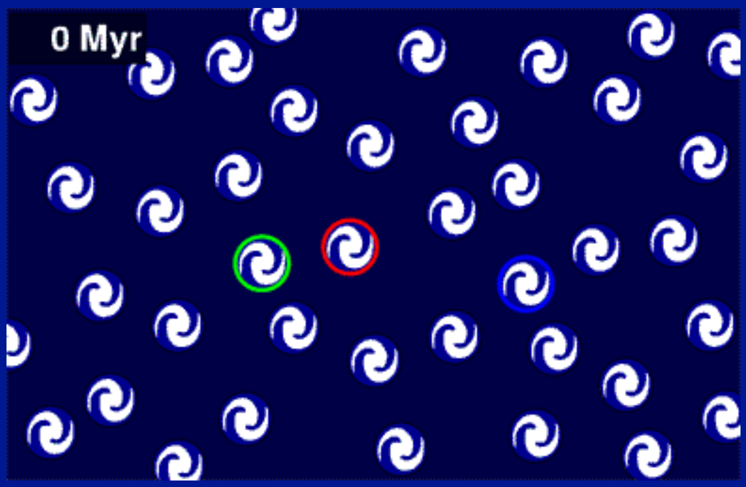

Cosmological Redshift

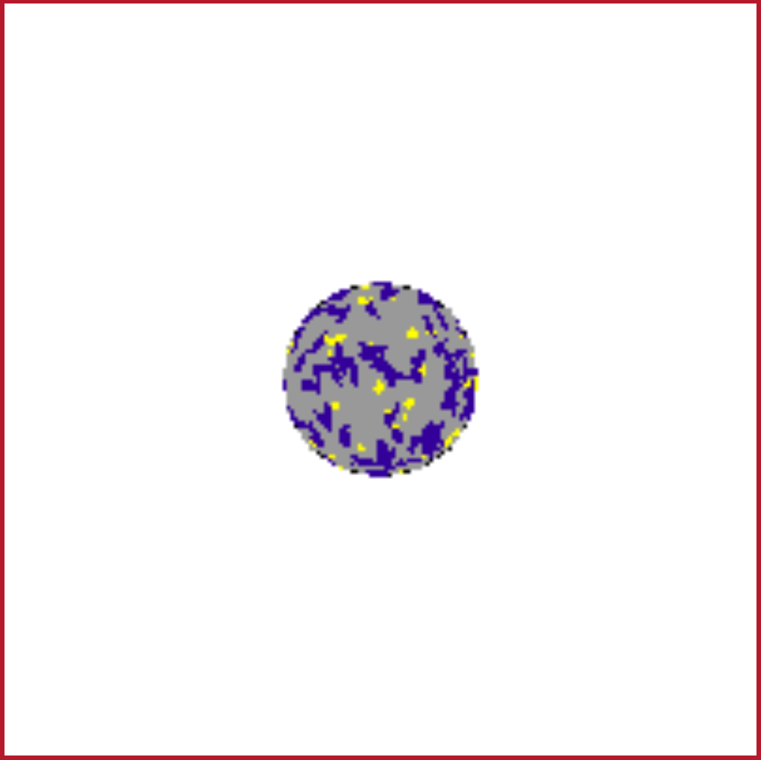

Cosmological Redshift

$$z = \frac{\lambda_{\text{obs}} - \lambda_{\text{emit}}}{\lambda_{\text{emit}}} \rightarrow 1 + z = \frac{\lambda_{\text{obs}}}{\lambda_{\text{emit}}}$$

Cosmic scale factor:

$$a(t) = \frac{R(t)}{R(t_0)}$$

Wavelengths stretch with scale factor:

$$1 + z = \frac{a(t_0)}{a(t)} = \frac{1}{a(t)}$$

Hubble Law

$$v_r = H_0 \times d$$

$$H_0 \approx 70 \frac{km}{s} Mpc^{-1}$$

$$H_0 \equiv 100h \frac{km}{s} Mpc^{-1}$$

$$h \approx 0.7$$

Hubble Law

THE ASTROPHYSICAL JOURNAL, 553:47–72, 2001 May 20

FINAL RESULTS FROM THE *HUBBLE SPACE TELESCOPE* KEY PROJECT TO MEASURE THE HUBBLE CONSTANT[1]

WENDY L. FREEDMAN,[2] BARRY F. MADORE,[2,3] BRAD K. GIBSON,[4] LAURA FERRARESE,[5] DANIEL D. KELSON,[6] SHOKO SAKAI,[7] JEREMY R. MOULD,[8] ROBERT C. KENNICUTT, JR.,[9] HOLLAND C. FORD,[10] JOHN A. GRAHAM,[6] JOHN P. HUCHRA,[11] SHAUN M. G. HUGHES,[12] GARTH D. ILLINGWORTH,[13] LUCAS M. MACRI,[11] AND PETER B. STETSON[14,15]

Received 2000 July 30; accepted 2000 December 19

ABSTRACT

We present here the final results of the *Hubble Space Telescope* (*HST*) Key Project to measure the Hubble constant. We summarize our method, the results, and the uncertainties, tabulate our revised distances, and give the implications of these results for cosmology. Our results are based on a Cepheid calibration of several secondary distance methods applied over the range of about 60–400 Mpc. The analysis presented here benefits from a number of recent improvements and refinements, including (1) a larger LMC Cepheid sample to define the fiducial period-luminosity (PL) relations, (2) a more recent *HST* Wide Field and Planetary Camera 2 (WFPC2) photometric calibration, (3) a correction for Cepheid metallicity, and (4) a correction for incompleteness bias in the observed Cepheid PL samples. We adopt a distance modulus to the LMC (relative to which the more distant galaxies are measured) of μ_0(LMC) = 18.50 ± 0.10 mag, or 50 kpc. New, revised distances are given for the 18 spiral galaxies for which Cepheids have been discovered as part of the Key Project, as well as for 13 additional galaxies with published Cepheid data. The new calibration results in a Cepheid distance to NGC 4258 in better agreement with the maser distance to this galaxy. Based on these revised Cepheid distances, we find values (in km s^{-1} Mpc^{-1}) of $H_0 = 71 \pm 2$ (random) ± 6 (systematic) (Type Ia supernovae), $H_0 = 71 \pm 3 \pm 7$ (Tully-Fisher relation), $H_0 = 70 \pm 5 \pm 6$ (surface brightness fluctuations), $H_0 = 72 \pm 9 \pm 7$ (Type II supernovae), and $H_0 = 82 \pm 6 \pm 9$ (fundamental plane). We combine these results for the different methods with three different weighting schemes, and find good agreement and consistency with $H_0 = 72 \pm 8$ km s^{-1} Mpc^{-1}. Finally, we compare these results with other, global methods for measuring H_0.

Subject headings: Cepheids — cosmology: observations — distance scale — galaxies: distances and redshifts

Hubble Law

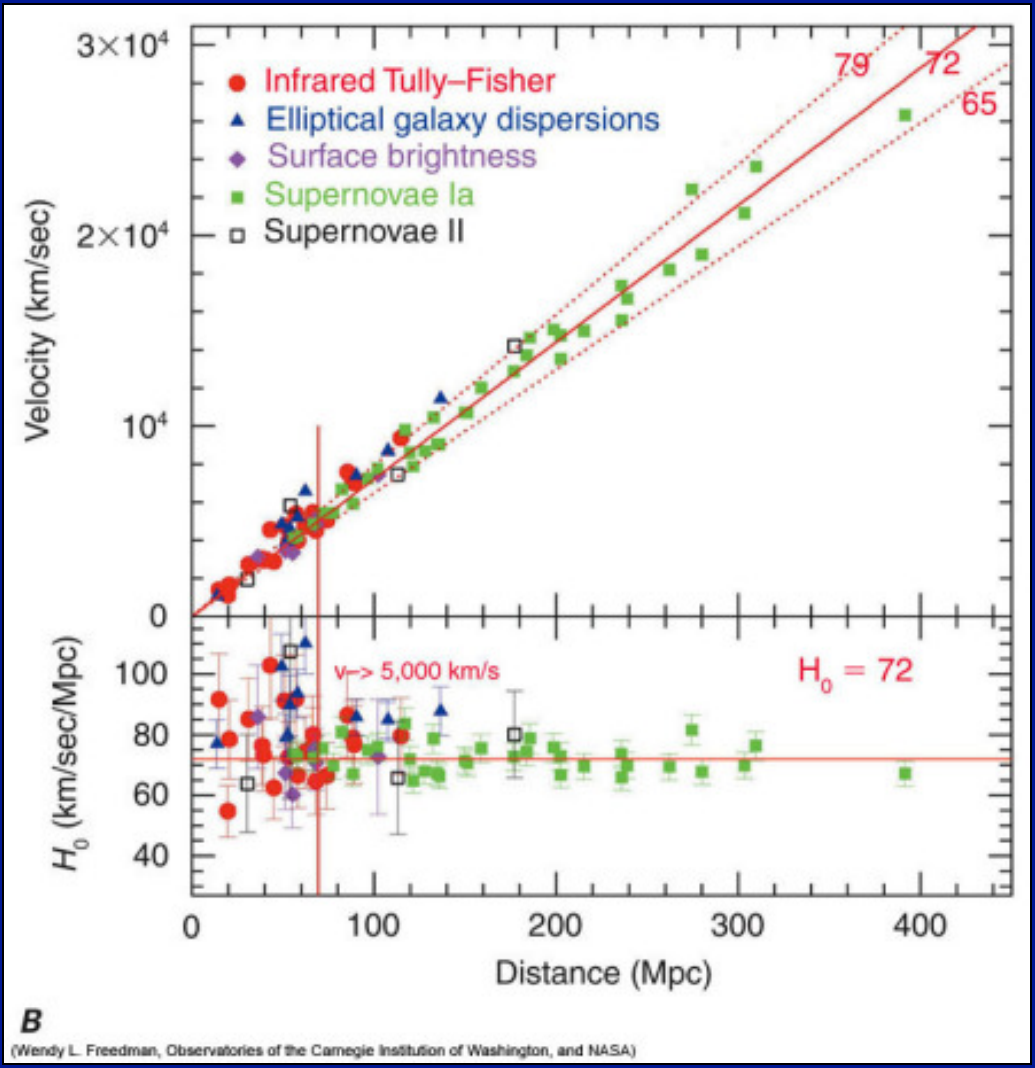

Infrared Tully–Fisher
Elliptical galaxy dispersions
Surface brightness
Supernovae Ia
Supernovae II
79
72
65
3×10⁴
2×10⁴
10⁴
0
Velocity (km/sec)
v–> 5,000 km/s
H0 = 72
100
80
60
40
H0 (km/sec/Mpc)
0
100
200
300
400
Distance (Mpc)
B
(Wendy L. Freedman, Observatories of the Carnegie Institution of Washington, and NASA)

Hubble Law

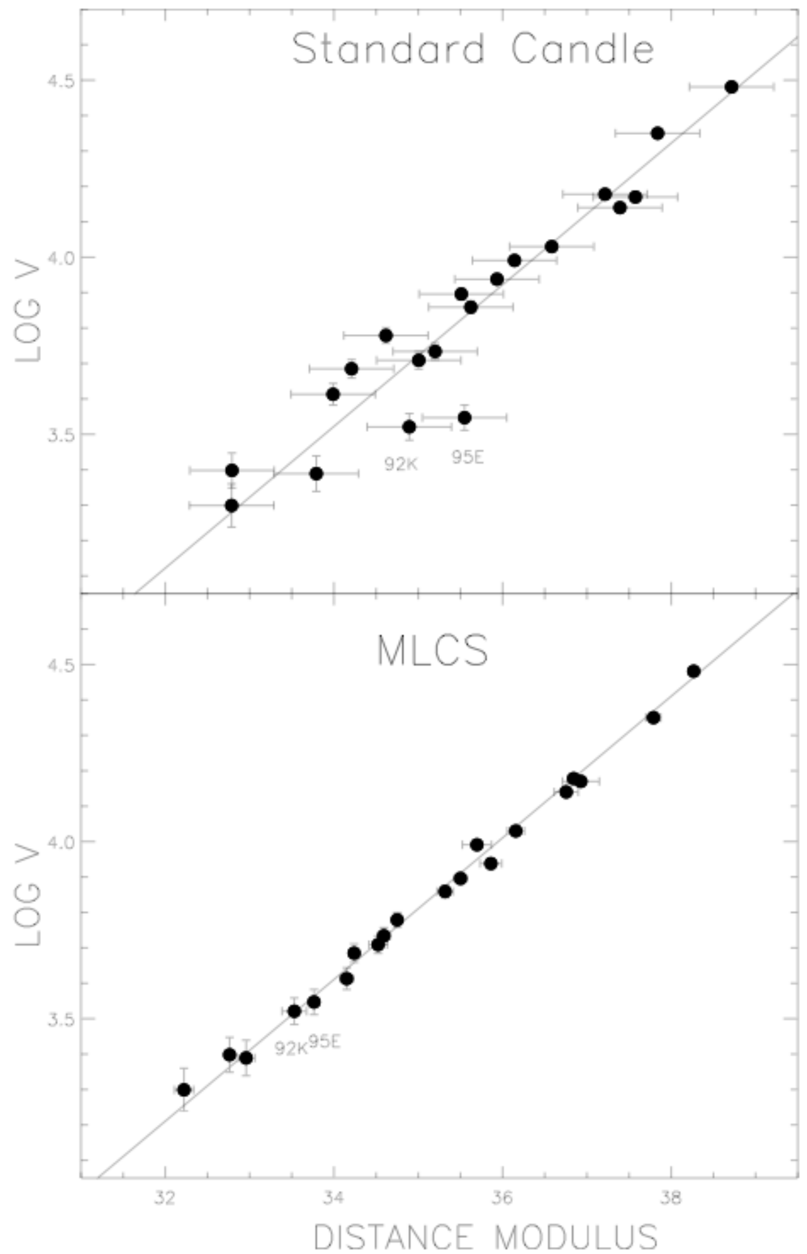

Riess et al. (2006)

Redshift Surveys

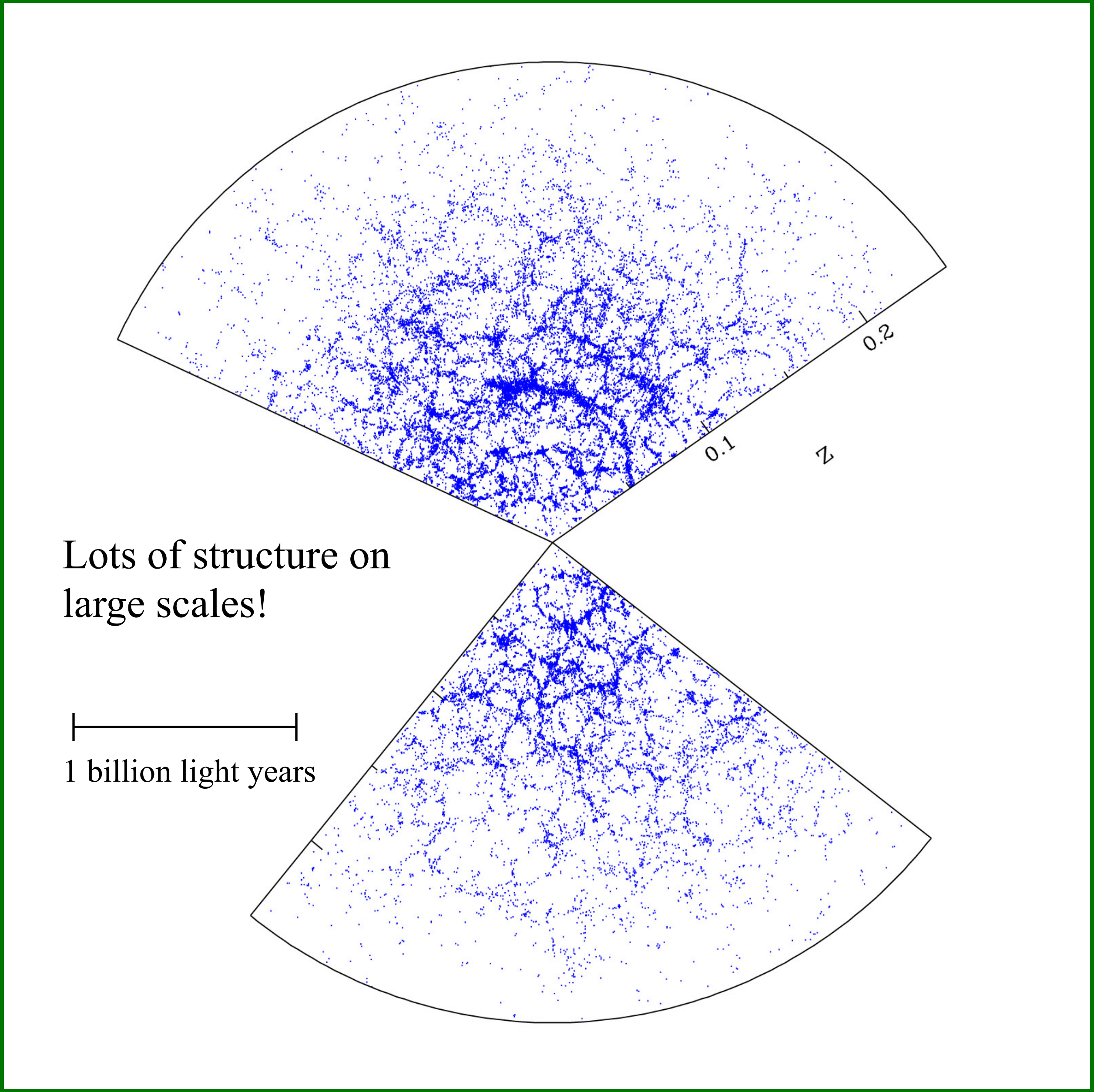

Sloan Digital Sky Survey

An international collaboration of 14 institutions with more than 200 involved scientists.

38 institutions including Vanderbilt

Apache Point, New Mexico

Elevation: 9100 feet

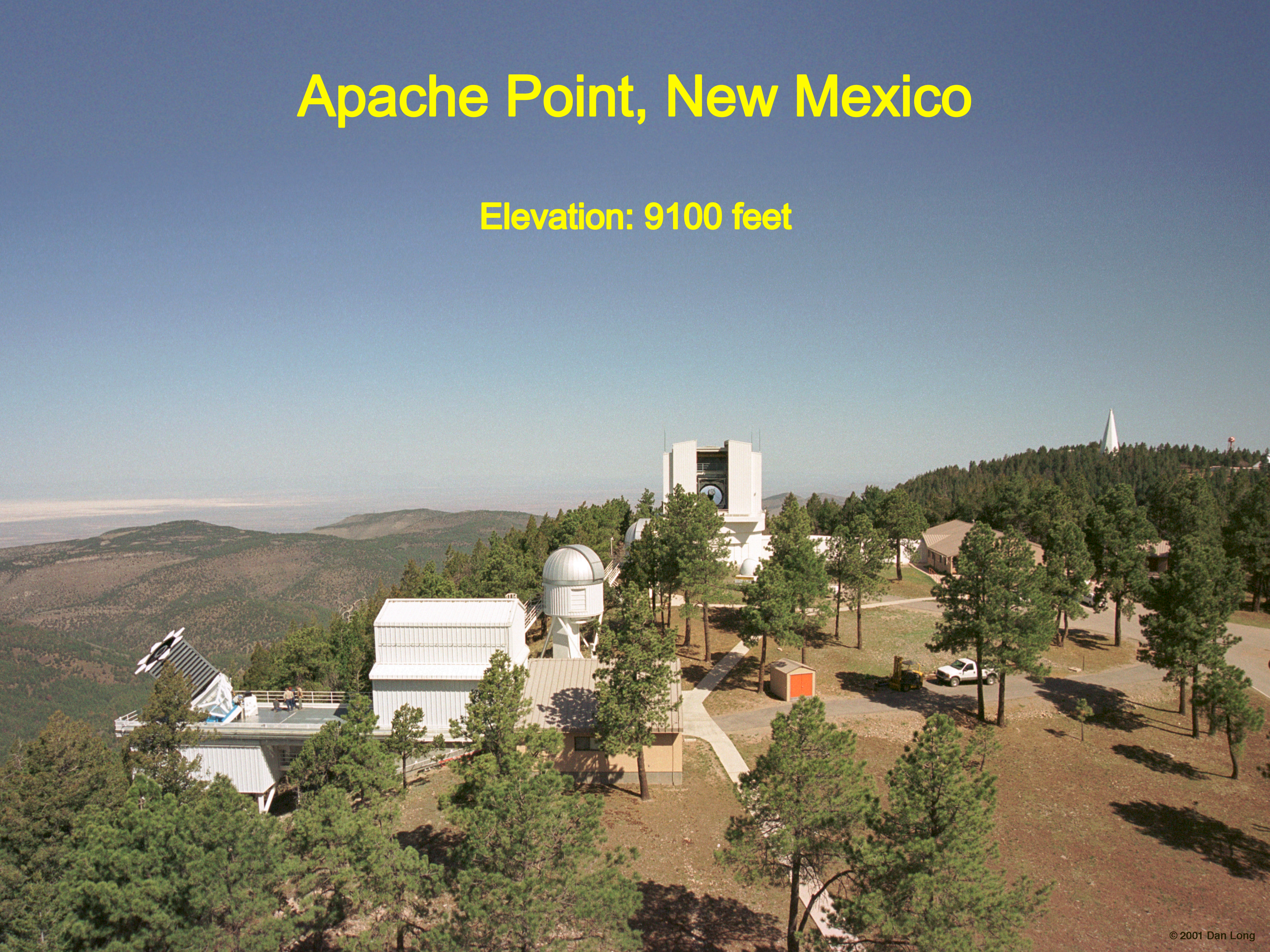

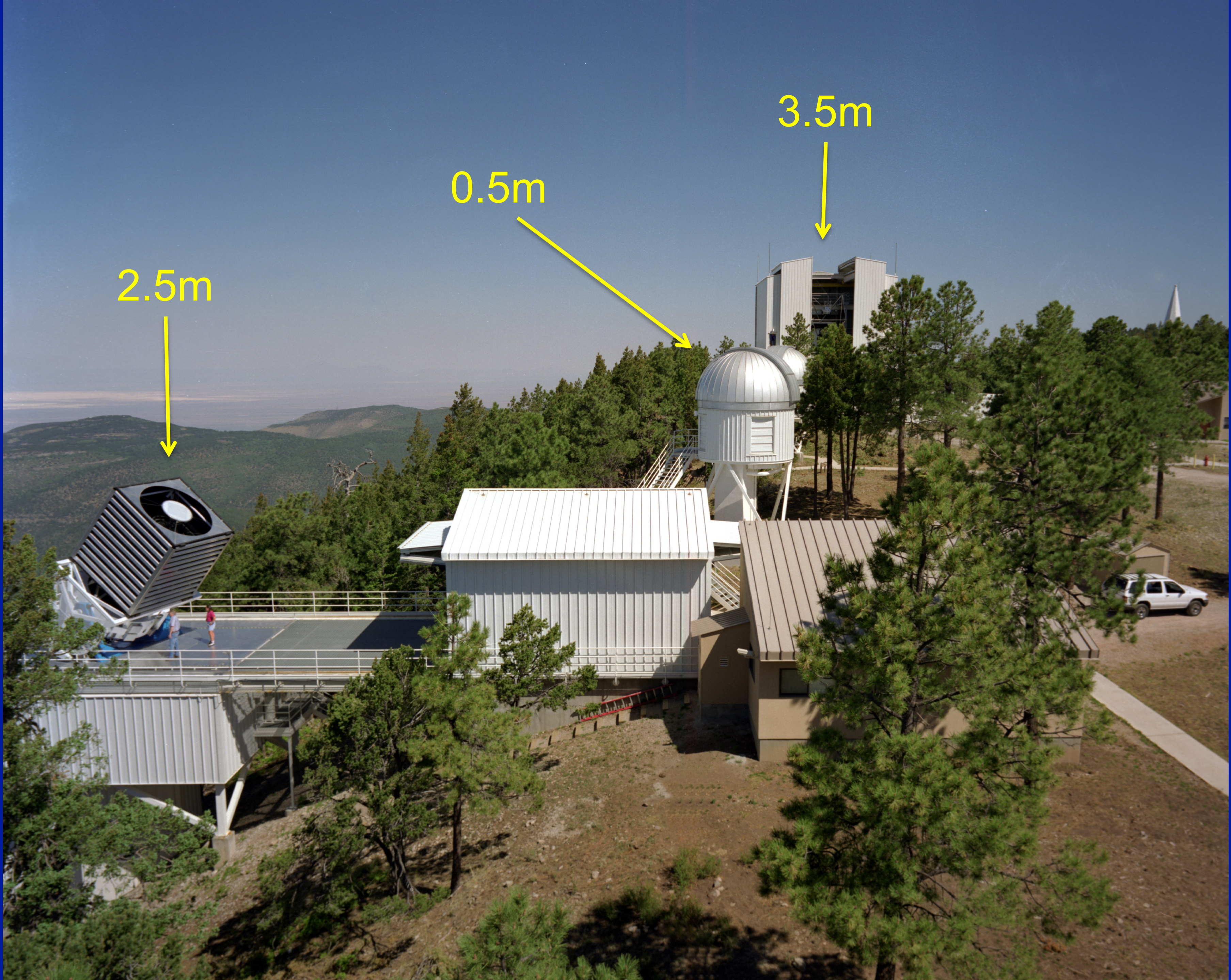
3.5m
0.5m
2.5m

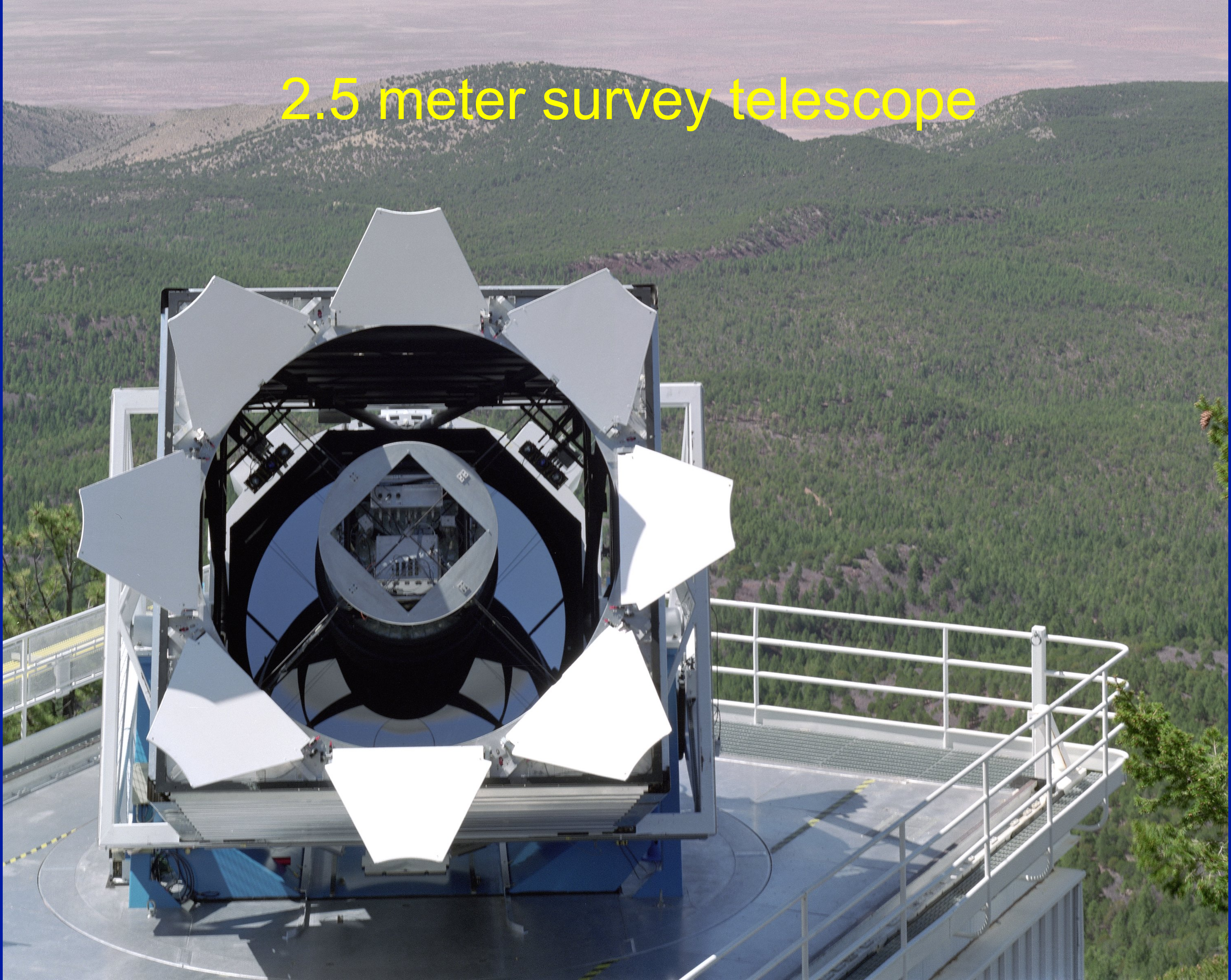
2.5 meter survey telescope

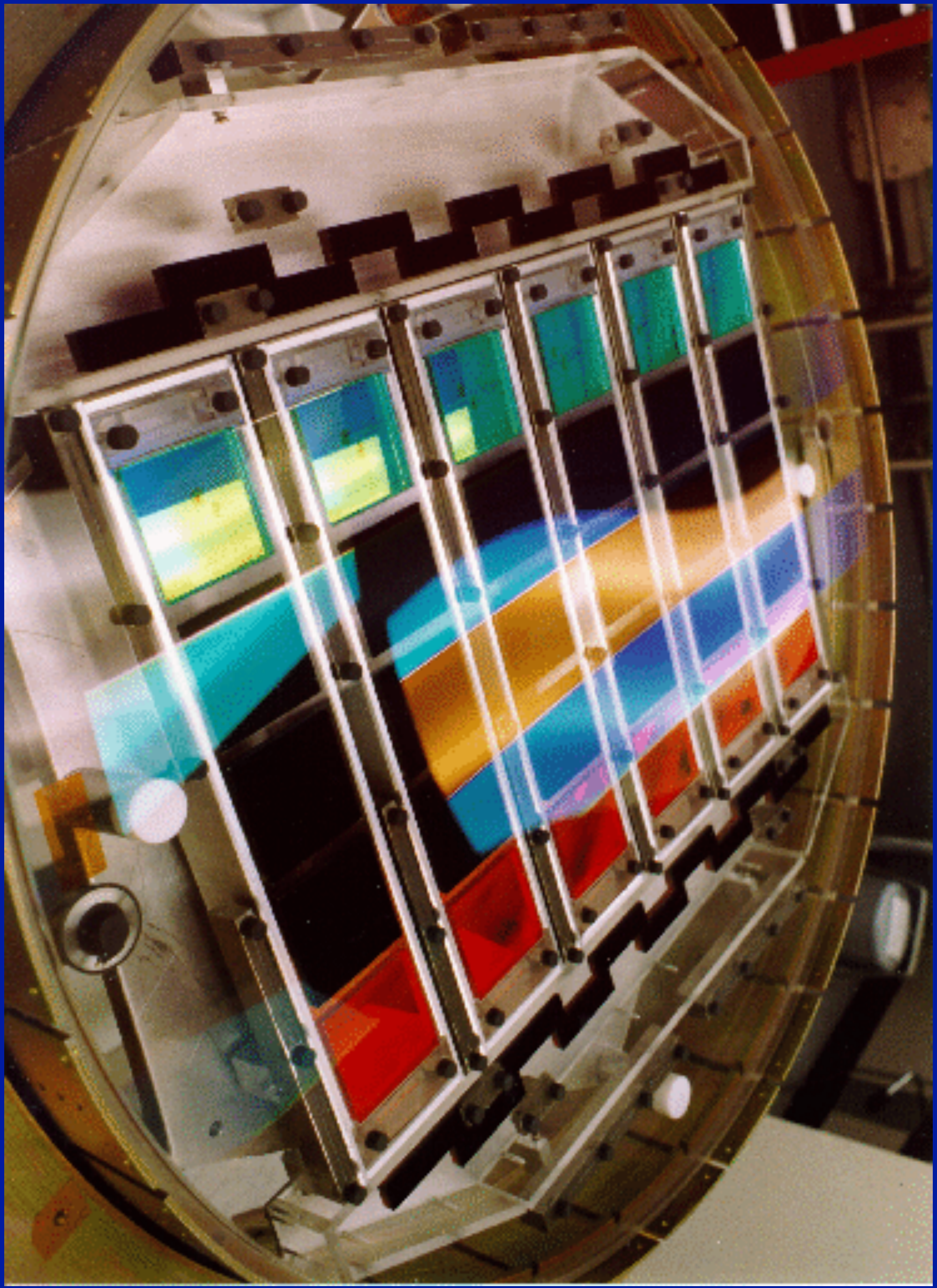

SDSS imaging camera

- 30 2048x2048 CCDs
- 5 color filters
- 126 megapixels!

SDSS imaging camera

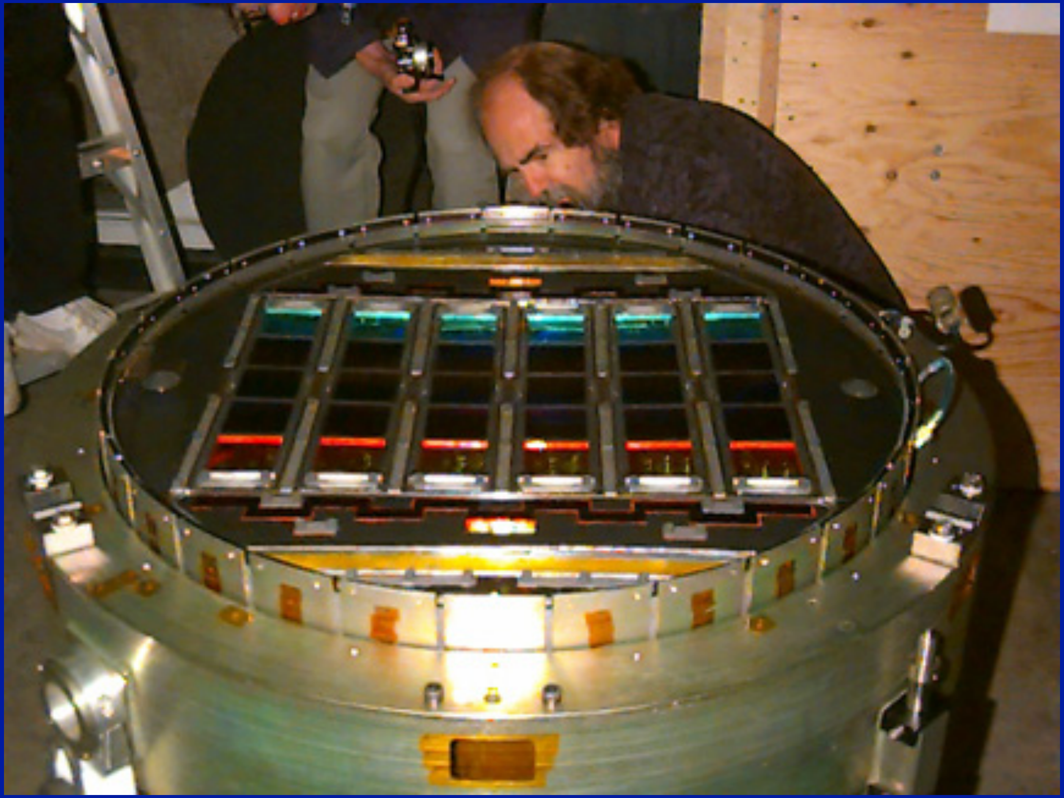

First light image! May 1998

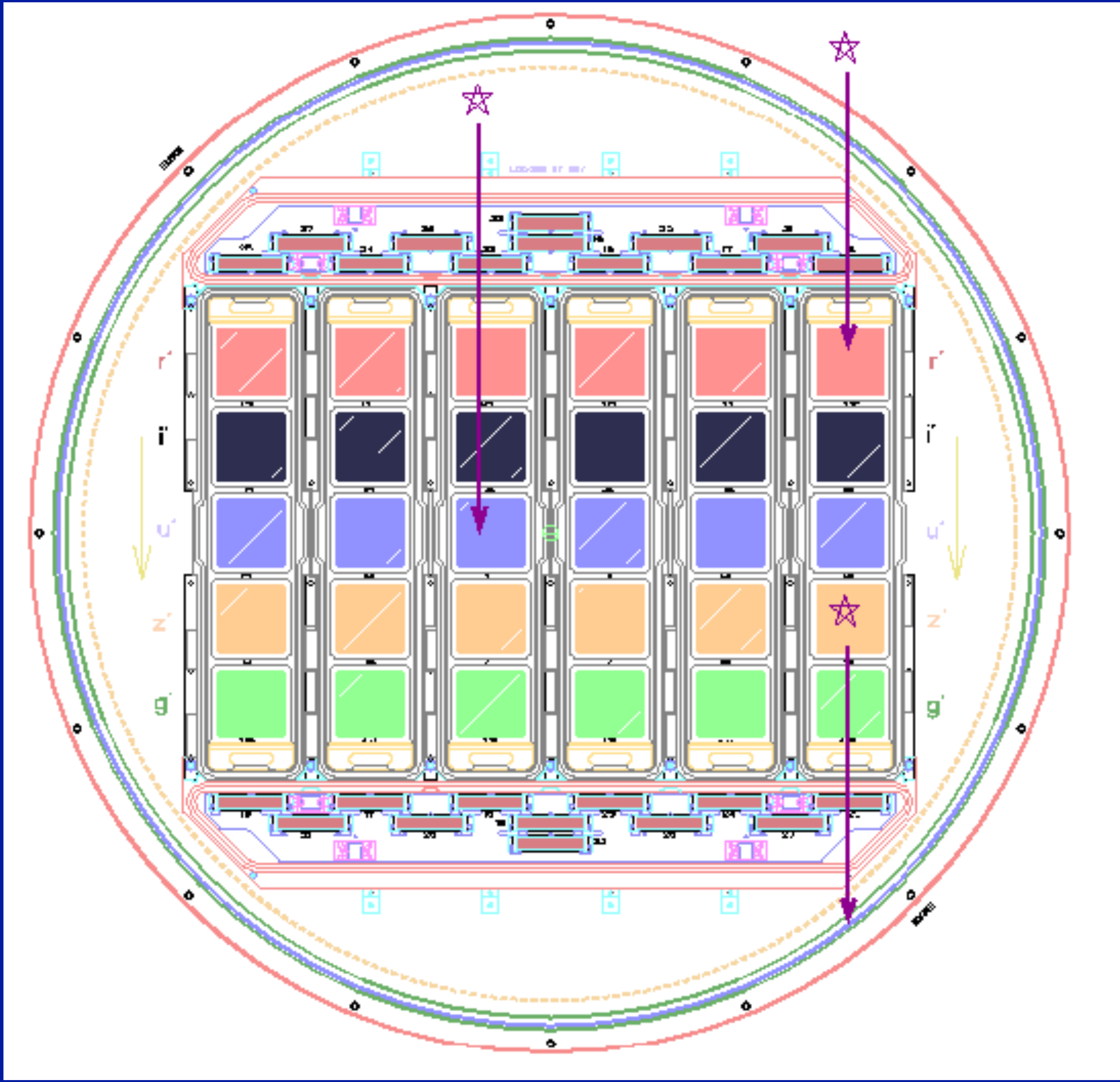
r'
i'
u'
z'
g'

Drift scanning

Drift scanning

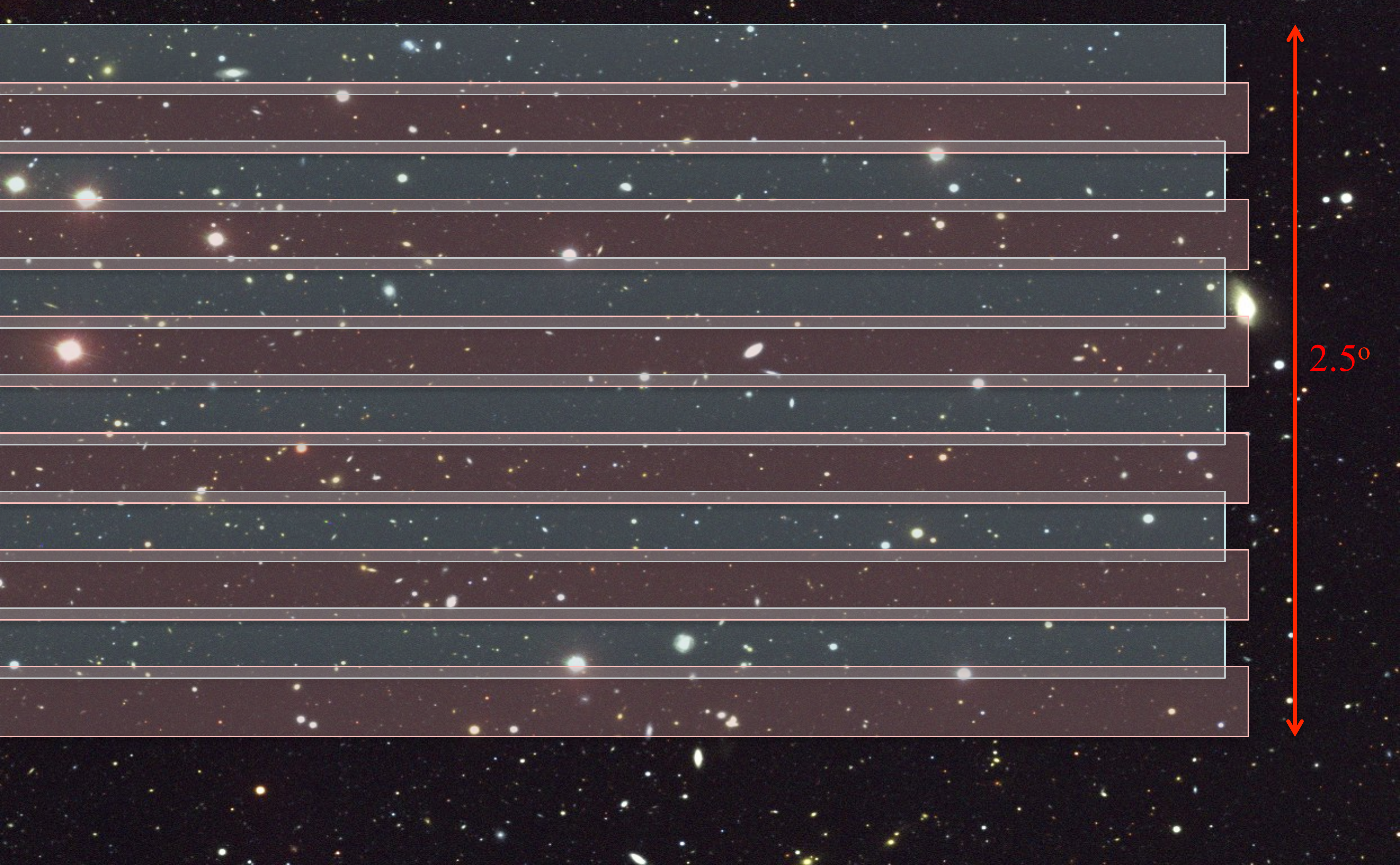

June 2003 53 million objects

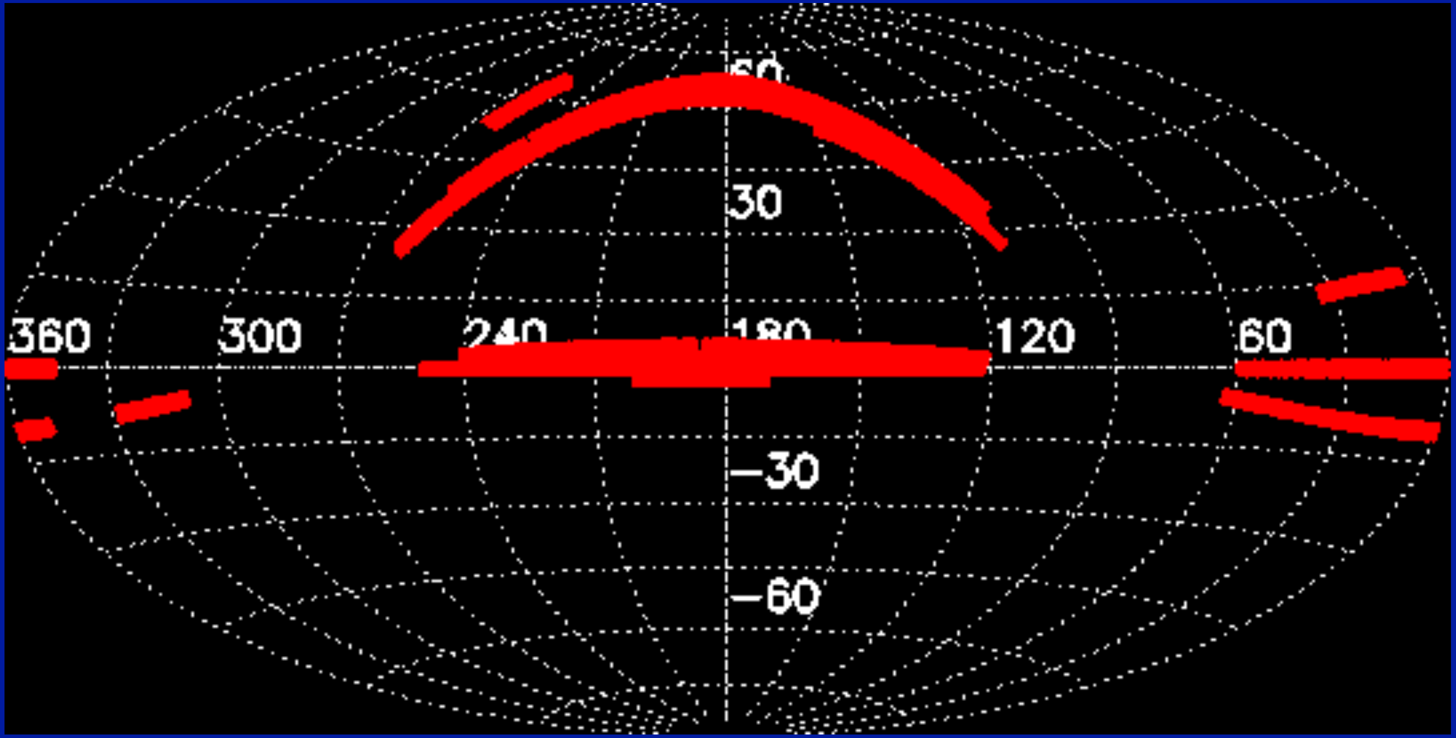

March 2004 88 million objects

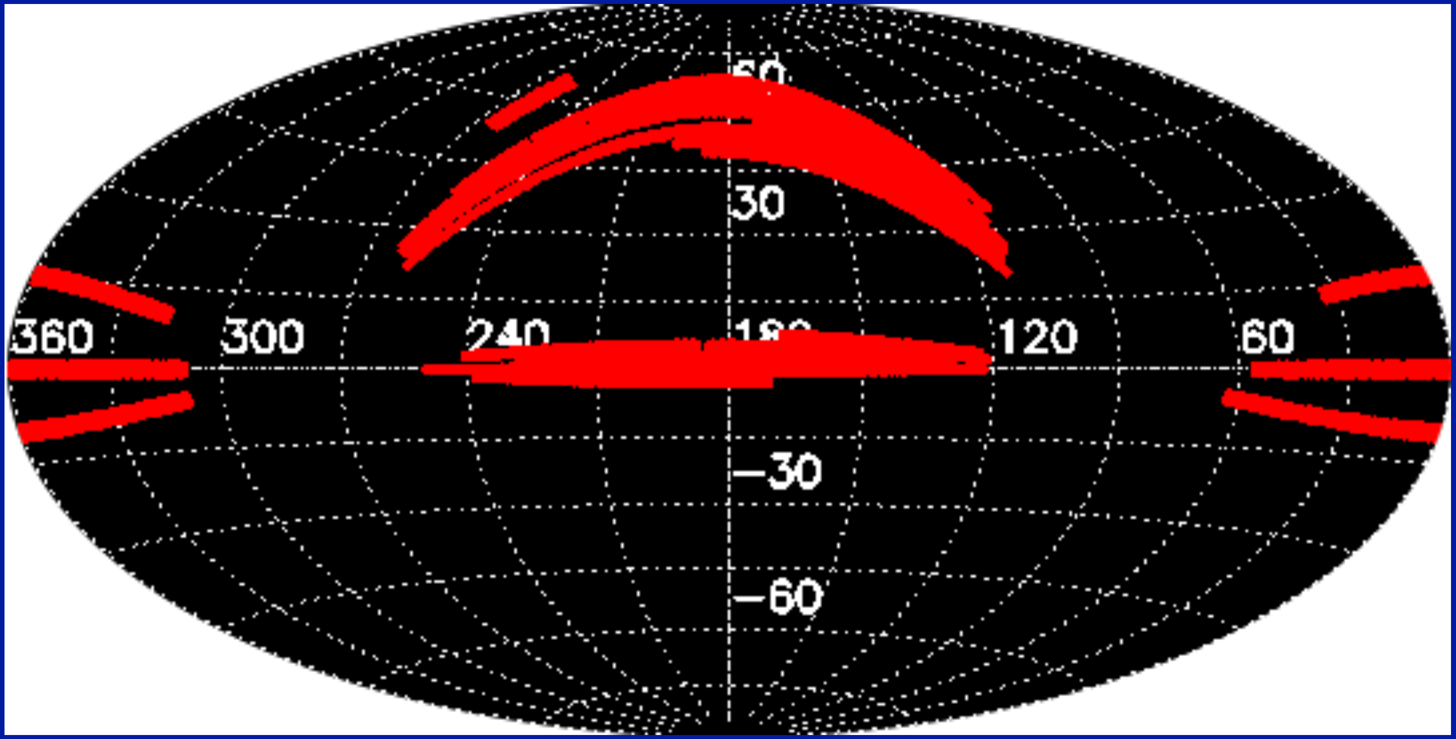

Sept 2004 141 million objects

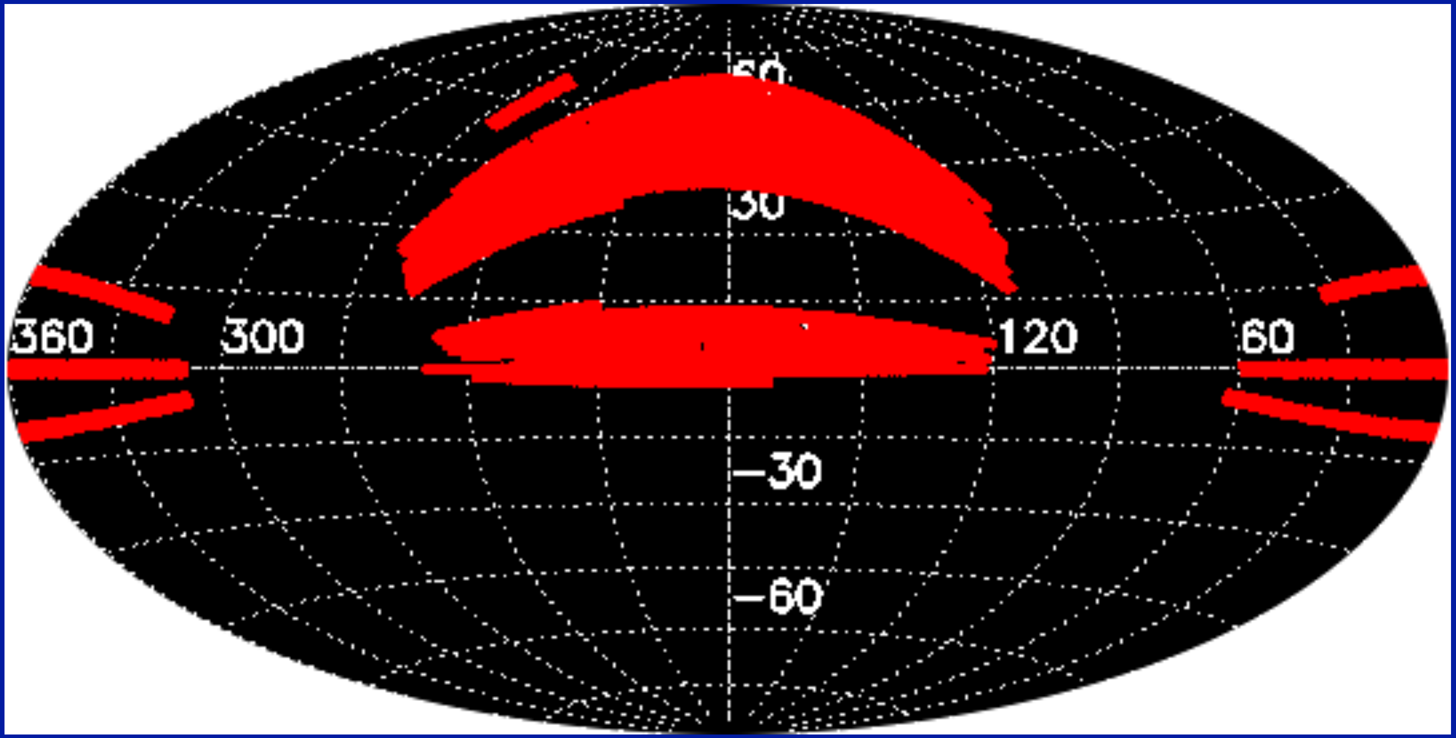

June 2005 180 million objects

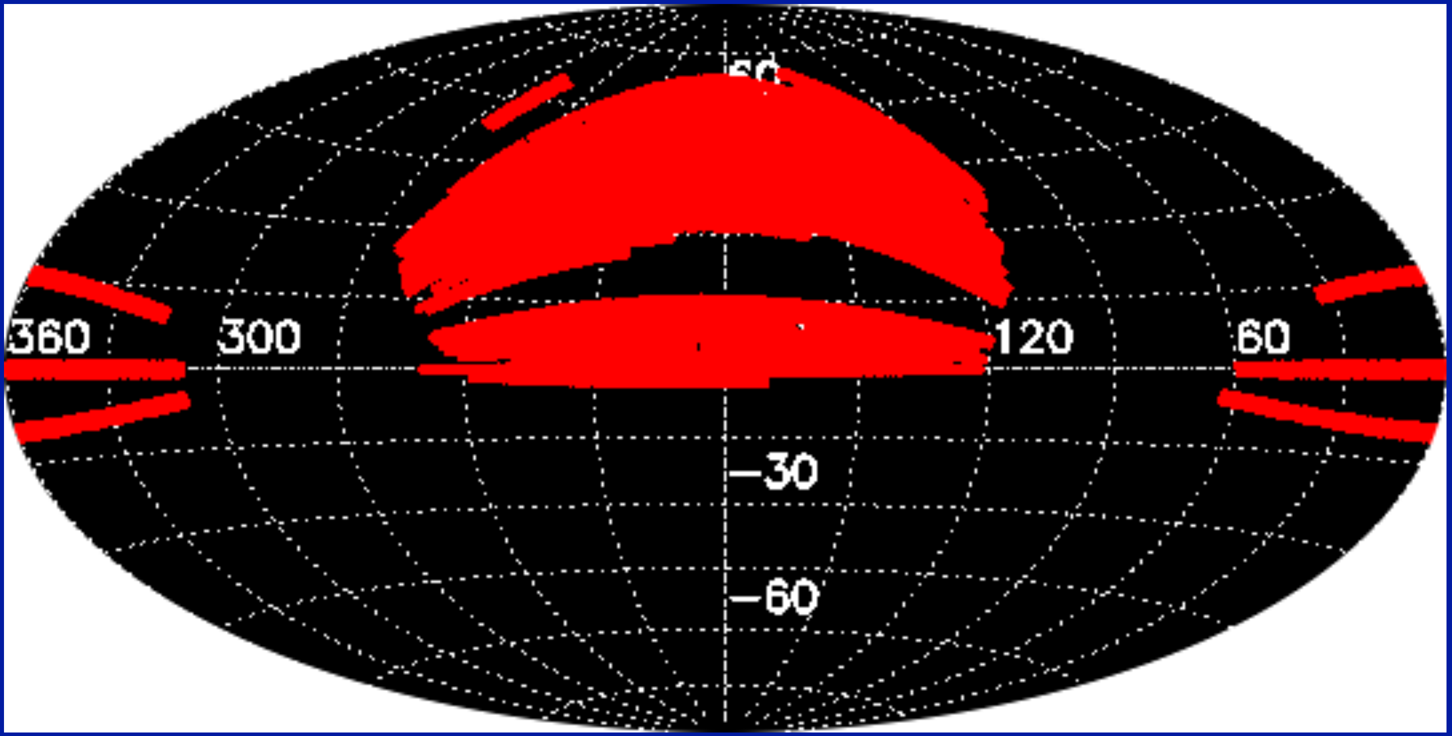

June 2006 215 million objects

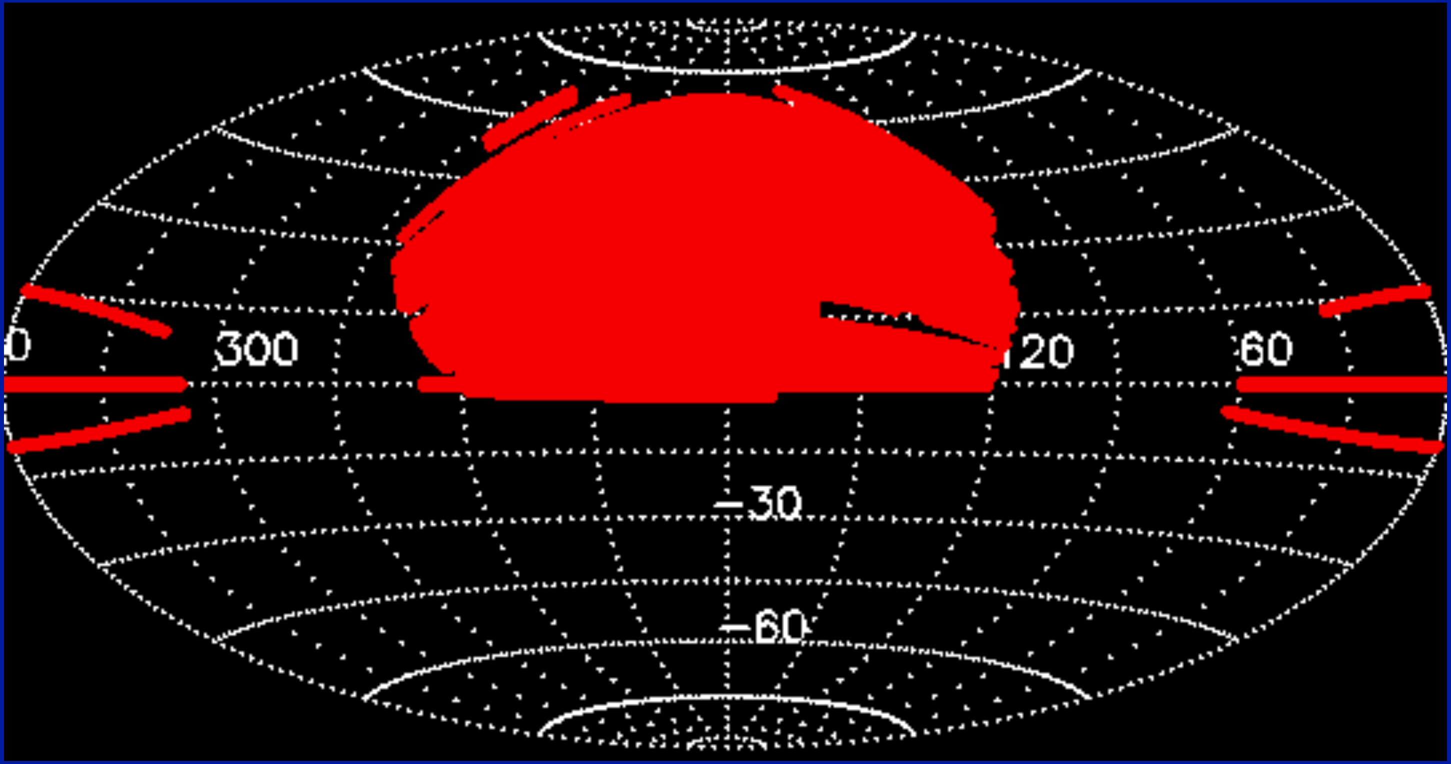

June 2007 287 million objects

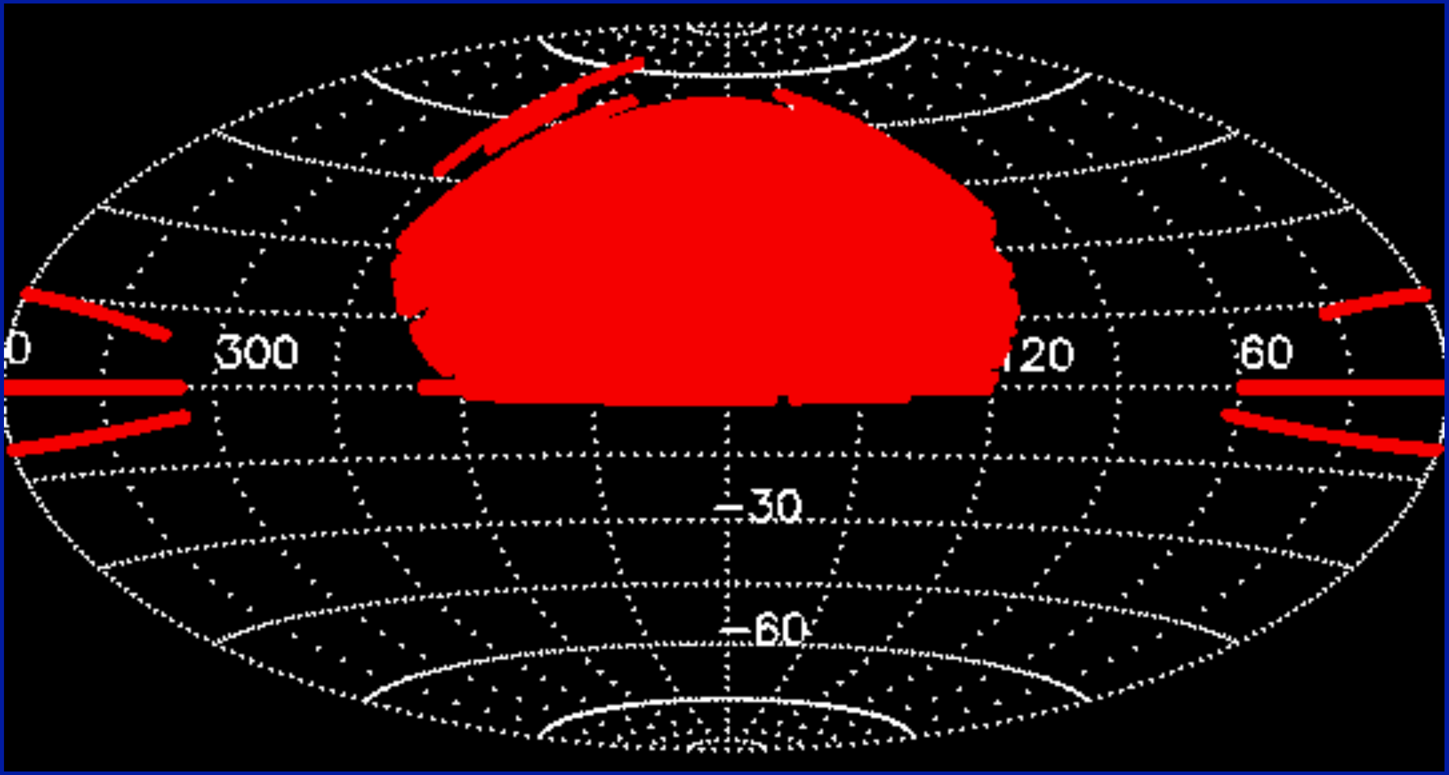

Oct 2008 357 million objects

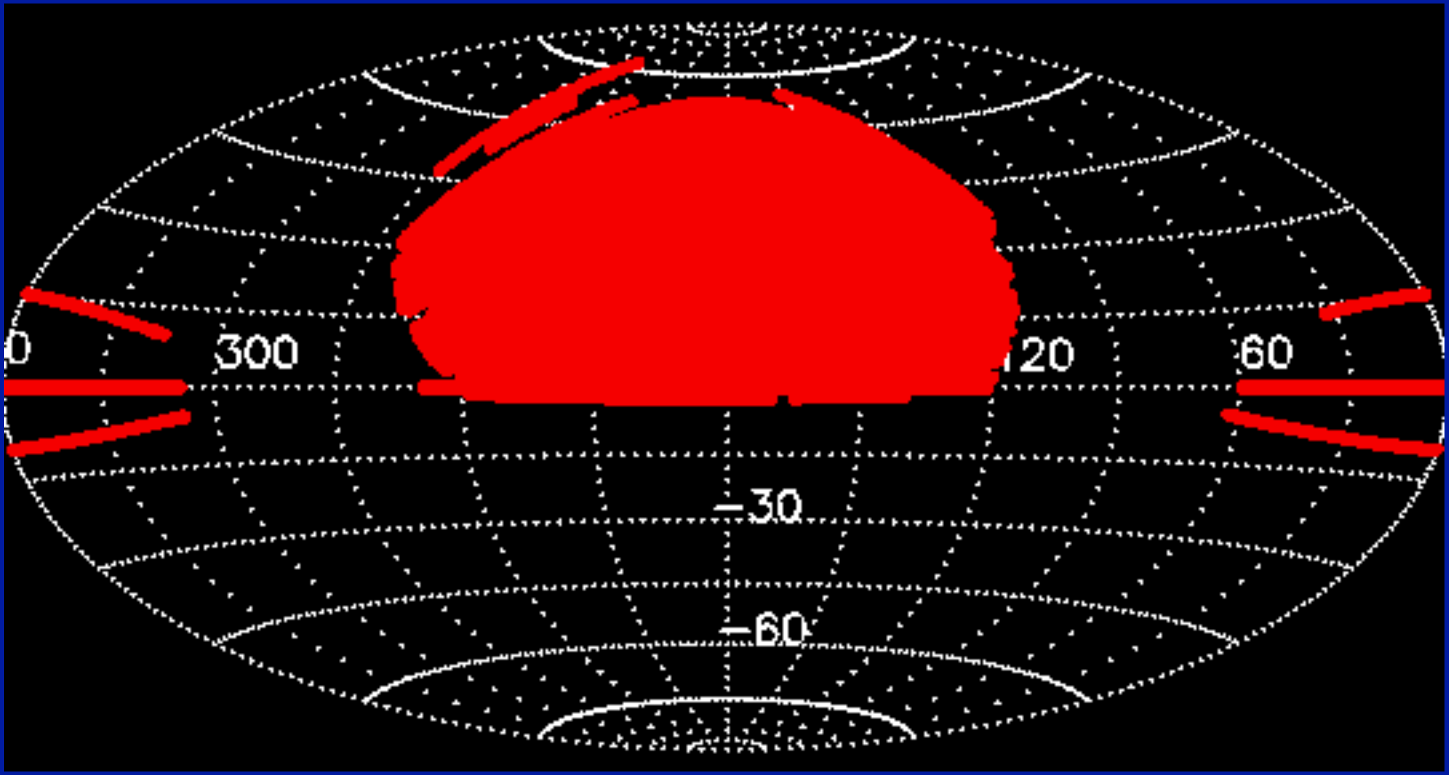

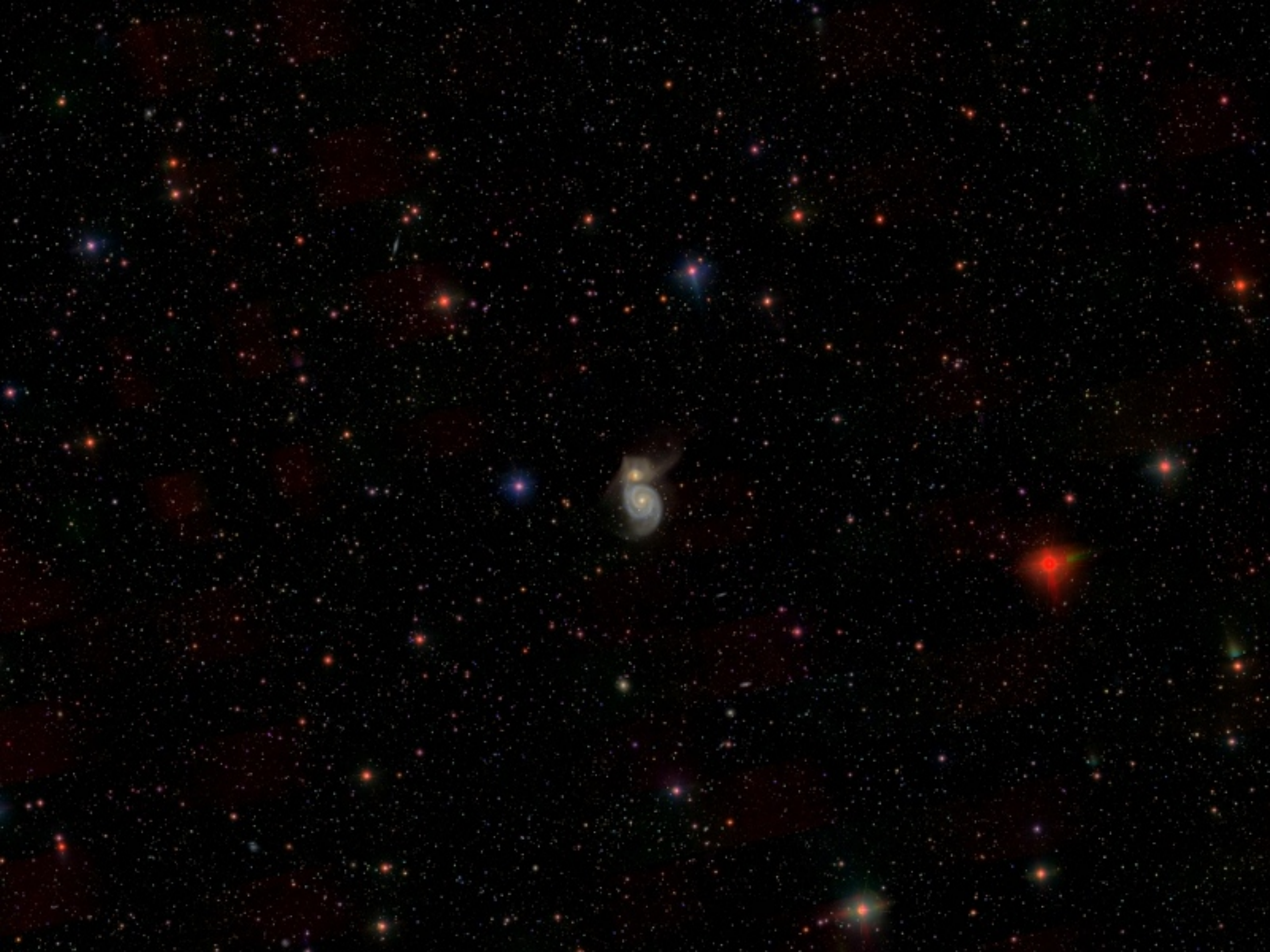

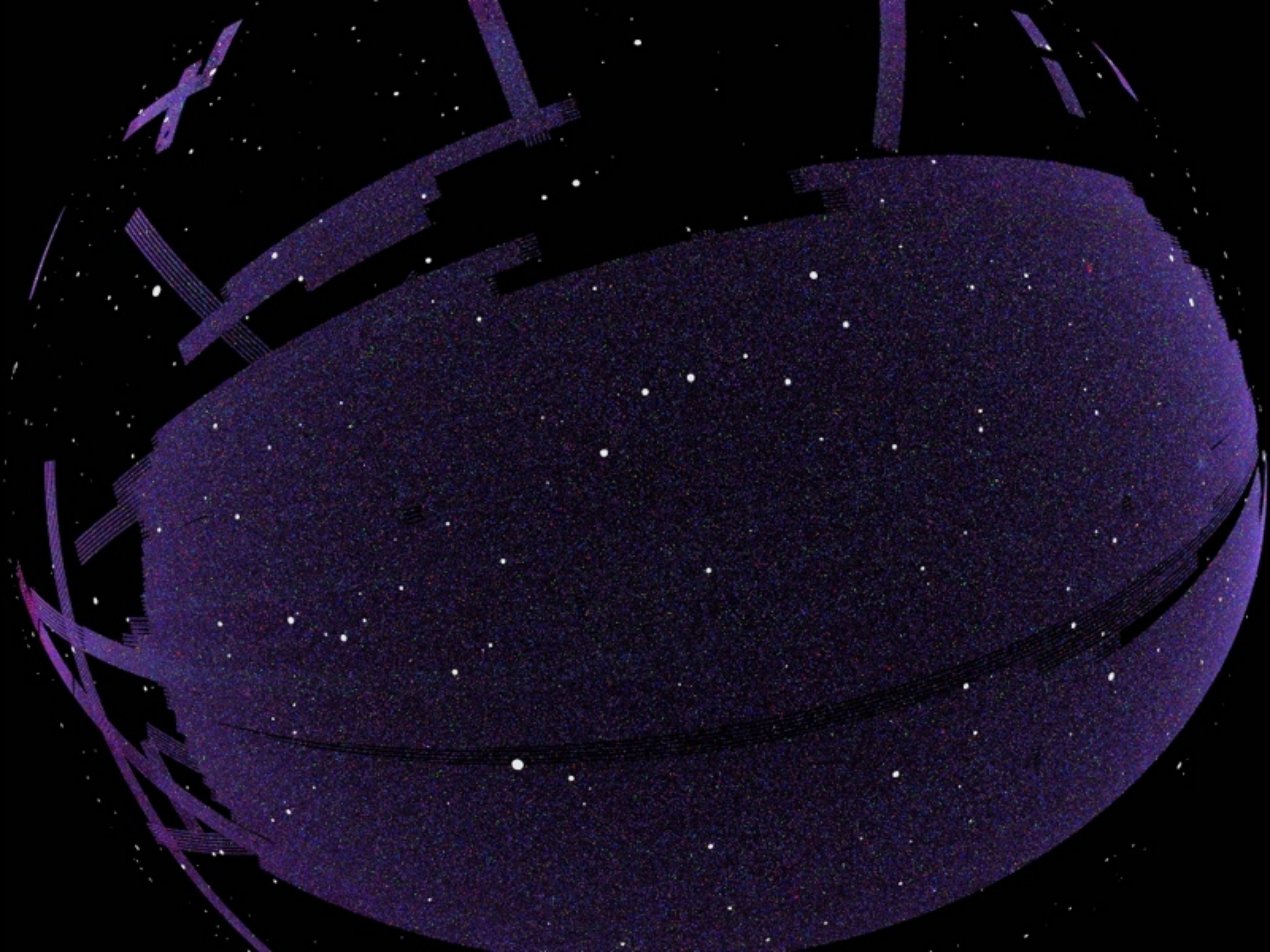

Pal 5 star cluster

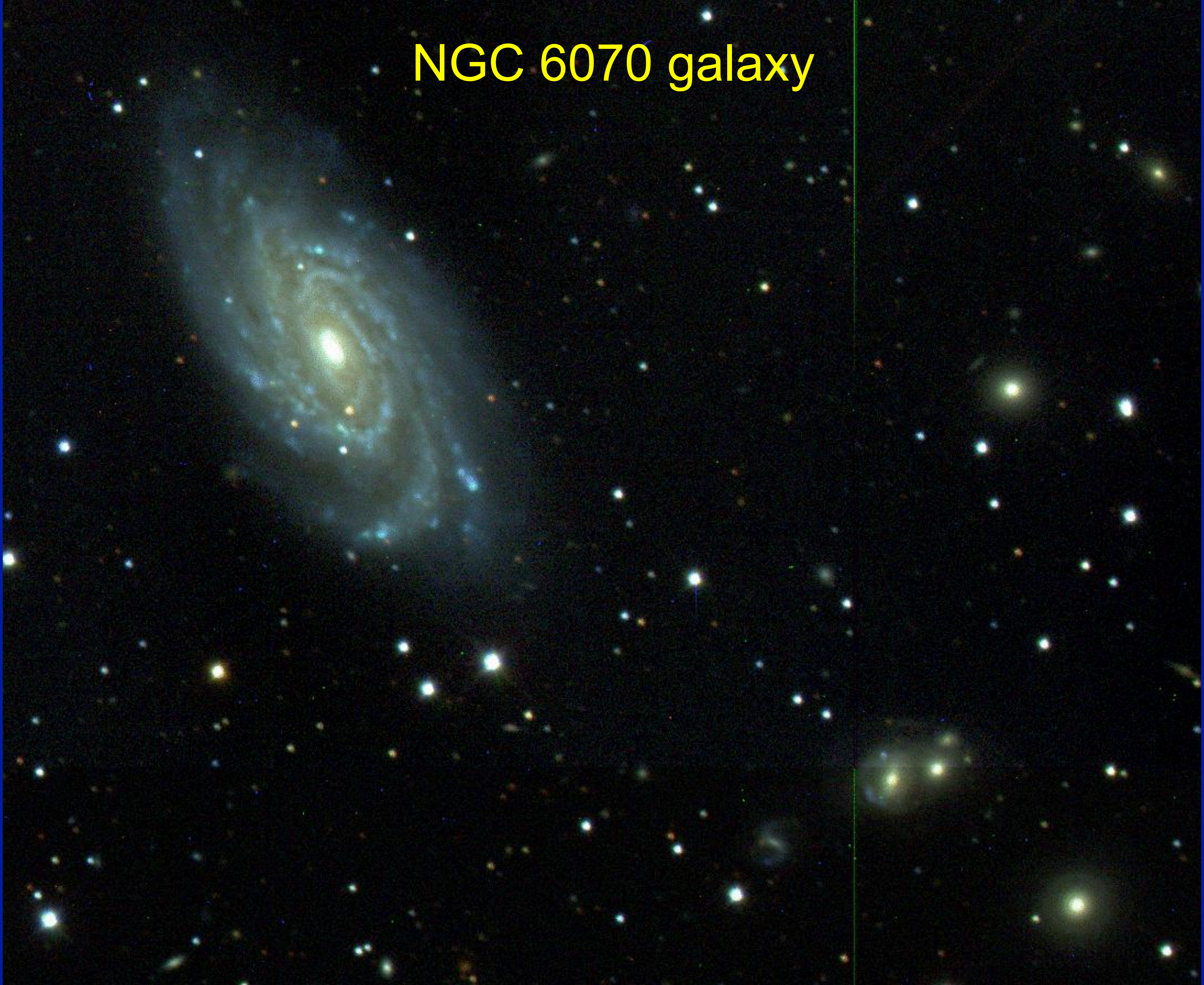
NGC 6070 galaxy

Perseus galaxy cluster

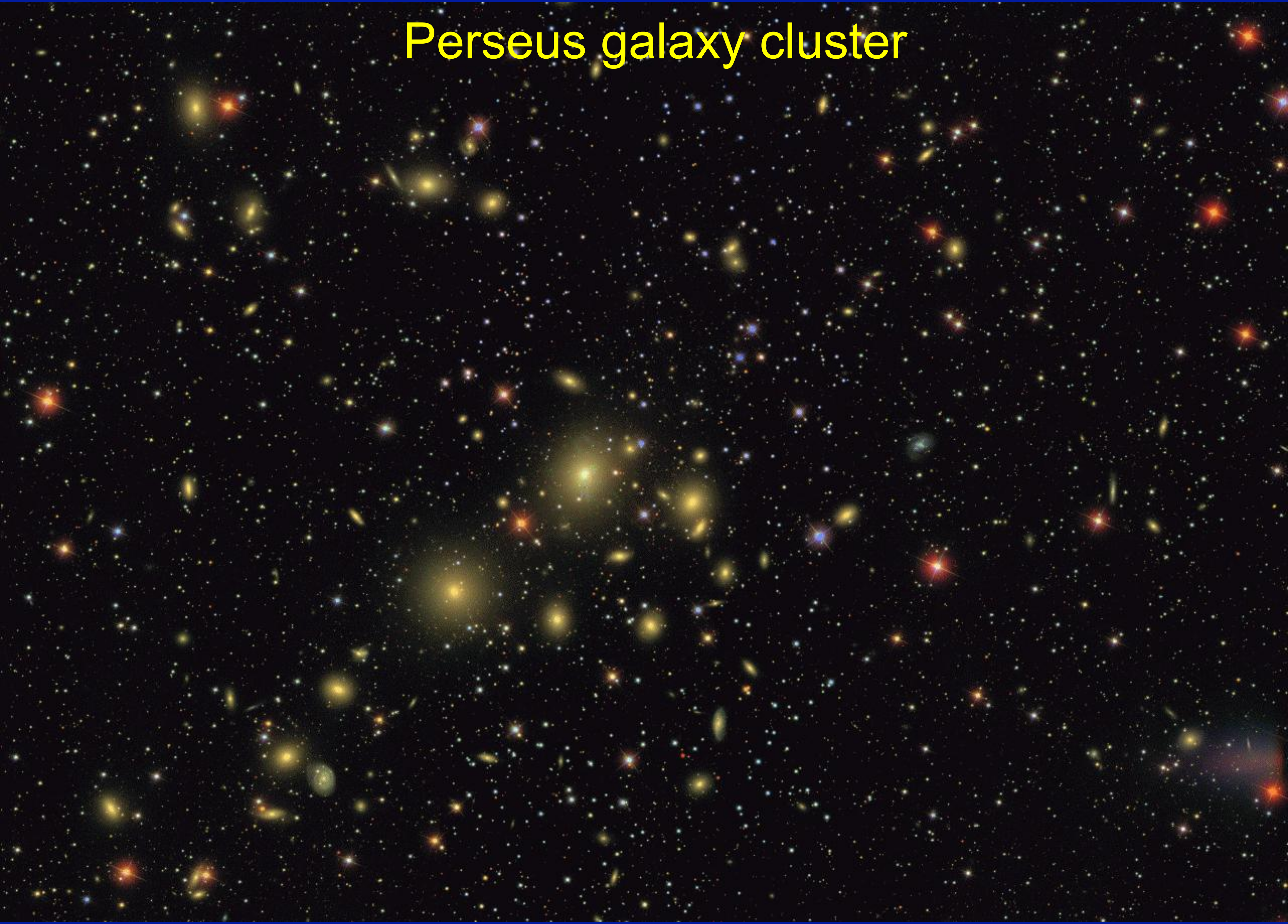

Selecting objects for spectroscopy

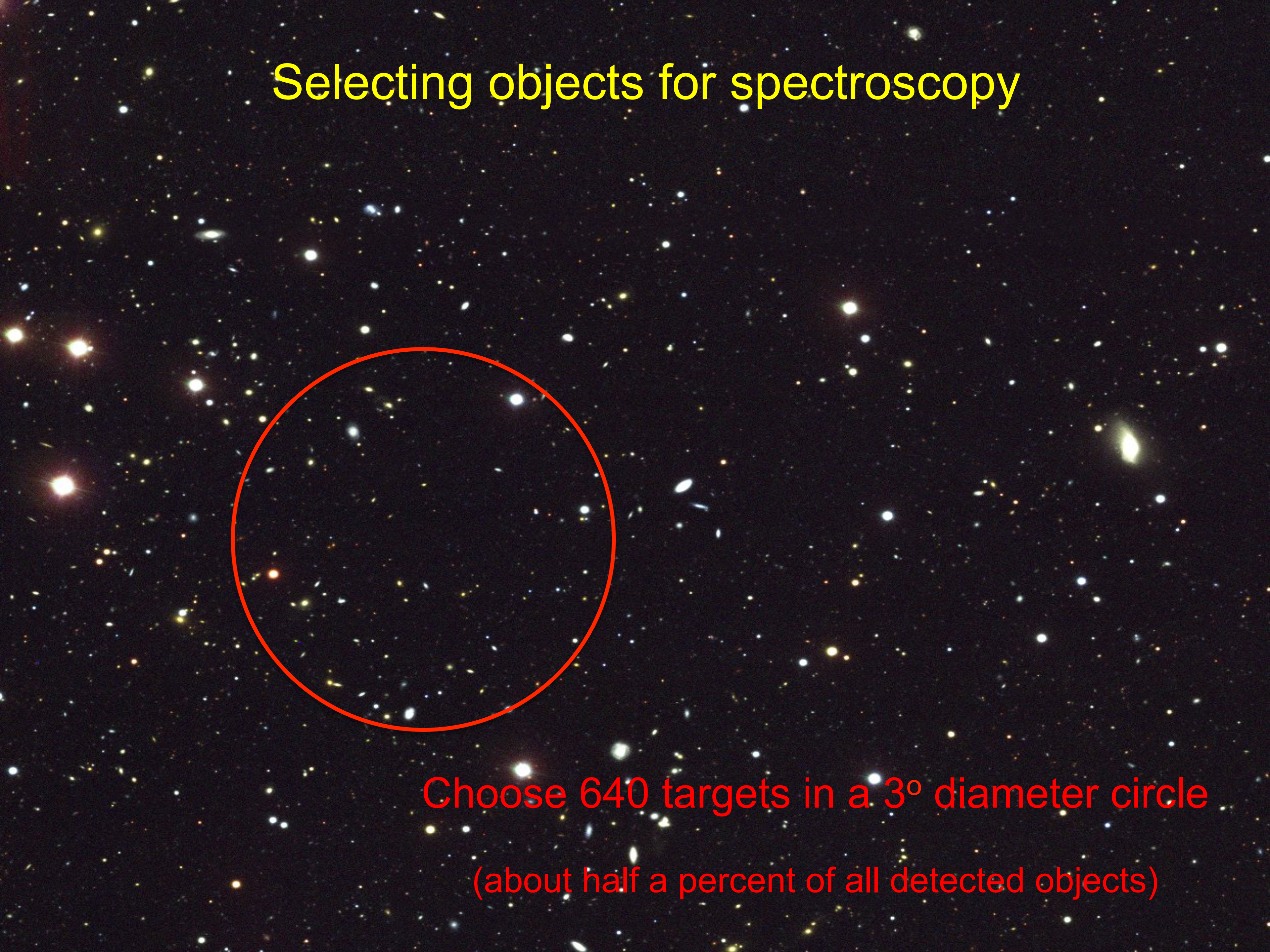

Drill Plate

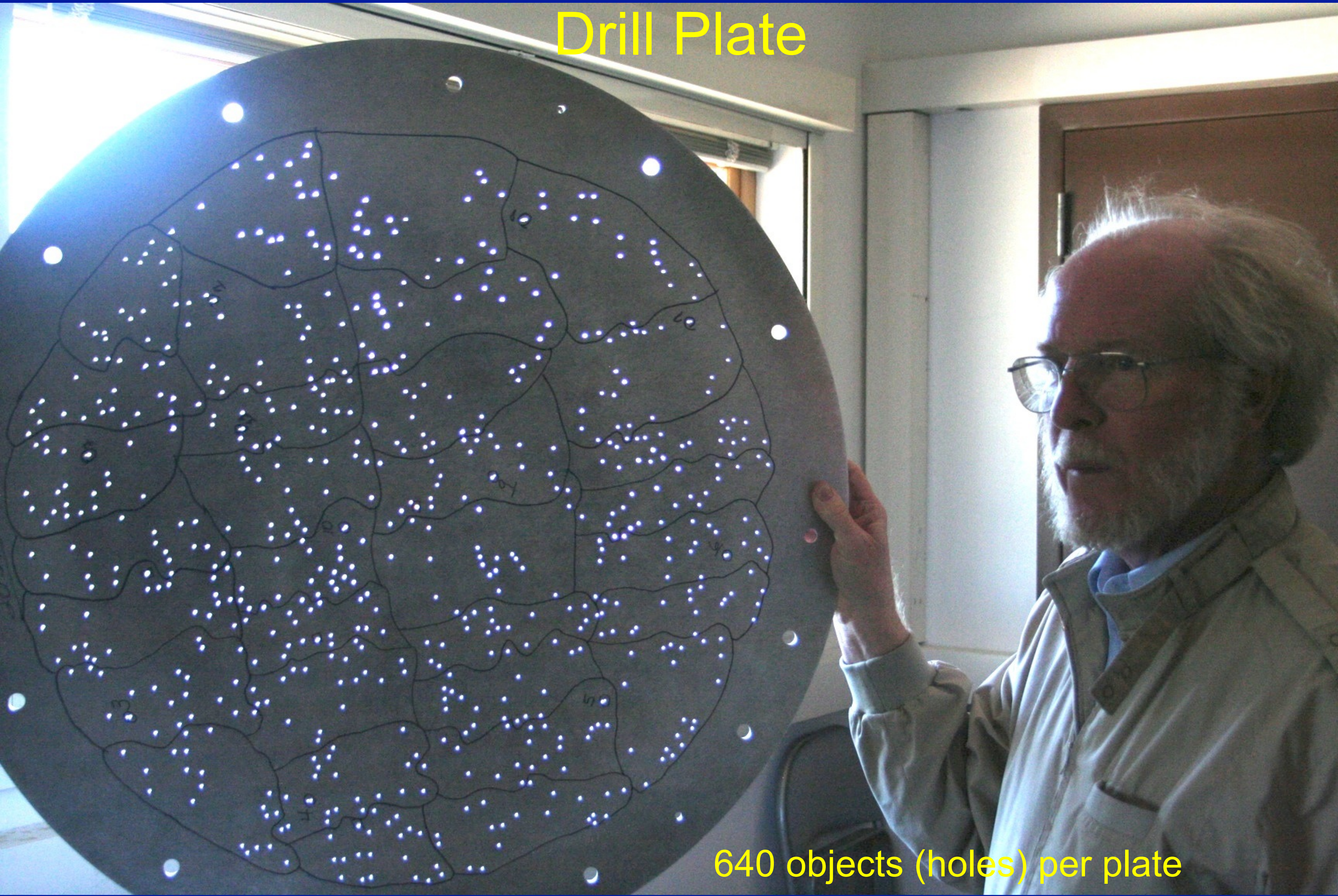

640 objects (holes) per plate

Fiber-optic cables

Plugging plates

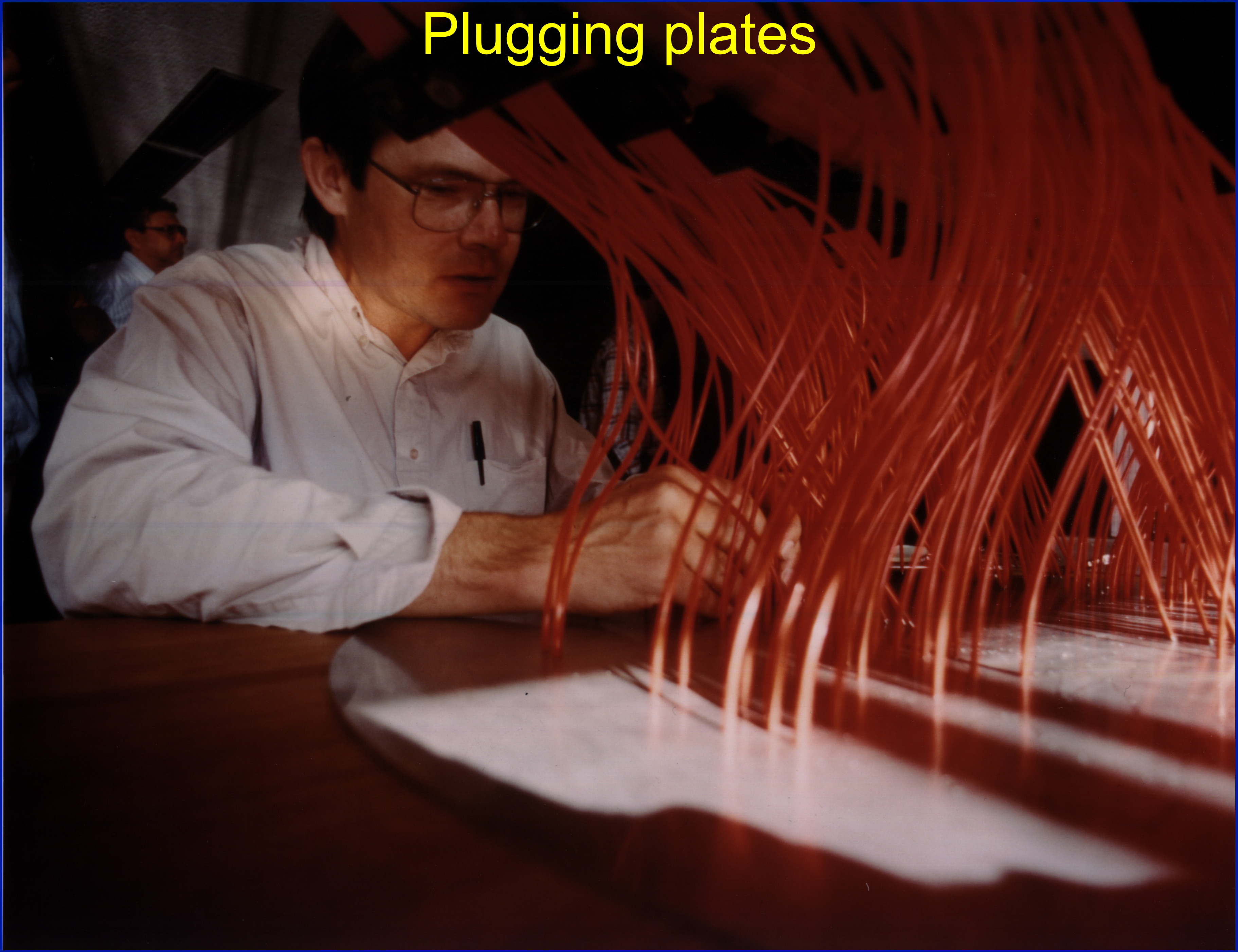

Spectrum

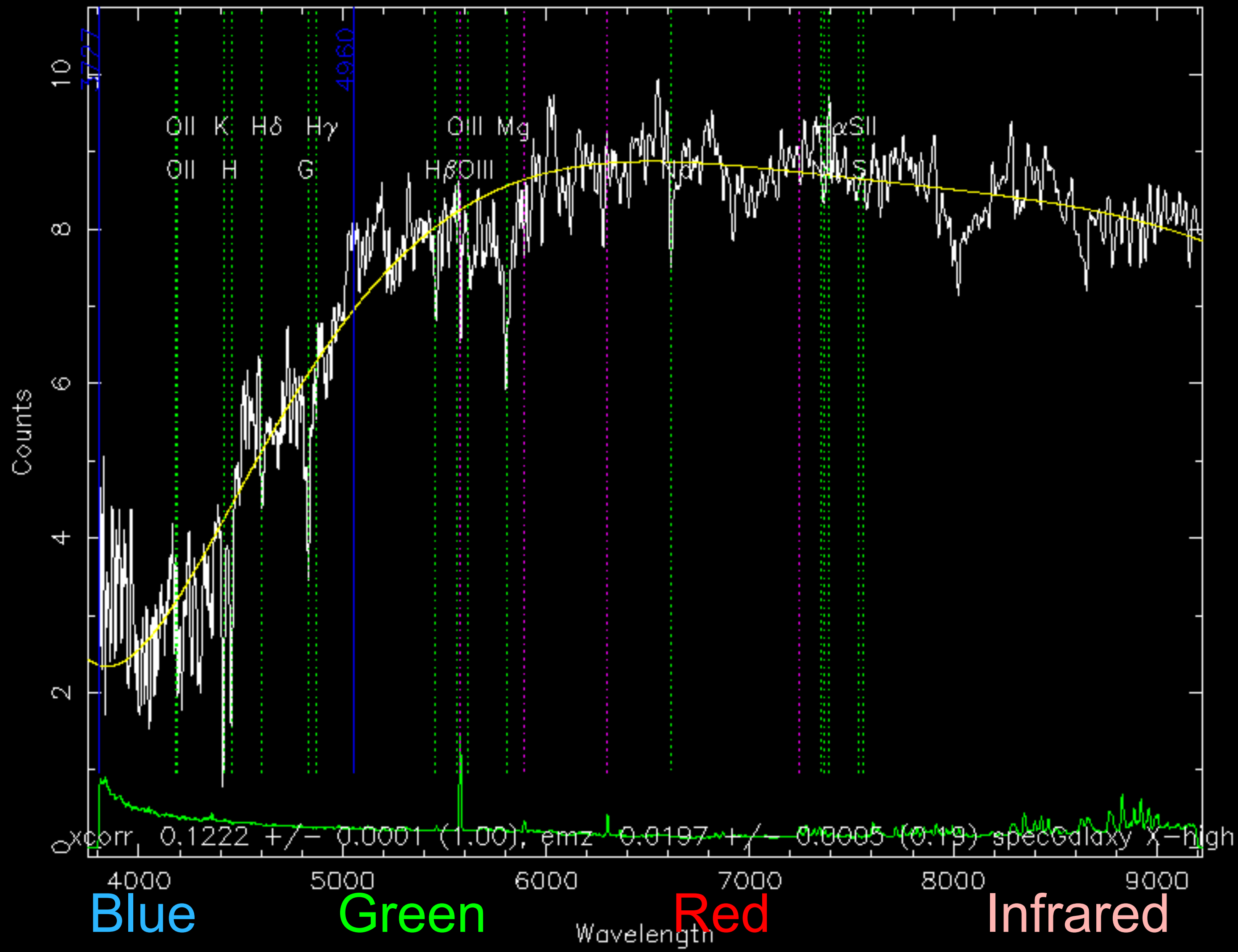

Wavelength of light


Over 2000 plates!

SDSS is state of the art!

- Imaging covering ¼ of sky : 100,000,000 galaxies detected
- Spectra of 1,500,000 galaxies and redshifts
- Also seen: stars in our galaxy, asteroids, quasars, etc…

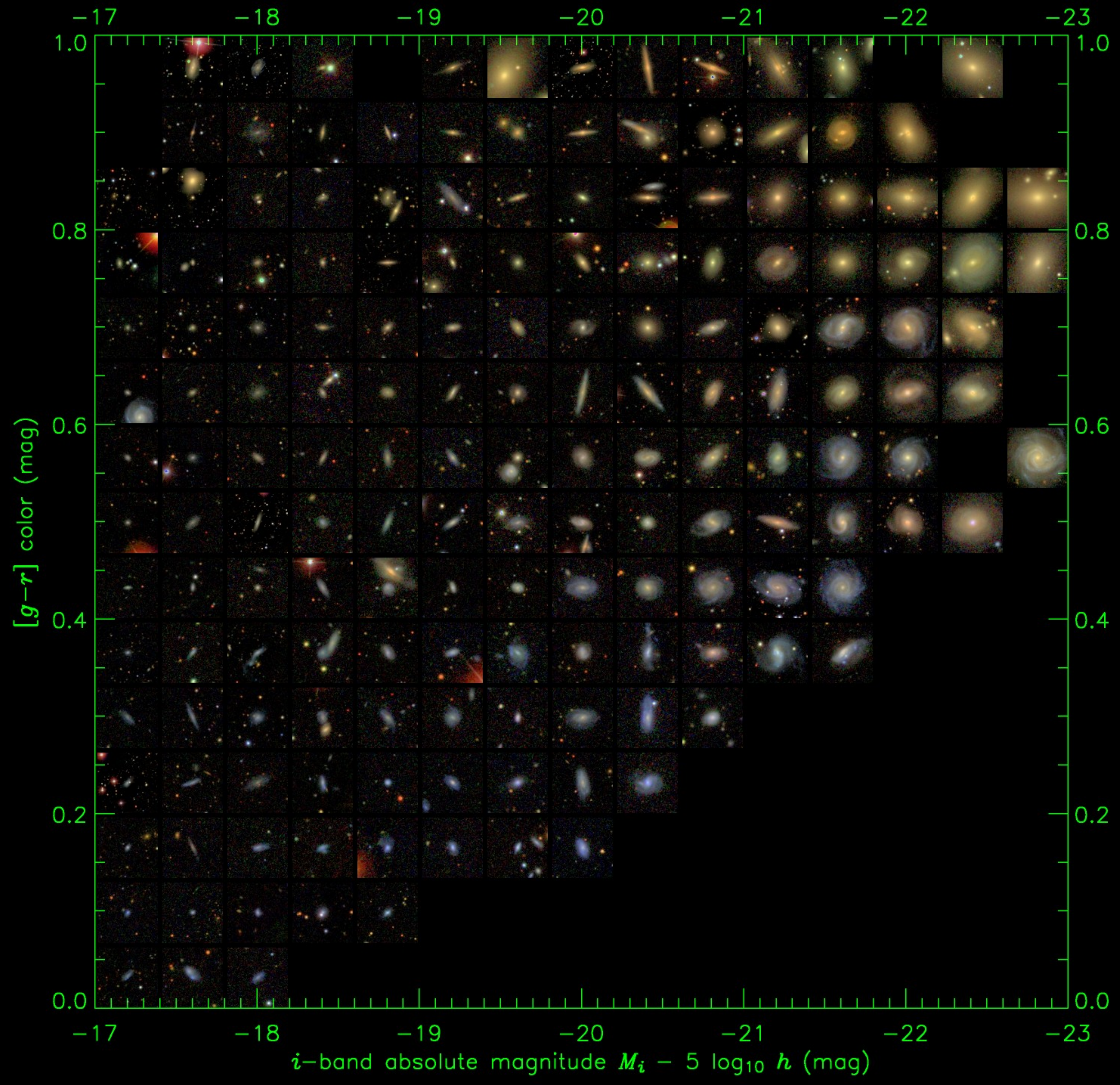

−17
−18
−19
−20
−21
−22
−23
1.0
0.8
0.6
0.4
0.2
0.0
[g−r] color (mag)
i−band absolute magnitude $M_i - 5 \log_{10} h$ (mag)

redshift-space distortions

Most galaxies move through space due to the gravitational pull of surrounding structures.

This motion is called *peculiar* motion.

Peculiar velocities cause doppler shifts, which add to the redshift.

Hubble flow "velocity": $H_0 d$

Radial component of peculiar velocity: v_r

Total radial "velocity": $H_0 d + v_r$

redshift-space distortions

Redshift according to the doppler effect is: $z = \frac{v_r}{c}$

So the inferred velocity from a measured redshift is: cz

And the inferred distance is: $d = \frac{cz}{H_0}$

But what is really being measured is: $\frac{cz}{H_0} = d + \frac{v_r}{H_0}$

redshift-space distortions

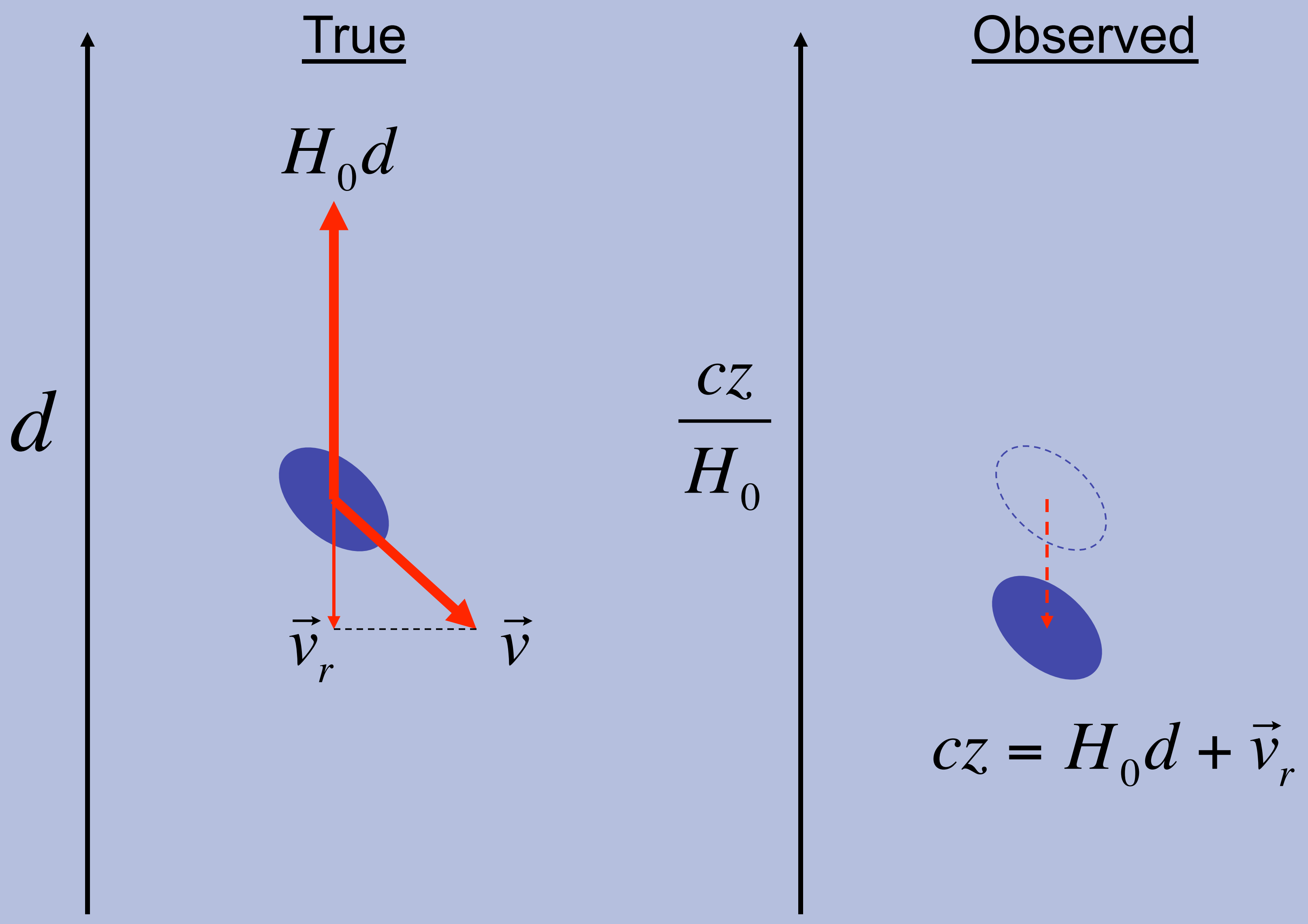

redshift-space distortions

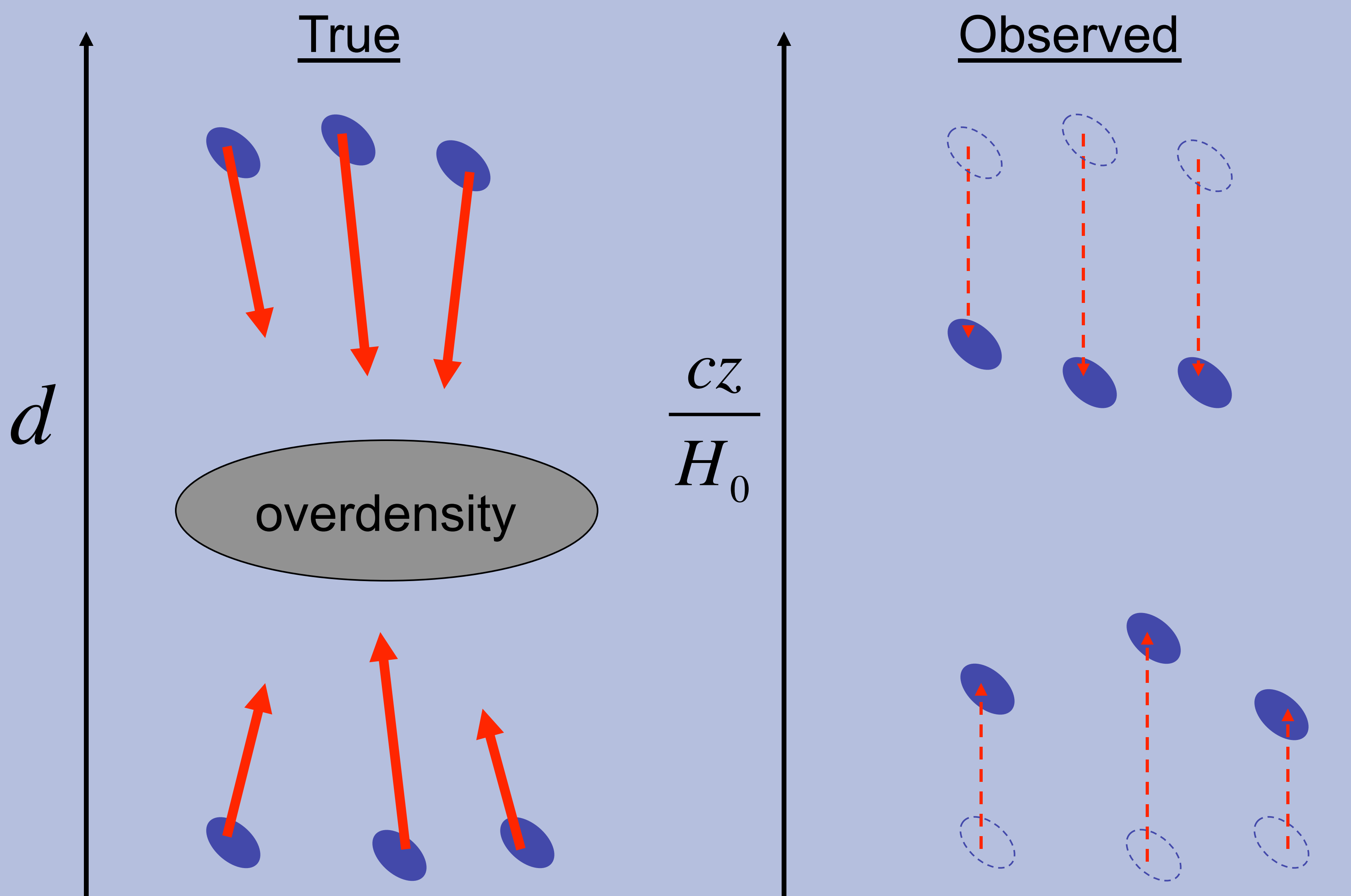

redshift-space distortions

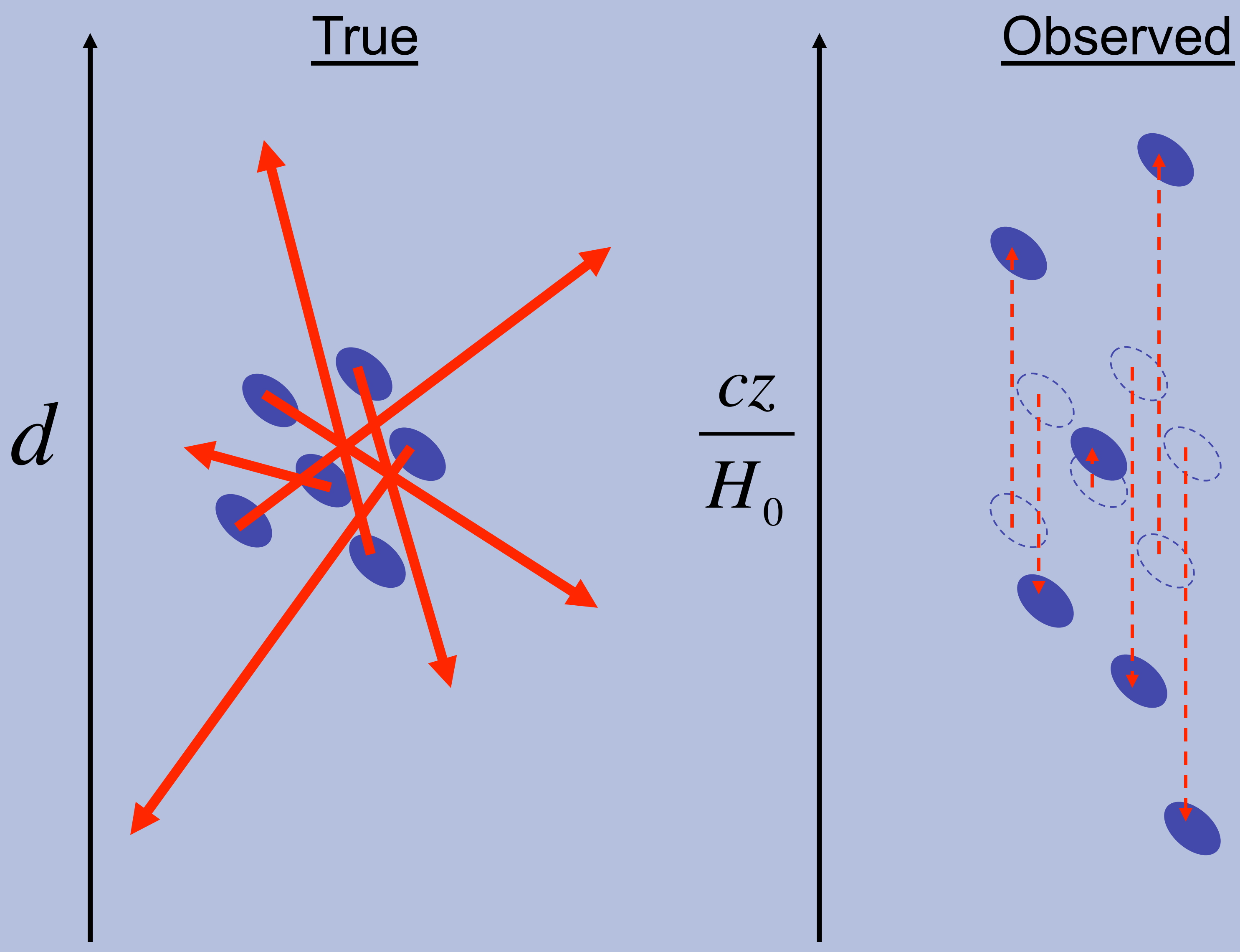

redshift-space distortions

real-space

$9.9 \times 10^{14} M_{\odot}$

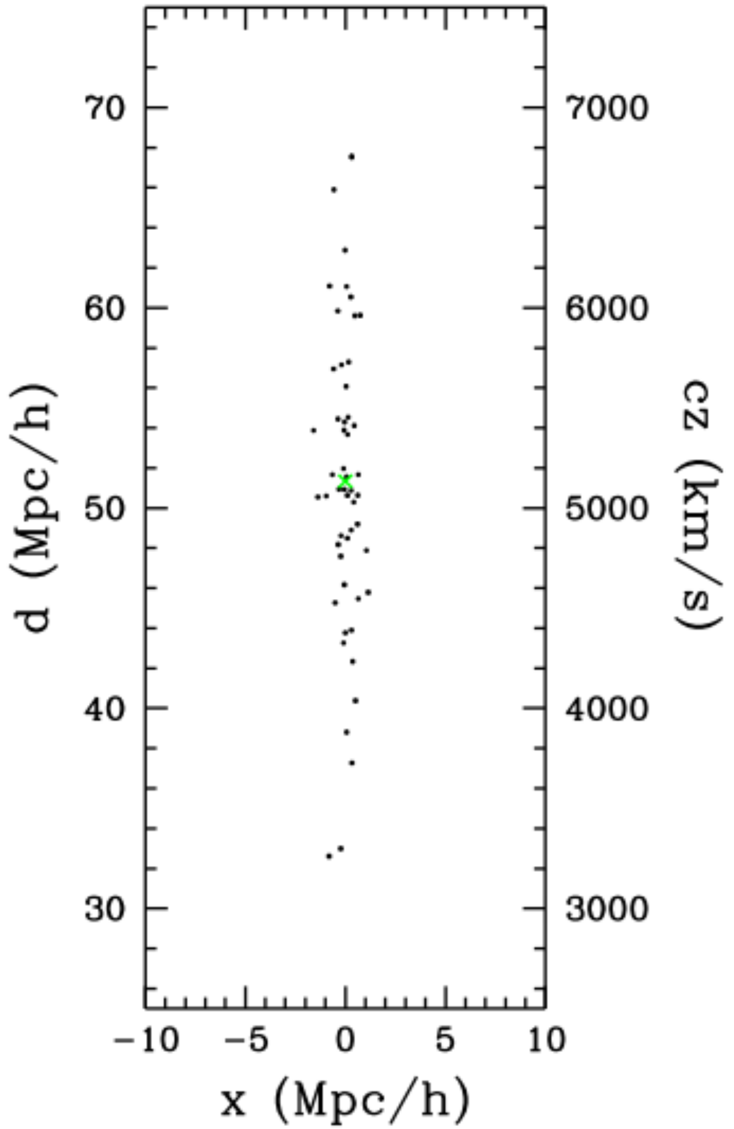

$9.5 \times 10^{13} M_{\odot}$

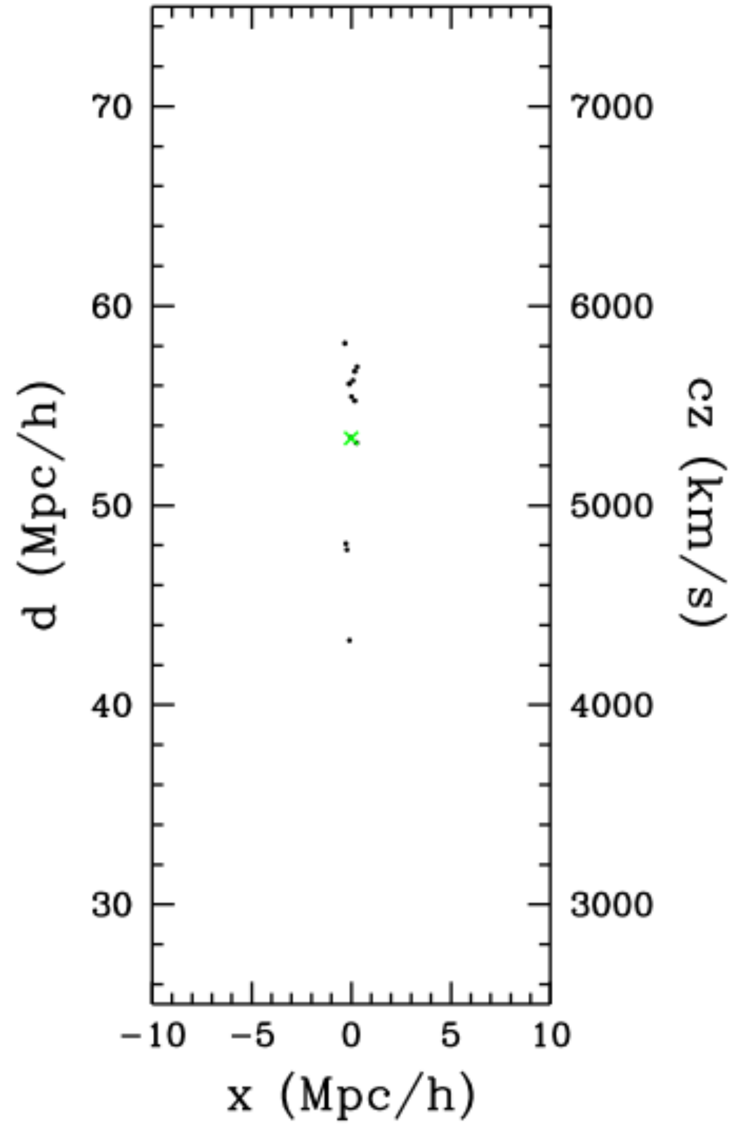

redshift-space distortions

- Large scales: compression

$$H_0 R > \langle v_{\rm pec} \rangle$$

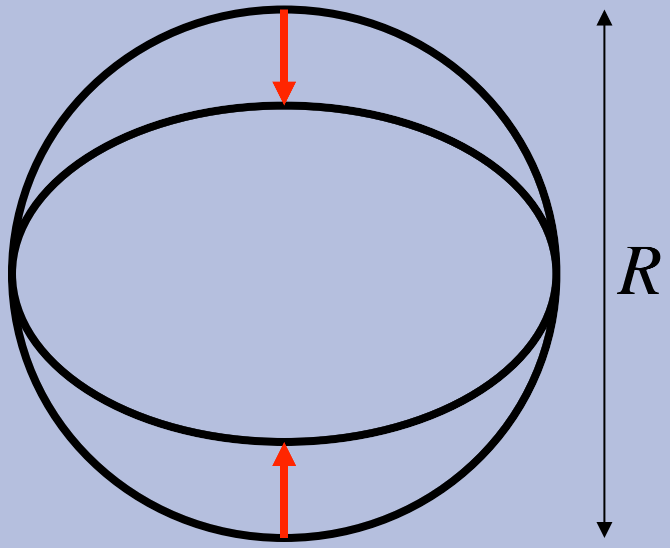

- Small scales: smearing (fingers of God)

$$H_0 R < \langle v_{\rm pec} \rangle$$

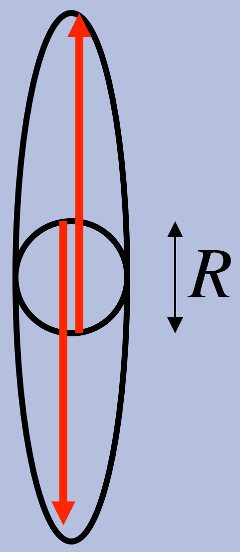

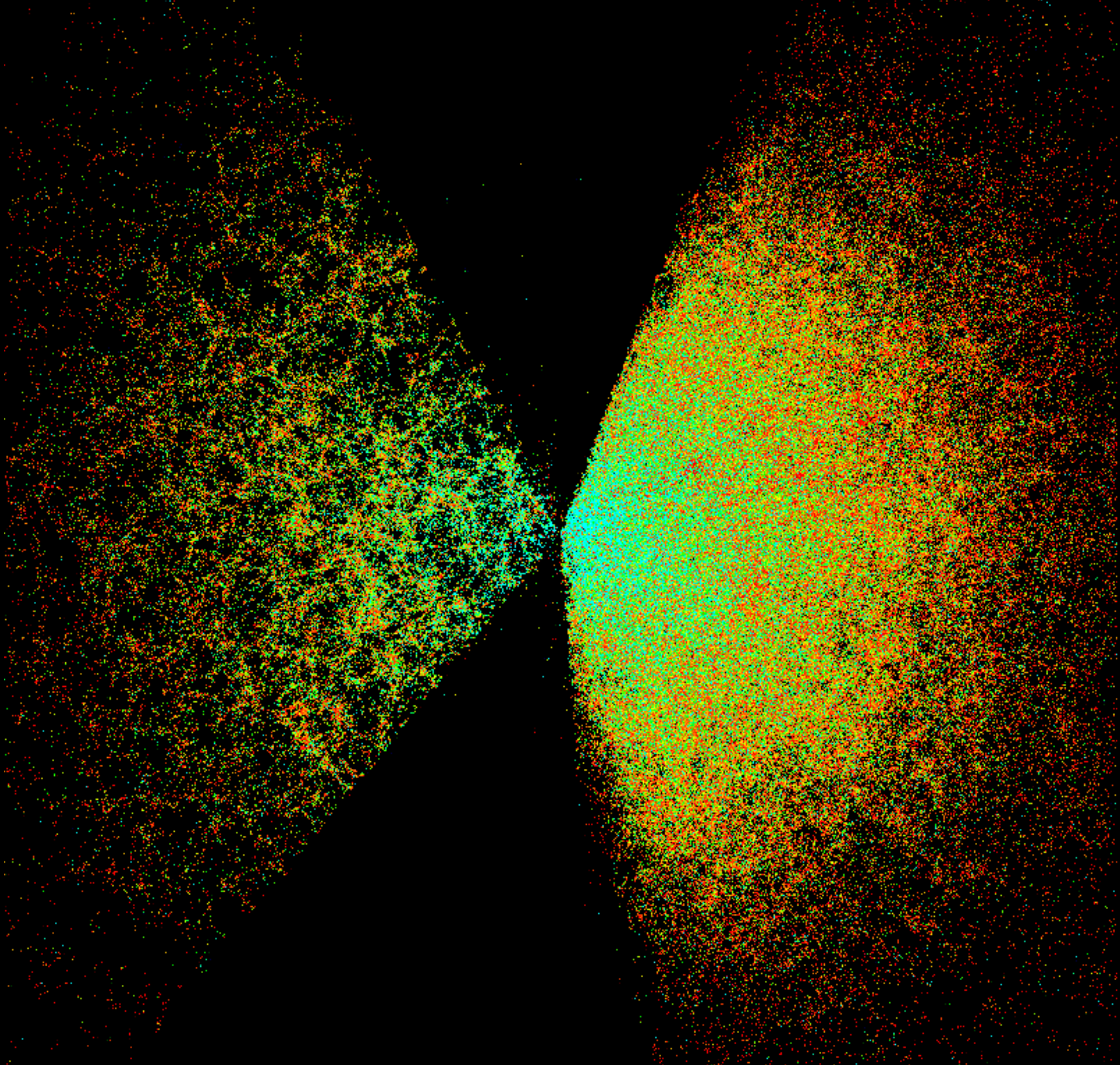

Redshift as distance estimator

$$d = \frac{cz}{H_0} - \frac{v_r}{H_0}$$

$$\sigma_d = \frac{v_r}{H_0} \rightarrow \frac{\sigma_d}{d} = \frac{v_r}{H_0 d}$$

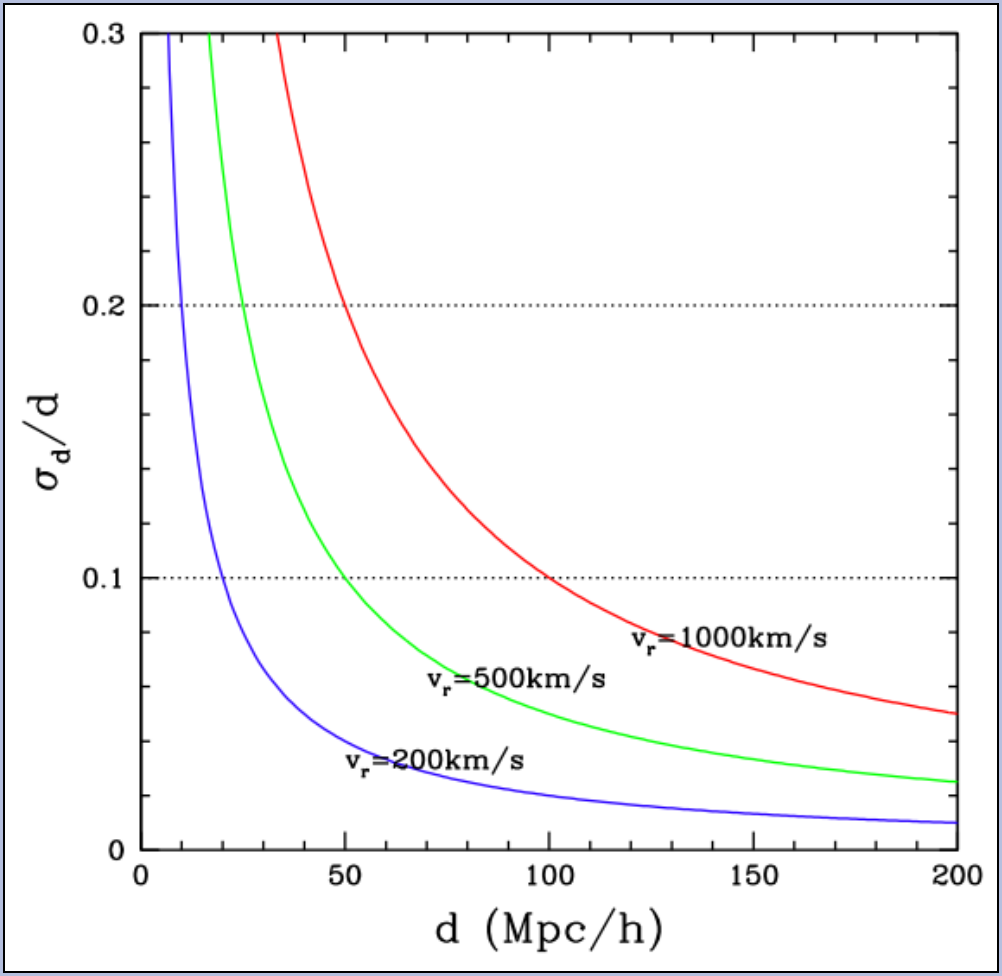

Redshift wins over other distance indicators at large distance.

Redshift

$$z = \frac{\lambda_{\text{obs}} - \lambda_{\text{emit}}}{\lambda_{\text{emit}}}$$

Cosmological + Doppler redshift

$$1 + z_{\text{cosm}} = \frac{1}{a(t)}$$

$$z_{\text{doppler}} \simeq \frac{v_r}{c}$$

$$1 + z = \left(1 + z_{\text{cosm}}\right)\left(1 + z_{\text{doppler}}\right)$$

Redshift Surveys

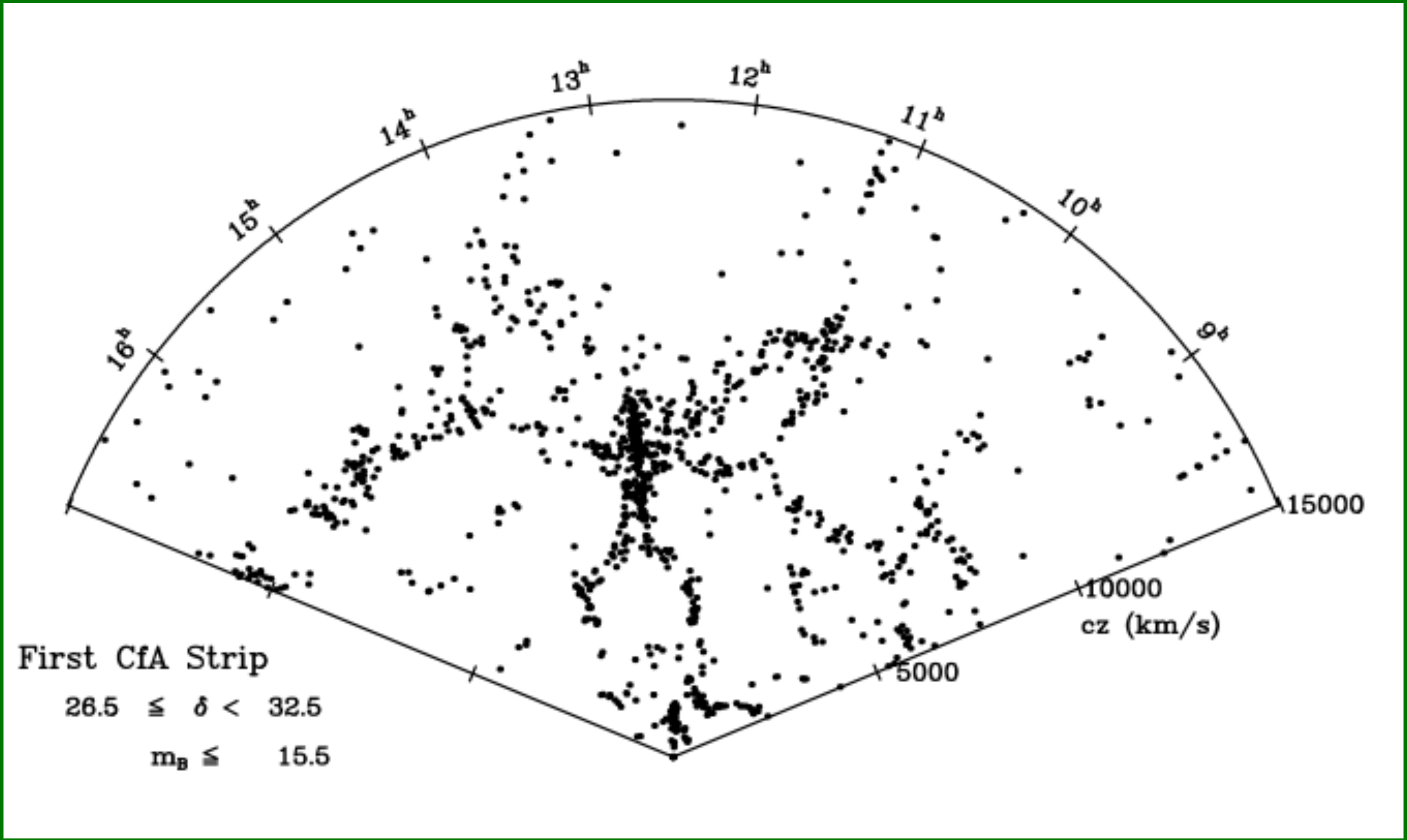

CfA survey

Redshift Surveys

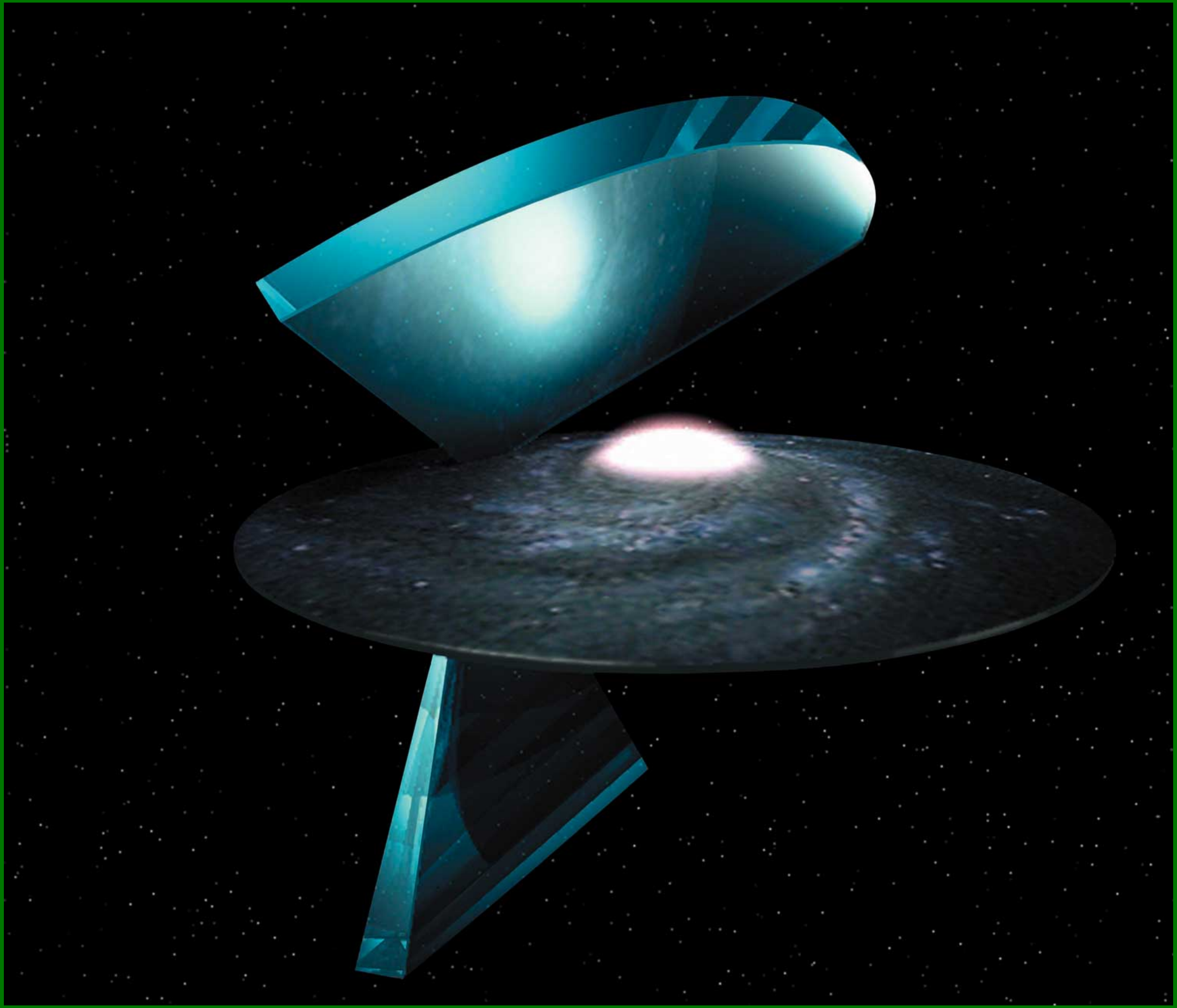

2dF survey

Redshift Surveys

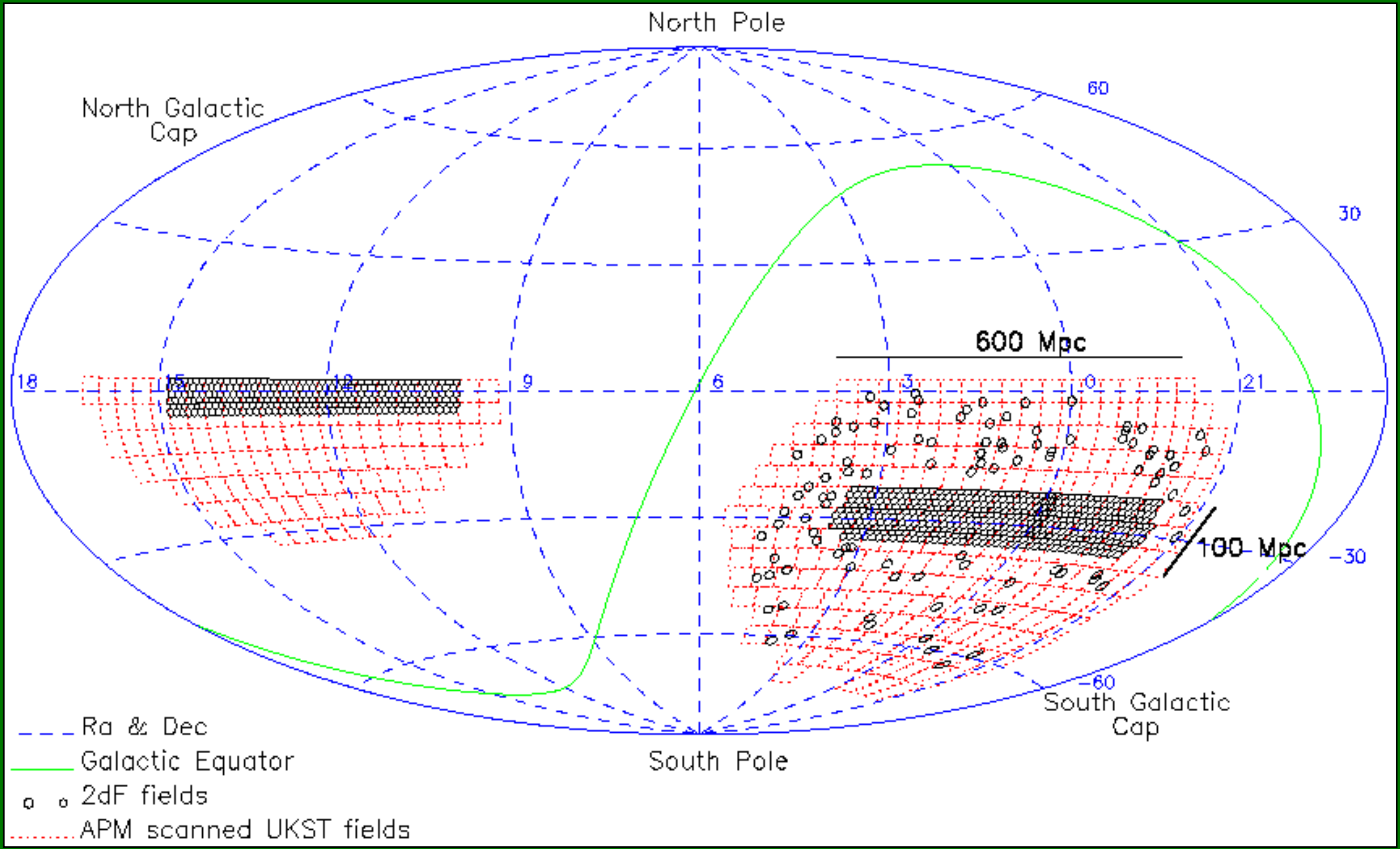

2dF survey

Redshift Surveys

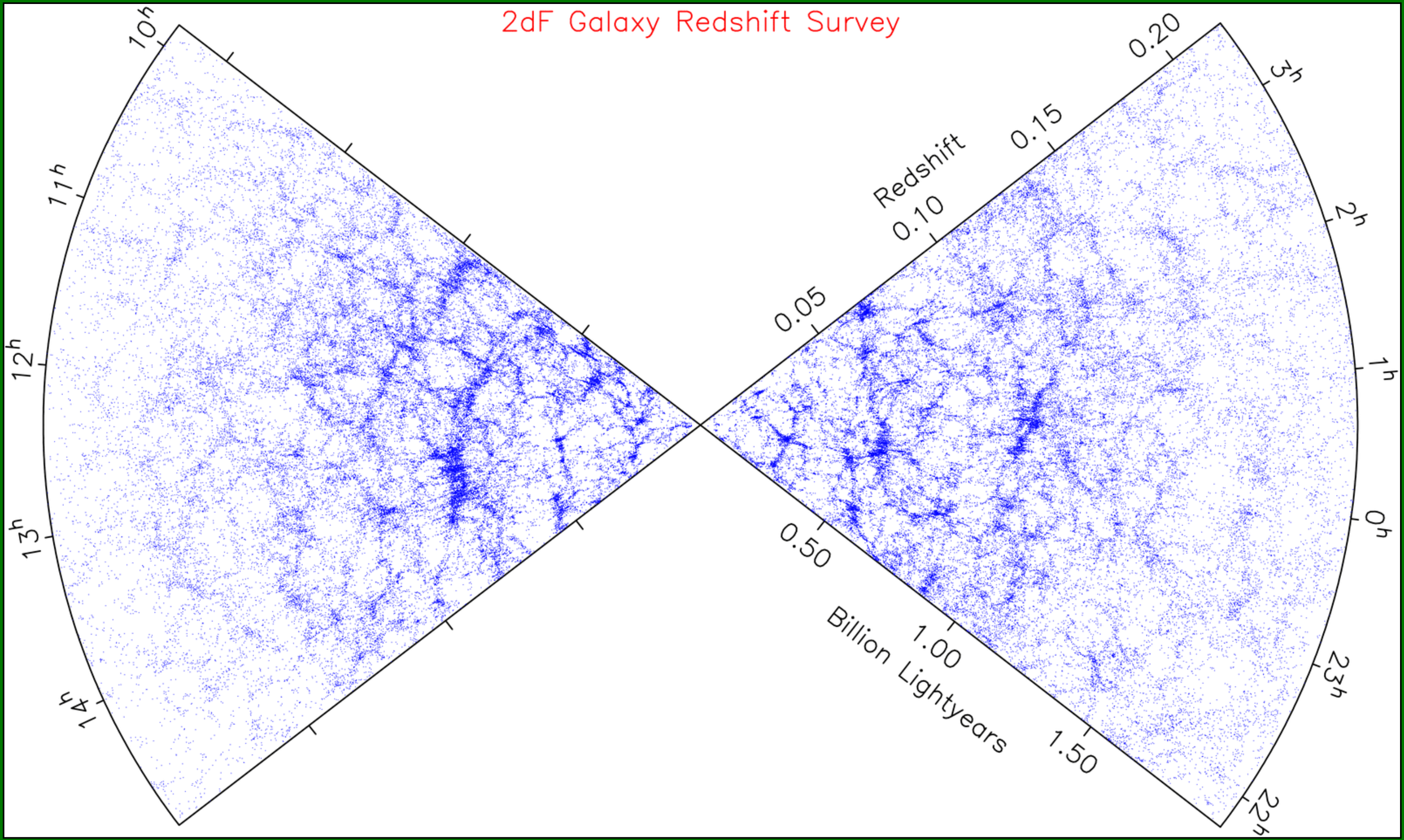

2dF survey

Redshift Surveys

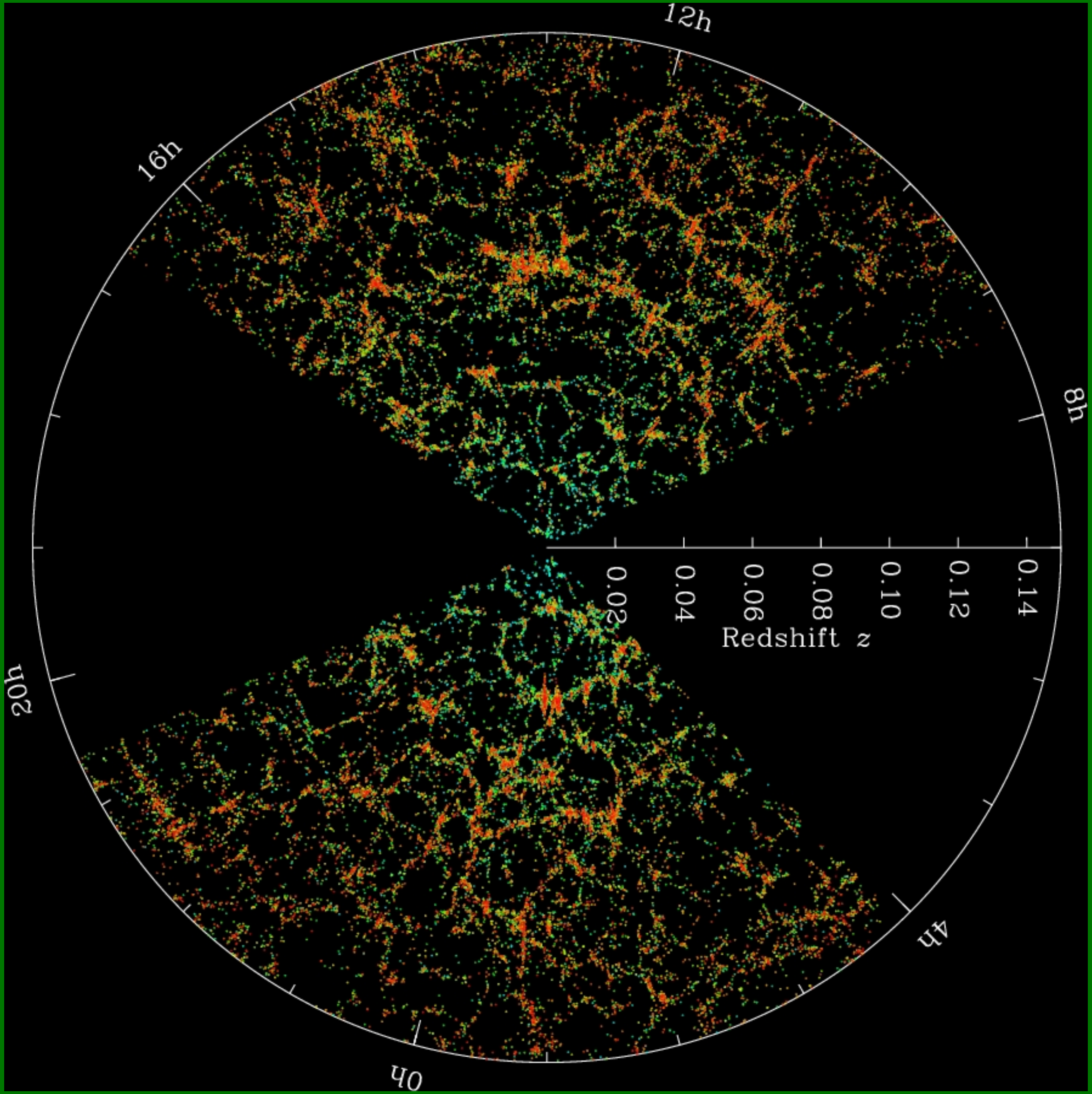

SDSS Main

Redshift Surveys

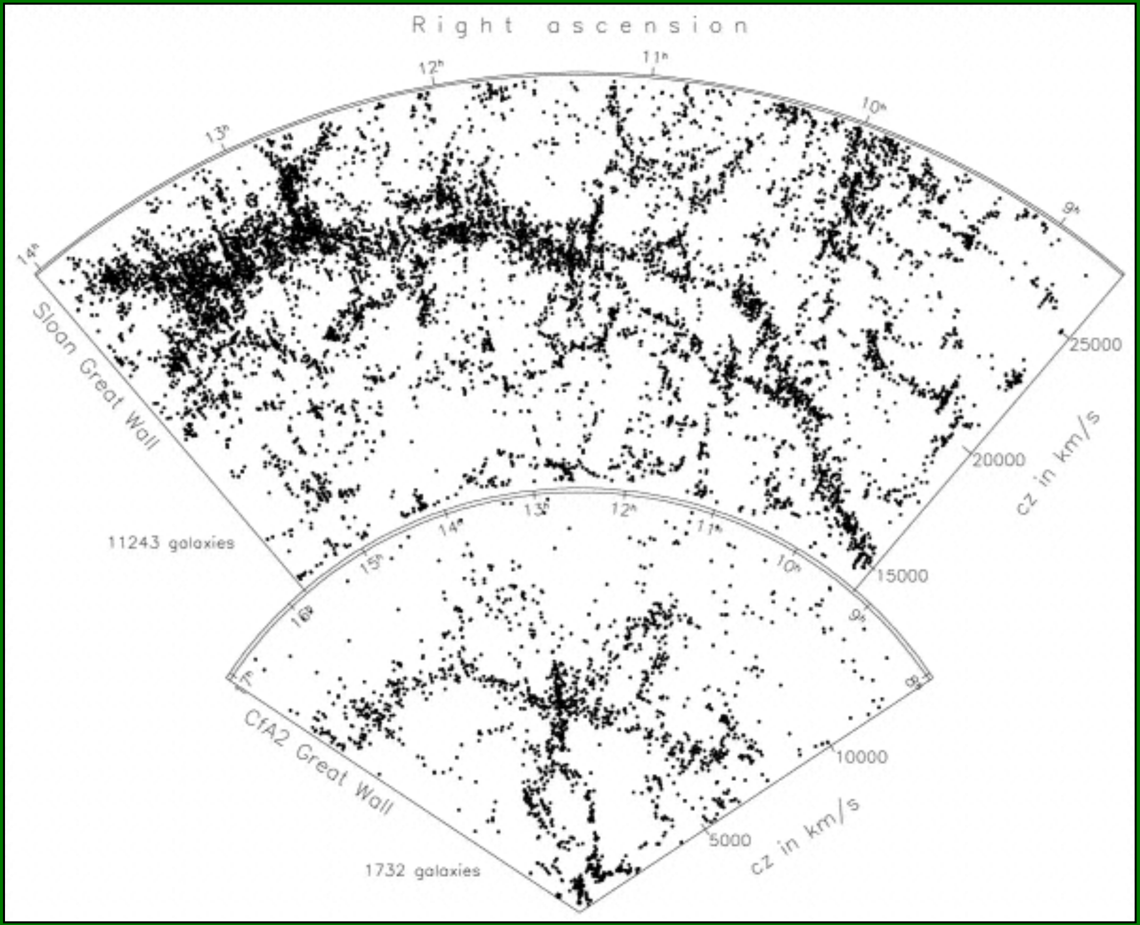

SDSS Main

Redshift Surveys

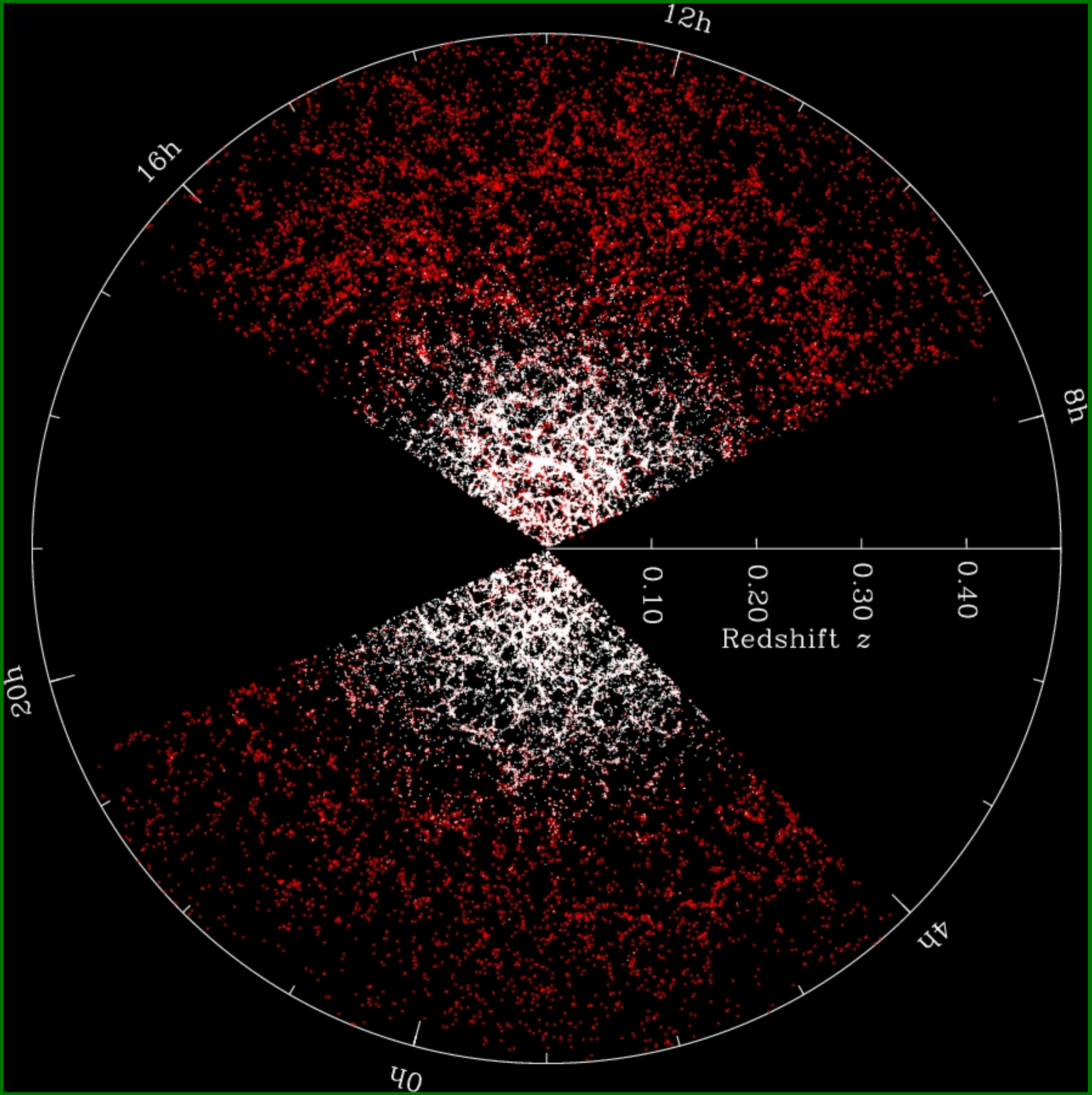

SDSS LRG

Redshift Surveys

SURVEY	YEARS	N_{gals}	d_{max}	Area
CfA	1977-1982	2,395	150 Mpc	N
CfA2	1985-1995	18,000	150 Mpc	N
SSRS2	1994	5,500	150 Mpc	S
PSCz	1998	15,000	150 Mpc	All-sky
LCRS	1996	25,000	600 Mpc	N+S Slices 700 deg^2
2dF	2001	250,000	600 Mpc	N+S 1500 deg^2
SDSS	1998-2008	1 million	600 Mpc	1/5 of sky
SDSS LRG	1998-2008	100,000	1 Gpc	1/5 of sky
DEEP2	2002-2005	50,000	2-3 Gpc	3 deg^2
VVDS	2002-2010	150,000	2-3 Gpc	16 deg^2
SDSS 3	2008-2014	1.5 million	1.8 Gpc	1/4 of sky
SDSS 4	2014-2020	?	2.4 Gpc	1/4 of sky

Redshift Surveys

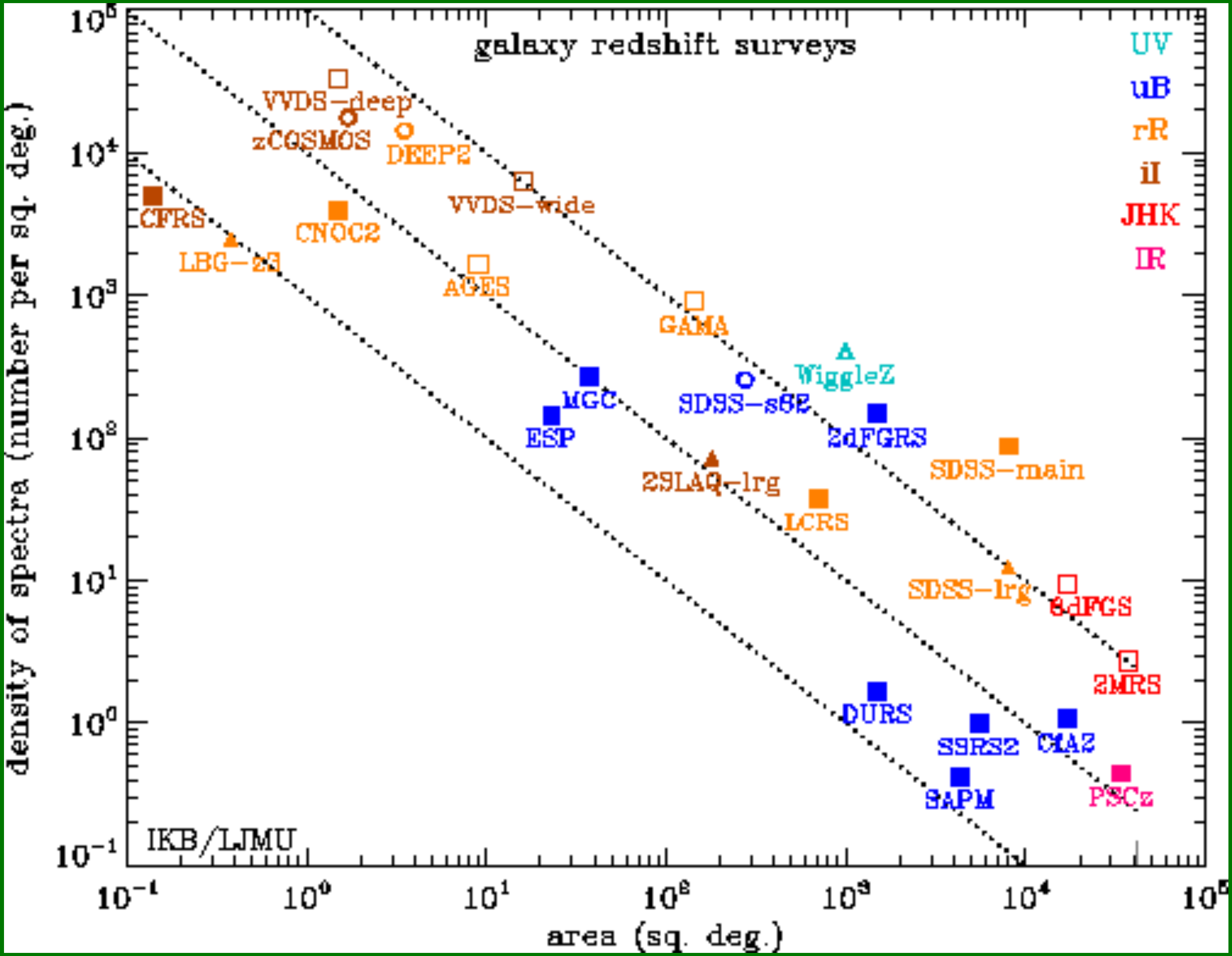

Flux/Magnitude-limited and Volume-limited samples

Surveys typically have a flux limit (i.e., minimum detectable flux) that corresponds to integration time and instrument sensitivity.

SDSS imaging detected galaxies down to *r ~ 22.2*
(telescope diameter=2.5m, integration time=54.1s)

SDSS spectra were taken for galaxies down to *r ~ 17.77*
(integration time=45-60min)

$$f = \frac{L}{4\pi d^2} \rightarrow L_{\min} = 4\pi d^2 f_{\lim}$$

$$m - M = 5\log d - 5 \rightarrow M_{\max} = m_{\lim} - 5\log d + 5$$

Flux/Magnitude-limited and Volume-limited samples

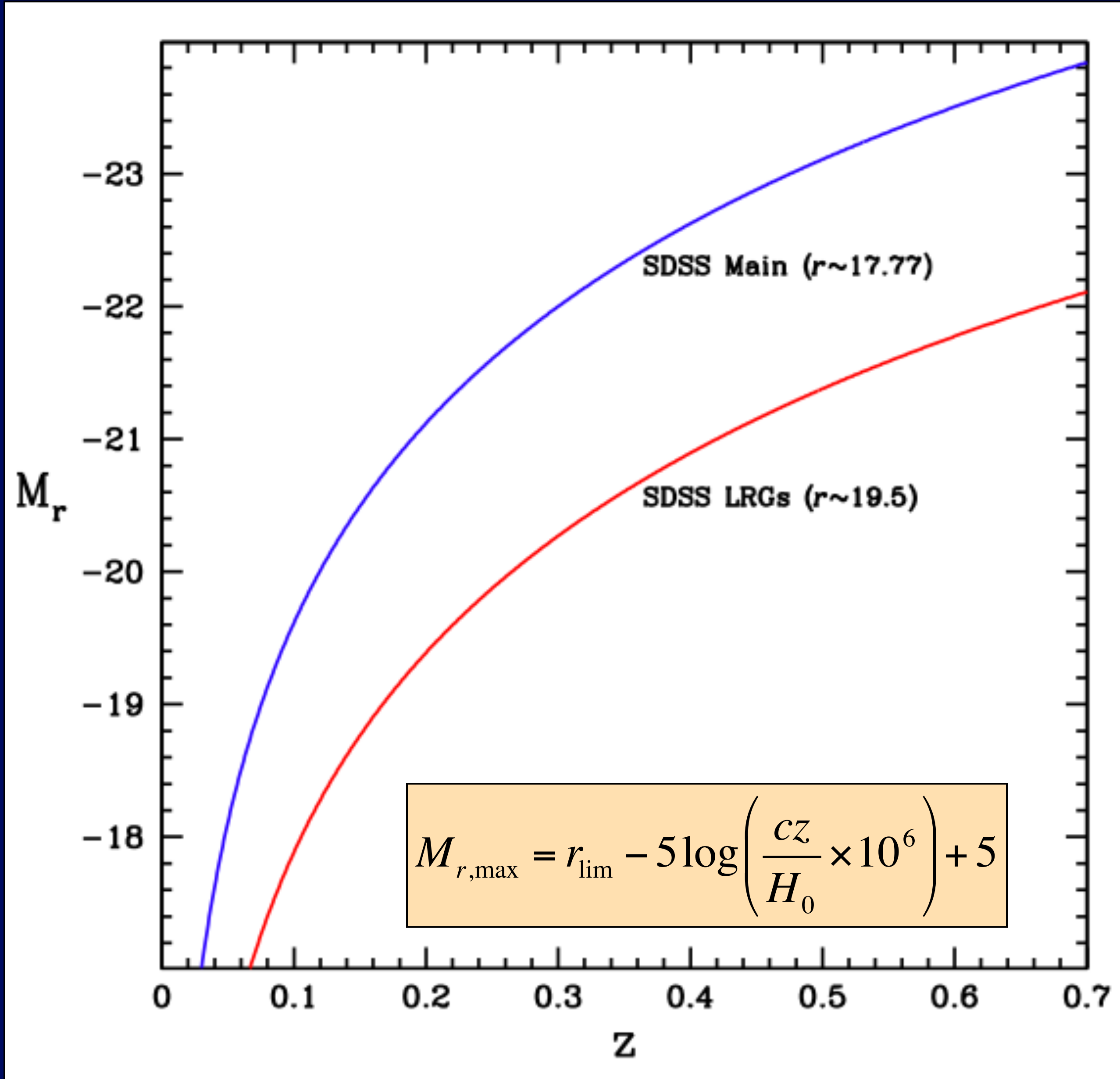

$$M_{r,\max} = r_{\lim} - 5\log\left(\frac{cz}{H_0}\times 10^6\right) + 5$$

Flux/Magnitude-limited and Volume-limited samples

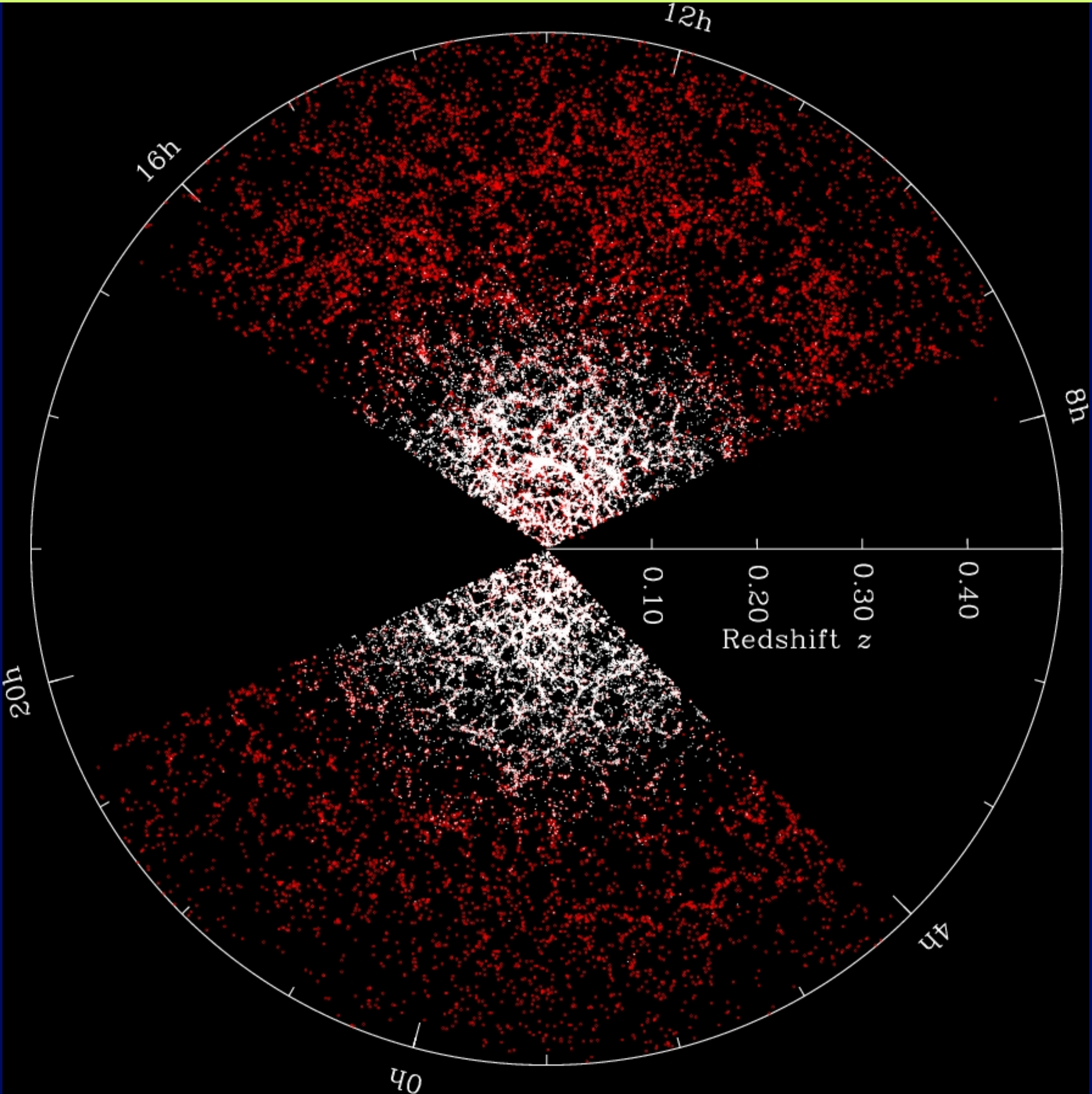

Flux/Magnitude-limited and Volume-limited samples

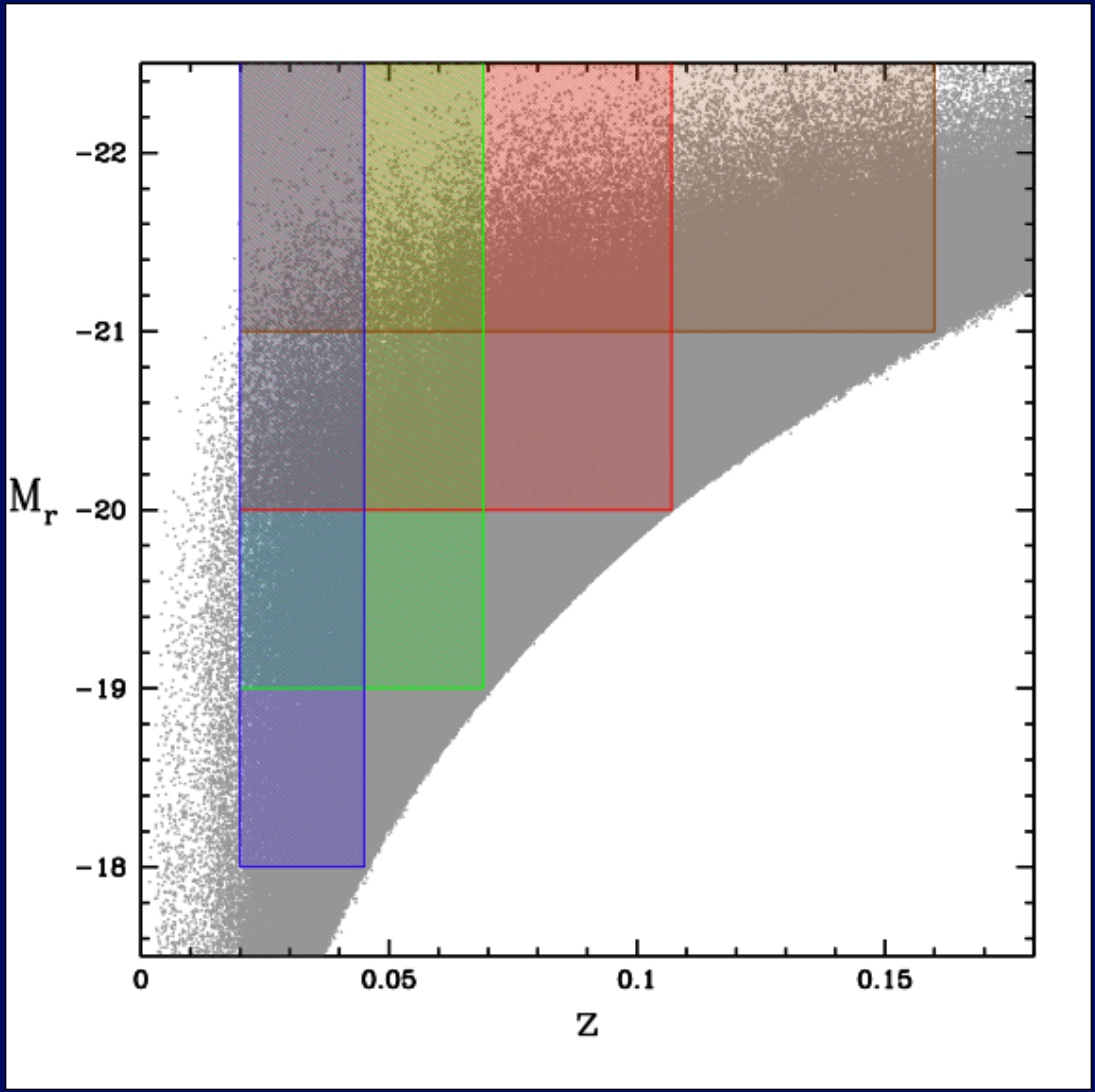

Flux/Magnitude-limited and Volume-limited samples

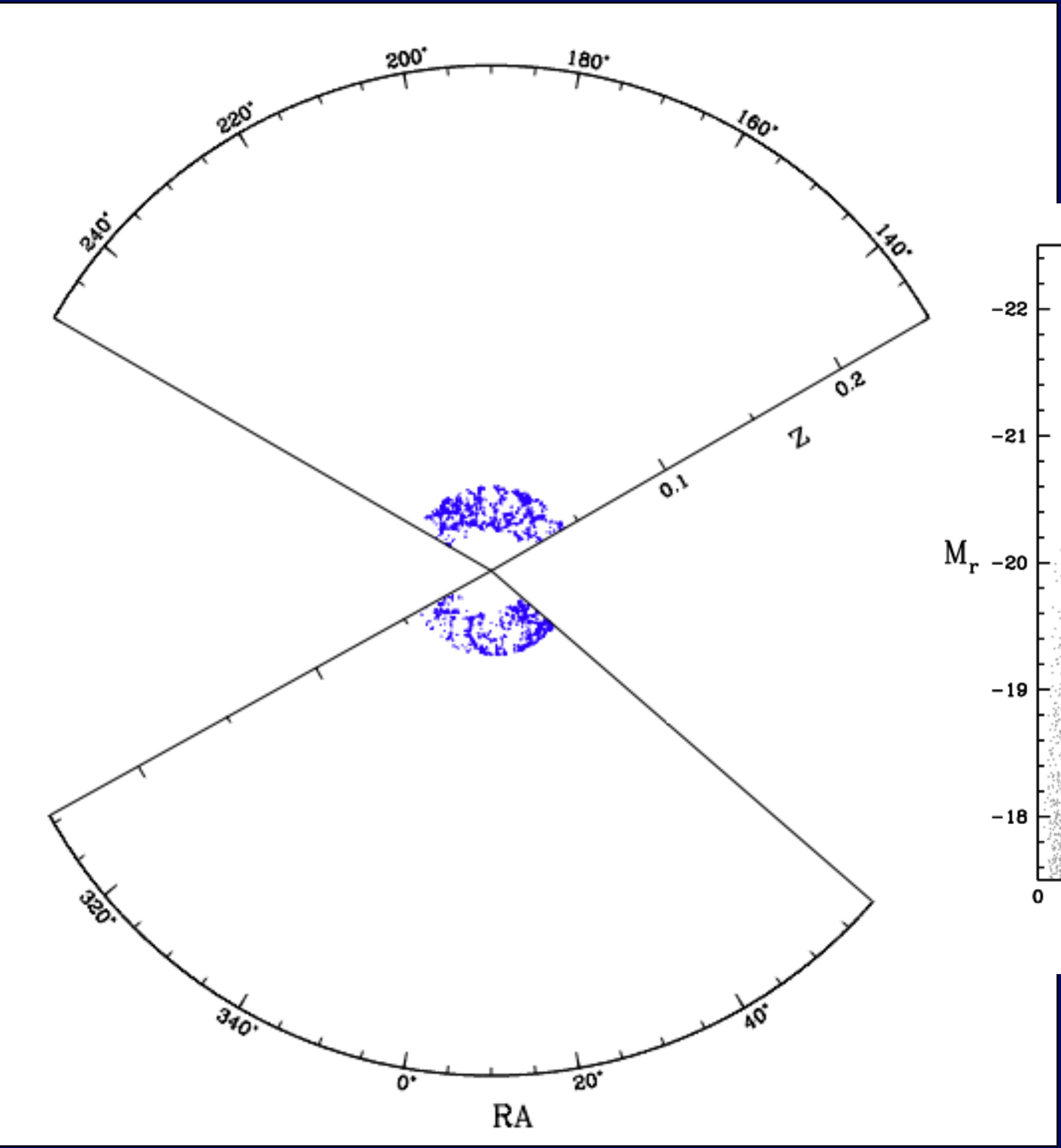

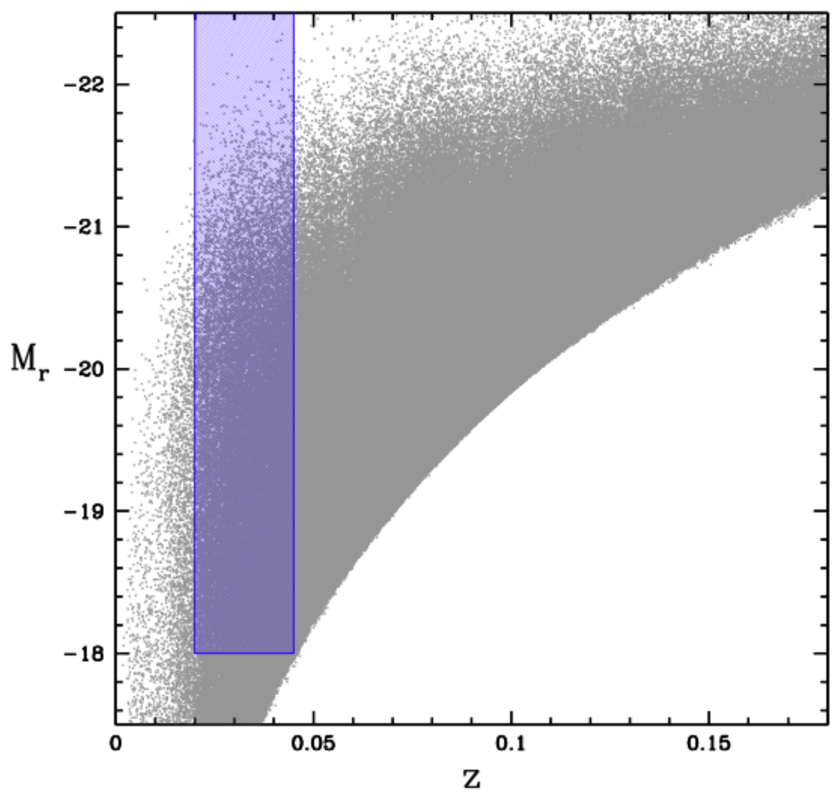

A simple example

What is the fraction of red and blue galaxies in the universe?

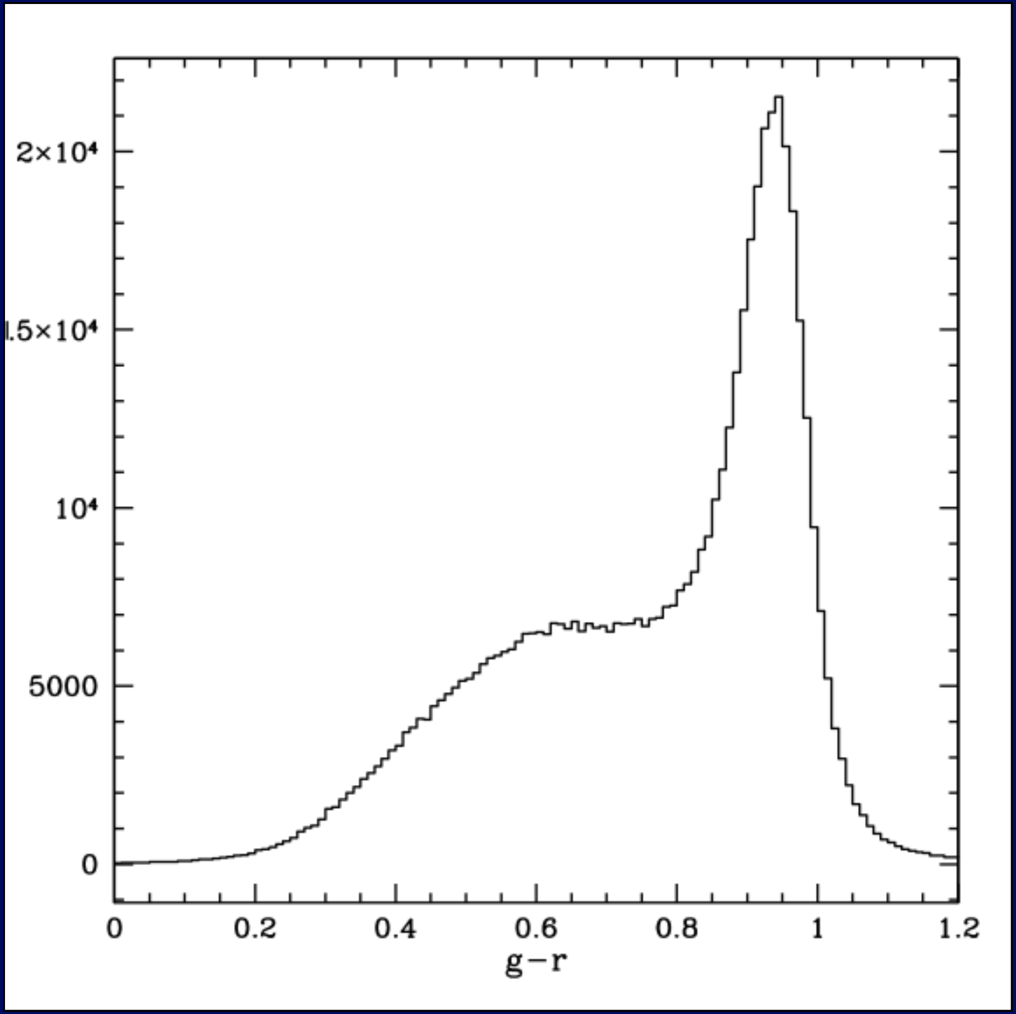

A simple example

What is the fraction of red and blue galaxies in the universe?

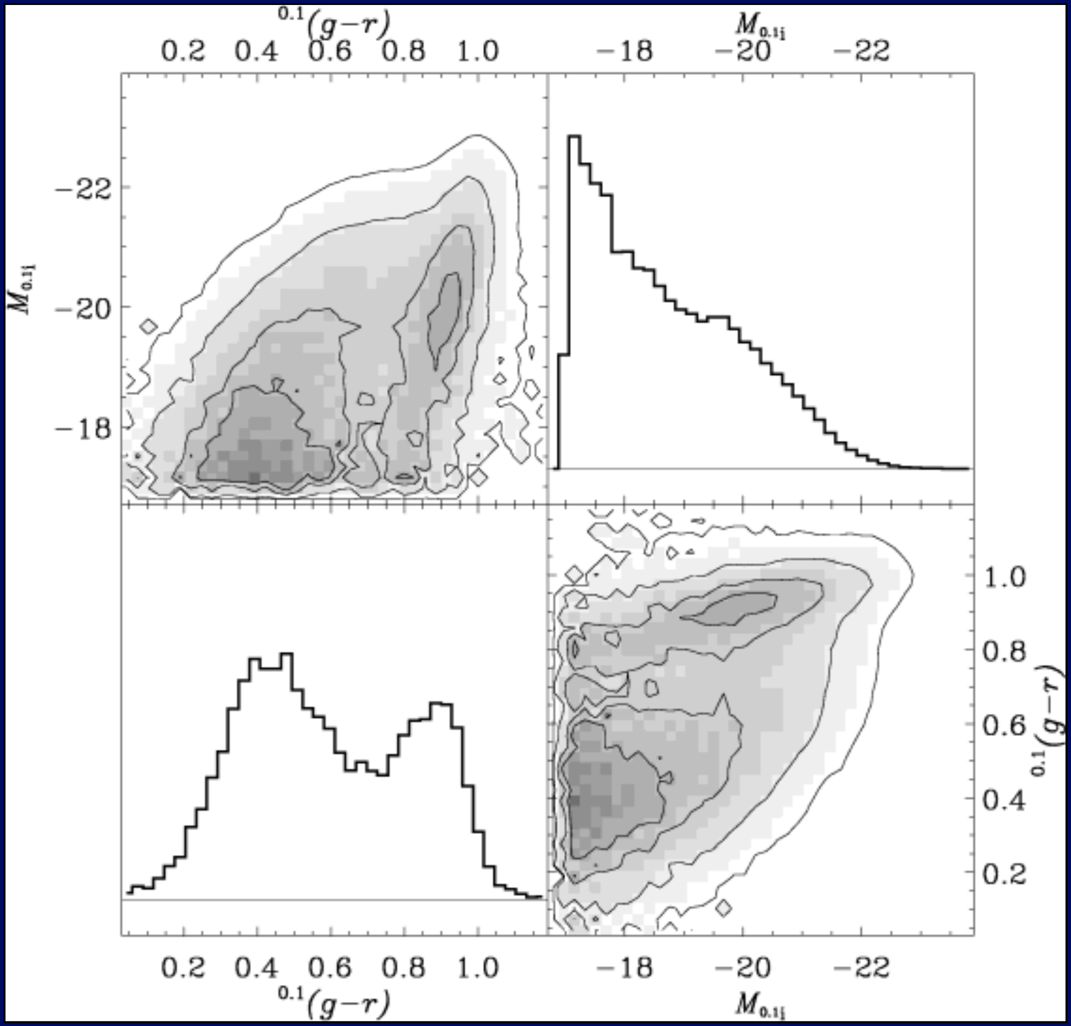

A simple example

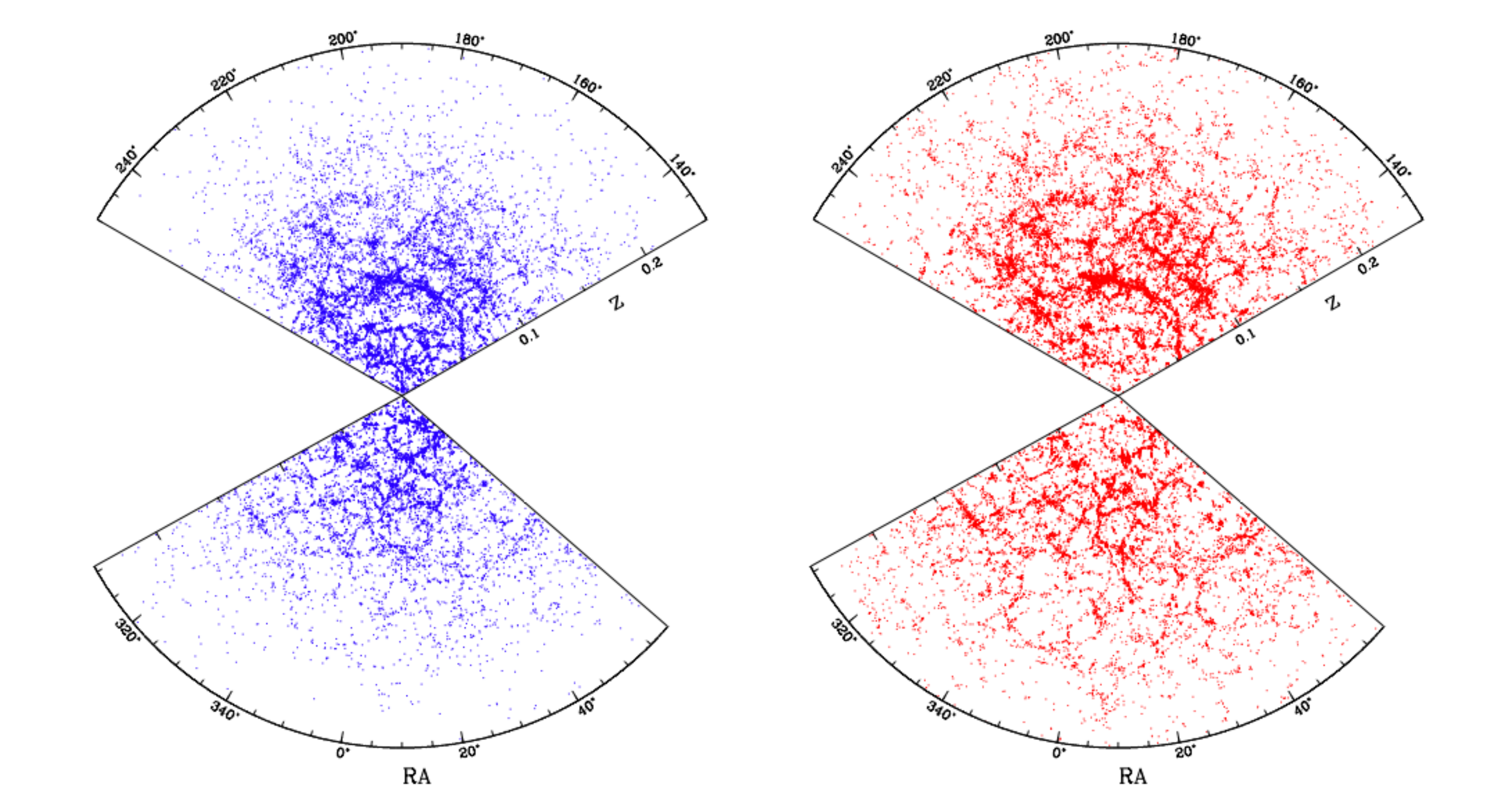

A simple example

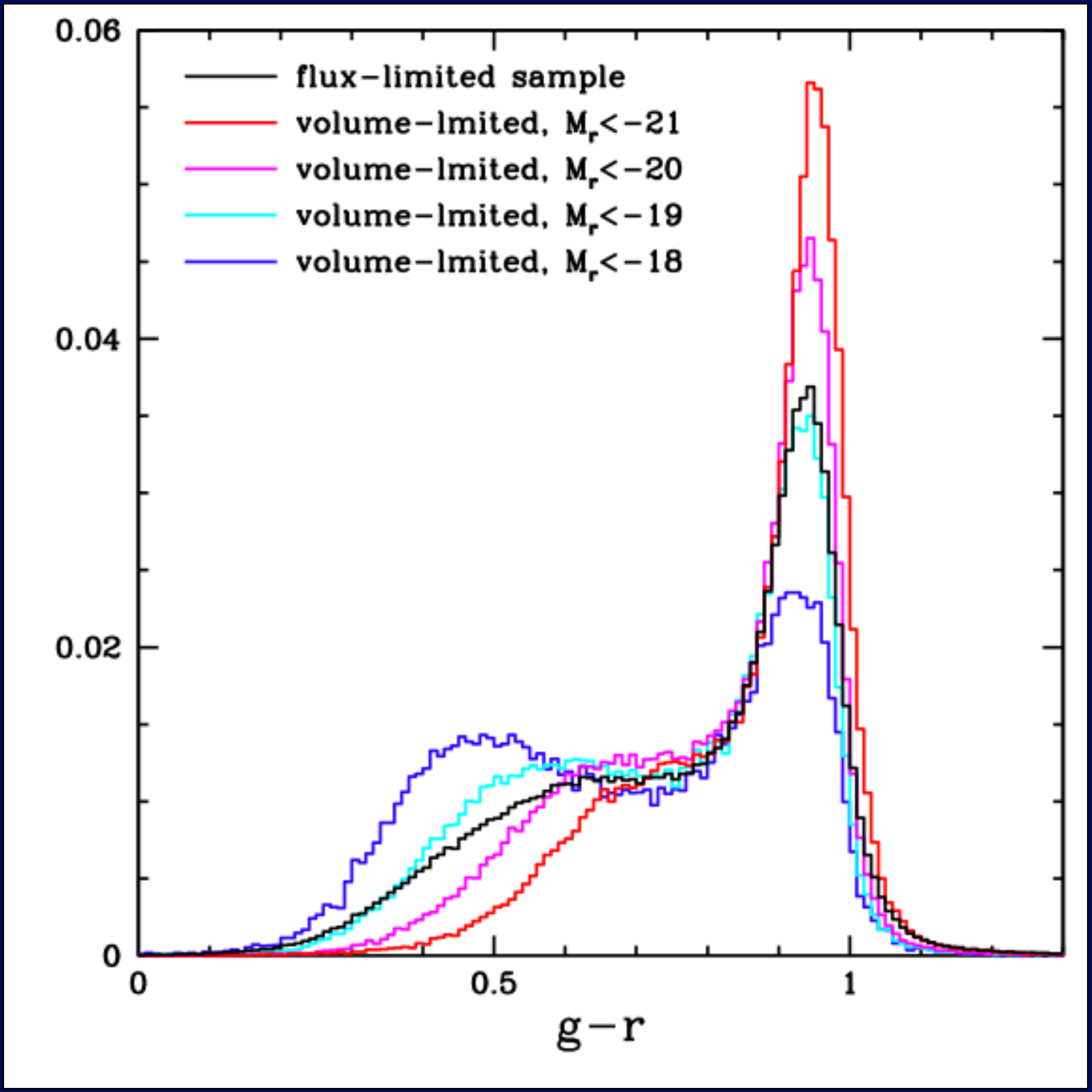

Bimodality

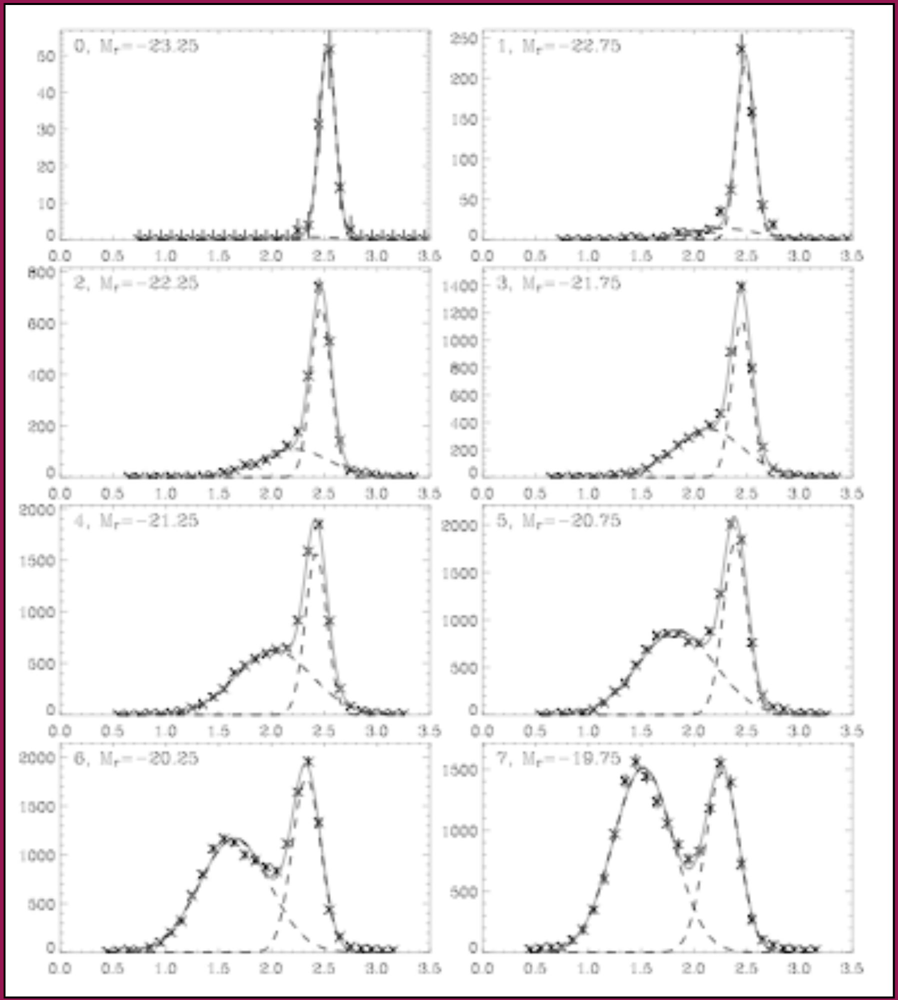

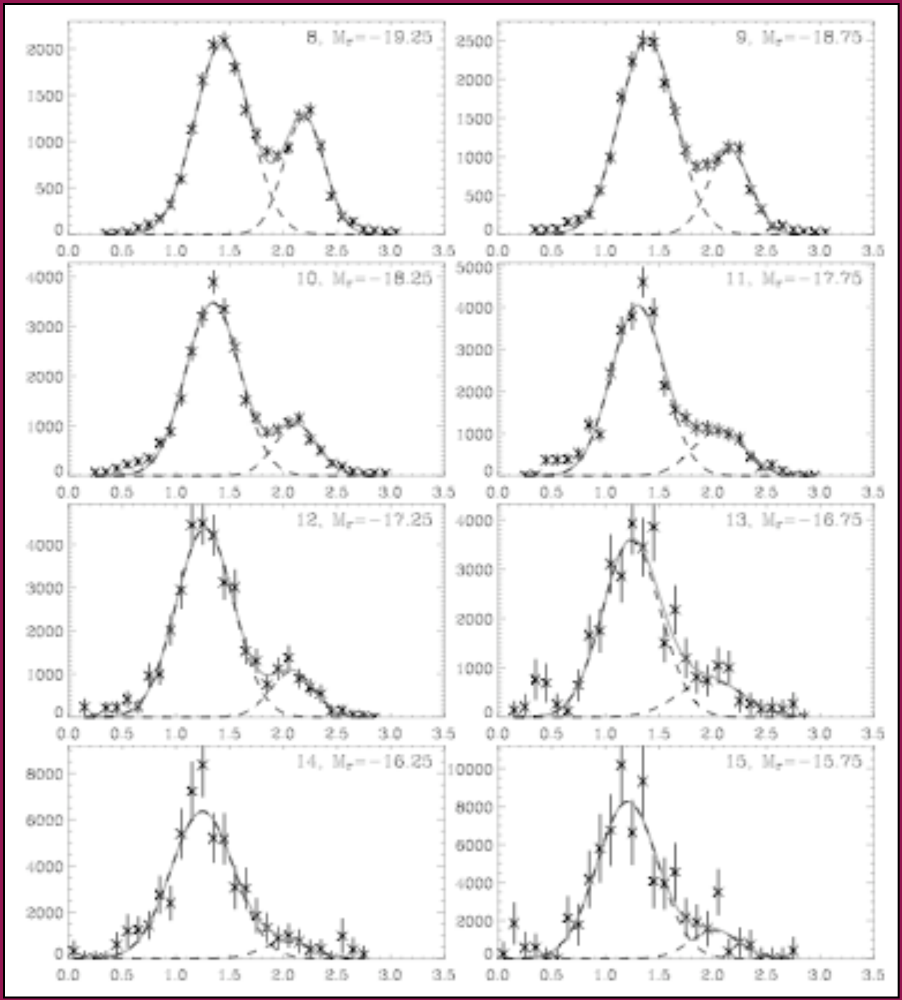

u-r

Baldry et al. (2004)

Bimodality

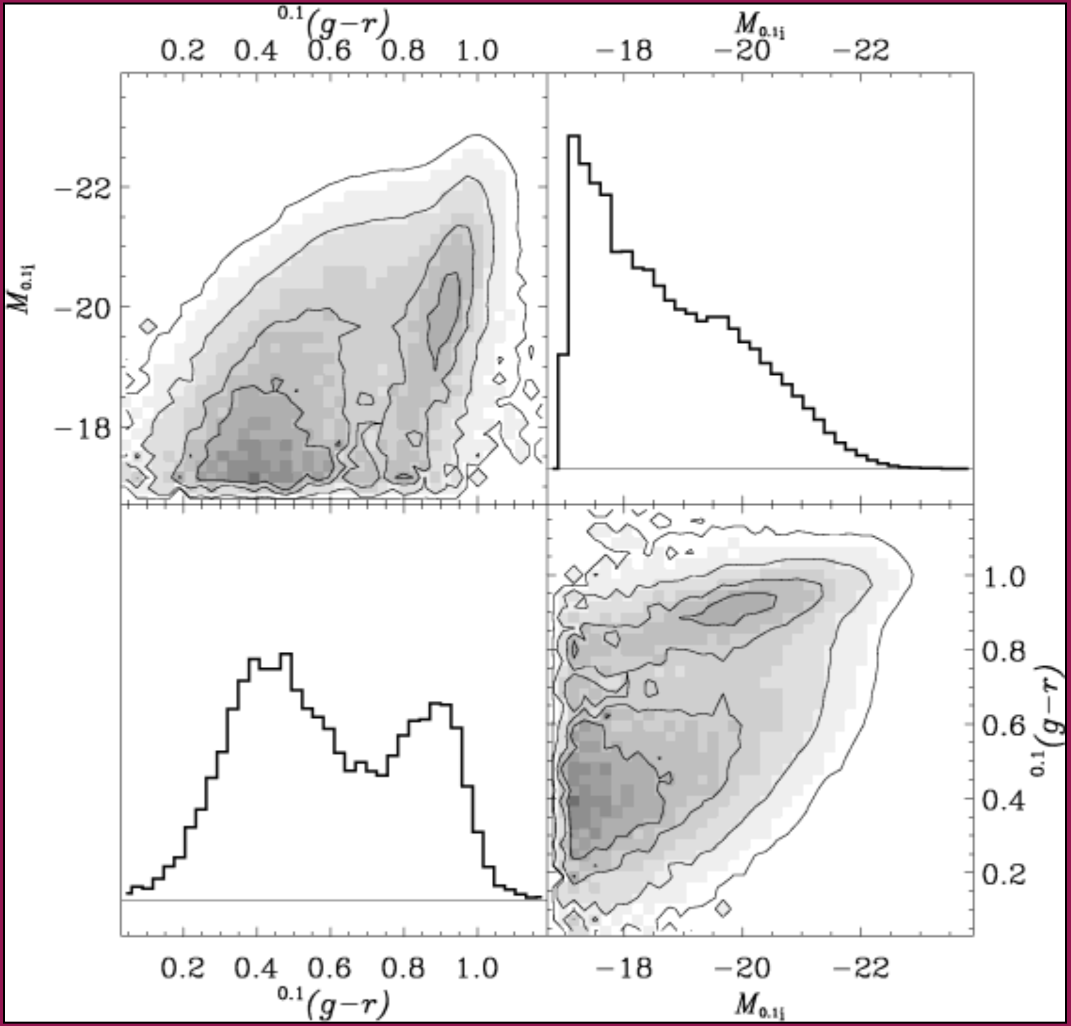

Blanton et al. (2004)

Stellar mass

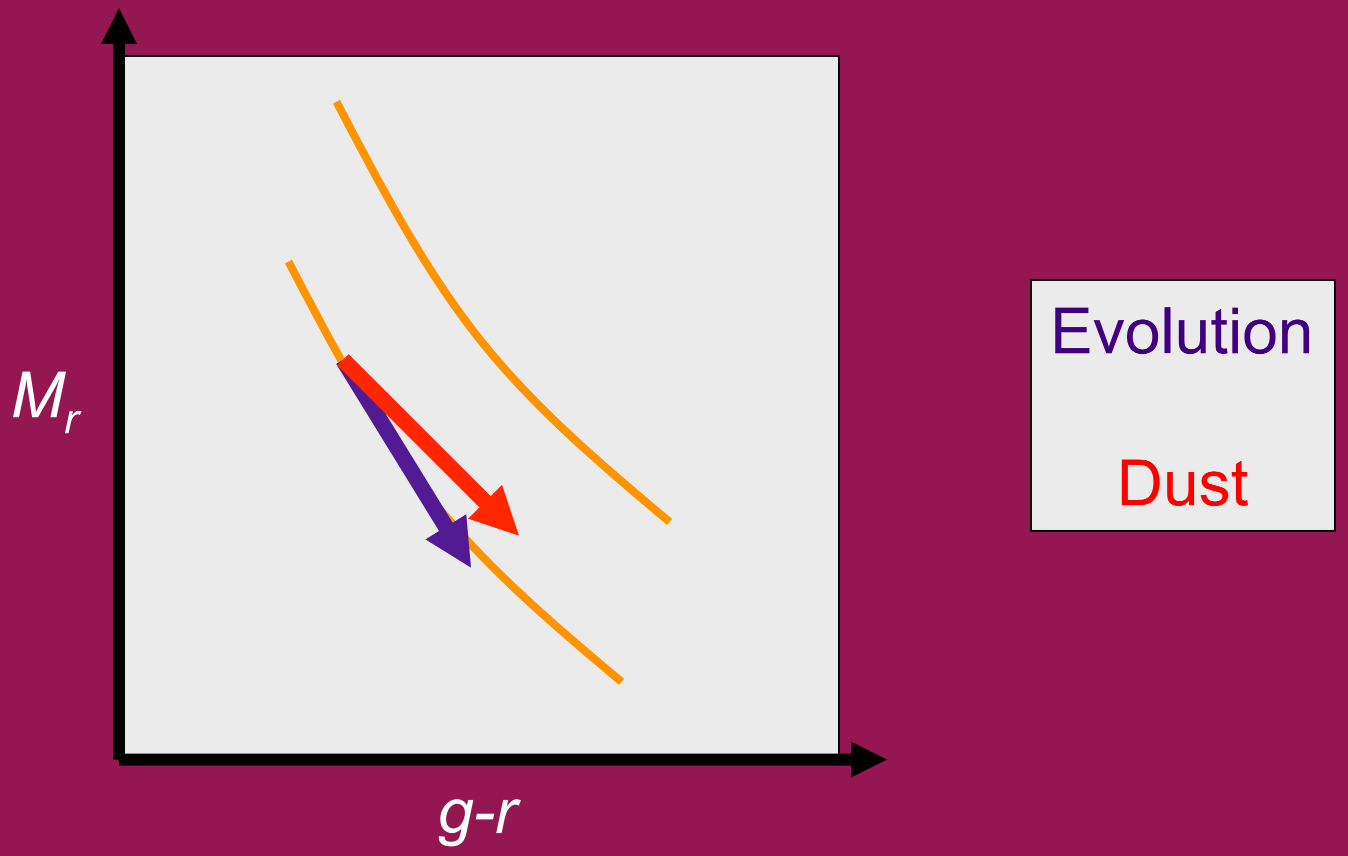

Bell & de Jong (2001)

Bimodality

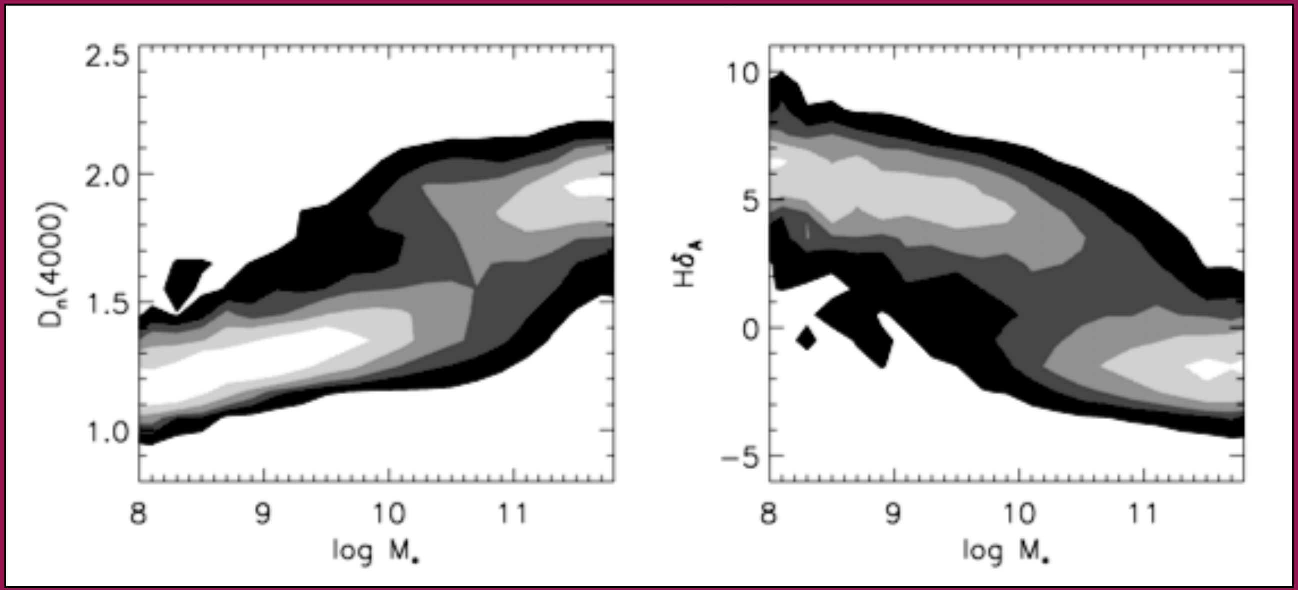

Kauffmann et al. (2004)

K-corrections

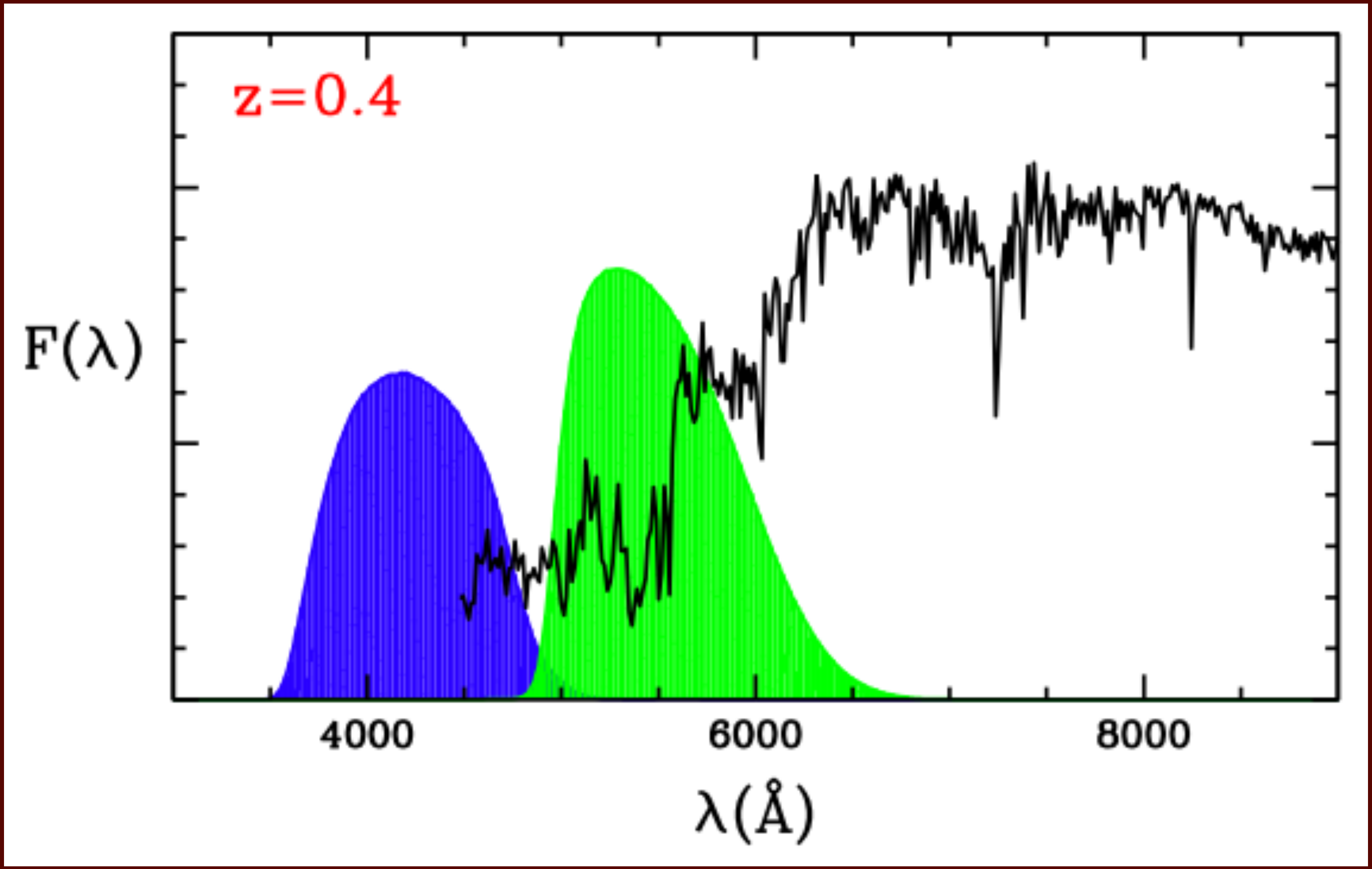

K-corrections

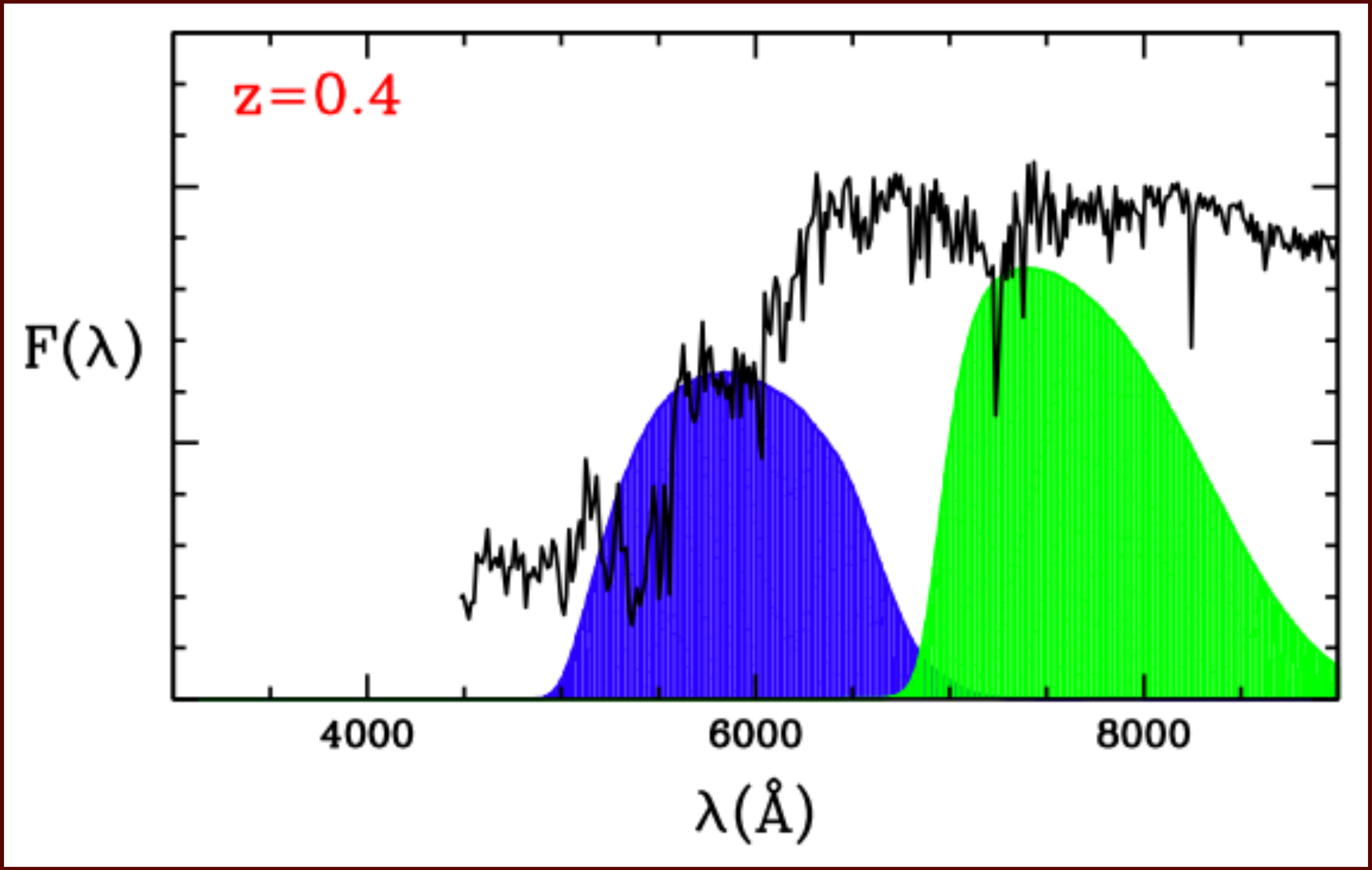

K-corrections

Galaxy magnitudes at different redshifts cannot be compared directly because photometric filters cover a different part of the rest-frame galaxy spectrum.

$$\frac{\lambda_{\text{observed}}}{\lambda_{\text{emitted}}} = 1 + z$$

$$\frac{f_{\text{intrinsic}}}{f_{\text{observed}}} = \frac{\int_0^{\infty} F(\lambda) S(\lambda) d\lambda}{\int_0^{\infty} F\left(\frac{\lambda}{1+z}\right) S(\lambda) \frac{d\lambda}{1+z}}$$

K-corrections

$$m_{\text{intrinsic}} = m_{\text{observed}} - K(z)$$

$$K(z) = 2.5\log\left((1+z)\frac{\int_0^\infty F(\lambda)S(\lambda)\,d\lambda}{\int_0^\infty F\left(\frac{\lambda}{1+z}\right)S(\lambda)\,d\lambda} \right)$$

$$= 2.5\log(1+z) + 2.5\log\left(\frac{\int_0^\infty F(\lambda)S(\lambda)\,d\lambda}{\int_0^\infty F\left(\frac{\lambda}{1+z}\right)S(\lambda)\,d\lambda} \right)$$

K-corrections

$$F(\lambda) = C\lambda^{\alpha}$$

$$K(z) = 2.5(\alpha + 1)\log(1 + z)$$

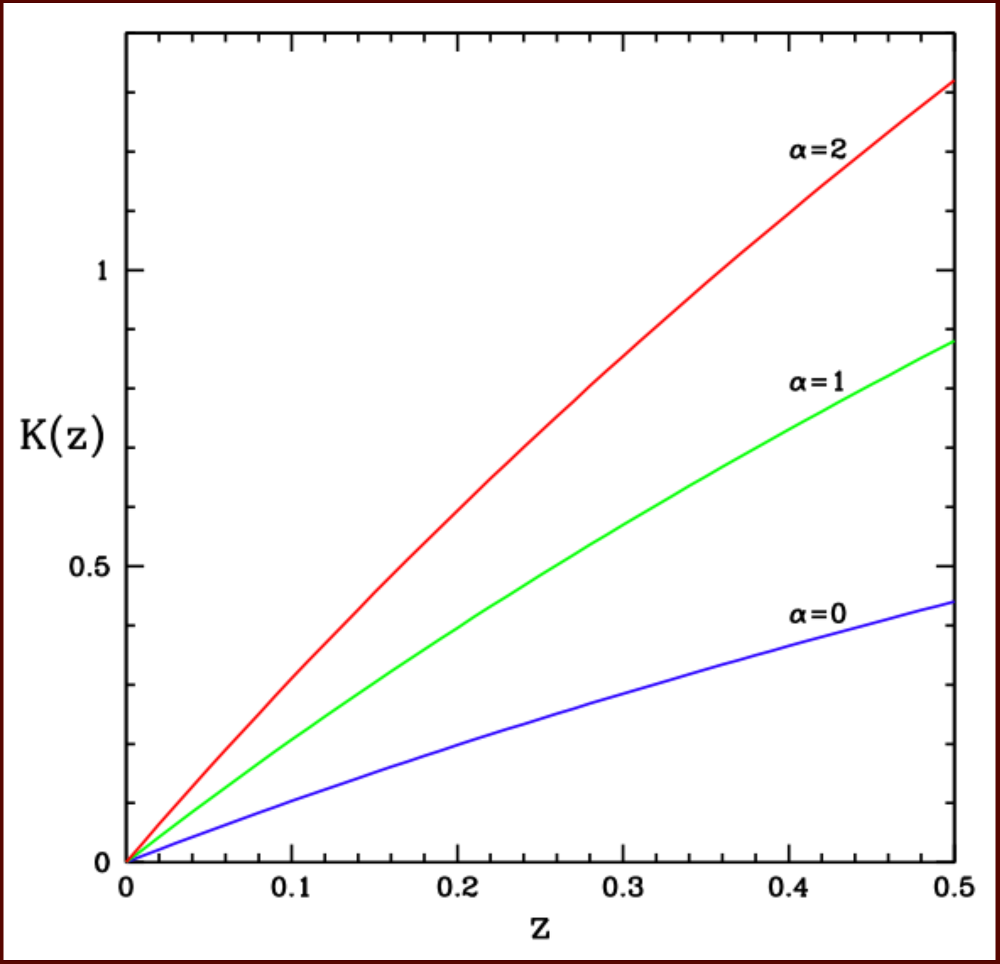

K-corrections

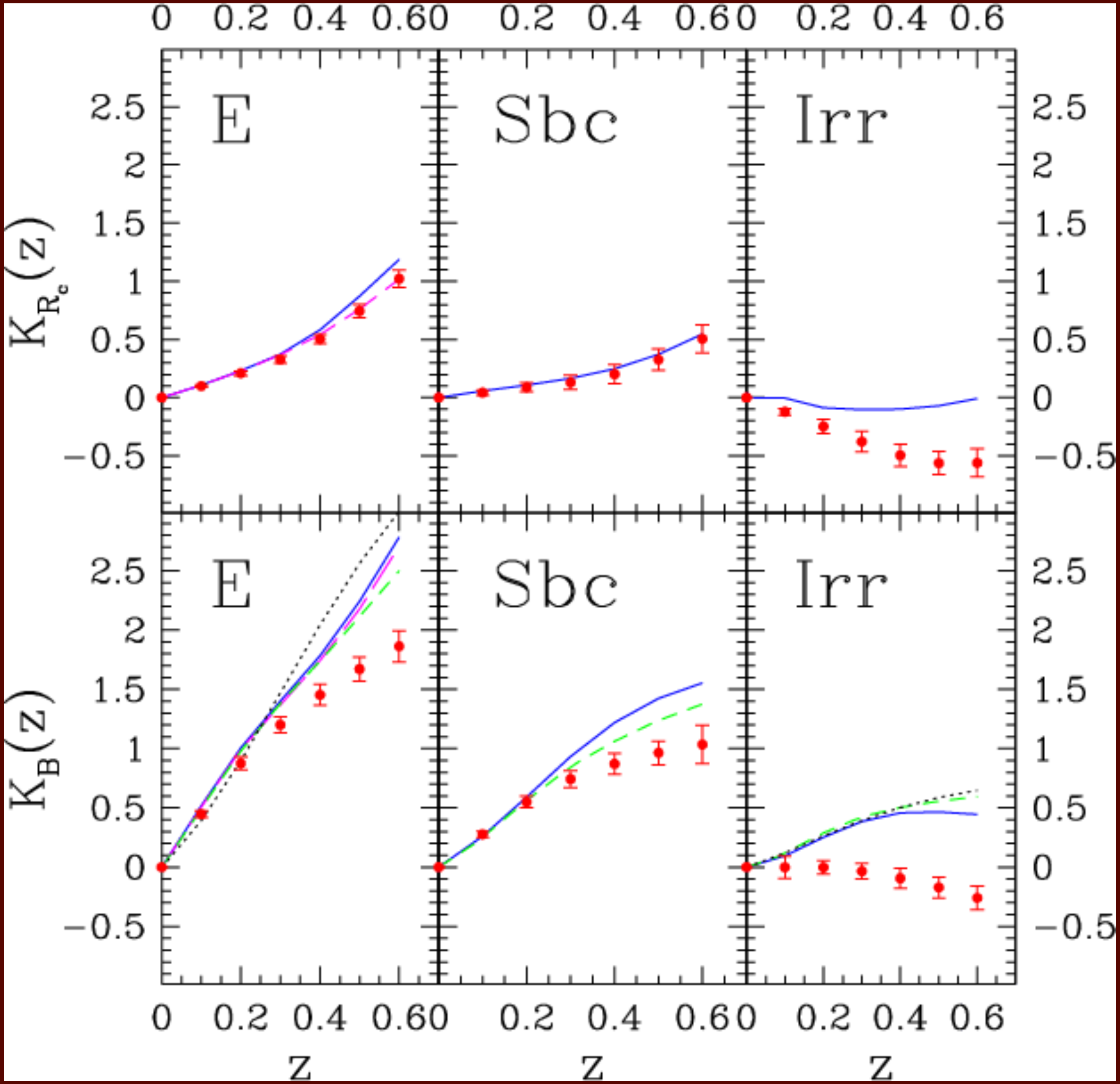

De Lapparent et al. (2003)

Evolution corrections

Galaxy luminosities evolve with redshift, making it difficult to compare galaxies at different redshifts.

Passive luminosity evolution: galaxies fade with time as their stellar populations age (*i.e, no new star formation*)

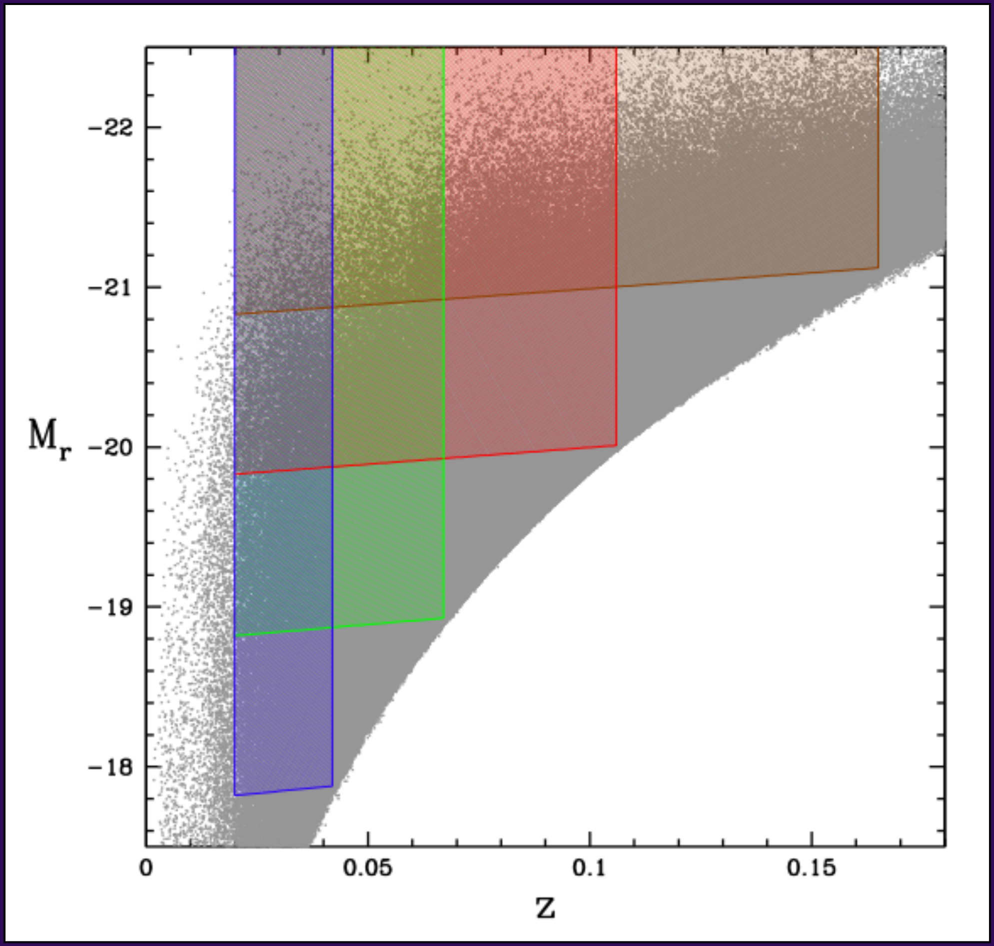

Luminosity Function

THE ASTROPHYSICAL JOURNAL, 203:297–306, 1976 January 15

AN ANALYTIC EXPRESSION FOR THE LUMINOSITY FUNCTION FOR GALAXIES*

PAUL SCHECHTER
California Institute of Technology and the Institute for Advanced Study
Received 1975 April 29; revised 1975 June 30

ABSTRACT

A new analytic approximation for the luminosity function for galaxies is proposed, which shows good agreement with both a luminosity distribution for bright nearby galaxies and a con luminosity distribution for cluster galaxies. The analytic expression is proportional to $L^{-5/4}$ where L^* is a characteristic luminosity corresponding to a characteristic absolute mag $M^*_{B(0)} = -20.6$. For an individual cluster, the characteristic magnitude may be dete with an accuracy of ~0.25 mag, suggesting its use as a standard candle. The analytic exp is used to compute an expected richness–absolute magnitude correlation for first ranked galaxies and an expected dispersion, which are compared with the data of Sandage and

Subject headings: galaxies: clusters of — galaxies: photometry

We propose here a new analytic approximation for the luminosity function for galaxies. Letting $\varphi(L)dL$ be number of galaxies per unit volume in the luminosity interval from L to $L + dL$, we investigate the expression

$$\varphi(L)dL = \varphi^*(L/L^*)^\alpha \exp(-L/L^*)d(L/L^*) \qquad (1)$$

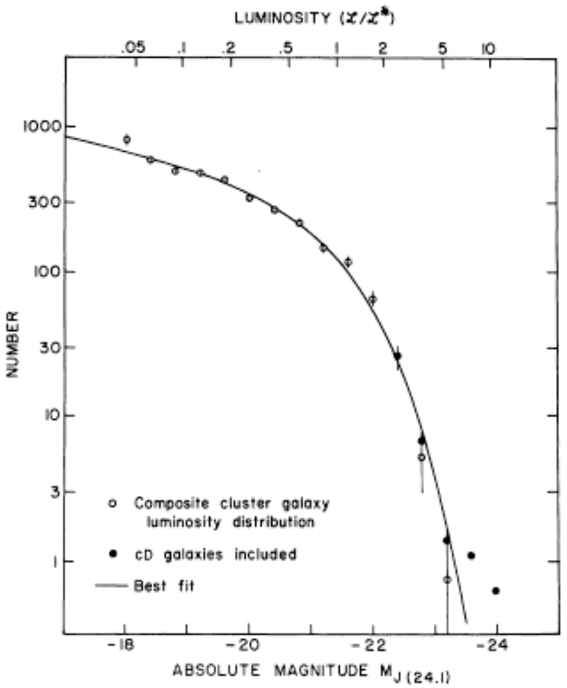

FIG. 2.—Best fit of analytic expression to observed composite cluster galaxy luminosity distribution. Filled circles show the effect of including cD galaxies in composite.

Luminosity Function

$$\Phi(L) = \frac{\Phi_*}{L_*}\left(\frac{L}{L_*}\right)^{\alpha} \exp\left(-\frac{L}{L_*}\right)$$

Luminosity Function

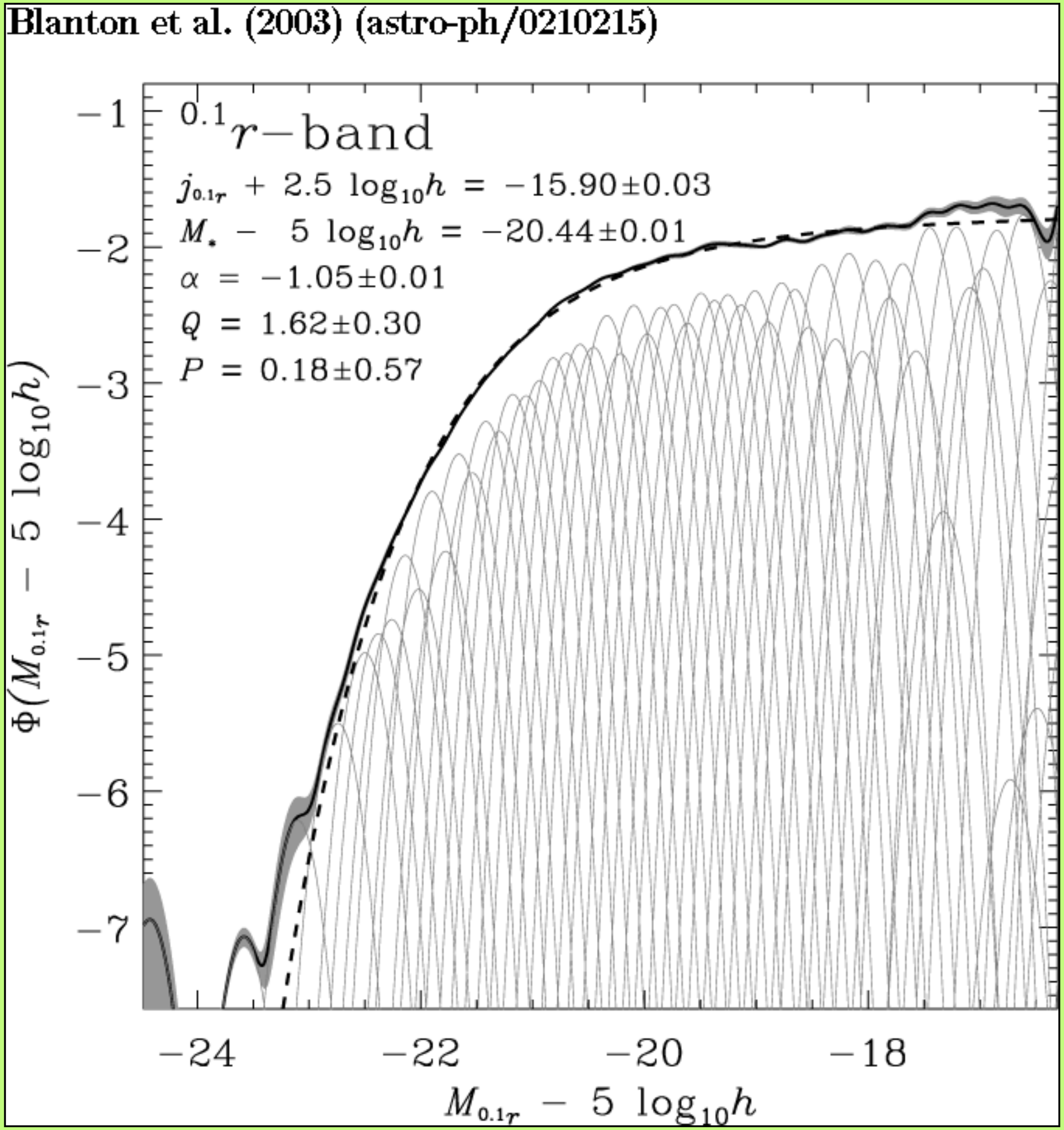

Blanton et al. (2003)

Luminosity Function

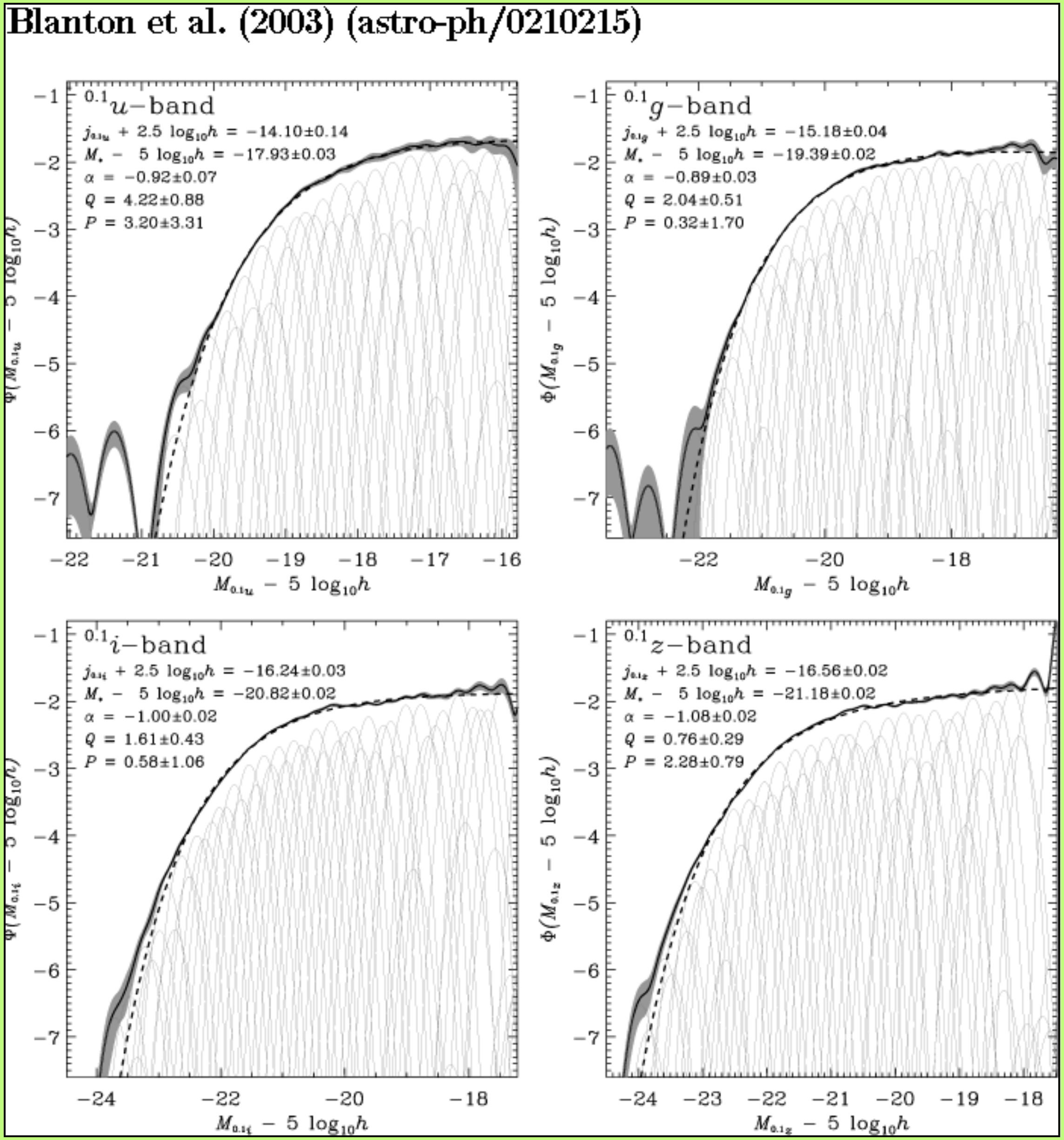

Blanton et al. (2003)

Luminosity Function

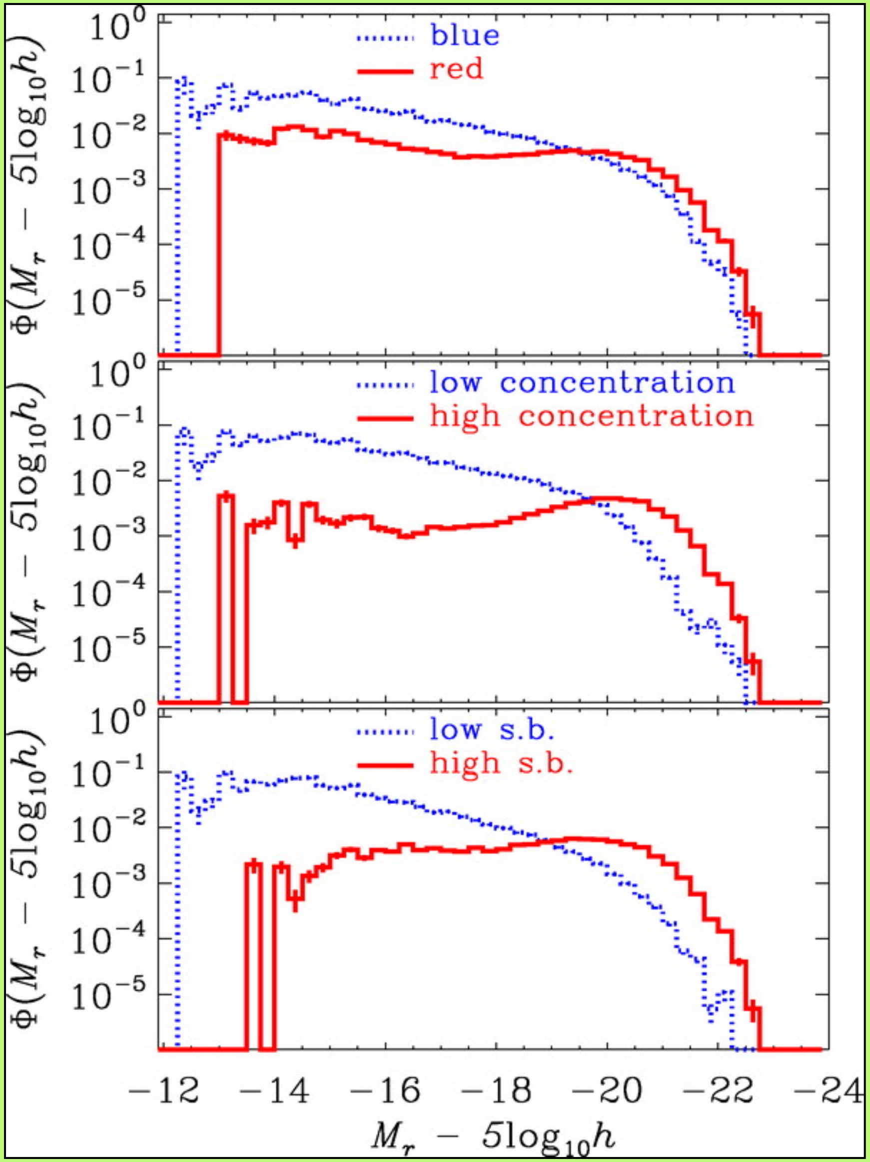

Blanton et al. (2005)

2dFGRS angular selection function

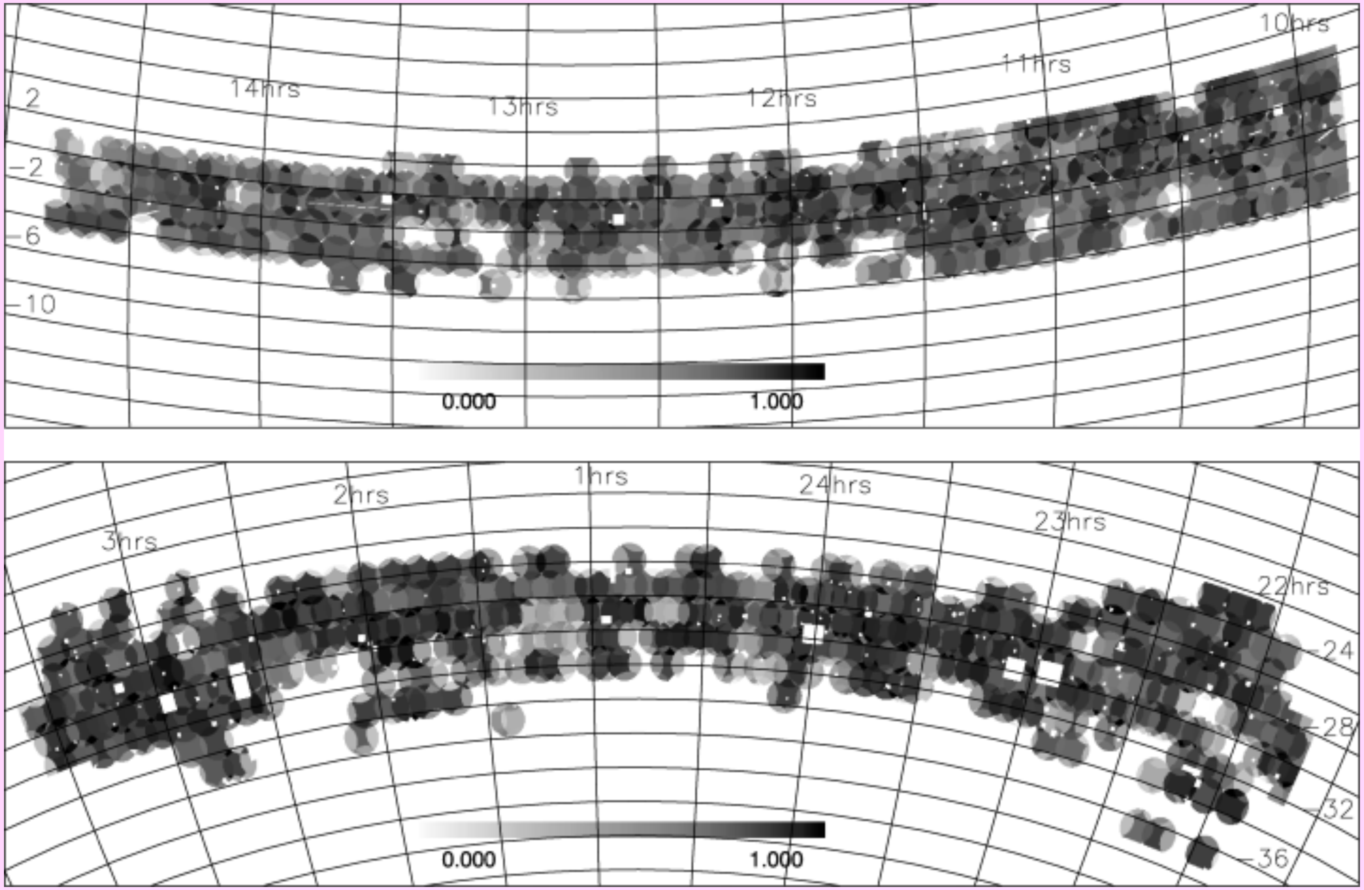

Norberg et al. (2002)

Radial selection function

$$\Phi(z) = \frac{\int_{M_{max}(z)}^{-\infty} dM\,\Phi(M)}{\int_{M_{cut}}^{-\infty} dM\,\Phi(M)}$$

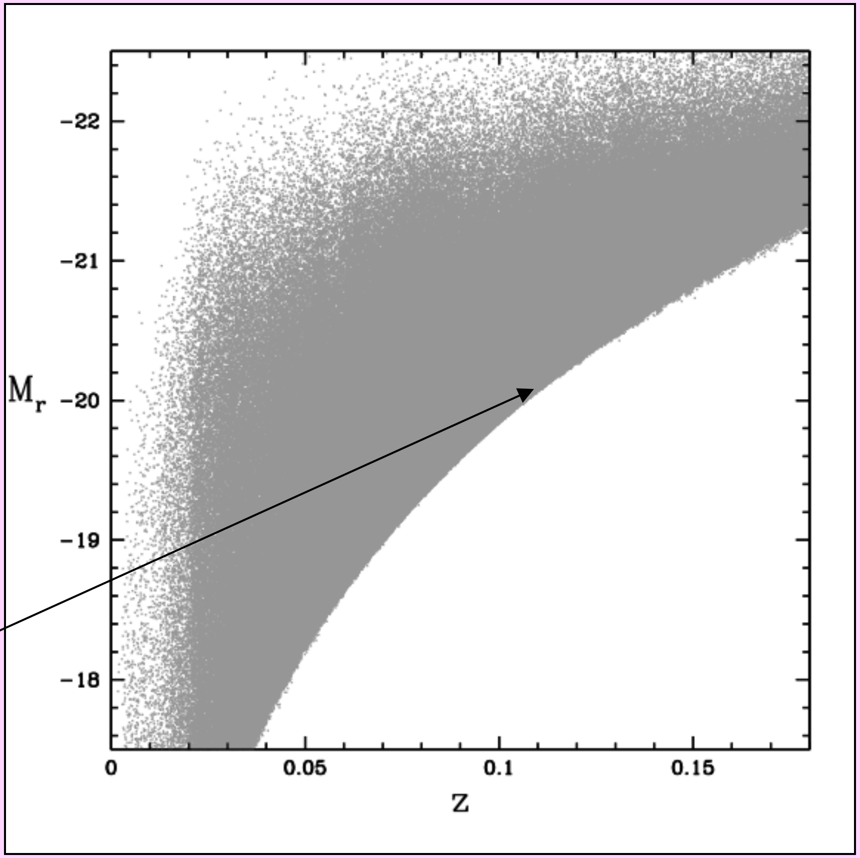

$$M_{max}(z) = m_{lim} - 5\log\left(\frac{cz}{H_0}\times 10^6\right) + 5 - K(z)$$

2dFGRS radial selection function

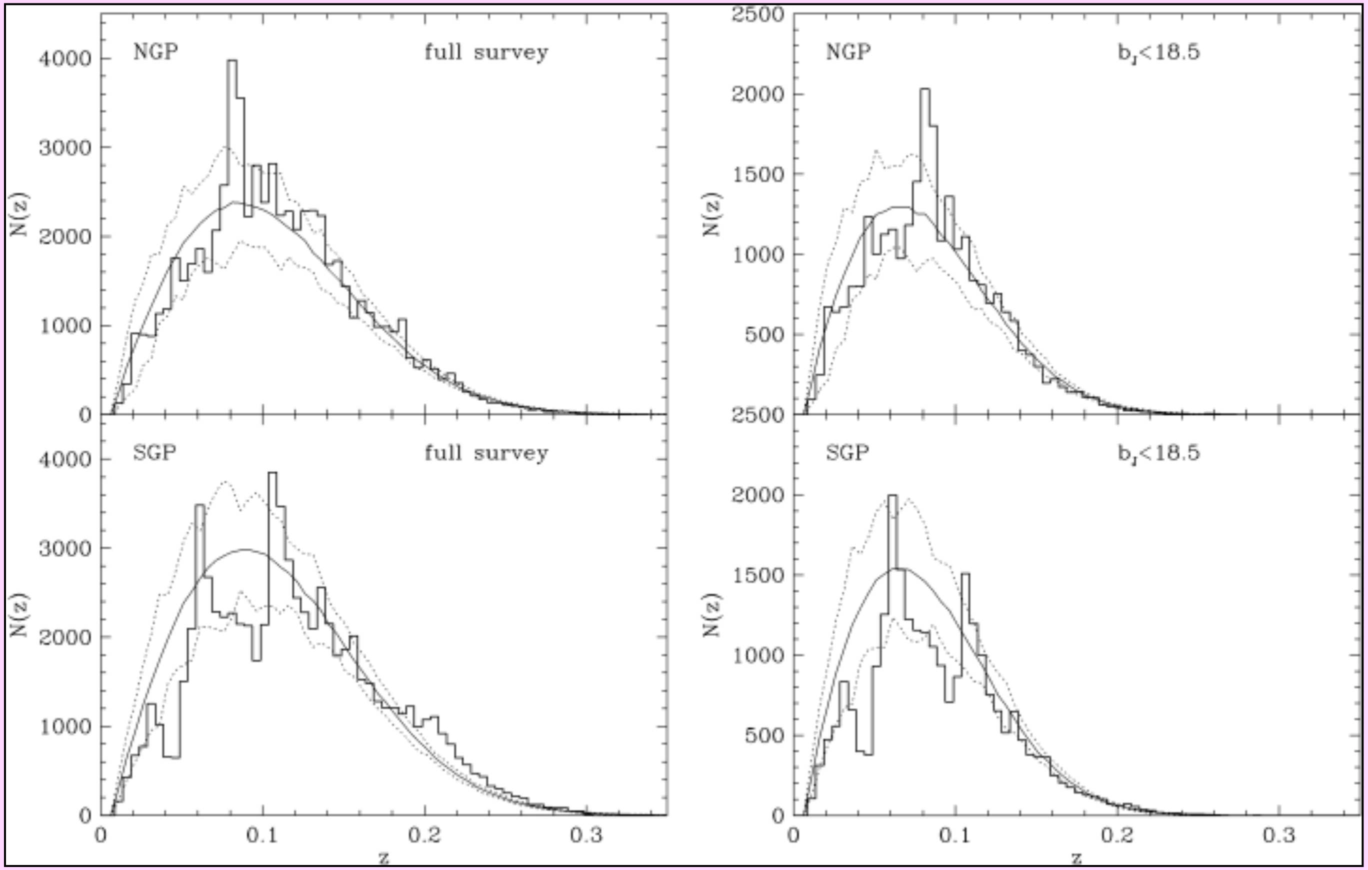

Norberg et al. (2002)

Photometric Redshifts

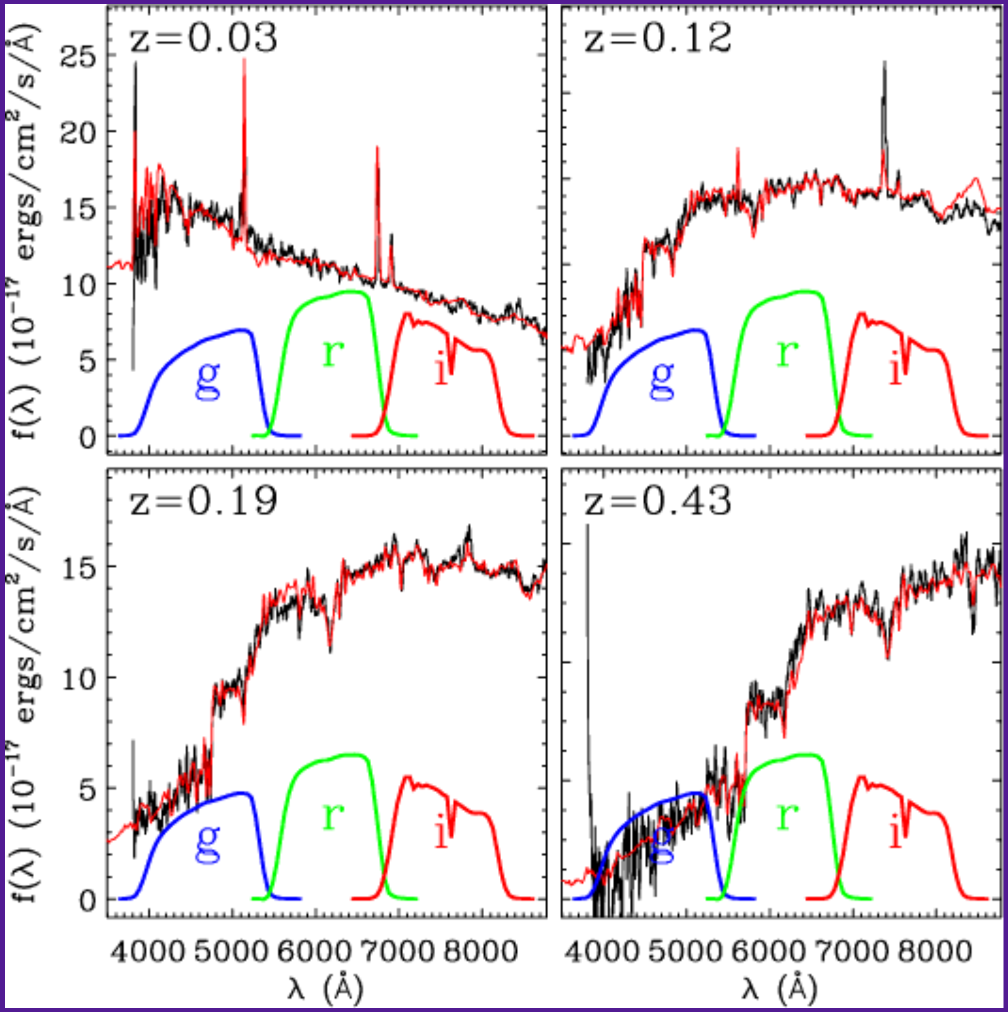

SDSS, Blanton

Photometric Redshifts

Where spectroscopic data are unavailable, one can still use photometric data in multiple bands to estimate redshift. Galaxy colors depend on:

- spectral type of galaxy
- redshift
- reddening due to dust

Since galaxies have a narrow range of spectral types, we can jointly fit for type and redshift.

- the more bands the better!
- photo-z's have accuracy of $\sigma_z \sim 0.1$
- allow us to exploit deep imaging surveys.

Photometric Redshifts

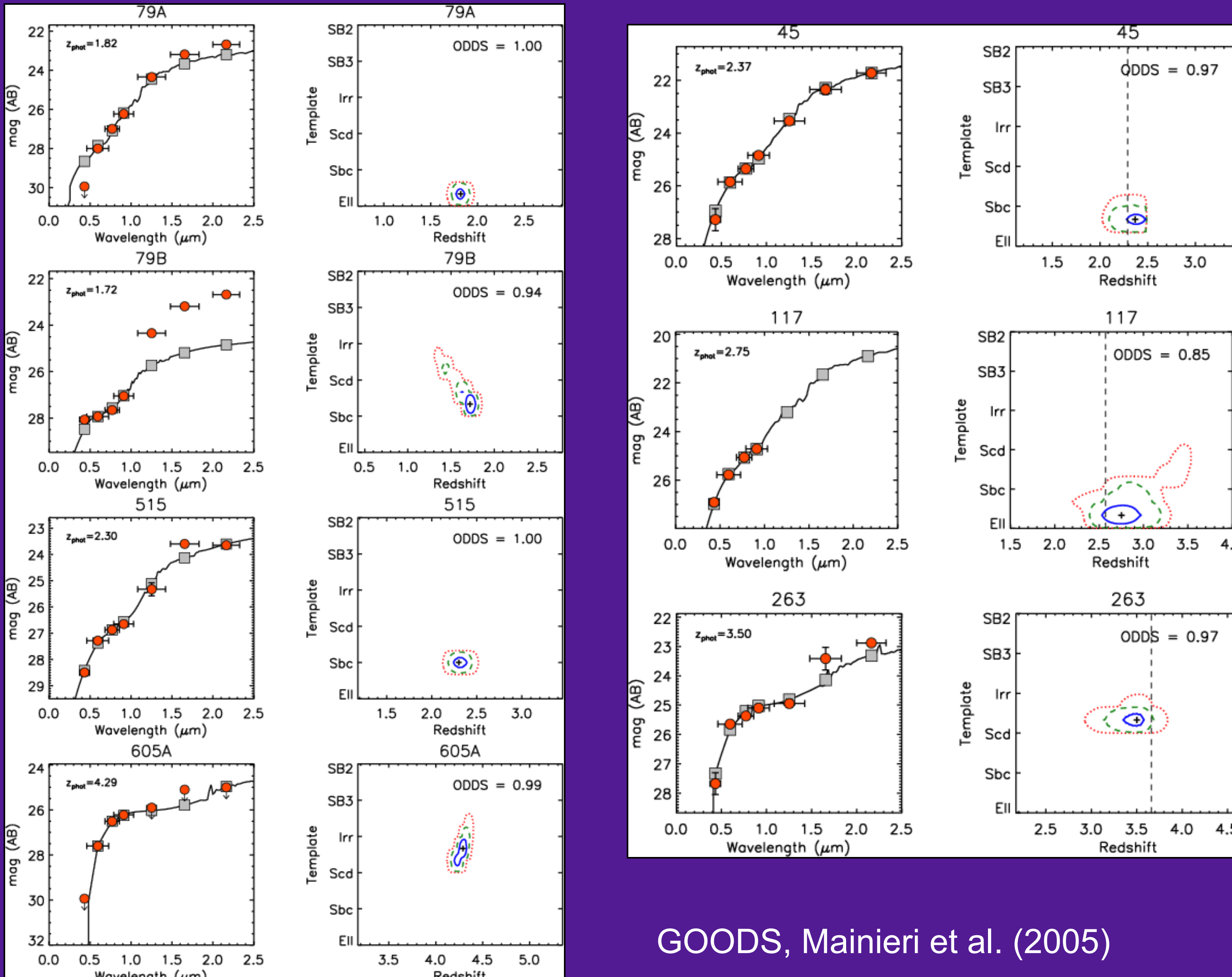

GOODS, Mainieri et al. (2005)

Photometric Redshifts

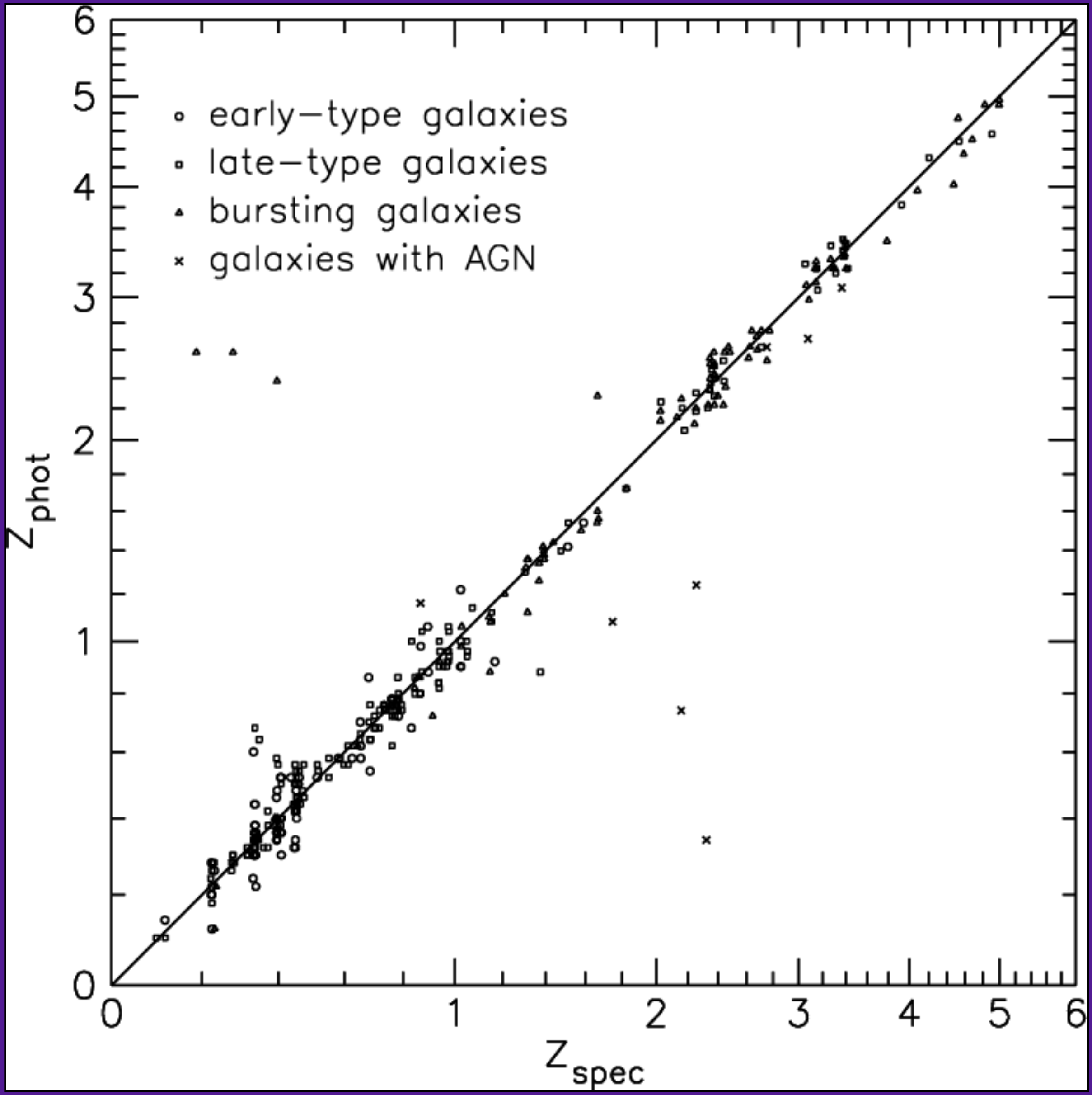

FORS Deep Field, Gabasch et al. (2004)

Photometric Redshifts

COMBO-17 Survey:

- 1 square degree
- 25,000 galaxies
- $\Delta z/z \sim 0.02$

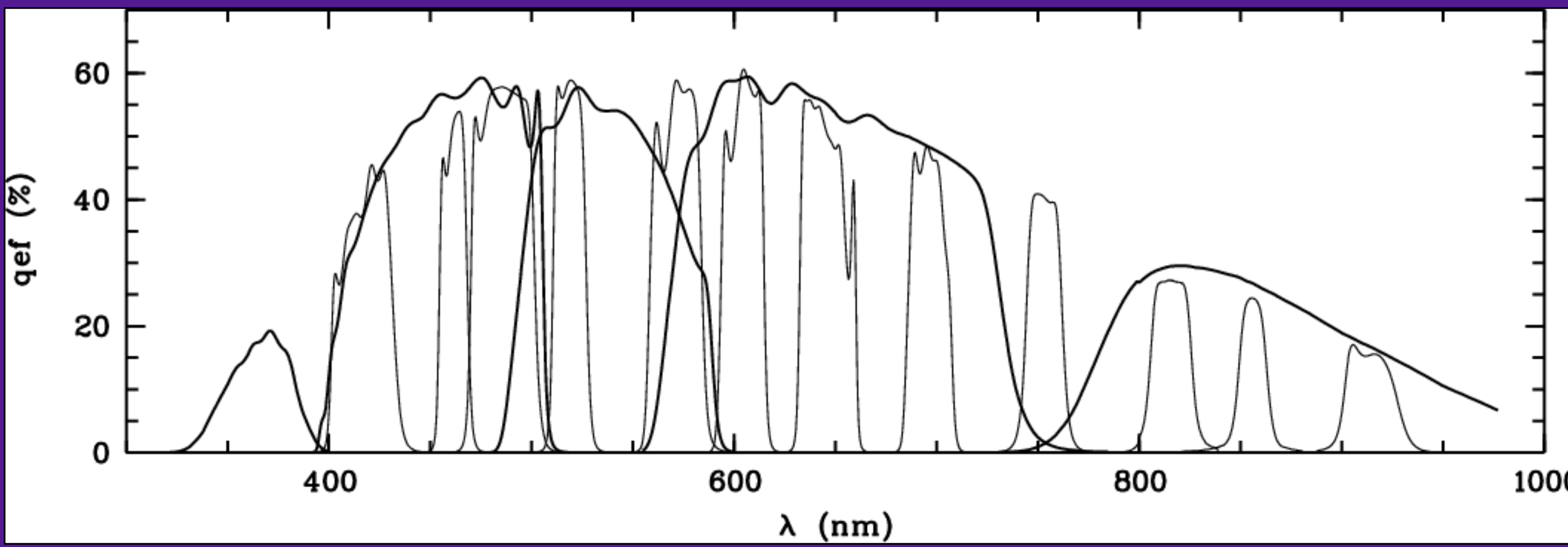

Wolf et al. (2003)

Measured galaxy properties

What can we measure from broadband galaxy images?

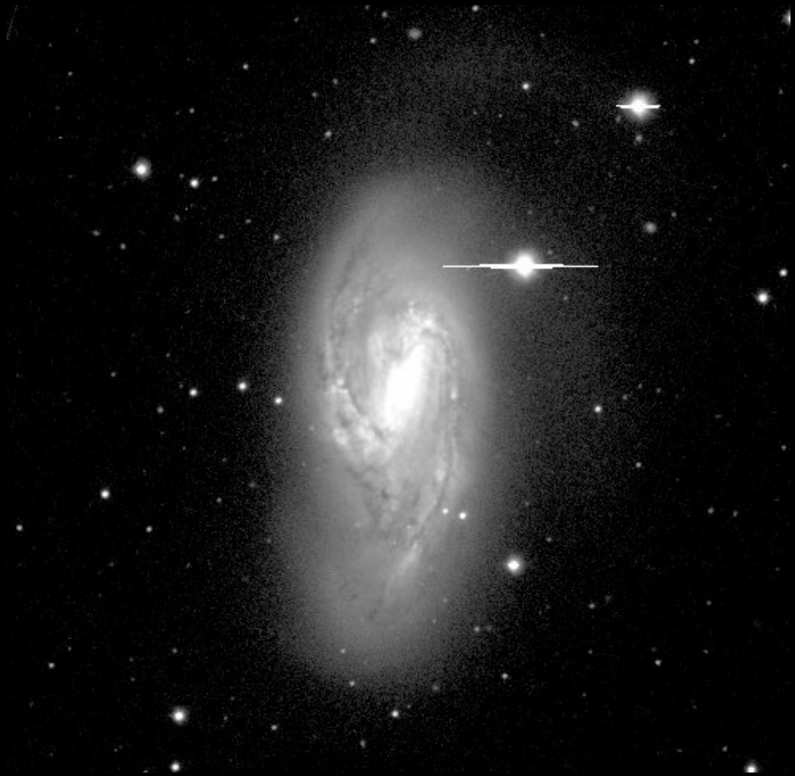

V band

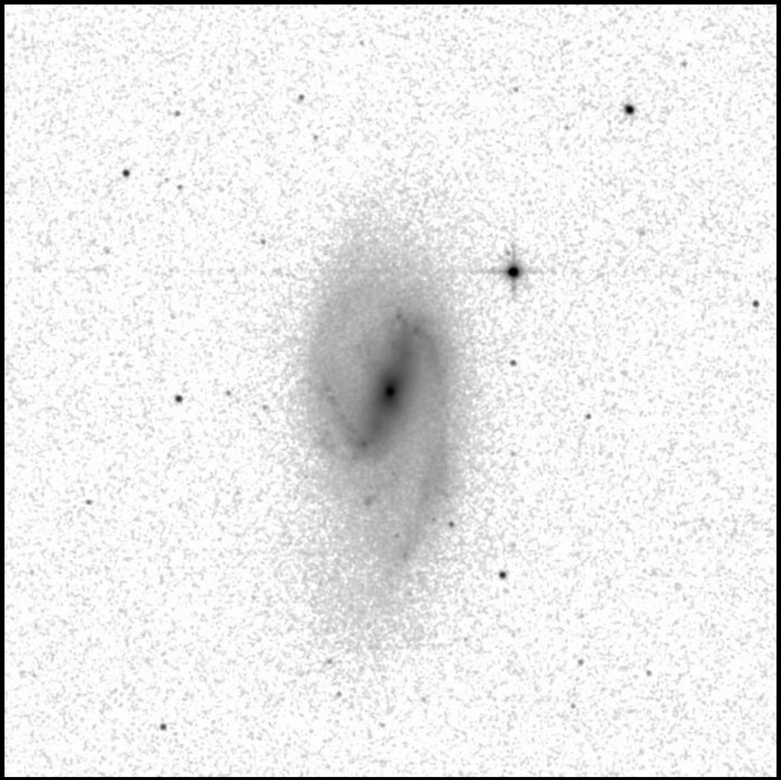

K band

Measured galaxy properties

What can we measure from broadband galaxy images?

- magnitudes (e.g., m_r)
- colors (e.g., g-r)
- surface brightness
- angular size
- 1D radial light profile
- morphology
- photometric redshift

Measured galaxy properties

What can we measure from galaxy spectra?

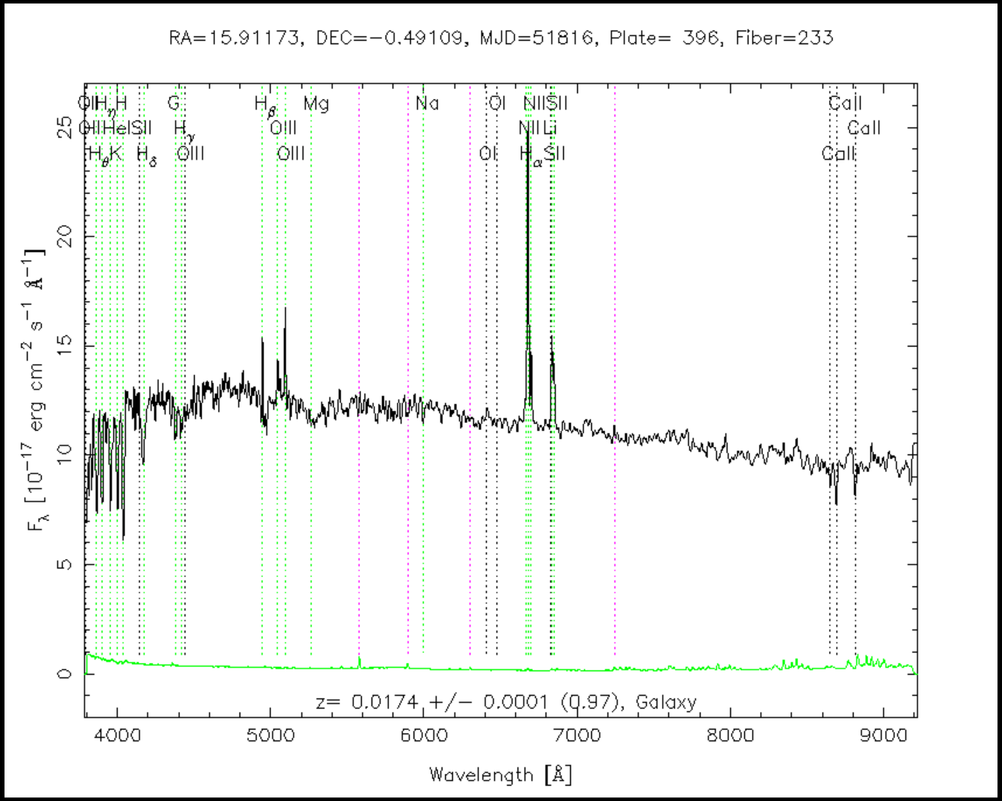

Measured galaxy properties

What can we measure from galaxy spectra?

- redshift
- absolute magnitude (e.g., M_r)
- physical size
- elemental abundances
- velocity dispersion / rotation
- stellar population
- star formation indicators

Galaxy light profiles

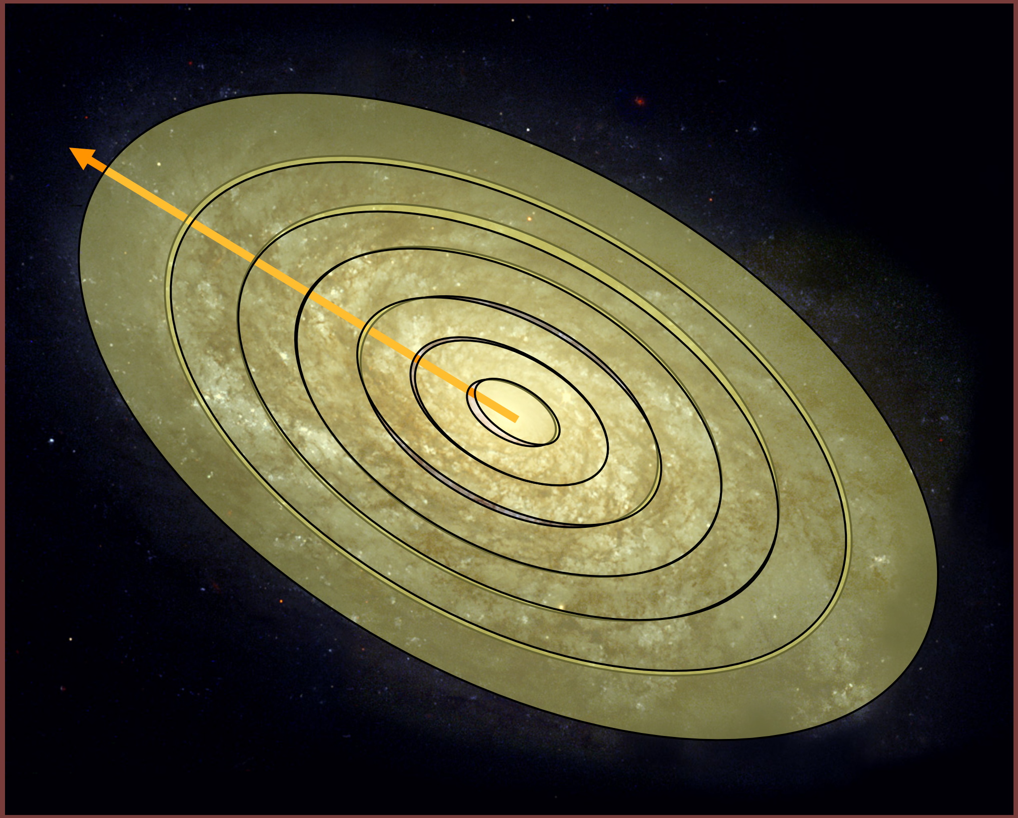

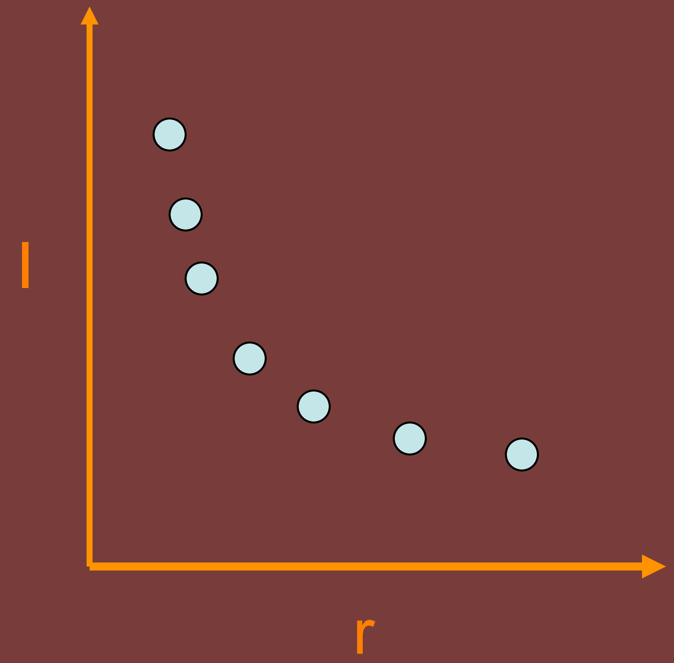

Galaxy light profiles

Disk galaxies: Exponential disk

$$I(r) = I_0 \exp(-r/r_0)$$

Galaxy light profiles

Elliptical galaxies: de Vaucouleurs profile

$$I(r) = I_0 \exp\left(-\left(r/r_0\right)^{\frac{1}{4}}\right)$$

More general: Sersic profile

$$I(r) = I_0 \exp\left(-\left(r/r_0\right)^{\frac{1}{n}}\right)$$

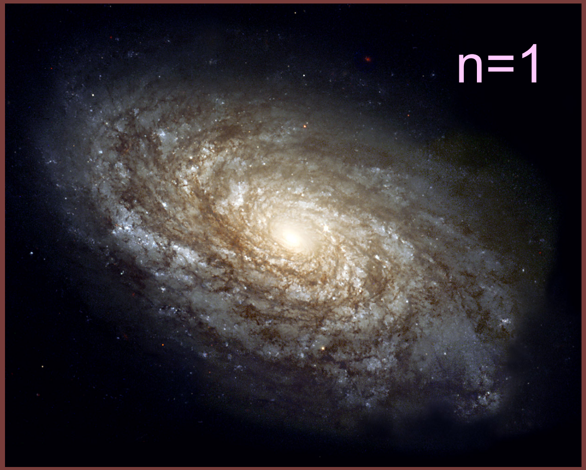

Galaxy light profiles

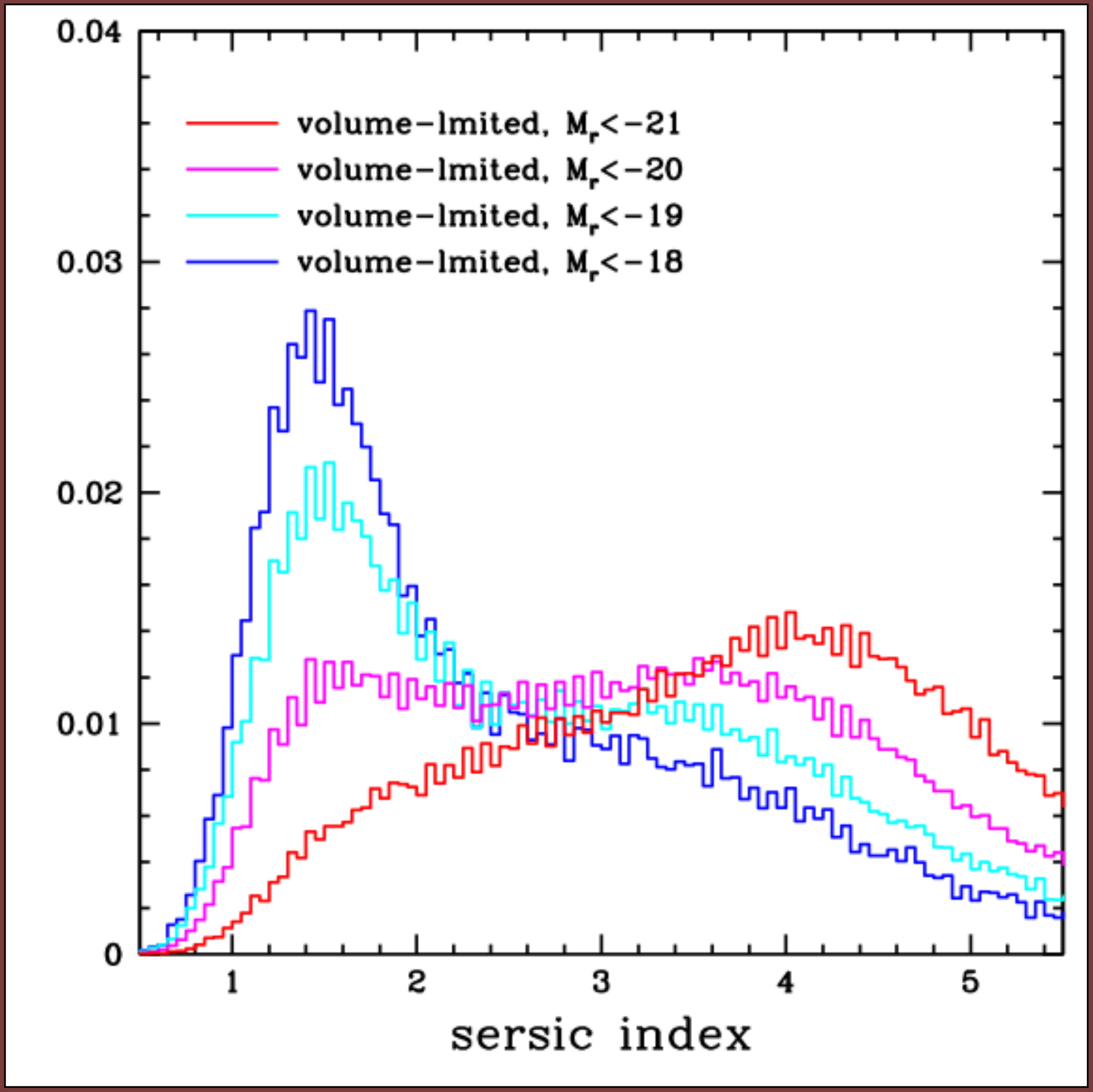

Galaxy light profiles

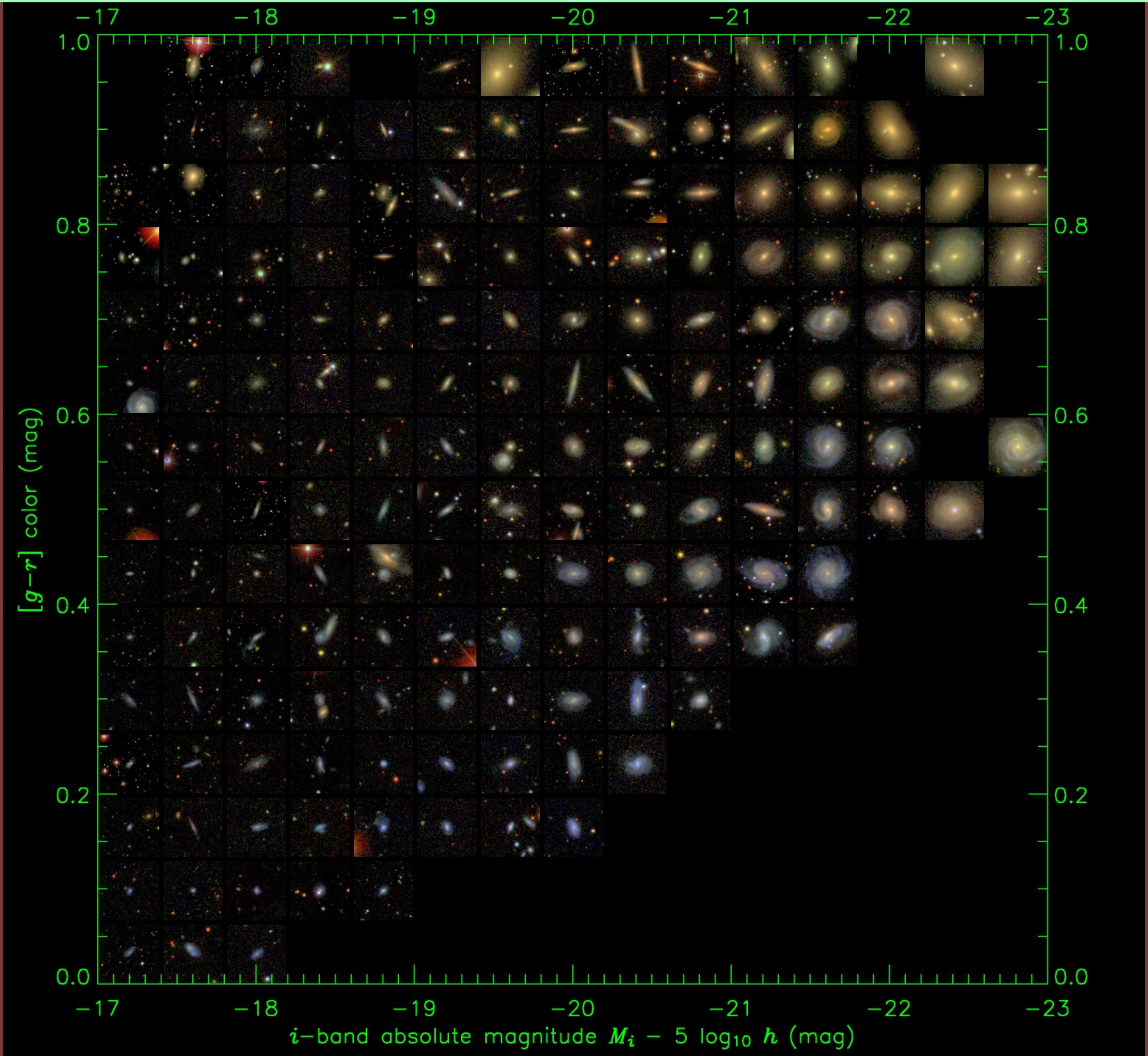

Galaxy light profiles

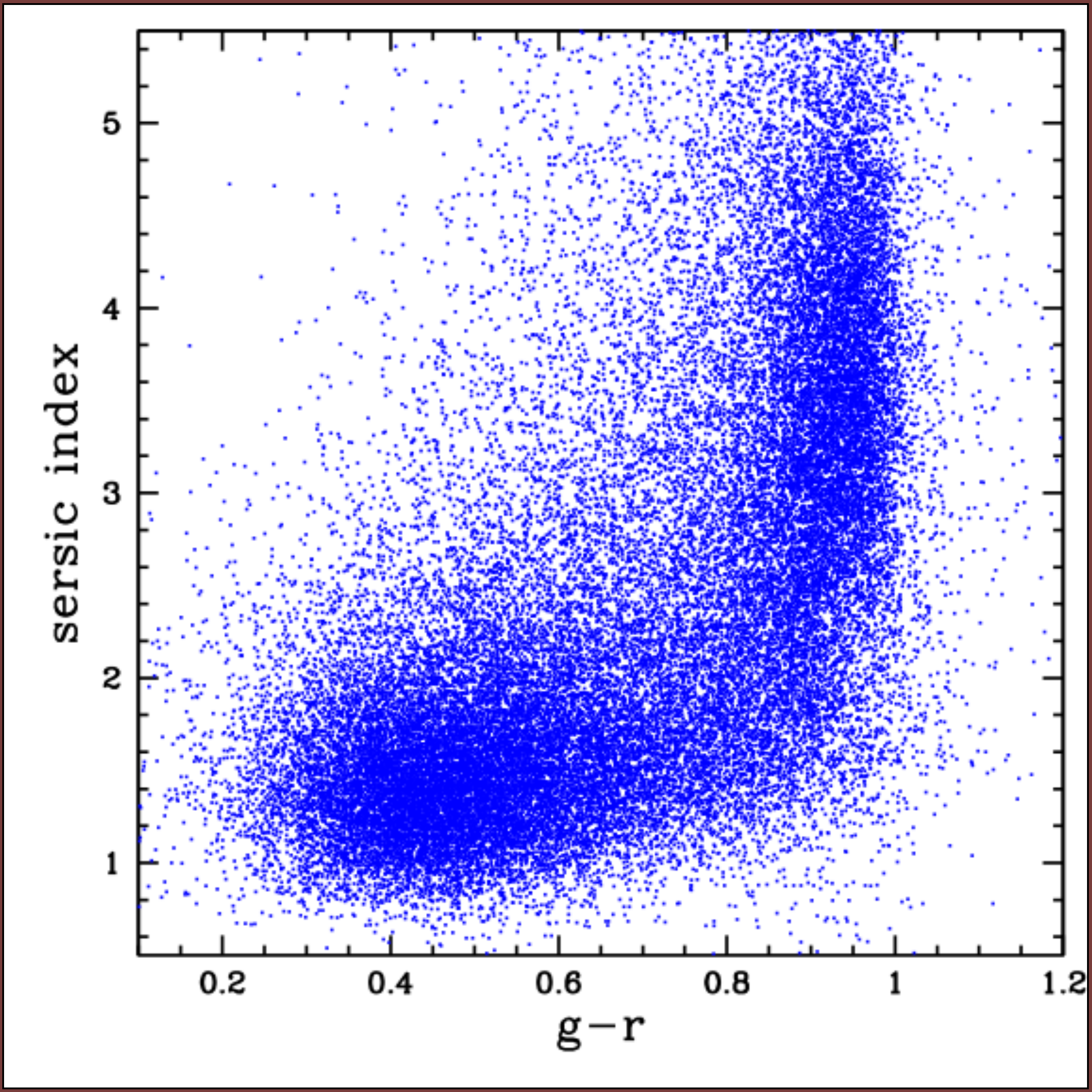

Galaxy morphology

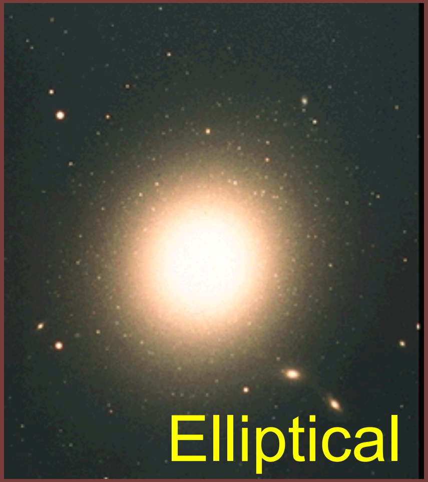

Galaxy morphology



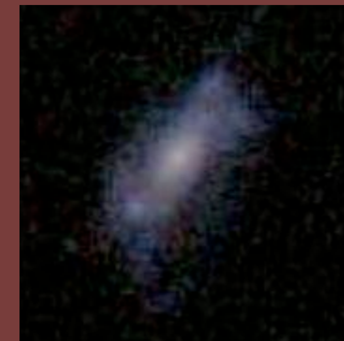




Galaxy morphology

Types

- Spiral structure
- Bars vs. no bars
- Disk vs. bulge
- Smooth vs. clumpy
- Tidal features

Method

- By eye
- 1D light profile fitting
- 2D light profile fitting
- Disk/bulge decomposition
- Spectro-Photometrically

Galaxy morphology

THE ASTRONOMICAL JOURNAL, 122:611–620, 2001 August

CALTECH FAINT GALAXY REDSHIFT SURVEY. XV. CLASSIFICATIONS OF GALAXIES WITH $0.2 < z < 1.1$ IN THE HUBBLE DEEP FIELD NORTH AND ITS FLANKING FIELDS[1]

SIDNEY VAN DEN BERGH
Dominion Astrophysical Observatory, Herzberg Institute of Astrophysics, National Research Council of Canada, 5071 West Saanich Road, Victoria, BC V9E 2E7, Canada; sidney.vandenbergh@nrc.ca

JUDITH G. COHEN
Palomar Observatory, Mail Stop 105-24, California Institute of Technology, Pasadena, CA 91125; jlc@astro.caltech.edu

AND

CHRISTOPHER CRABBE
California Institute of Technology, Mail Stop 185-54, Pasadena, CA 91125; crabbe@its.caltech.edu
Received 2001 April 15; accepted 2001 May 2

ABSTRACT

To circumvent the spatial effects of resolution on galaxy classification, the images of 233 objects of known redshift in the Hubble Deep Field (HDF) and its flanking fields that have redshifts in the range $0.20 < z < 1.10$ were degraded to the resolution that they would have had if they were all located at a redshift of $z = 1.00$. As in Paper XIV of the present series, the effects of shifts in rest wavelength were mitigated by using *R*-band images for the classification of galaxies with $0.2 < z < 0.6$ and *I*-band images for objects with redshifts $0.6 < z < 1.1$. A special effort was made to search for bars in distant galaxies. The present data strongly confirm the previous conclusion that the Hubble tuning fork diagram only provides a satisfactory framework for the classification of galaxies with $z < 0.3$. More distant disk galaxies are often difficult to shoehorn into the Hubble classification scheme. The paucity of barred spirals and grand-design spirals at large redshifts is confirmed. It is concluded that the morphology of disk galaxies observed at look-back times smaller than 3–4 Gyr differs systematically from that of more distant galaxies viewed at look-back times of 4–8 Gyr. The disks of late-type spirals at $z > 0.5$ are seen to be more chaotic than those of their nearer counterparts. Furthermore, the spiral structure in distant early-type spirals appears to be less well developed than it is in nearby early galaxies.

Key words: galaxies: evolution — galaxies: formation — surveys

1D fitting

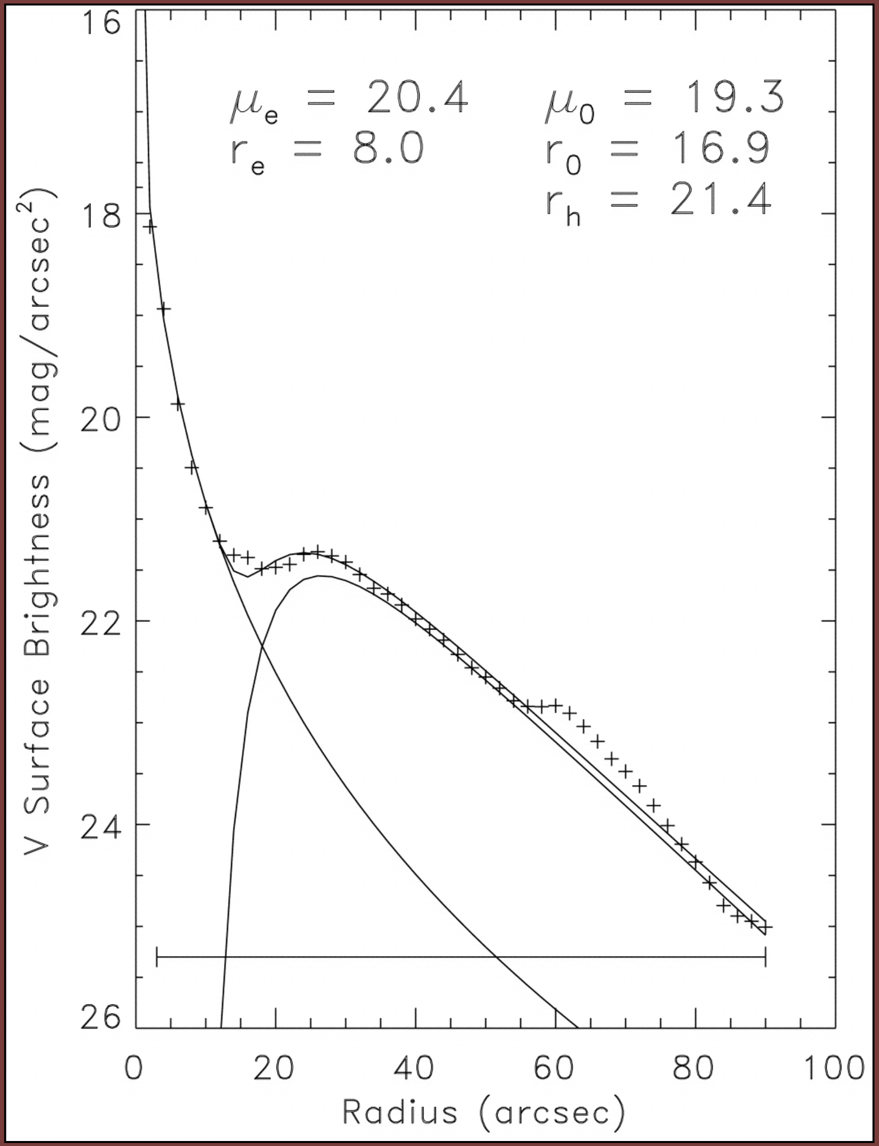

de Souza (2004)

Galaxy morphology

2D fitting

de Souza (2004)

Galaxy morphology

GALAXY ZOO 2

- 150,000 people
- 50 million galaxy classifications

Galaxy Zoo: Morphologies derived from visual inspection of galaxies from the Sloan Digital Sky Survey*

Chris J. Lintott[1]†, Kevin Schawinski[1]‡, Anže Slosar[1,2], Kate Land[1], Steven Bamford[3], Daniel Thomas[3], M. Jordan Raddick[4], Robert C. Nichol[3], Alex Szalay[4], Dan Andreescu[5], Phil Murray[6], Jan van den Berg[4]

[1] *Oxford Astrophysics, Denys Wilkinson Building, Keble Road, Oxford, OX1 3RH, UK*
[2] *Berkeley Centre for Cosmological Physics, Lawrence Berkeley National Laboratory and Physics Department, Berkeley, CA 94720*
[3] *Institute of Cosmology and Gravitation, University of Portsmouth, Mercantile House, Hampshire Terrace, Portsmouth, PO1 2EG, UK*
[4] *Department of Physics and Astronomy, Johns Hopkins University, 3400 N. Charles St., Baltimore, MD 21218, USA*
[5] *LinkLab, 4506 Graystone Ave., Bronx, NY 10471, USA*
[6] *Fingerprint Digital Media, 9 Victoria Close, Newtownards, Co. Down, Northern Ireland, BT23 7GY, UK*

Galaxy environments

The "environment" of a galaxy is a general term that has many different specific definitions, but is usually related to the local mass density.

Environment measures

- galaxy density on a scale *r*
- distance to N^{th} nearest neighbor
- group or cluster membership
- distance to nearest cluster
- void membership

Galaxy environments

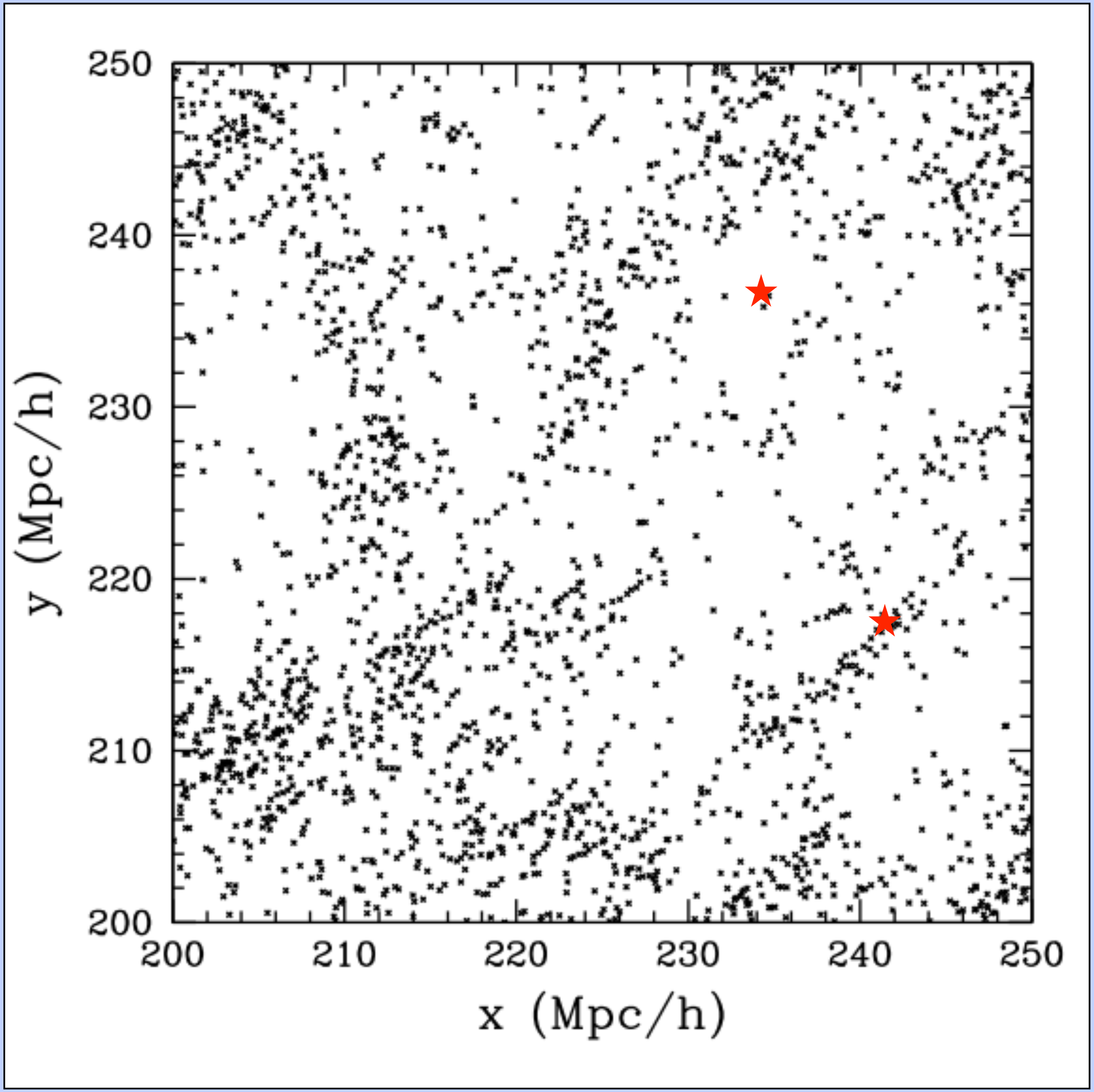

Galaxy environments

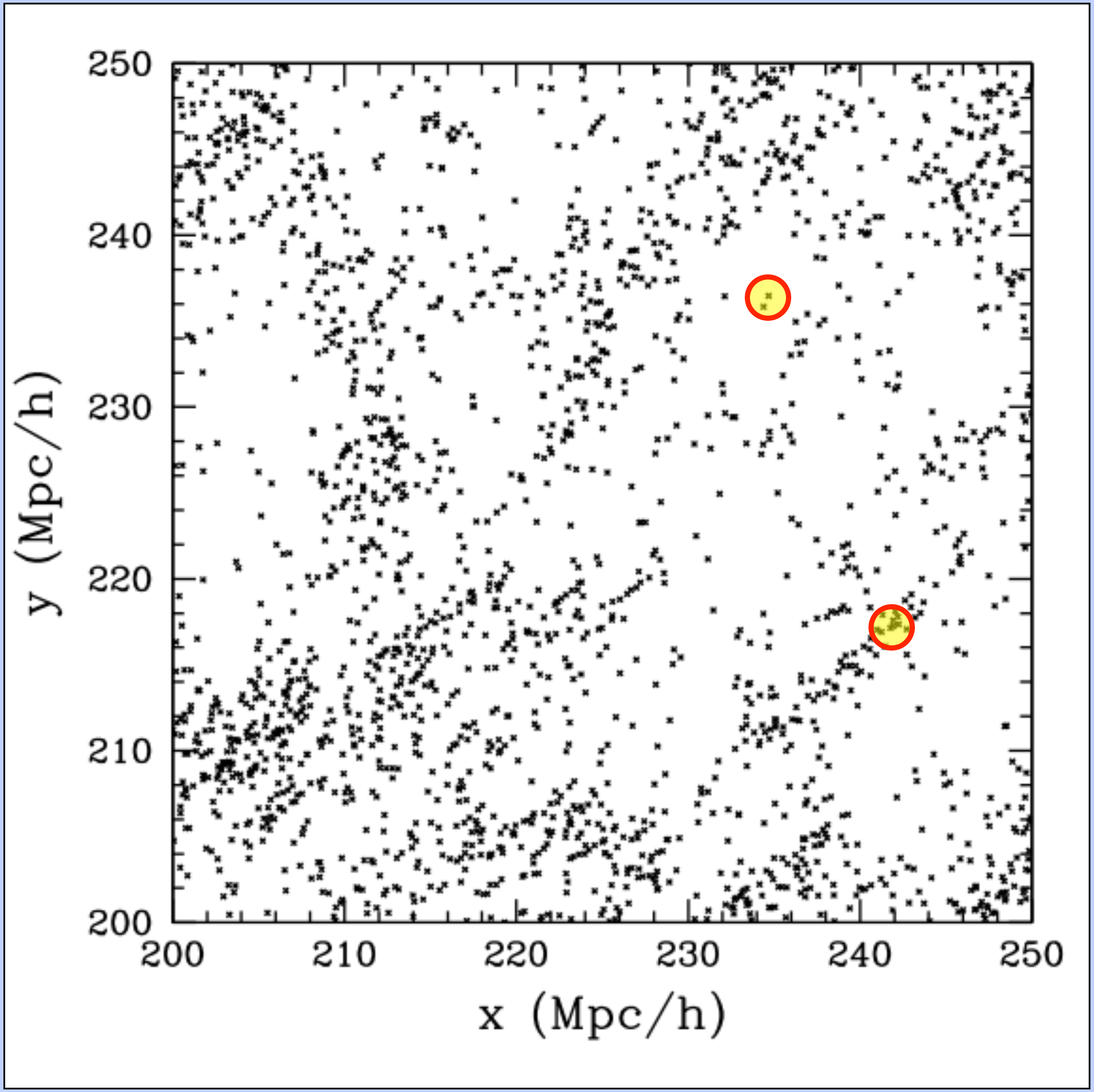

- Galaxy density on small scale (1 Mpc/h)

Galaxy environments

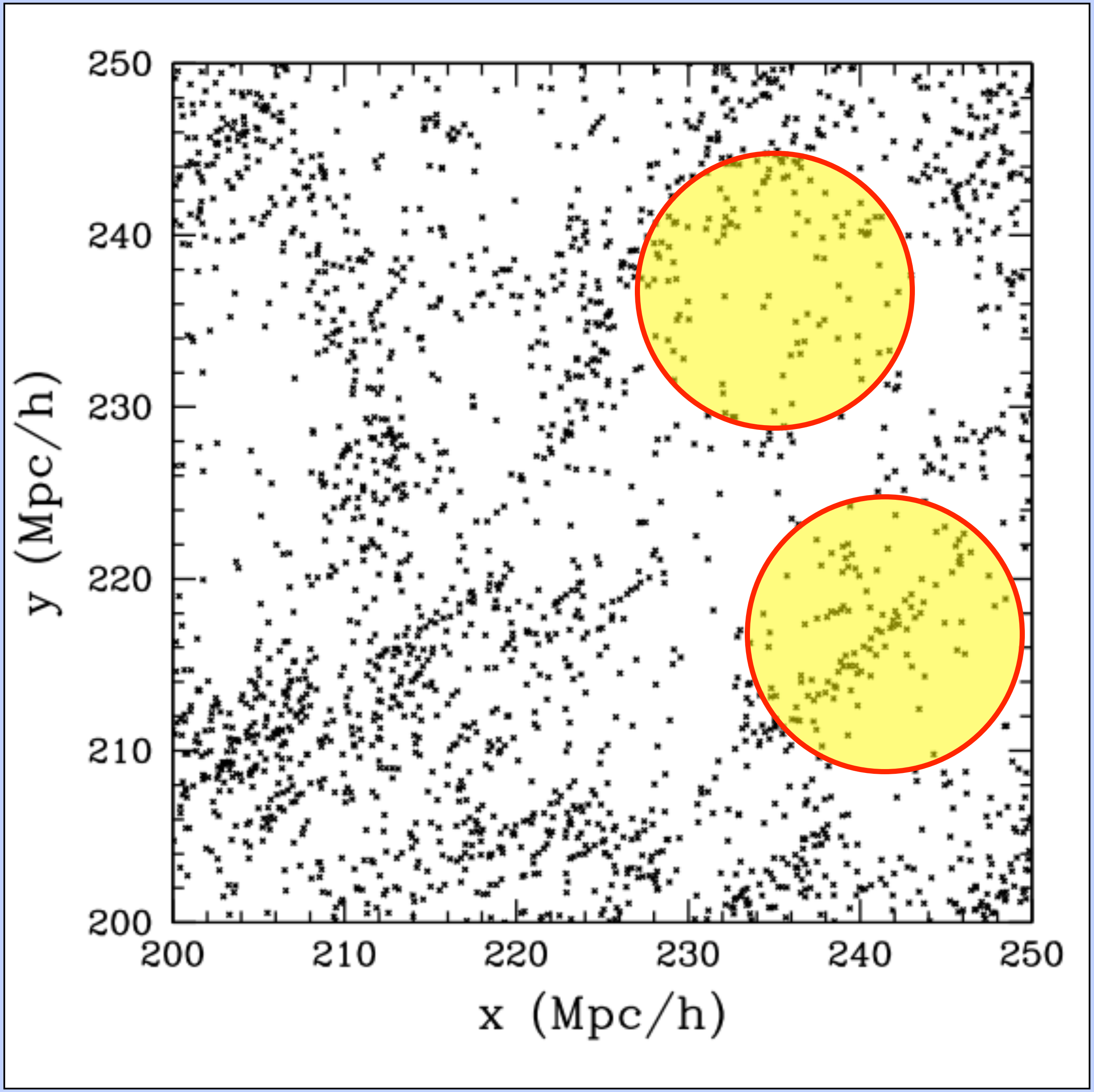

- Galaxy density on small scale (1 Mpc/h)
- Galaxy density on large scale (8 Mpc/h)

Galaxy environments

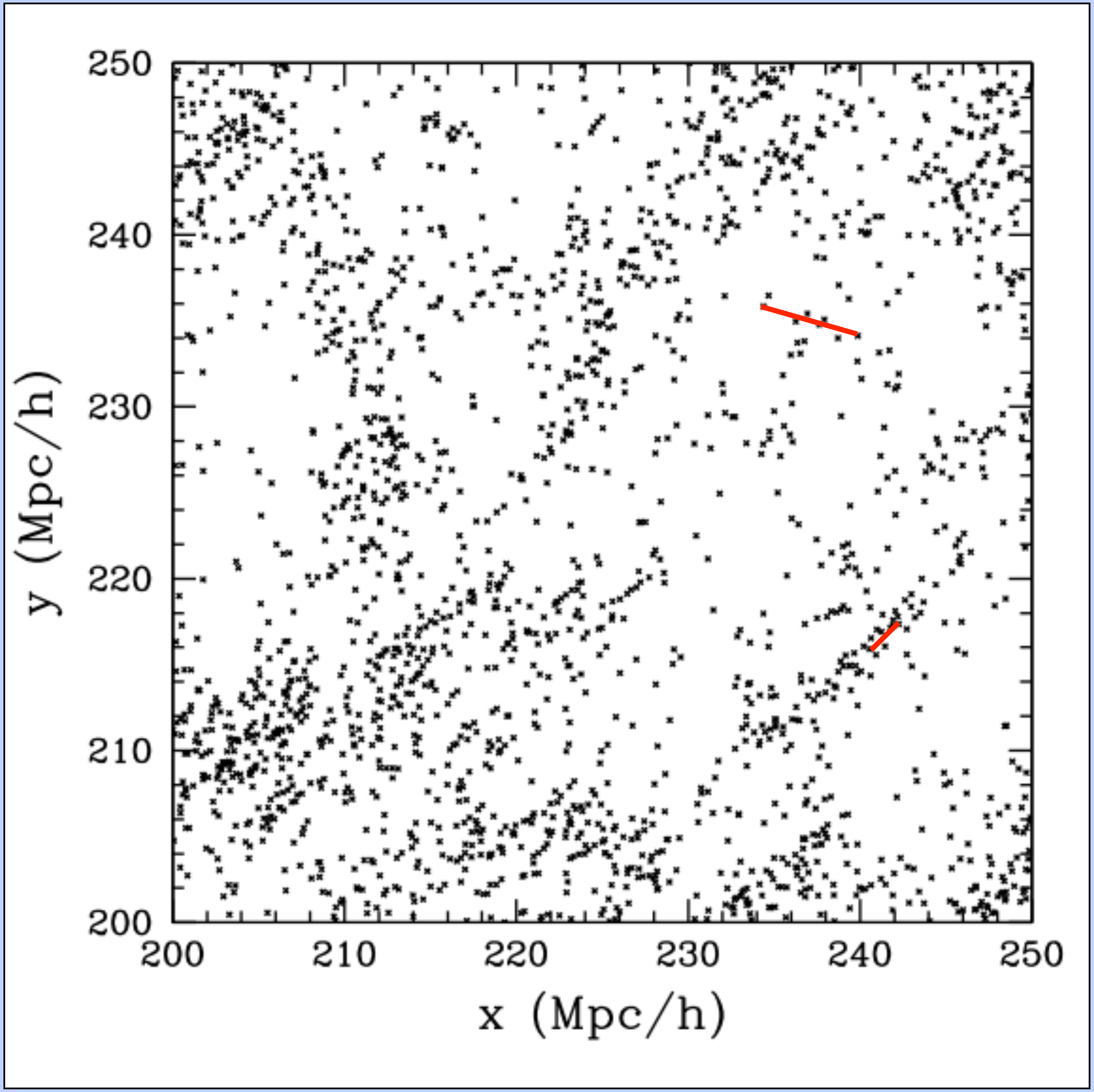

- Galaxy density on small scale (1 Mpc/h)
- Galaxy density on large scale (8 Mpc/h)
- Distance to N^{th} nearest neighbor

Galaxy environments

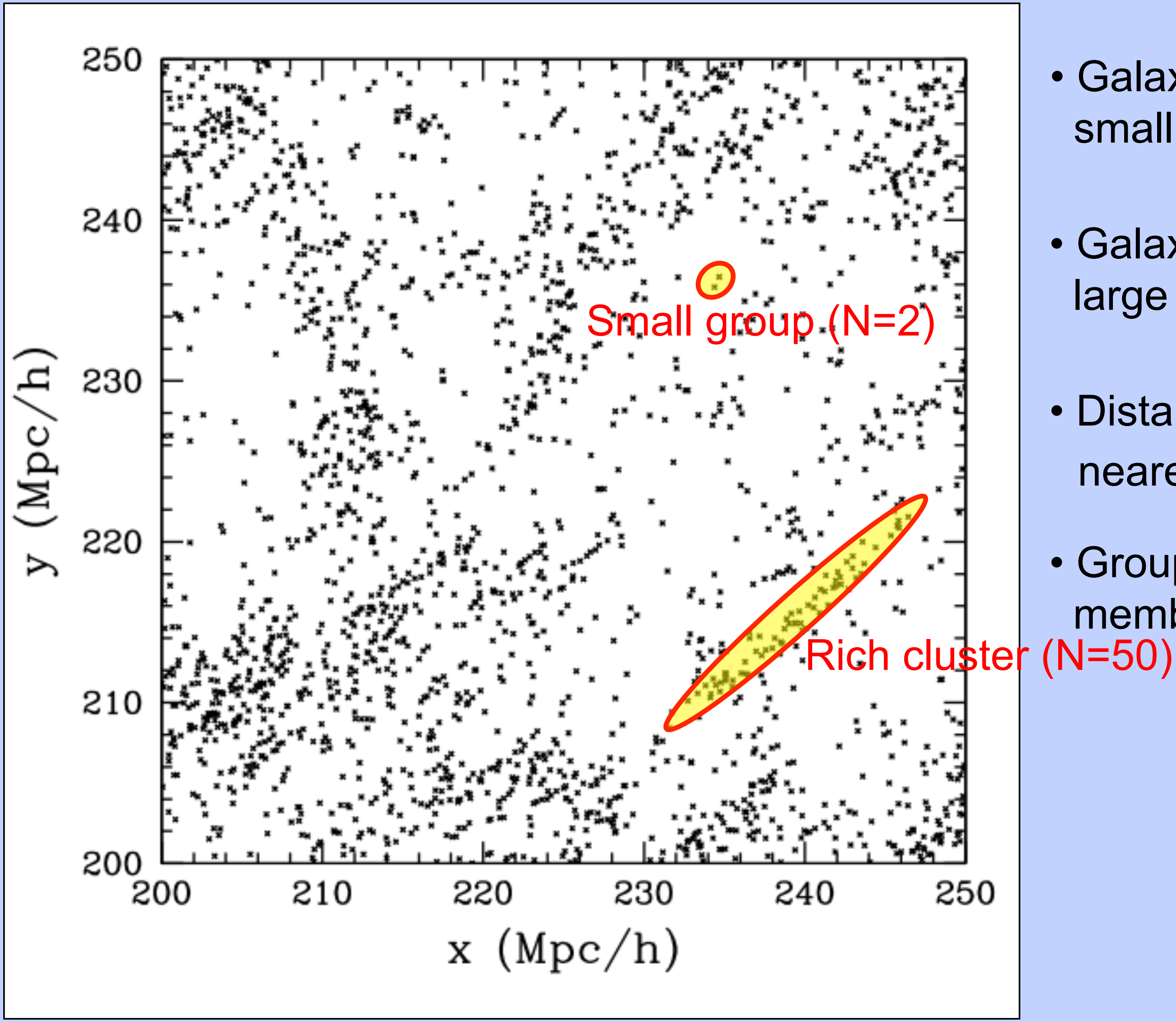

- Galaxy density on small scale (1 Mpc/h)
- Galaxy density on large scale (8 Mpc/h)
- Distance to N^{th} nearest neighbor
- Group or cluster membership

Galaxy environments

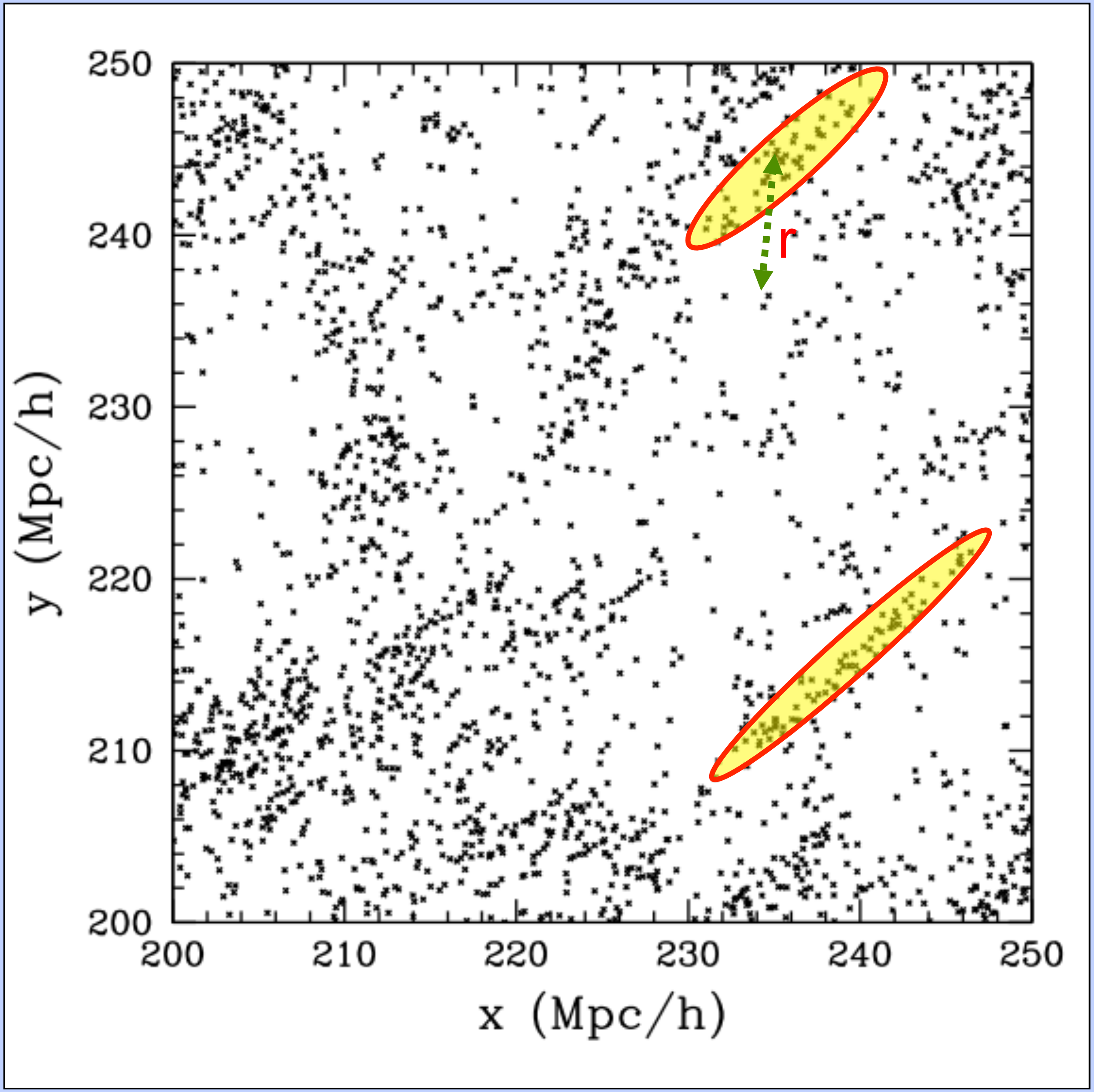

- Galaxy density on small scale (1 Mpc/h)
- Galaxy density on large scale (8 Mpc/h)
- Distance to N^{th} nearest neighbor
- Group or cluster membership
- Distance to nearest cluster

Galaxy environments

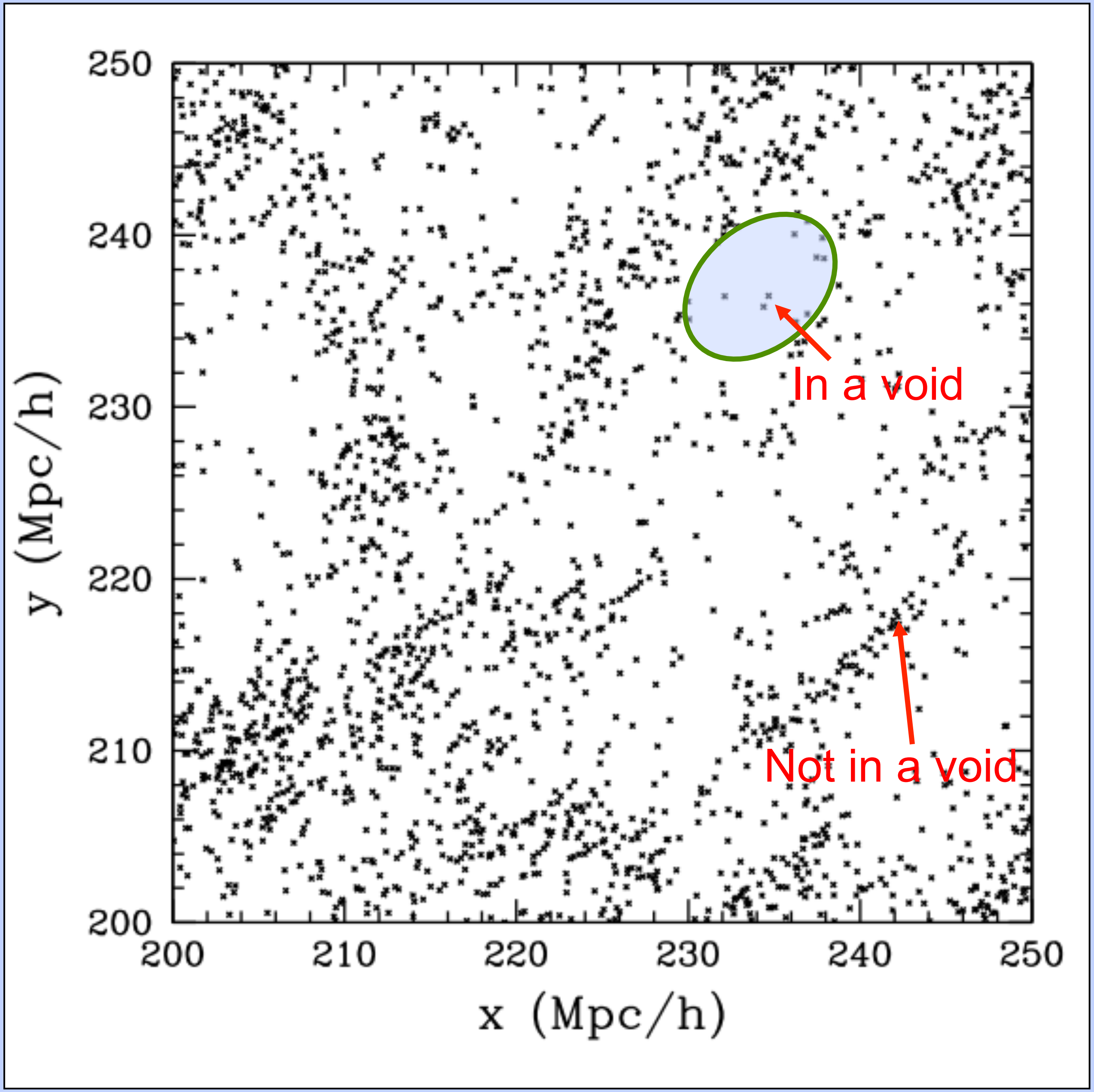

- Galaxy density on small scale (1 Mpc/h)
- Galaxy density on large scale (8 Mpc/h)
- Distance to Nth nearest neighbor
- Group or cluster membership
- Distance to nearest cluster
- Void membership

Morphology-density relations

Spirals

Fraction

S0

Ellipticals

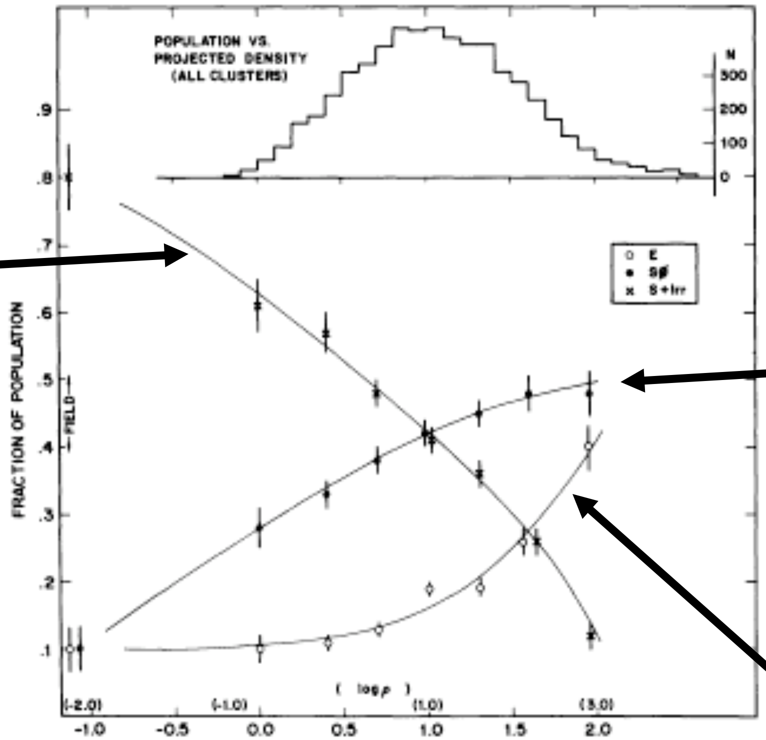

Density

FIG. 4.—The fractior … -I galaxies as a function of the log of the projected density, in galaxies Mpc^{-2}. The data shown are for all cluster galaxies in the sample and for the field. Also shown is an estimated scale of true space density in galaxies Mpc^{-3}. The upper histogram shows the number distribution of the galaxies over the bins of projected density.

Dressler 1980

Morphology-density relations

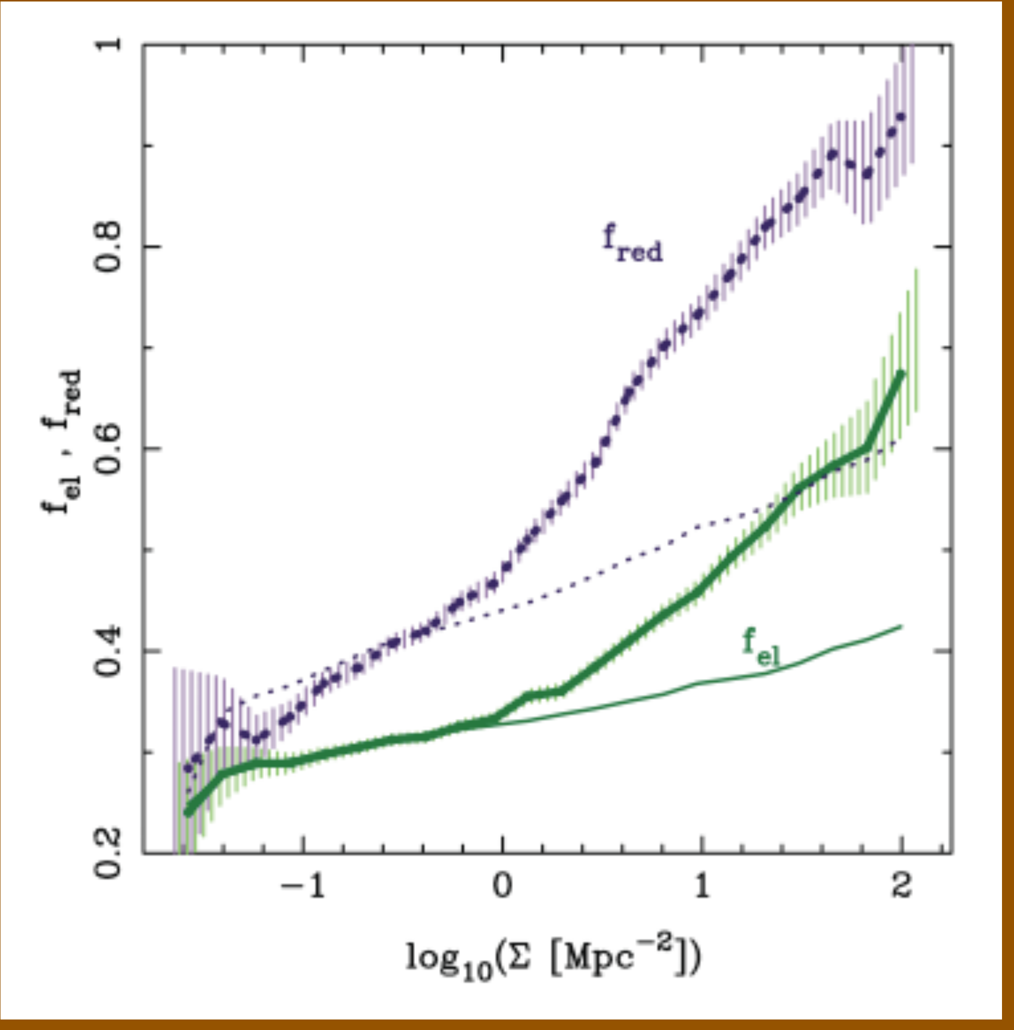

Bamford et al. 2009

Correlations of galaxy properties with environment

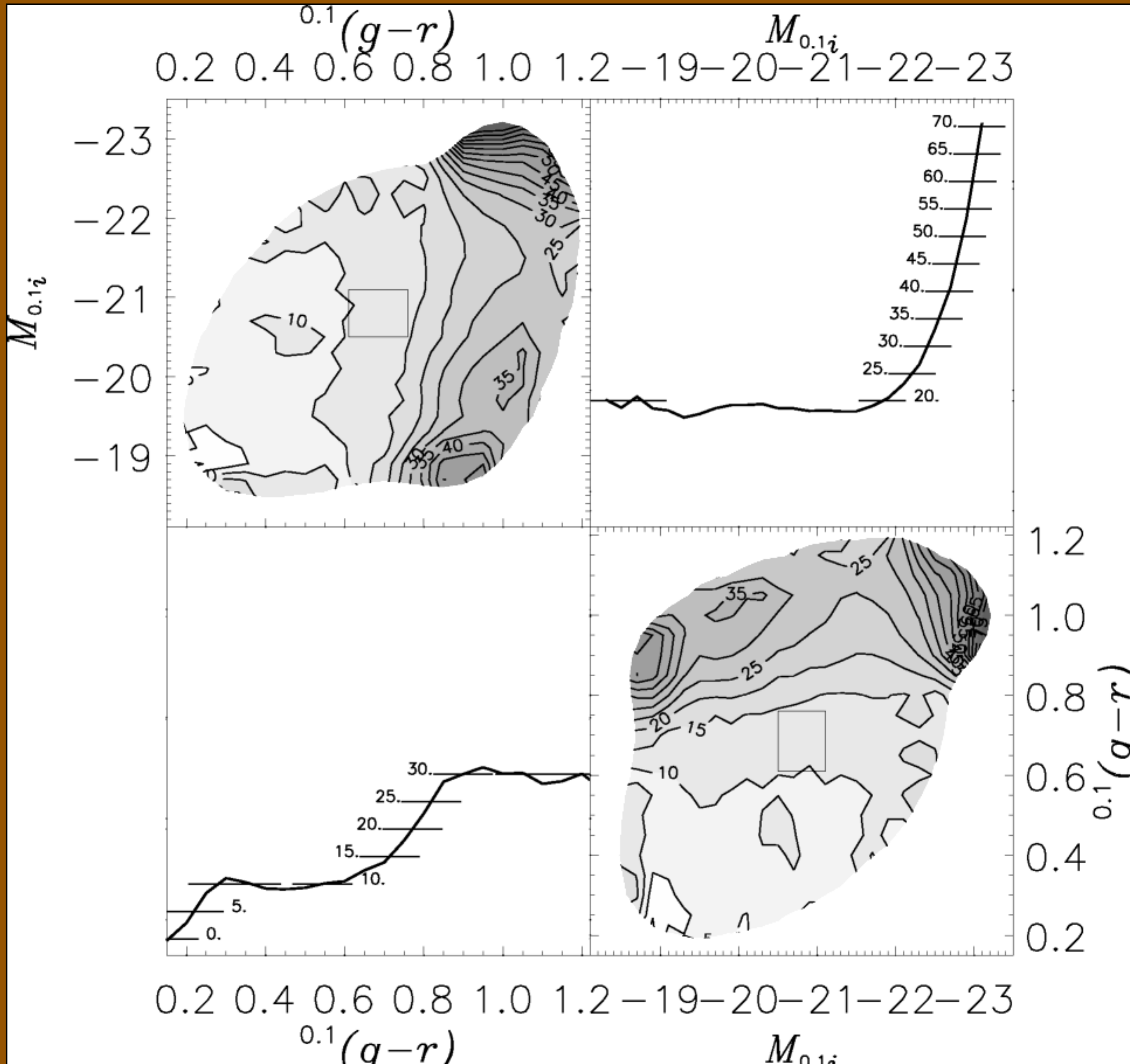

Blanton

Correlations of galaxy properties with environment

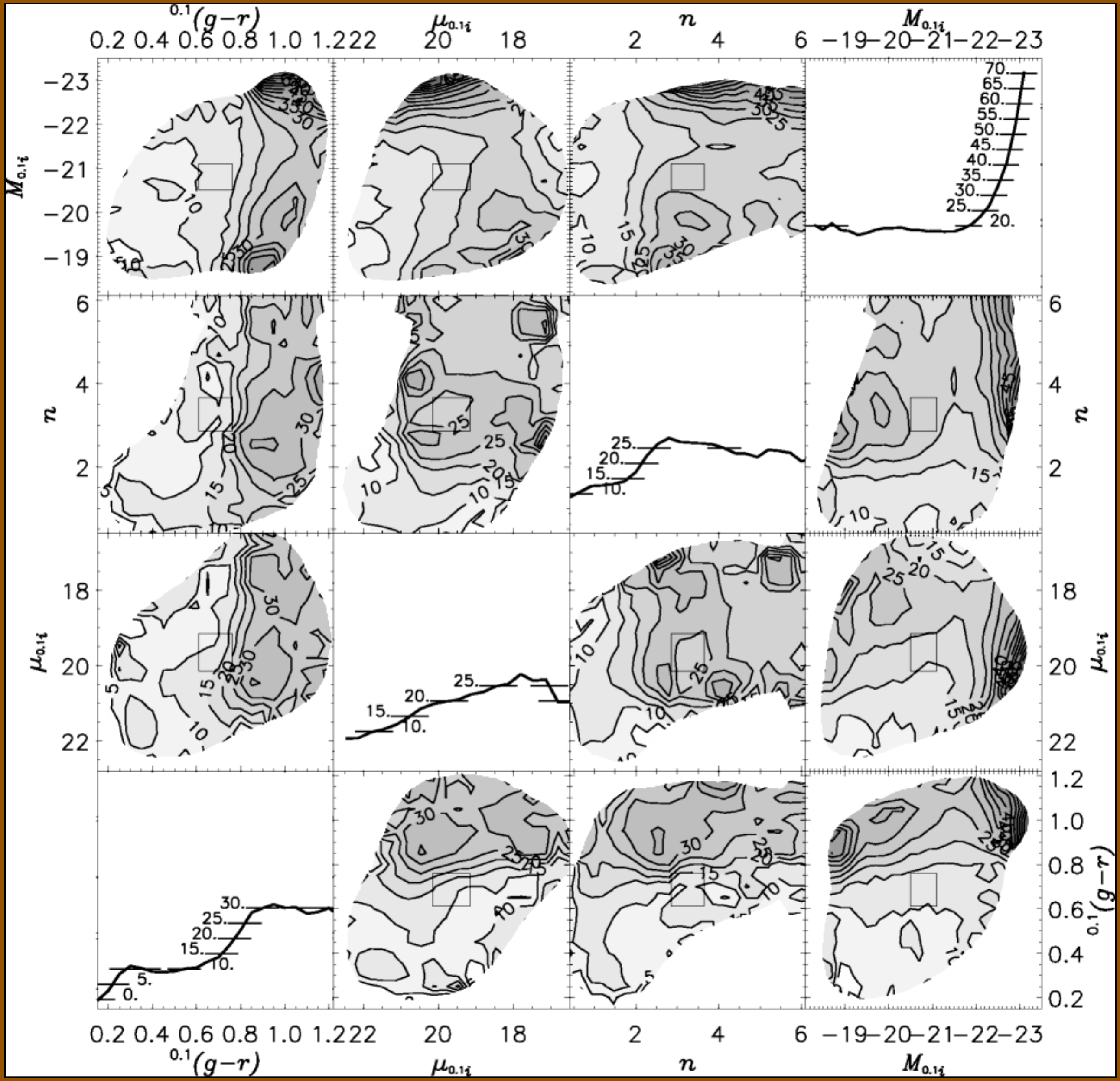

Blanton

Galaxies congregate on small scales to form groups and clusters.

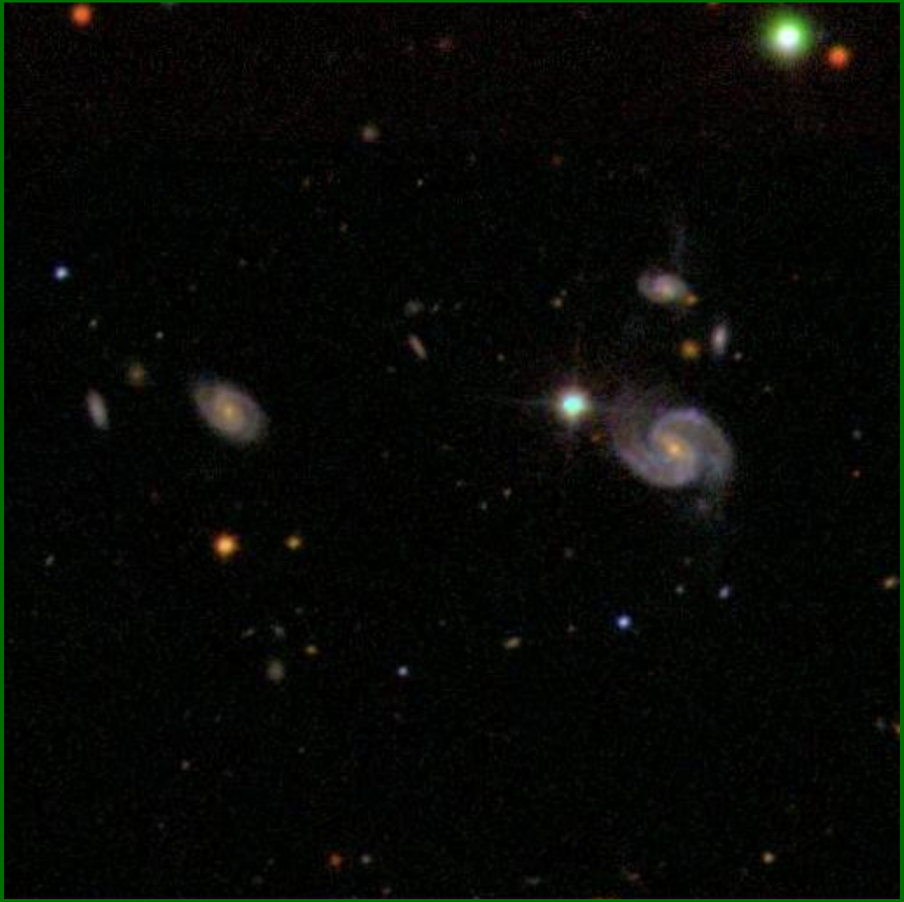

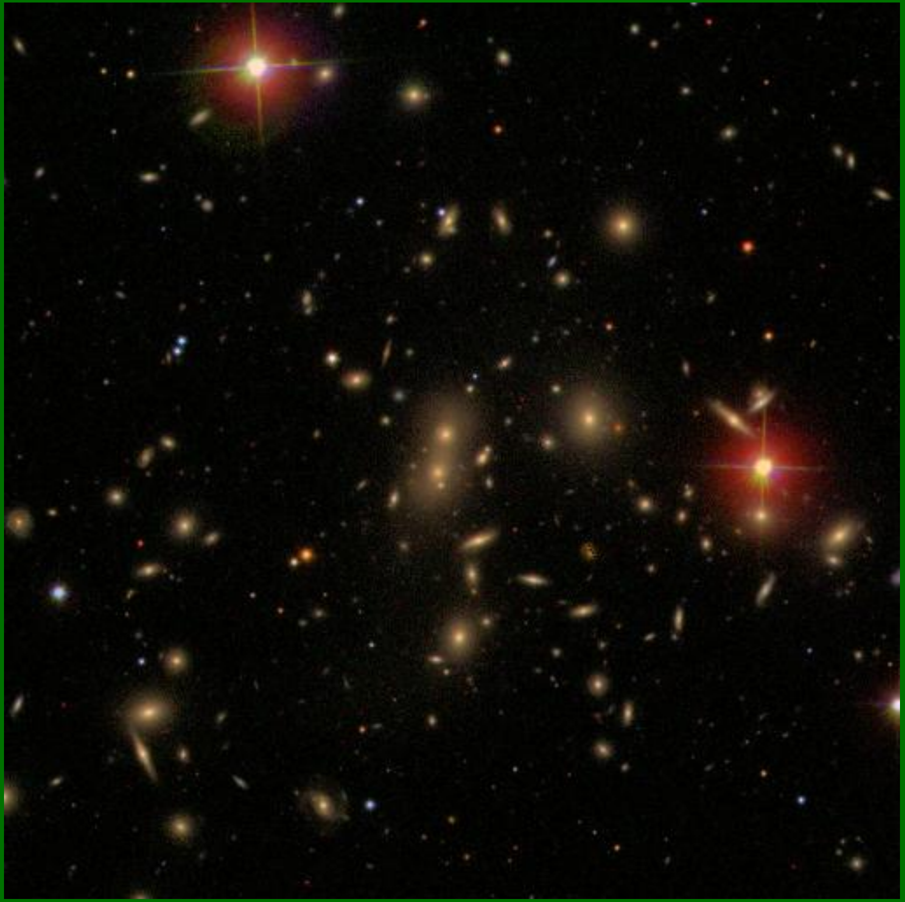

Galaxy groups and clusters

What defines a group or cluster?

In theory…

- Gravitationally bound system of galaxies
- System of galaxies in virial equilibrium
- Galaxies that live in the same dark matter halo

In practice…

- Whatever group-finding algorithm is used

Galaxy groups and clusters

There are as many algorithms as group/cluster catalogs

Three broad sets of classes:

- 2D vs. 3D
- purely geometric vs. spectro-photometric
- galaxies vs. gas vs. dark matter

All must deal with:

- incompleteness (missing galaxies that should be included)
- contamination (including galaxies that should not be)

Galaxy groups and clusters

Geometric method: <u>friends-of-friends</u>

Linking length:

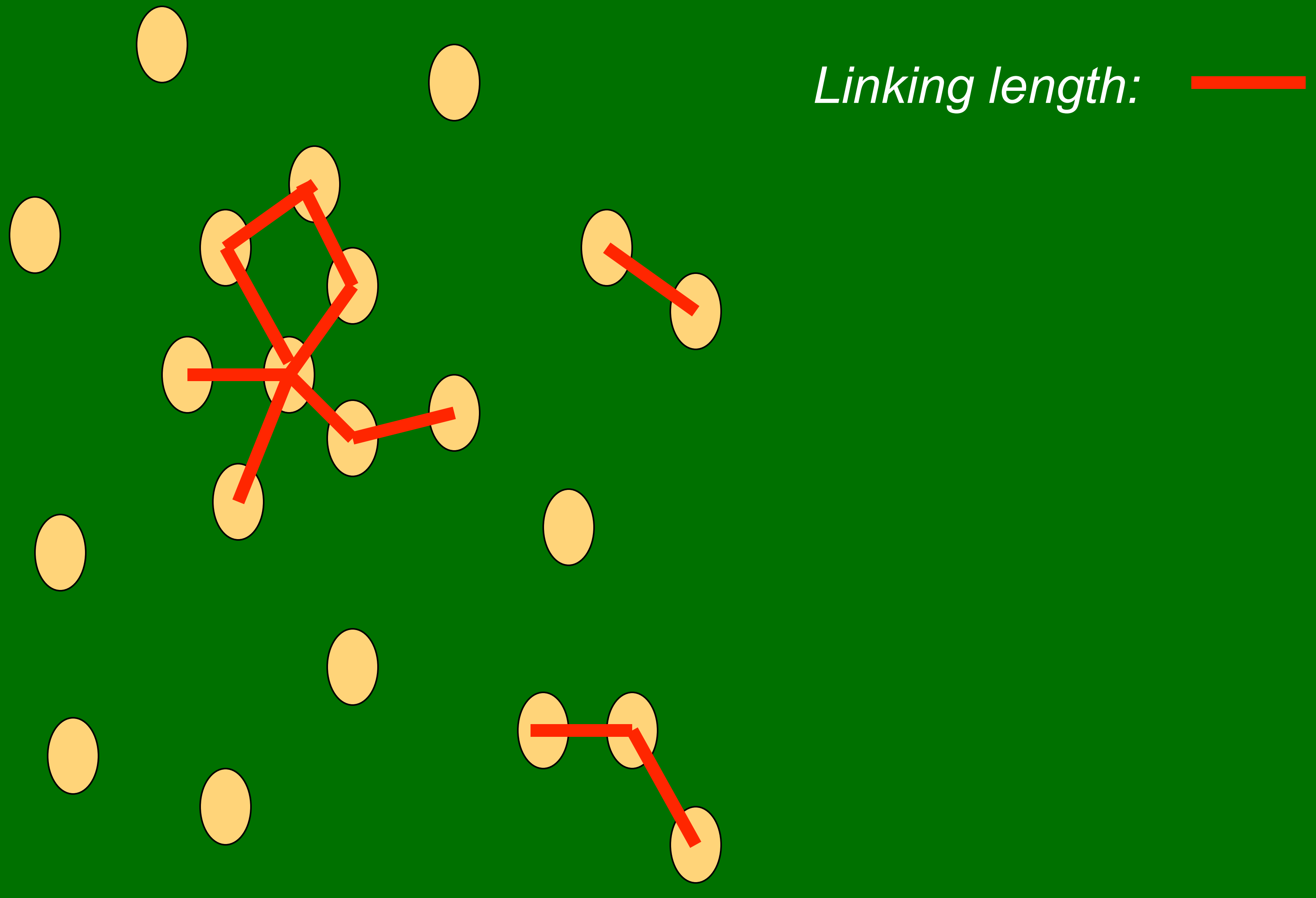

Galaxy groups and clusters

Geometric method: <u>friends-of-friends</u>

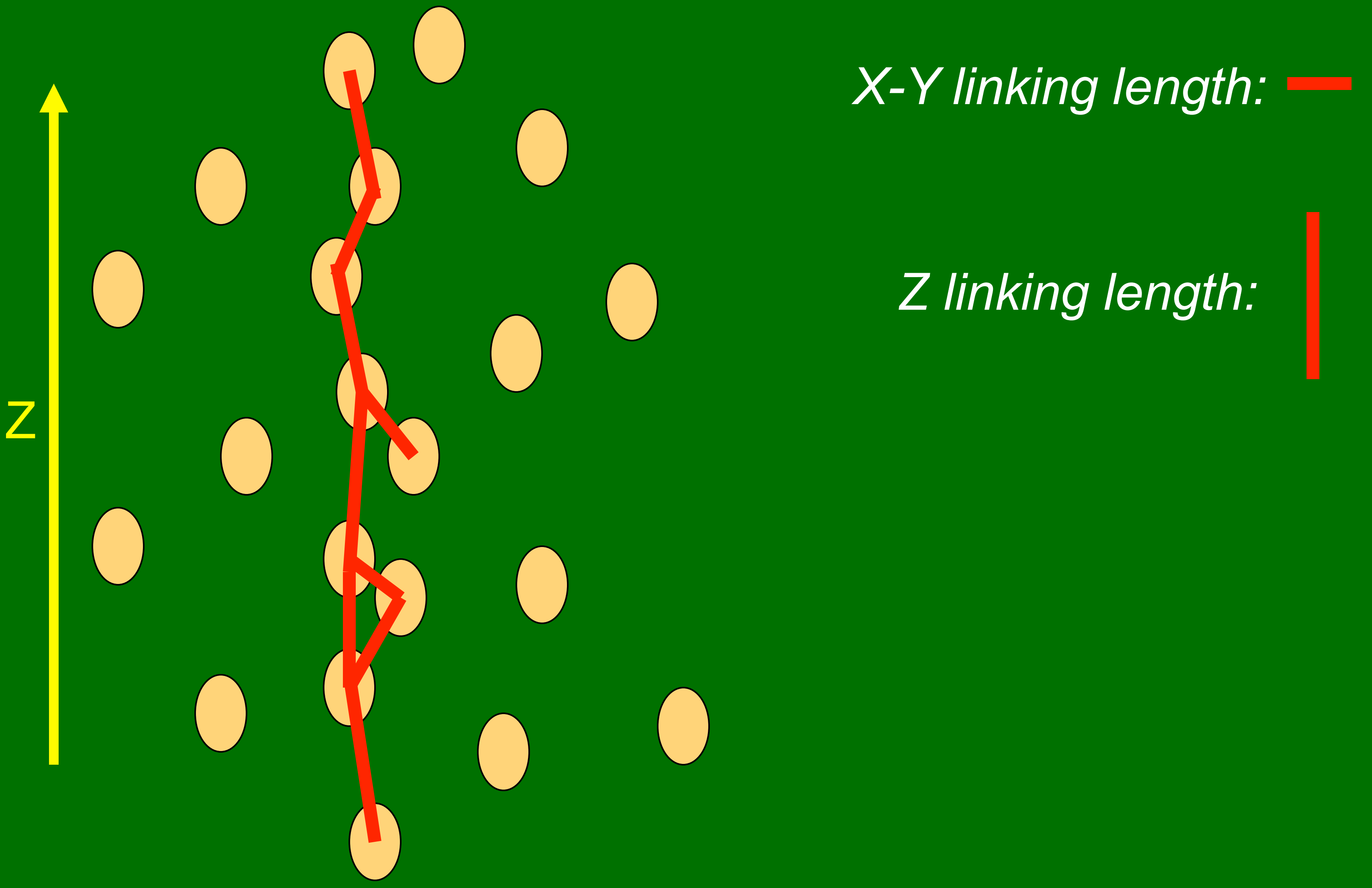

Galaxy groups and clusters

The Astrophysical Journal Supplement Series, 167:1–25, 2006 November

PERCOLATION GALAXY GROUPS AND CLUSTERS IN THE SDSS REDSHIFT SURVEY: IDENTIFICATION, CATALOGS, AND THE MULTIPLICITY FUNCTION

Andreas A. Berlind,[1,2] Joshua Frieman,[2] David H. Weinberg,[3] Michael R. Blanton,[1] Michael S. Warren,[4]
Kevork Abazajian,[4] Ryan Scranton,[5] David W. Hogg,[1] Roman Scoccimarro,[1] Neta A. Bahcall,[6]
J. Brinkmann,[7] J. Richard Gott III,[6] S. J. Kleinman,[7] J. Krzesinski,[8,9] Brian C. Lee,[10]
Christopher J. Miller,[11] Atsuko Nitta,[7] Donald P. Schneider,[12]
Douglas L. Tucker,[13] and Idit Zehavi[14,15]
(for The SDSS Collaboration)
Received 2006 January 13; accepted 2006 July 26

ABSTRACT

We identify galaxy groups and clusters in volume-limited samples of the Sloan Digital Sky Survey (SDSS) redshift survey, using a redshift-space friends-of-friends algorithm. We optimize the friends-of-friends linking lengths to recover galaxy systems that occupy the same dark matter halos, using a set of mock catalogs created by populating halos of *N*-body simulations with galaxies. Extensive tests with these mock catalogs show that no combination of perpendicular and line-of-sight linking lengths is able to yield groups and clusters that simultaneously recover the true halo multiplicity function, projected size distribution, and velocity dispersion. We adopt a linking length combination that yields, for galaxy groups with 10 or more members: a group multiplicity function that is unbiased with respect to the true halo multiplicity function; an unbiased median relation between the multiplicities of groups and their associated halos; a spurious group fraction of less than ∼1%; a halo completeness of more than ∼97%; the correct projected size distribution as a function of multiplicity; and a velocity dispersion distribution that is ∼20% too low at all multiplicities. These results hold over a range of mock catalogs that use different input recipes of populating halos with galaxies. We apply our group-finding algorithm to the SDSS data and obtain three group and cluster catalogs for three volume-limited samples that cover 3495.1 $\deg^2$ on the sky, go out to redshifts of 0.1, 0.068, and 0.045, and contain 57,138, 37,820, and 18,895 galaxies, respectively. We correct for incompleteness caused by fiber collisions and survey edges and obtain measurements of the group multiplicity function, with errors calculated from realistic mock catalogs. These multiplicity function measurements provide a key constraint on the relation between galaxy populations and dark matter halos.

Subject headings: galaxies: clusters: general — large-scale structure of universe

Online material: color figures, machine-readable tables

Berlind et al. (2006)

Galaxy groups and clusters

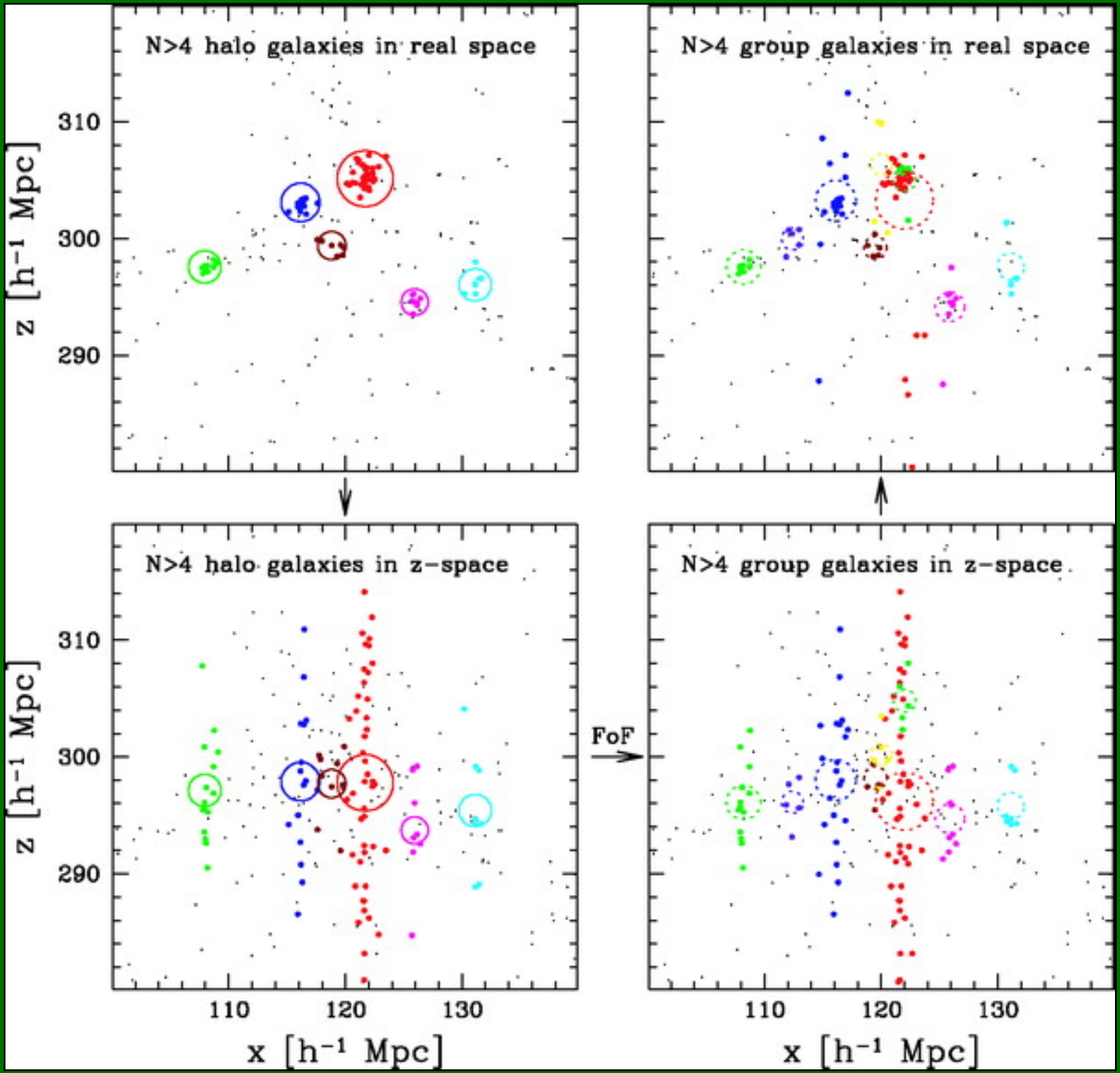

Berlind et al. (2006)

Galaxy groups and clusters

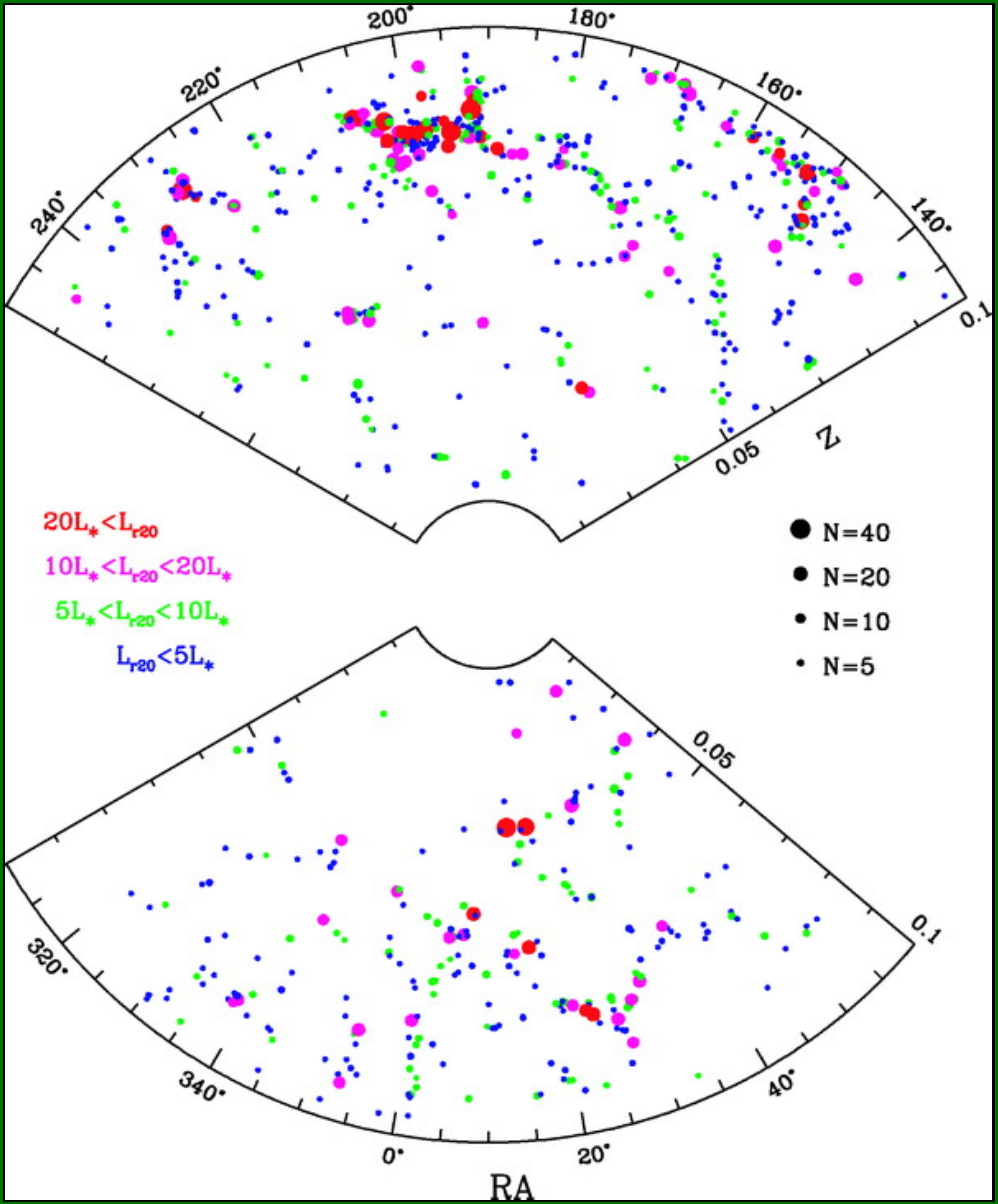

Berlind et al. (2006)

Group/cluster multiplicity/richness function

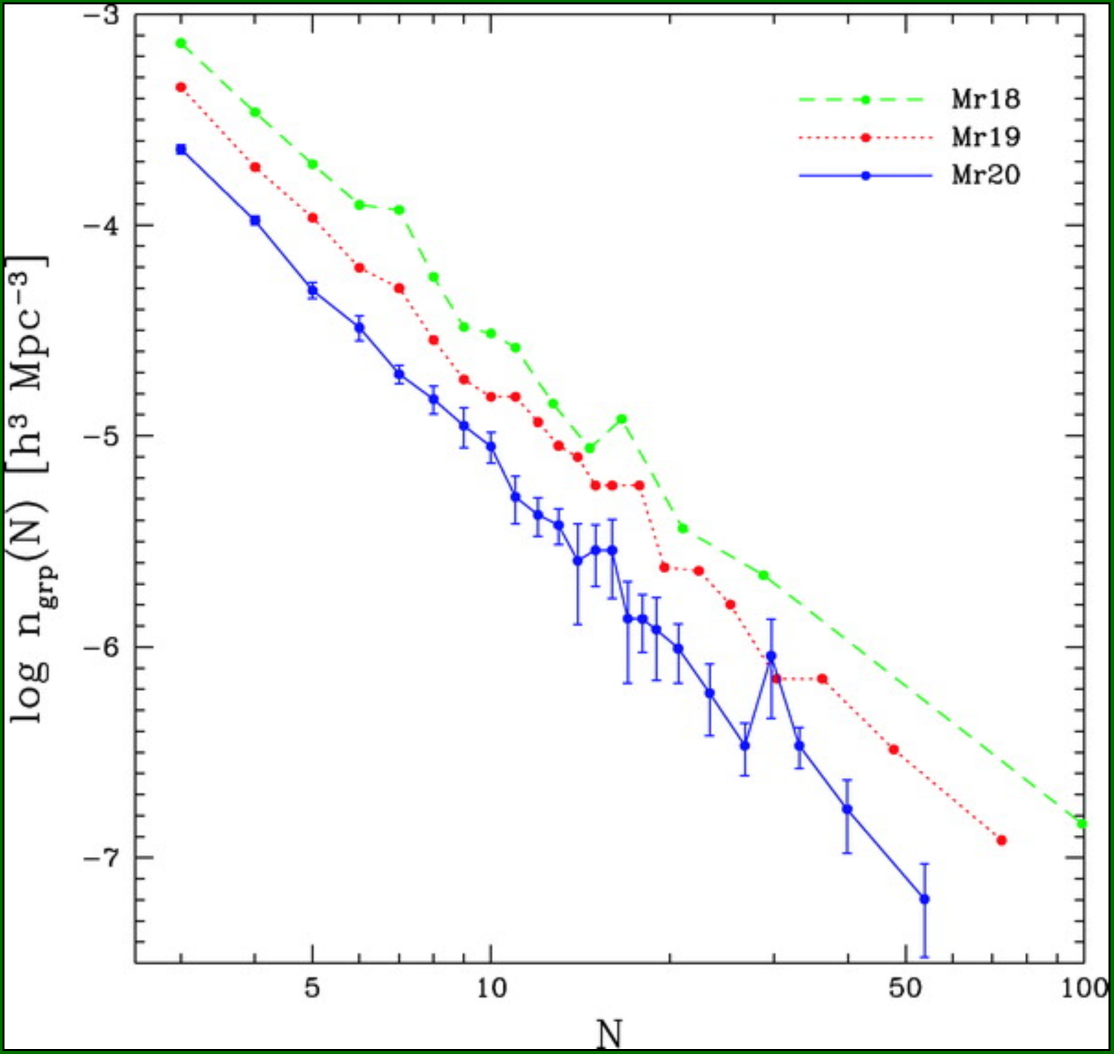

Berlind et al. (2006)

2D Photometric cluster finders: maxBCG

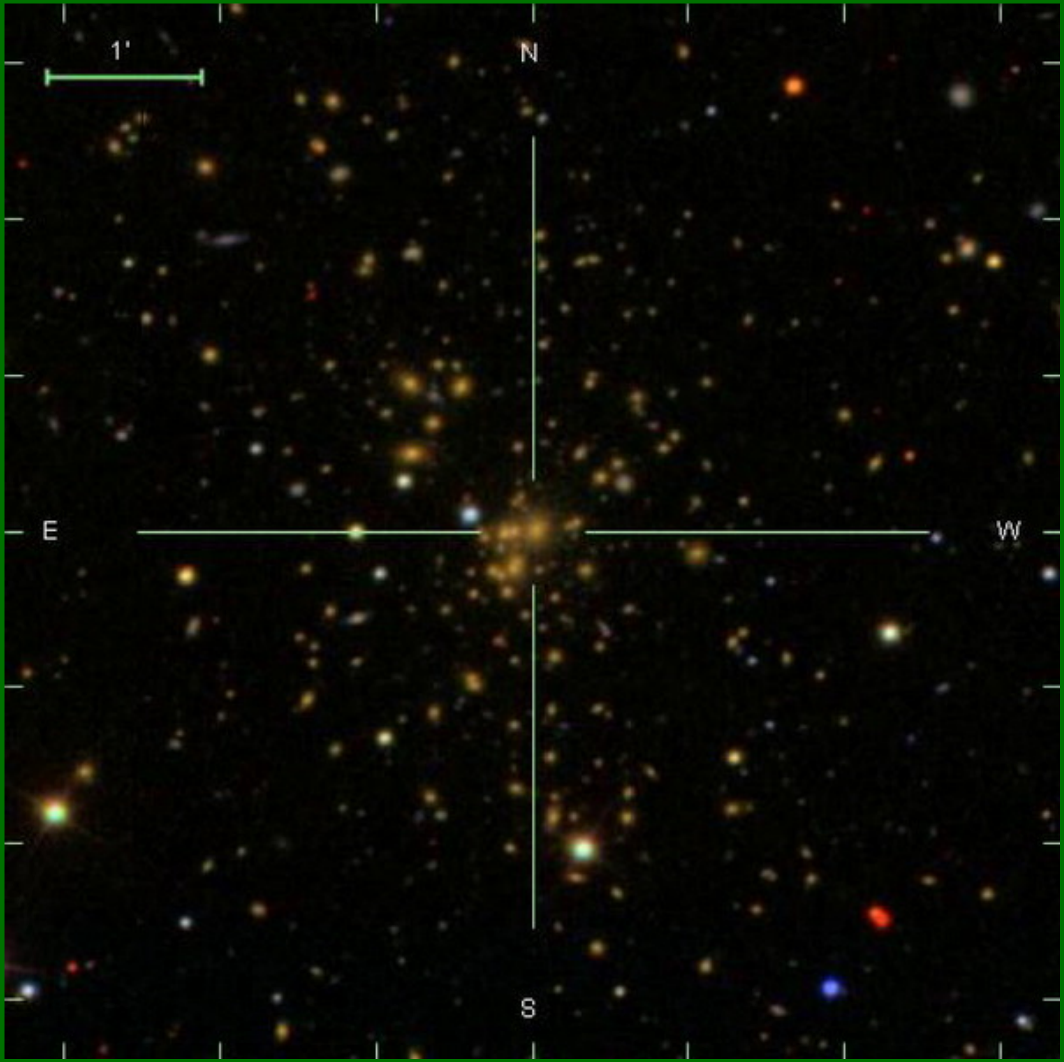

Koester et al. (2007)

Galaxy groups and clusters

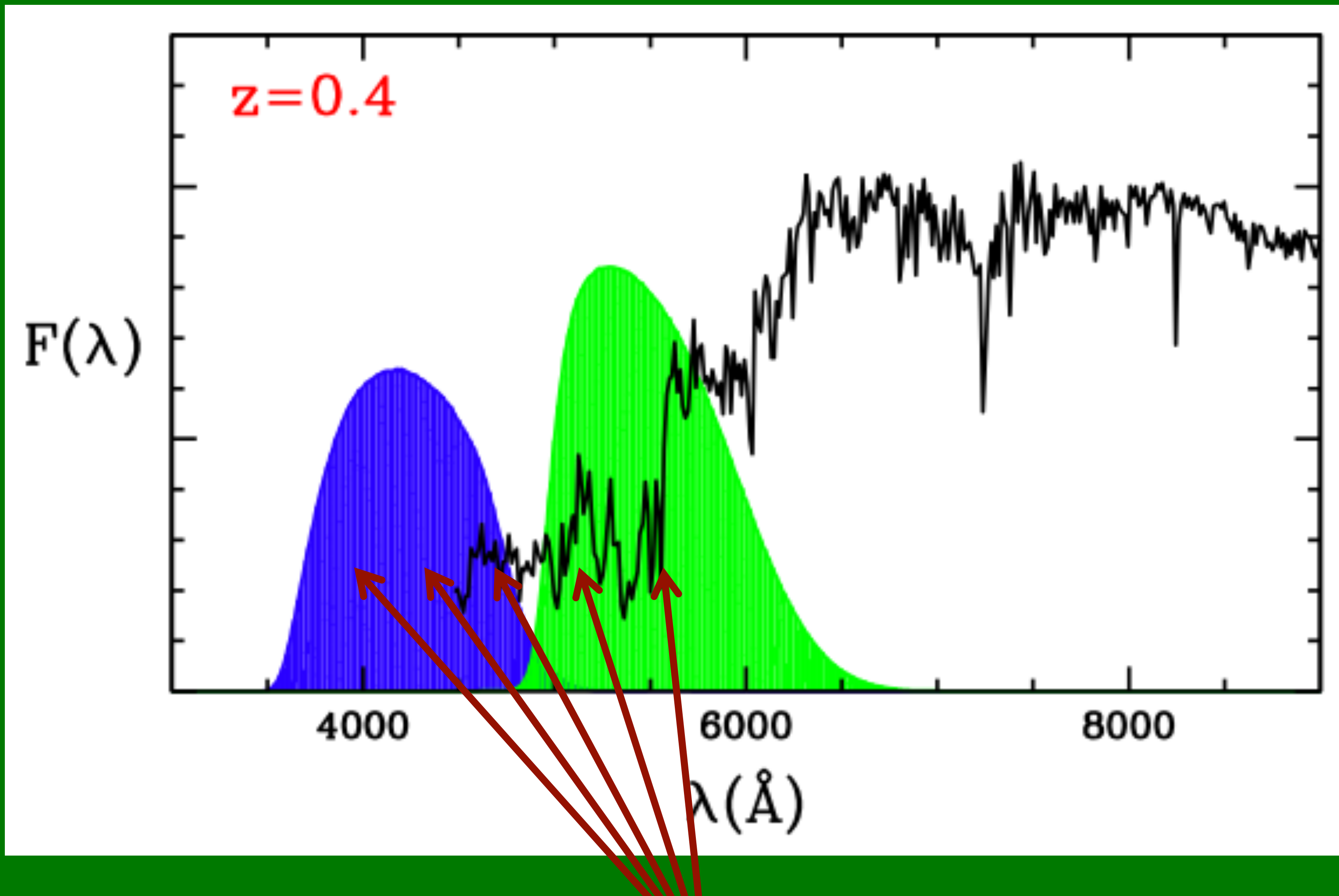

4000 Å break

Galaxy groups and clusters

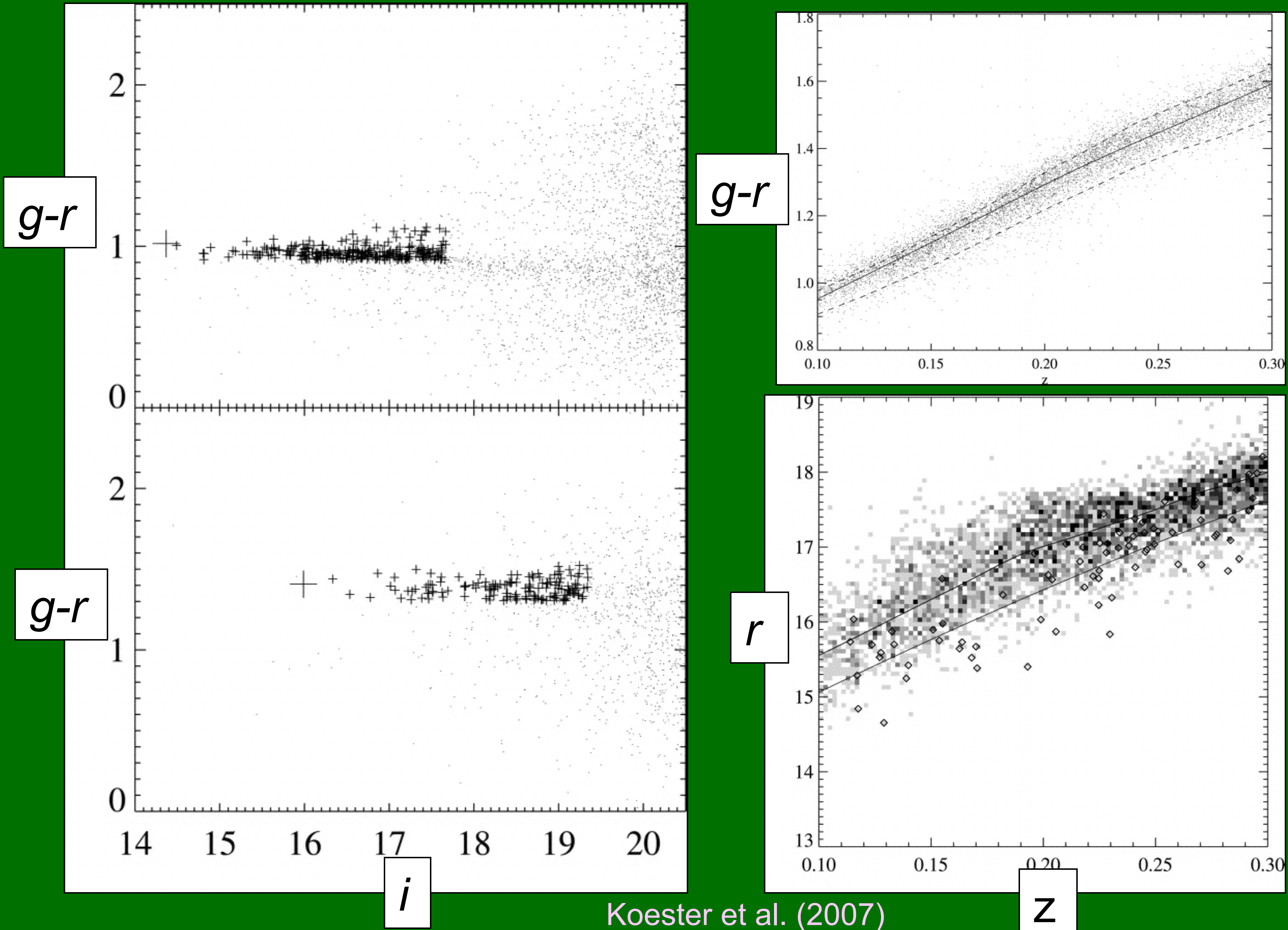

Koester et al. (2007)

Galaxy groups and clusters

X-ray clusters

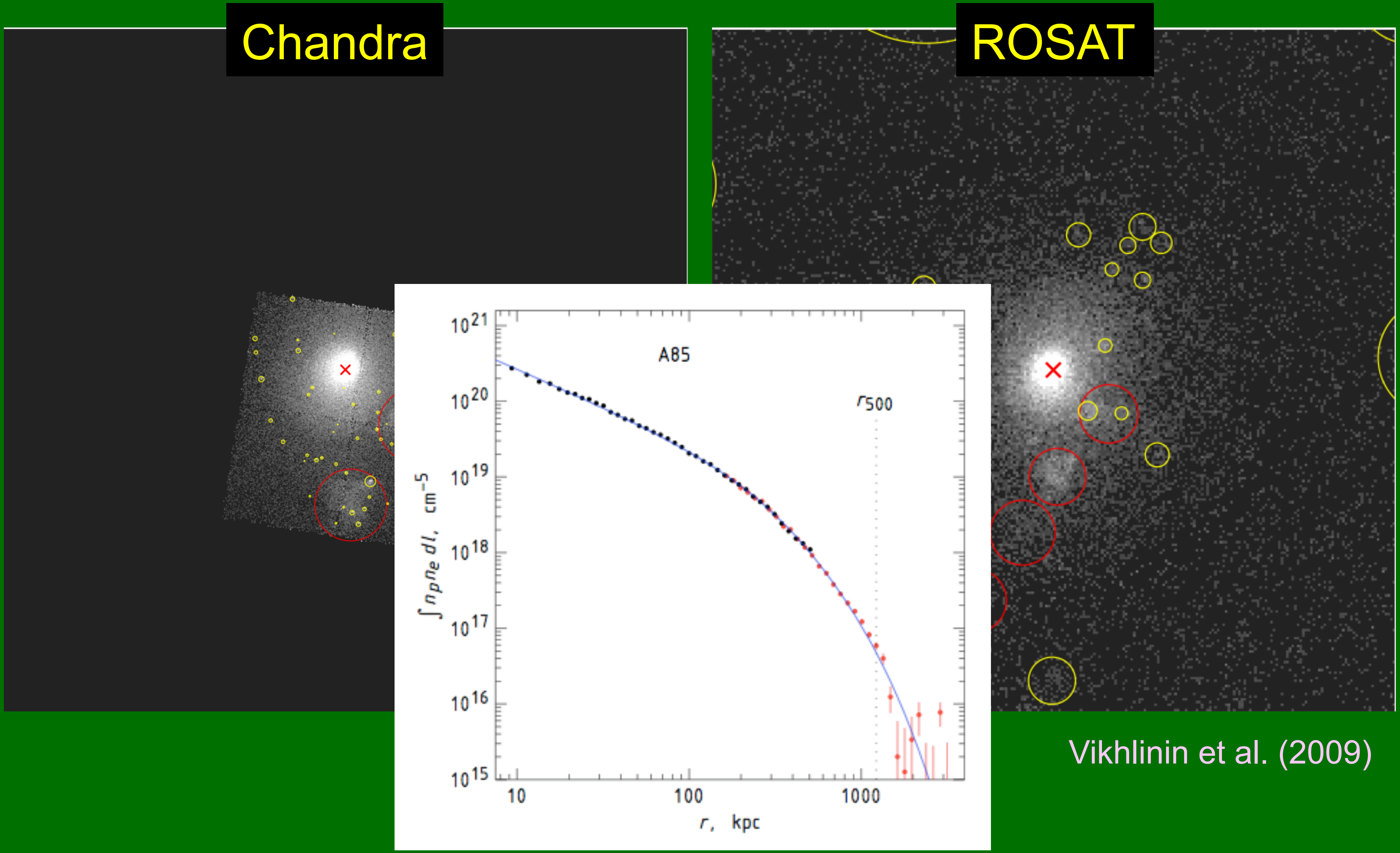

Vikhlinin et al. (2009)

X-ray clusters

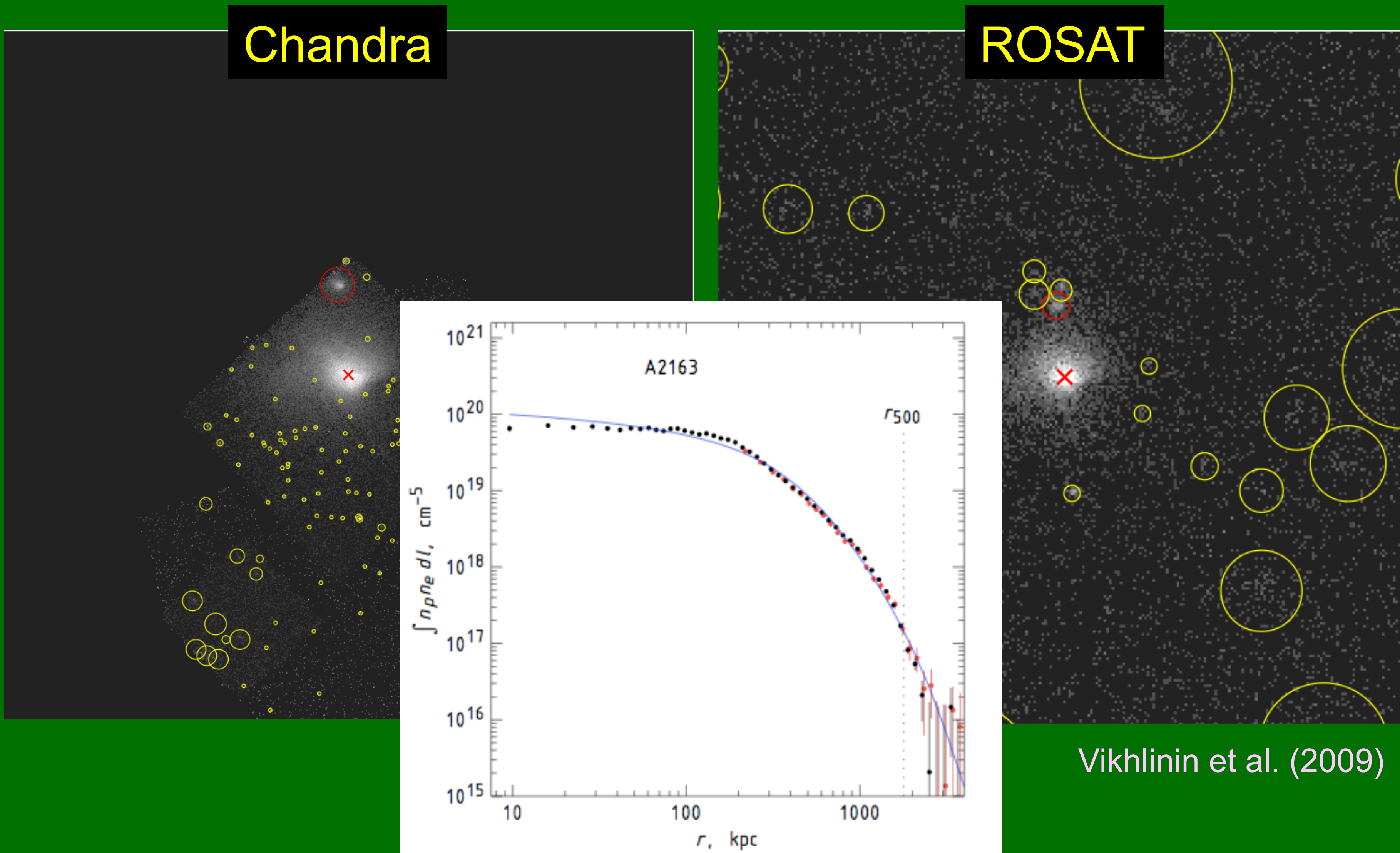

Vikhlinin et al. (2009)

X-ray clusters

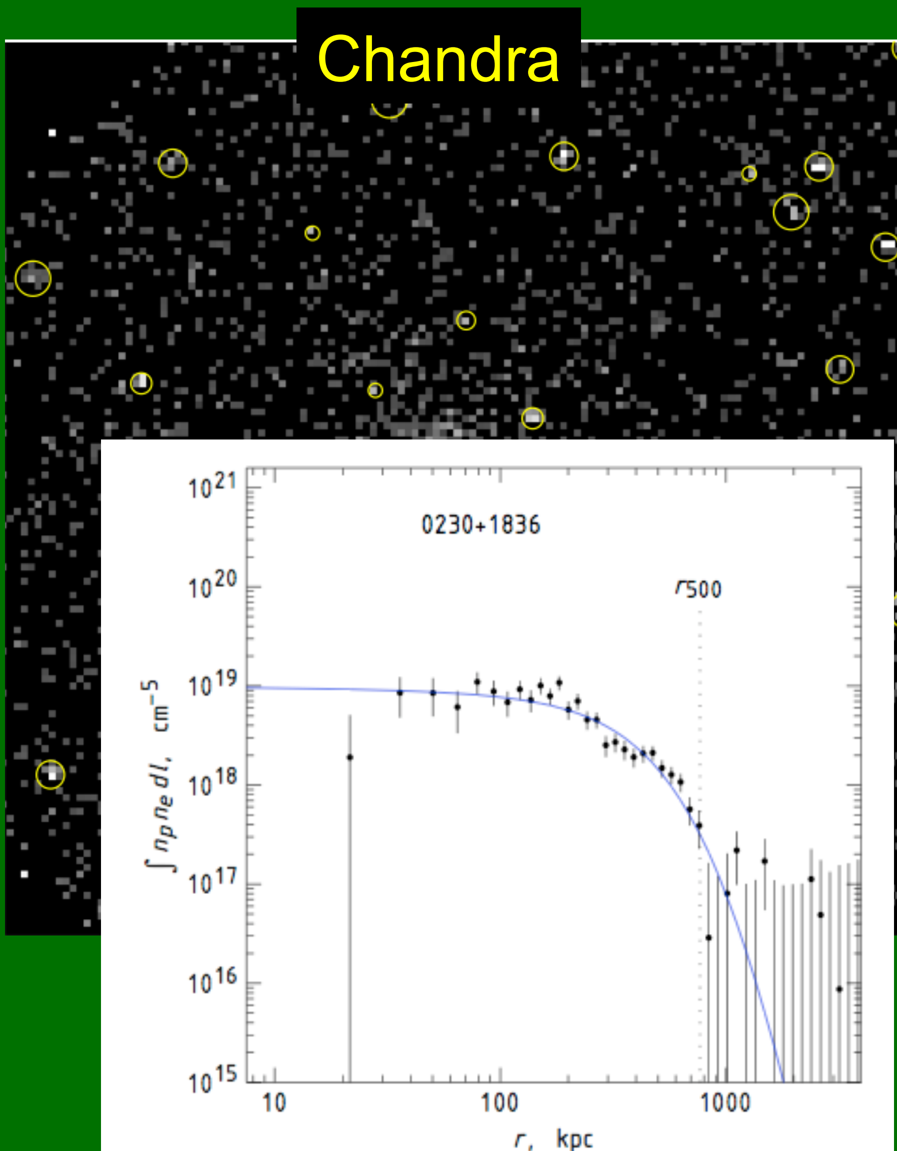

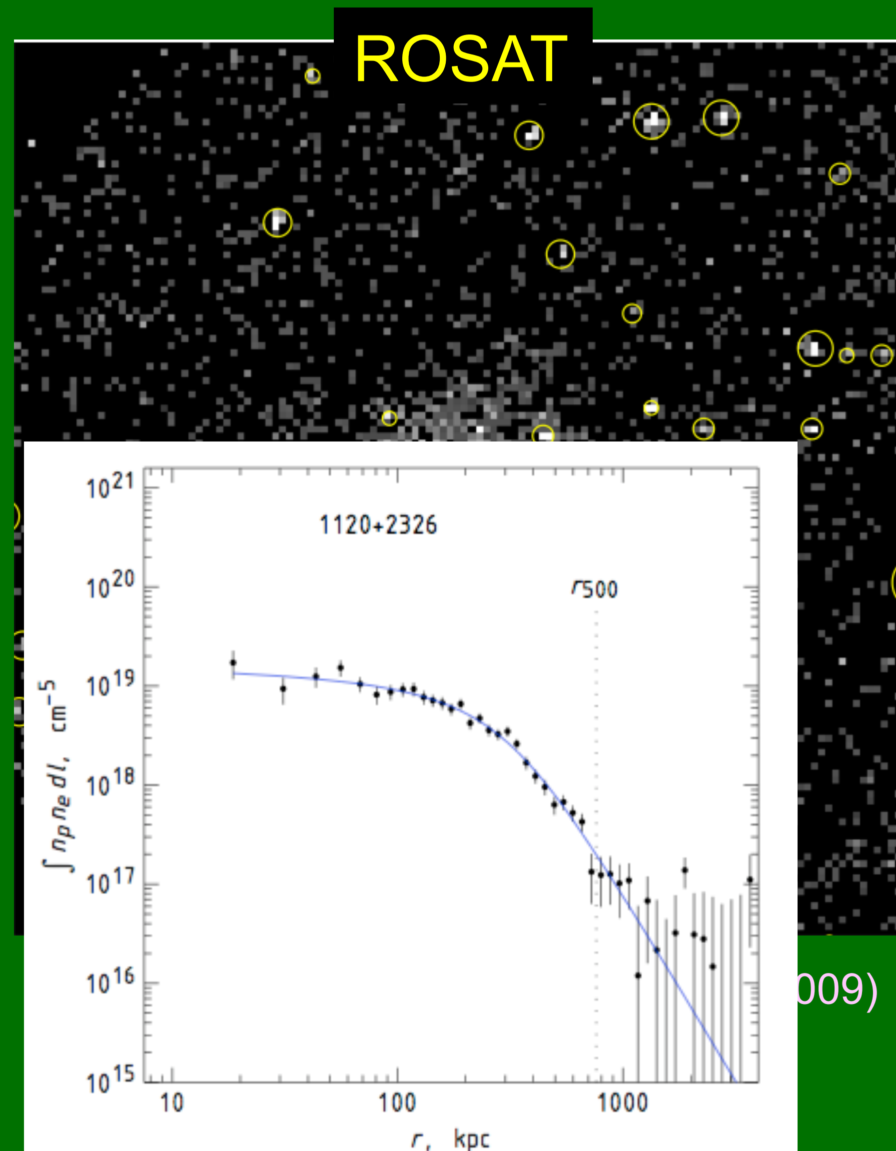

009)

X-ray clusters

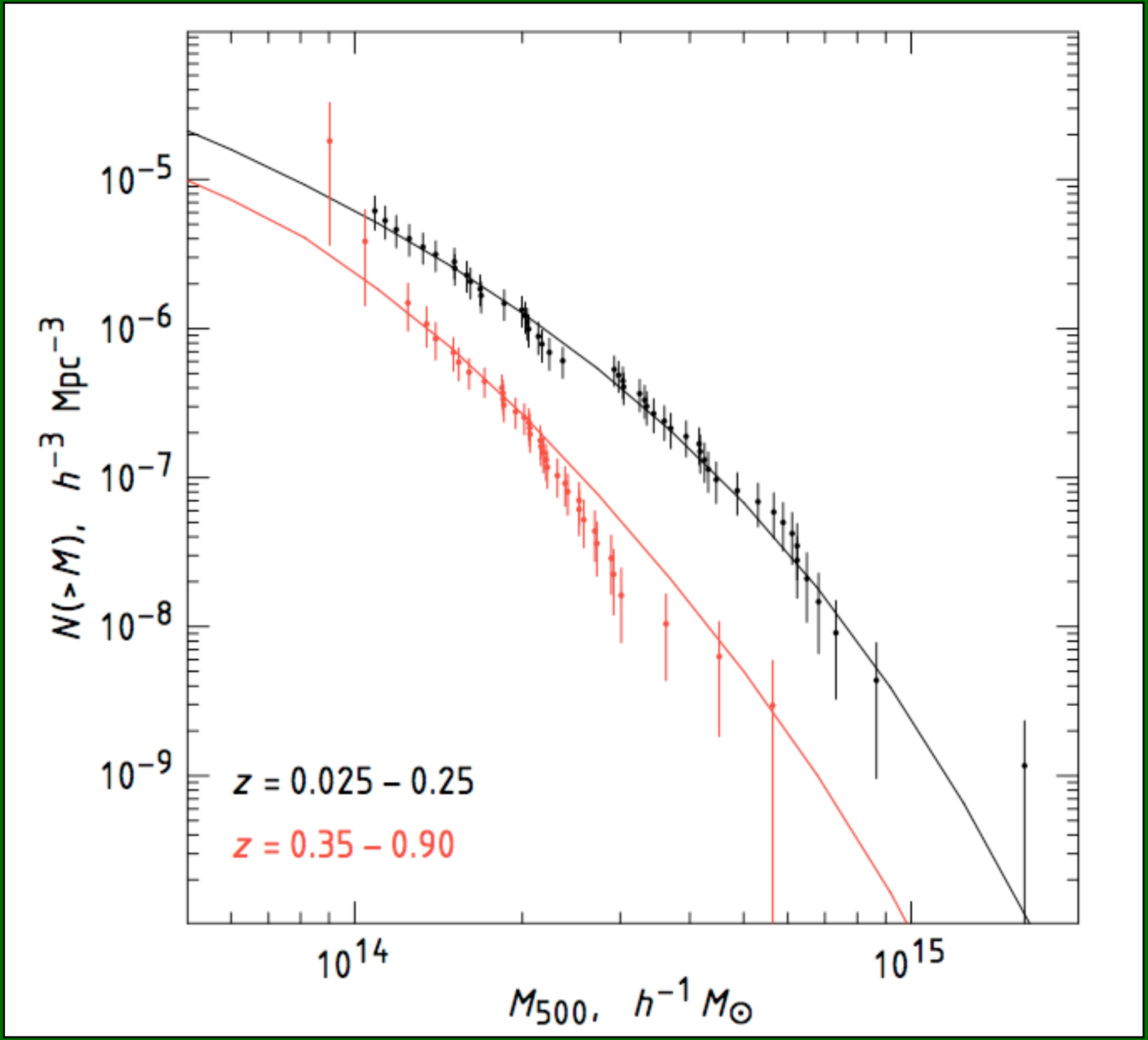

Vikhlinin et al. (2009)

Sunayev-Zel' dovich effect

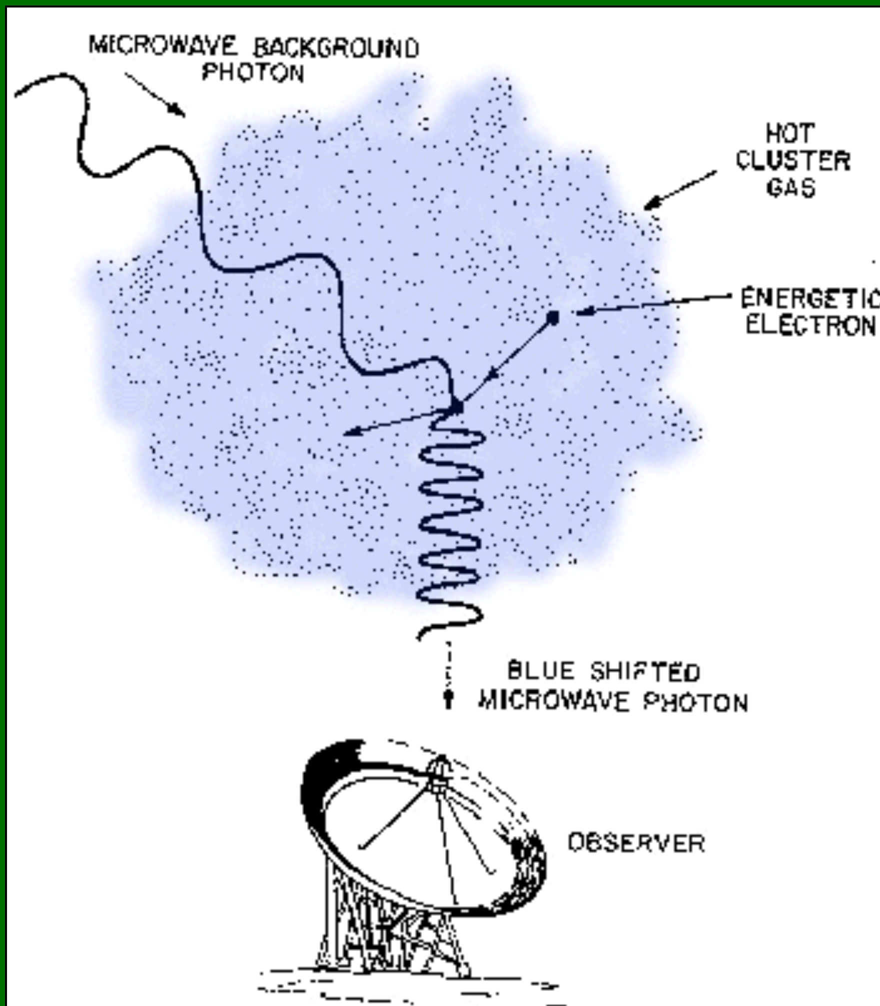

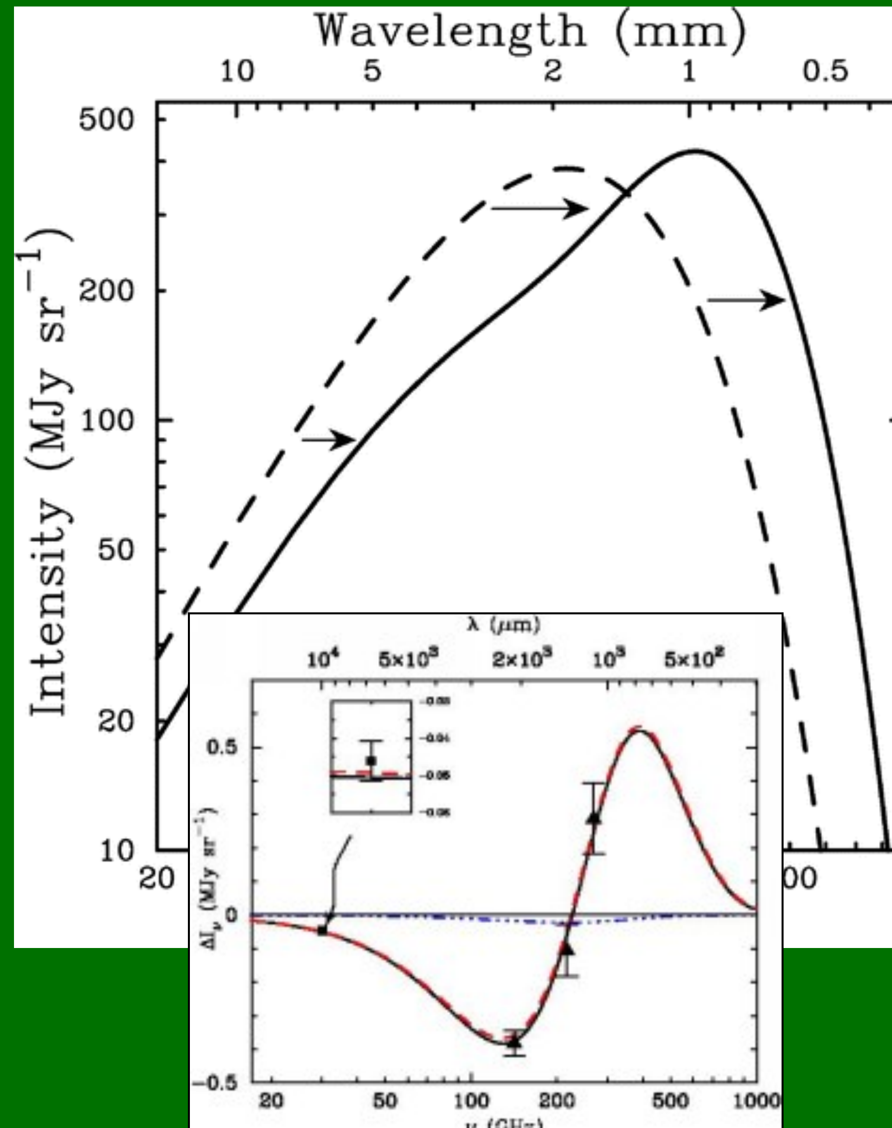

Carlstrom et al.

Galaxy groups and clusters

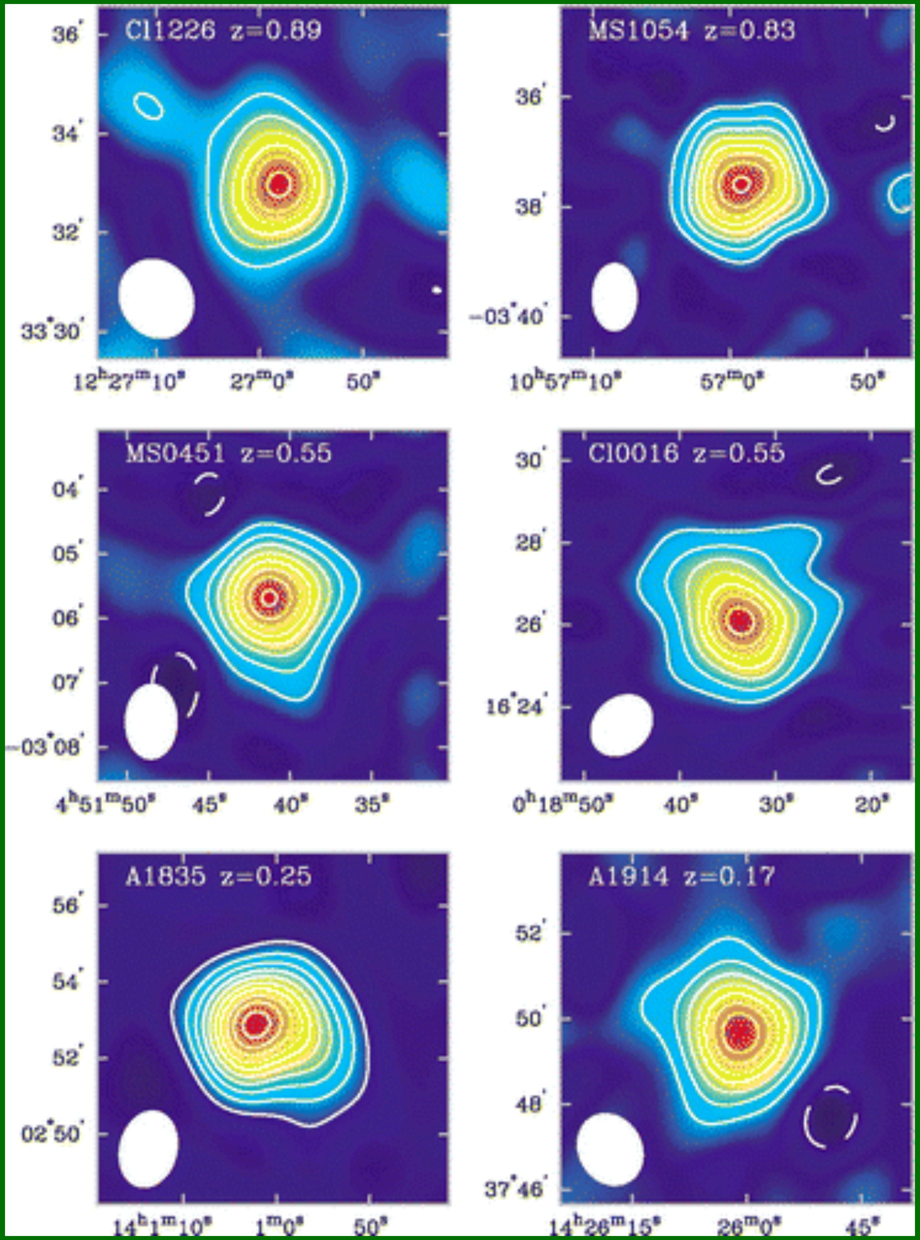

SZ clusters

Carlstrom et al.

Galaxy rotation curves

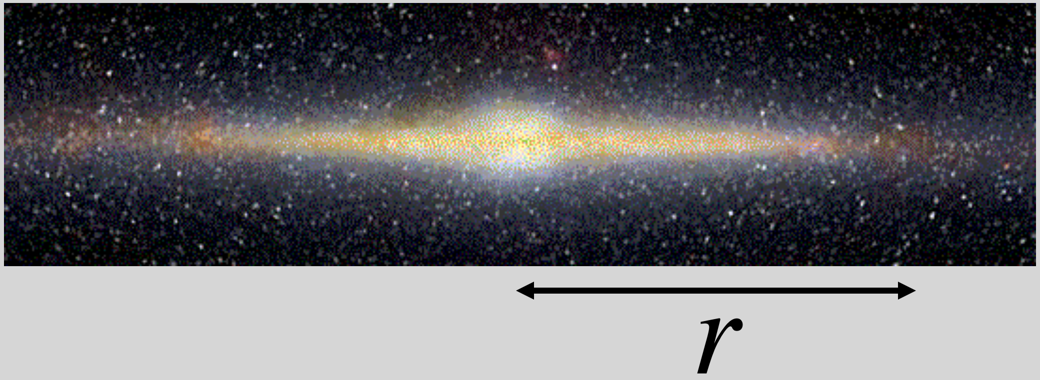

$$\frac{v^2(r)}{r} = \frac{GM(r)}{r^2} \rightarrow v(r) = \sqrt{\frac{GM(r)}{r}}$$

At large distances, where the galaxy runs out of light, the rotation speed should decrease as $r^{-1/2}$

Galaxy rotation curves

Instead, it stays flat.

$$v(r) = const \rightarrow M(r) = \frac{v^2}{G} r$$

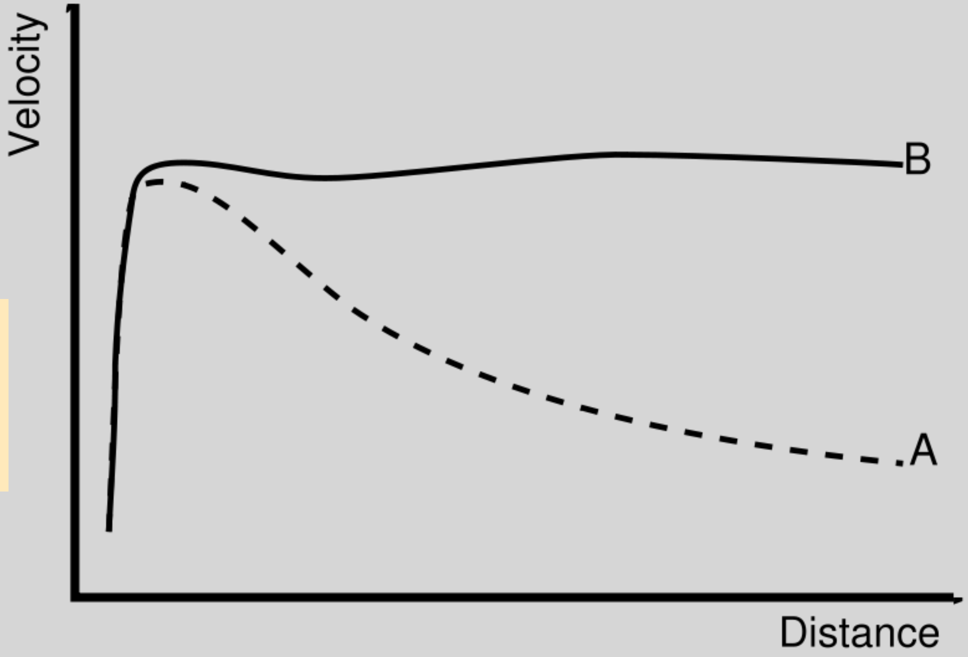

There must therefore be lots of mass that is not visible, out to very large distances. ---> Dark matter

Modified gravity?

Alternatively, our theory of gravity is wrong, and gravitational accelerations are stronger than Newton on very large scales.

Newton: $\vec{F} = m\vec{a}$

MOND: $$\vec{F} = m\mu\left(\frac{a}{a_0}\right)\vec{a} = \begin{cases} m\vec{a}, & a \gg a_0 \\ m\left(\frac{a}{a_0}\right)\vec{a}, & a \ll a_0 \end{cases}$$

How does MOND work?

$$F = \frac{GMm}{r^2} = \frac{ma^2}{a_0} \rightarrow a^2 = \frac{GMa_0}{r^2}$$

$$a = \frac{v^2}{r} \rightarrow v^2 = \left(\frac{GMa_0}{r^2}\right)^{1/2} r \rightarrow v = \sqrt[4]{GMa_0} = const!$$

Plugging in measured rotation speeds and visible masses of galaxies:

$$a_0 = 1.2 \times 10^{-10}\, ms^{-2}$$

A galaxy cluster: Dark matter

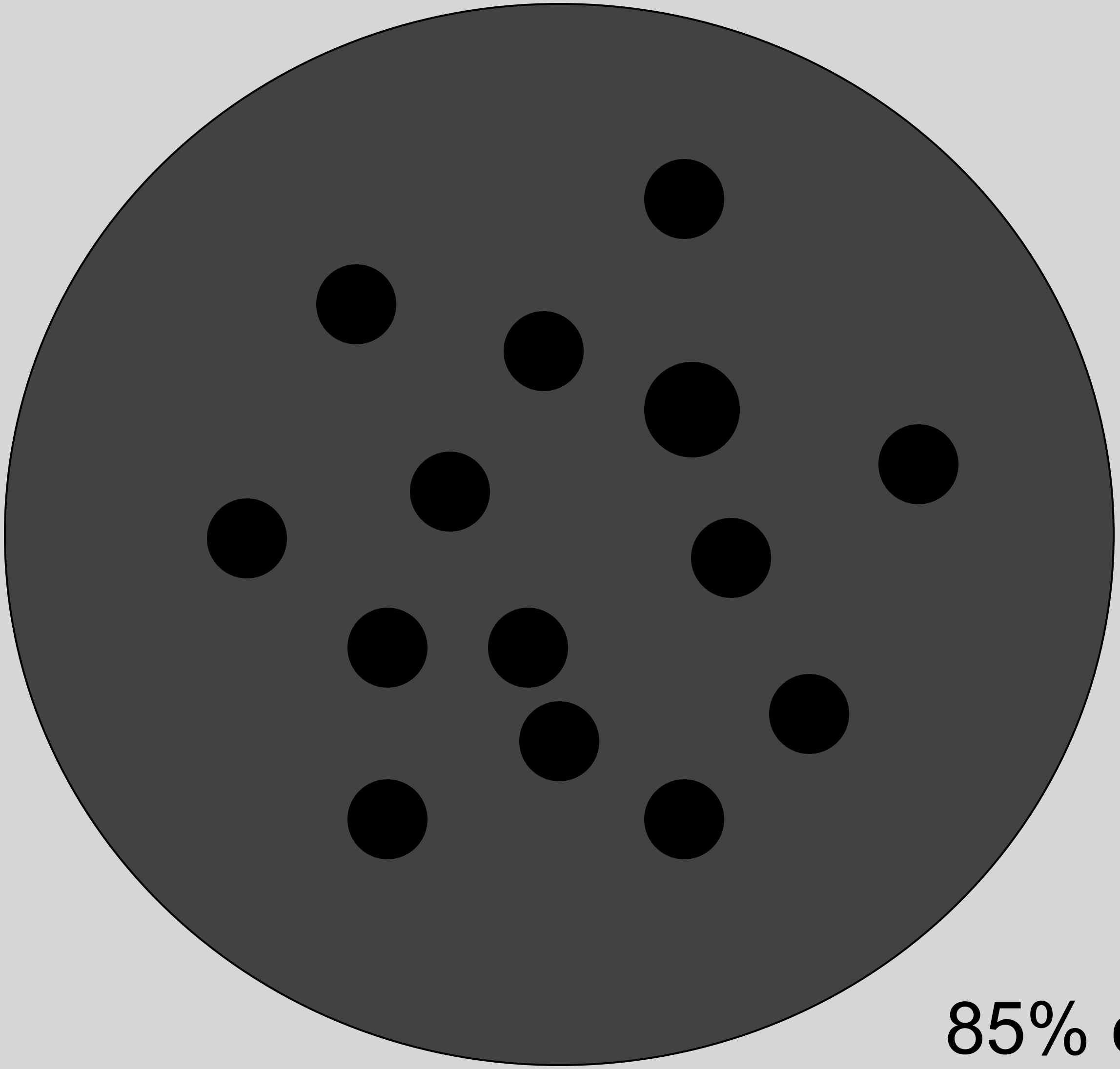

85% of mass

A galaxy cluster: Hot X-ray gas

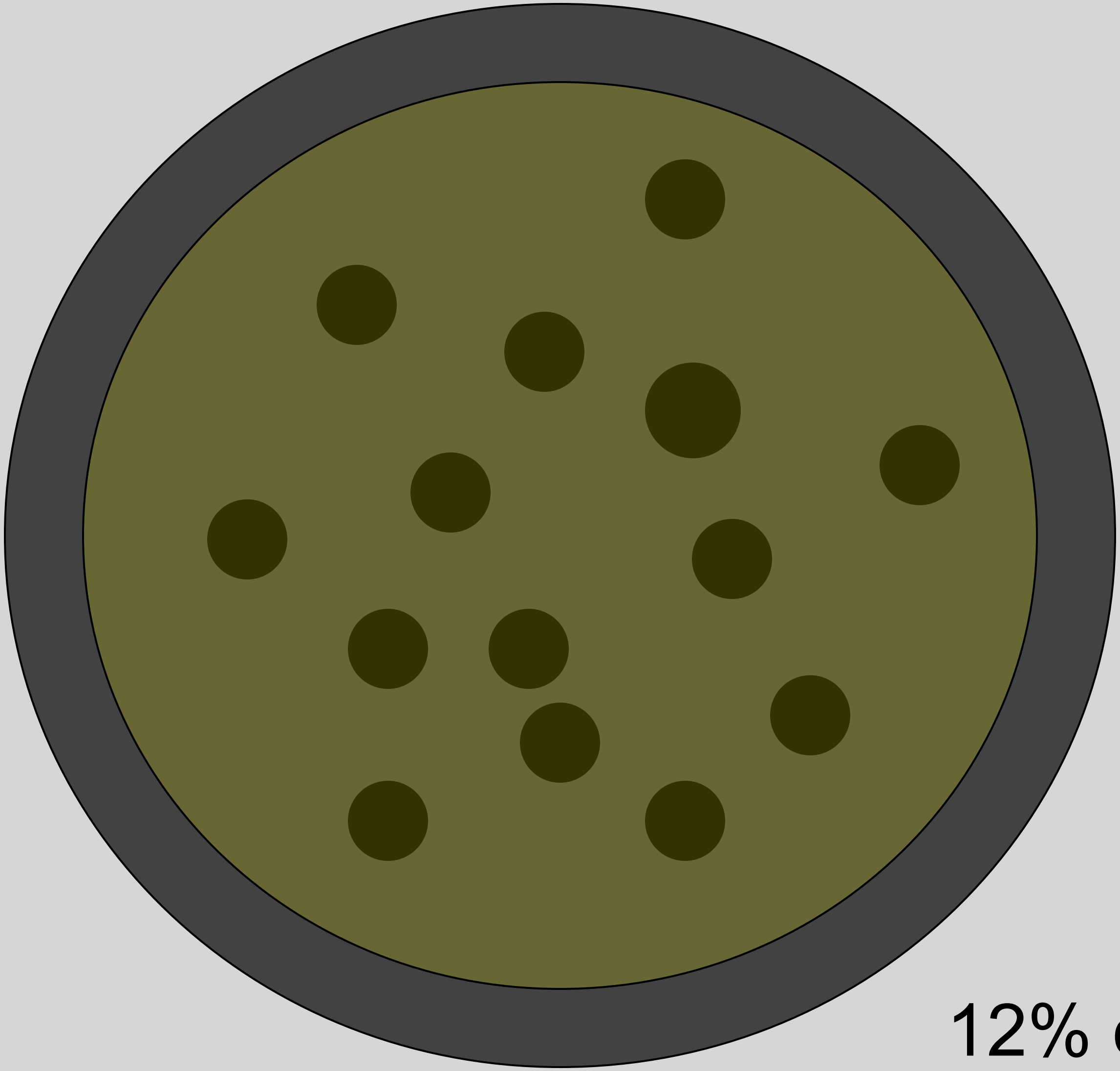

12% of mass

A galaxy cluster: Galaxies (stars + cold gas)

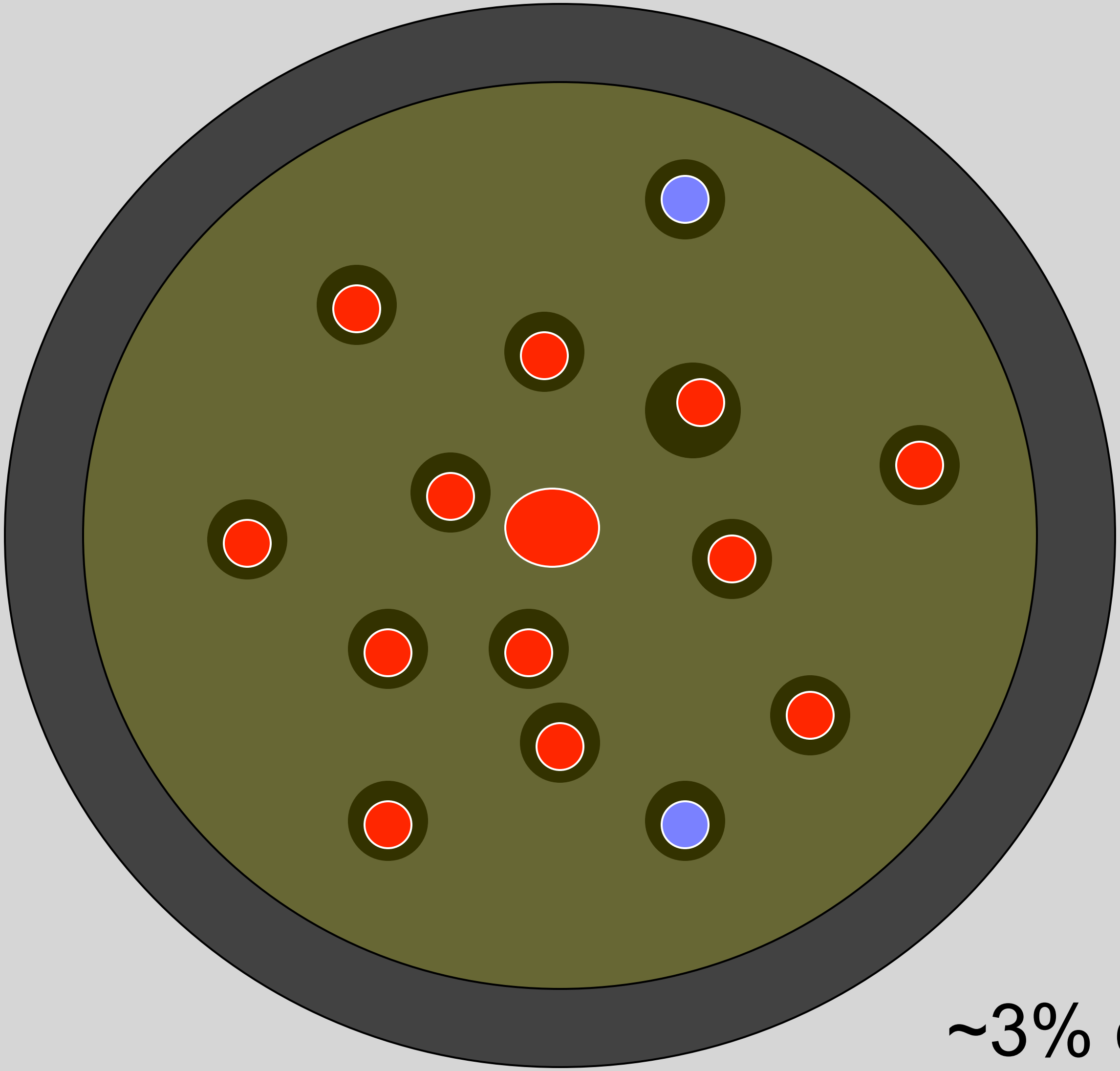

~3% of mass

Galaxies

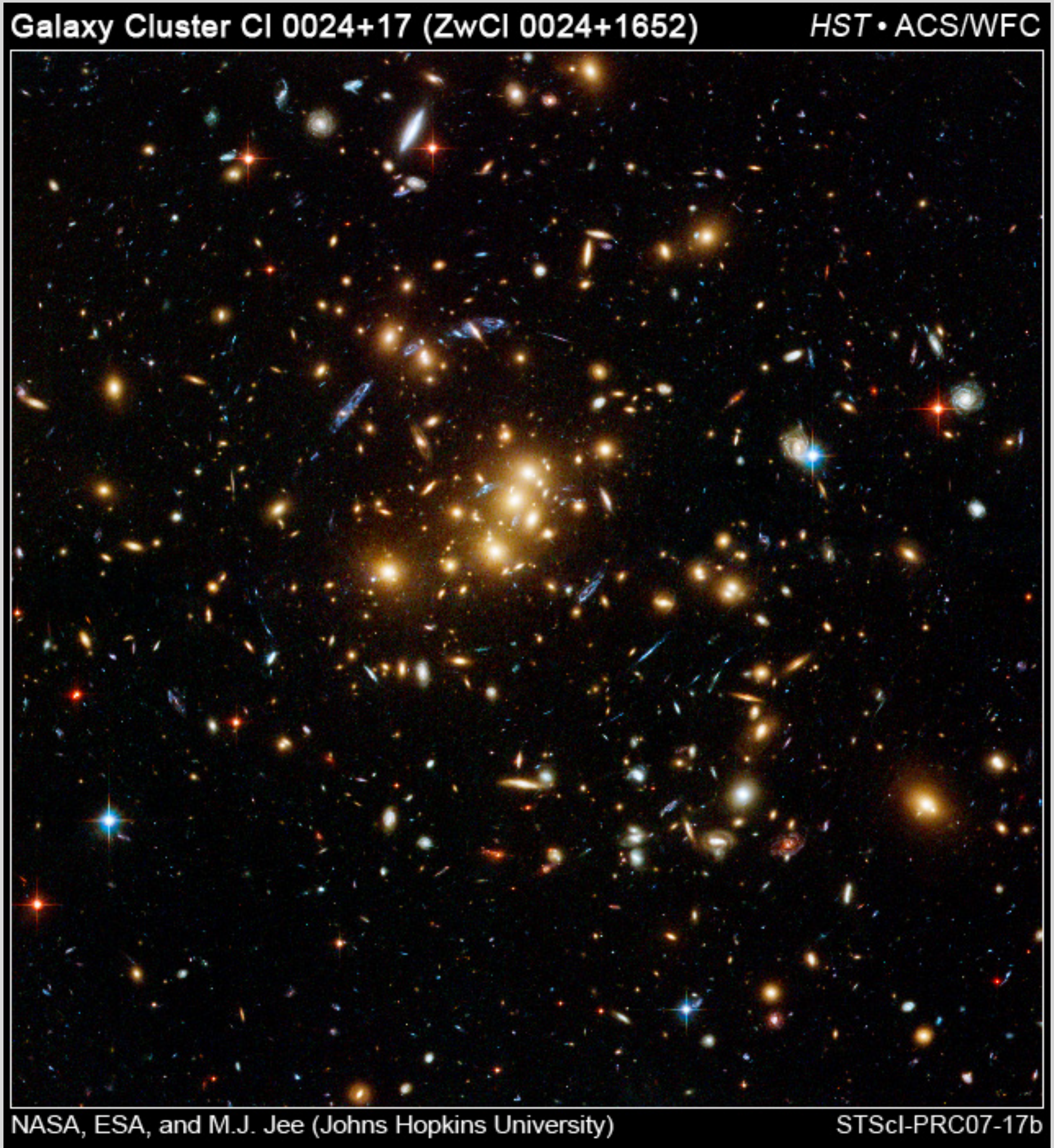
Galaxy Cluster Cl 0024+17 (ZwCl 0024+1652)
HST • ACS/WFC
NASA, ESA, and M.J. Jee (Johns Hopkins University)
STScI-PRC07-17b

X-ray gas

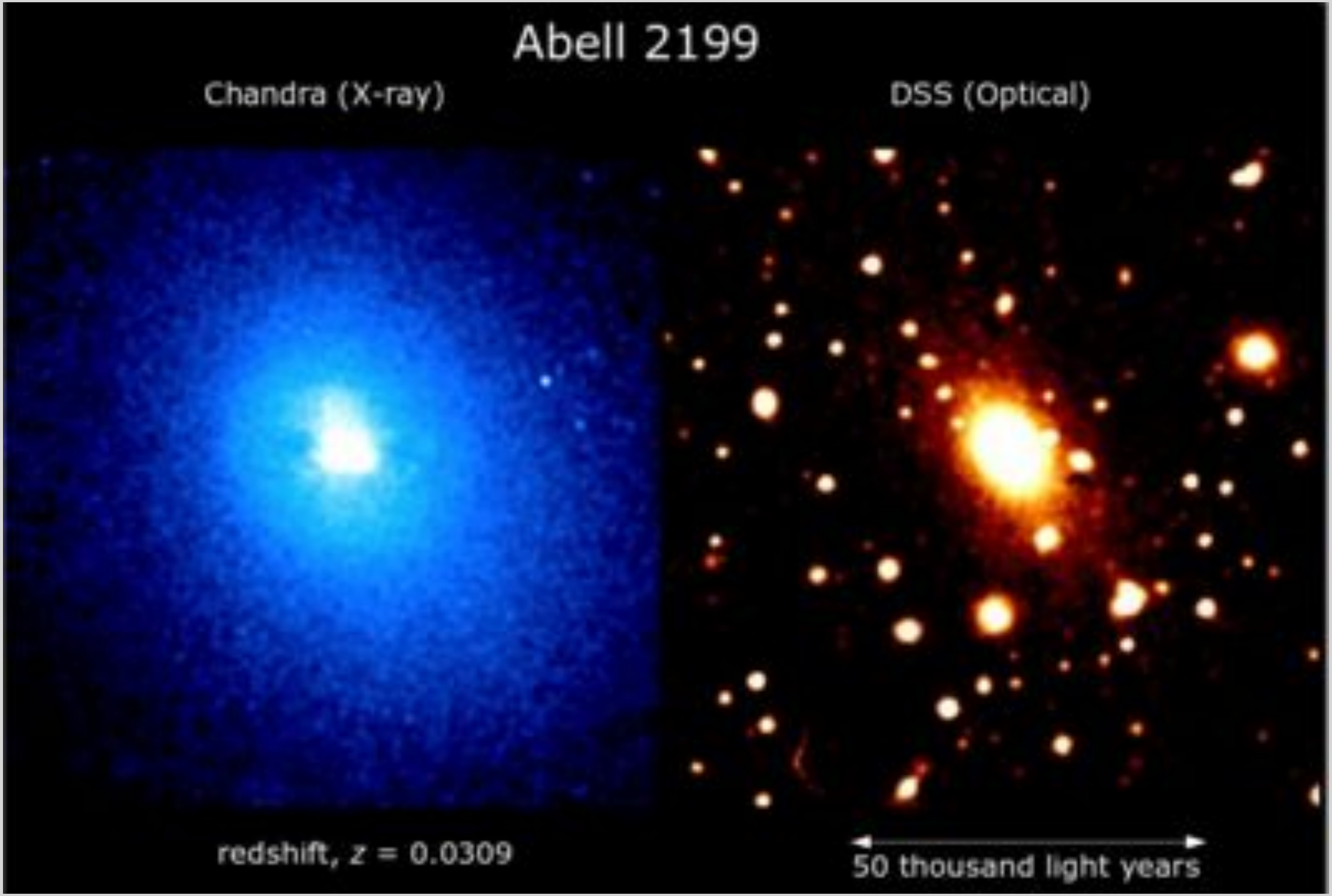

Abell 2199
Chandra (X-ray)
DSS (Optical)
redshift, z = 0.0309
50 thousand light years

Dark matter

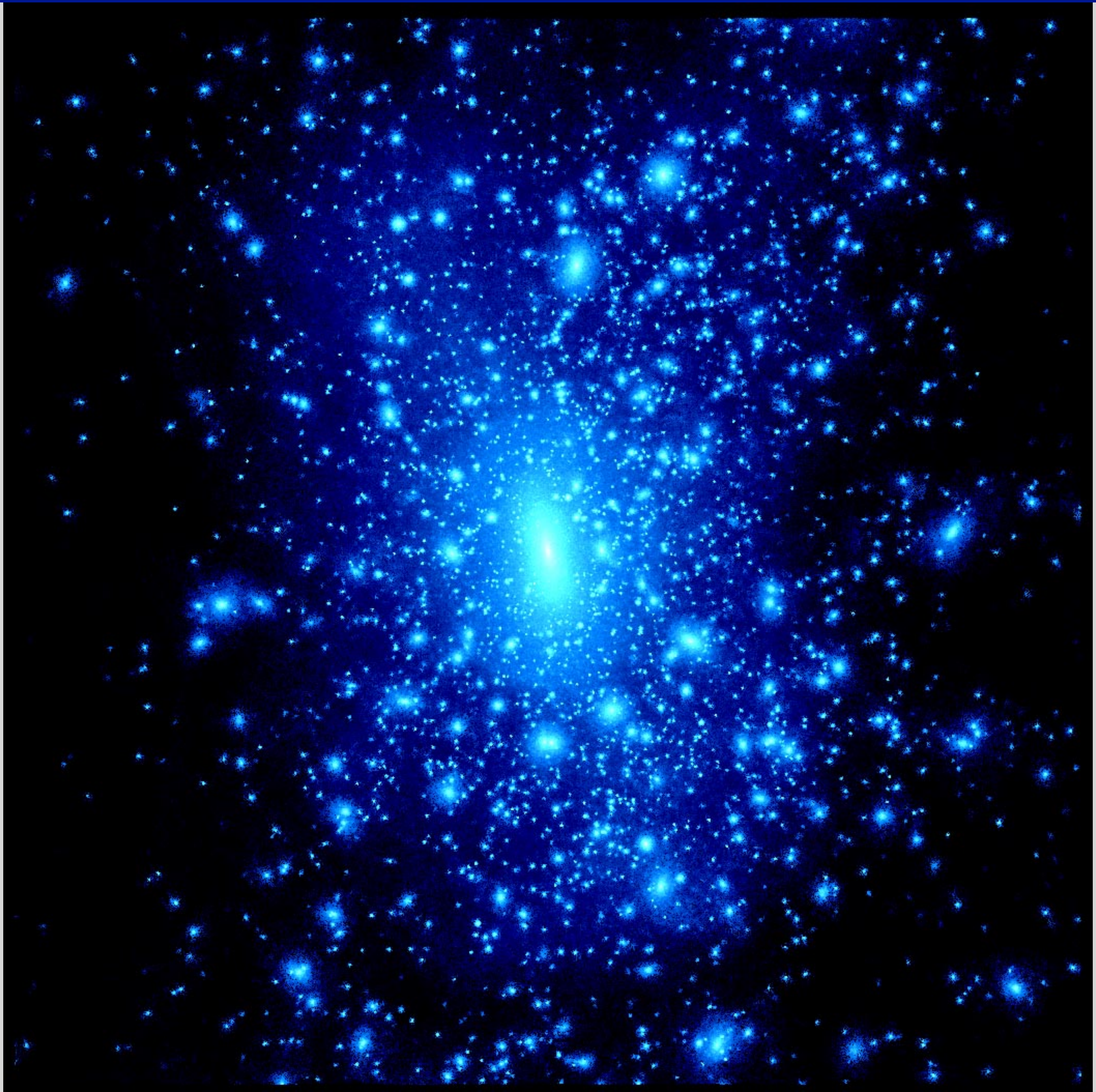

Gravitational lensing

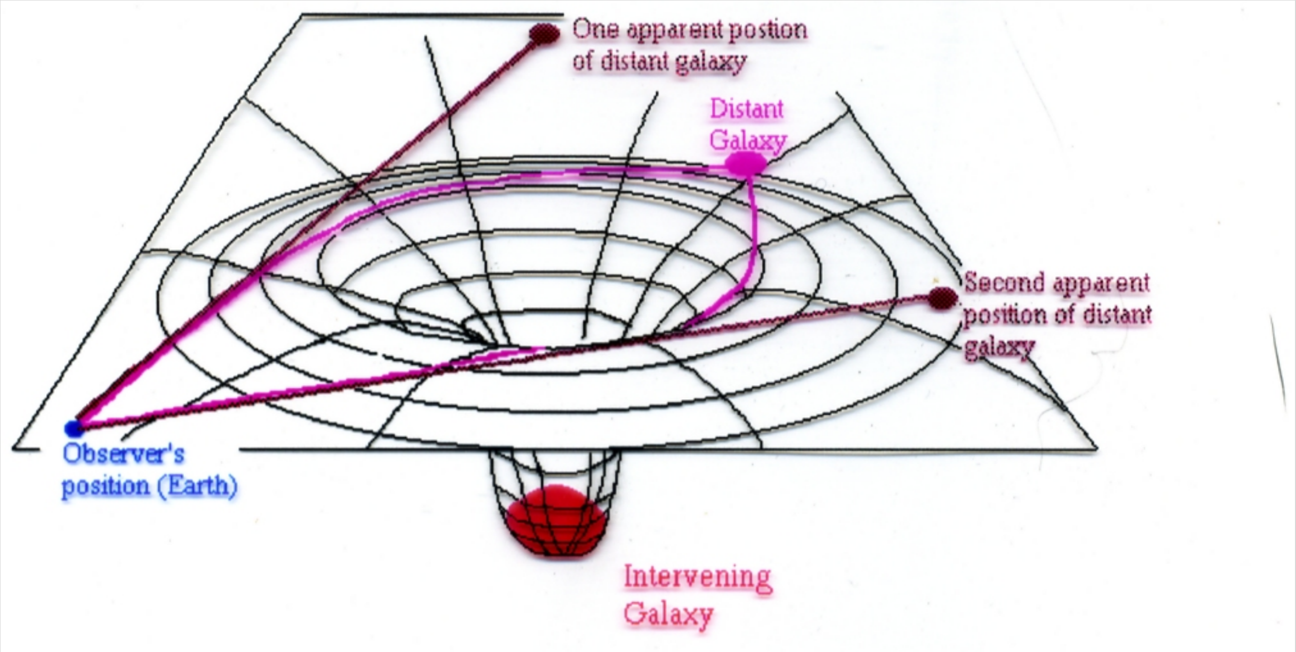

Gravitational lensing

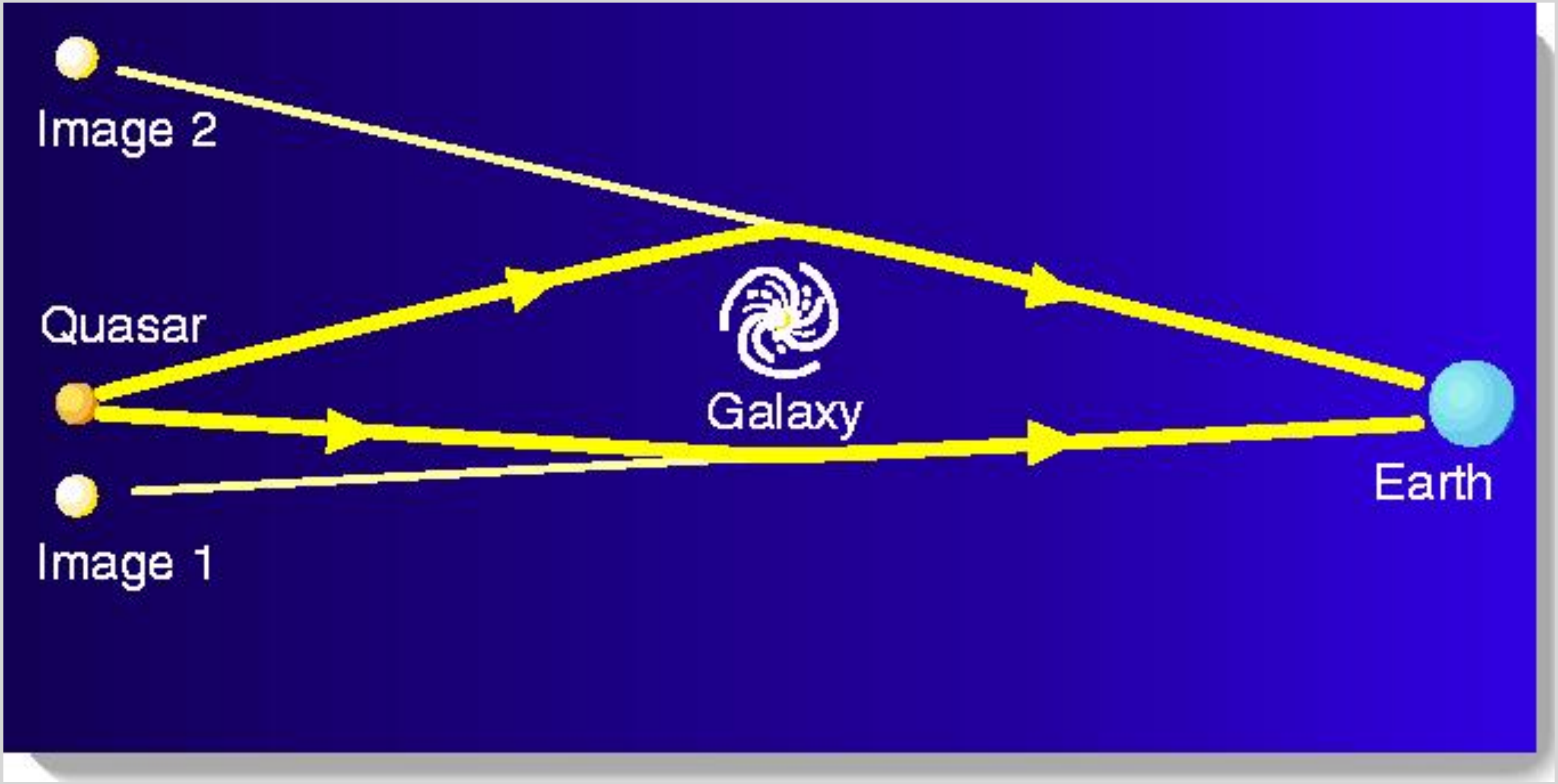

Gravitational lensing

Optical image

X-ray image

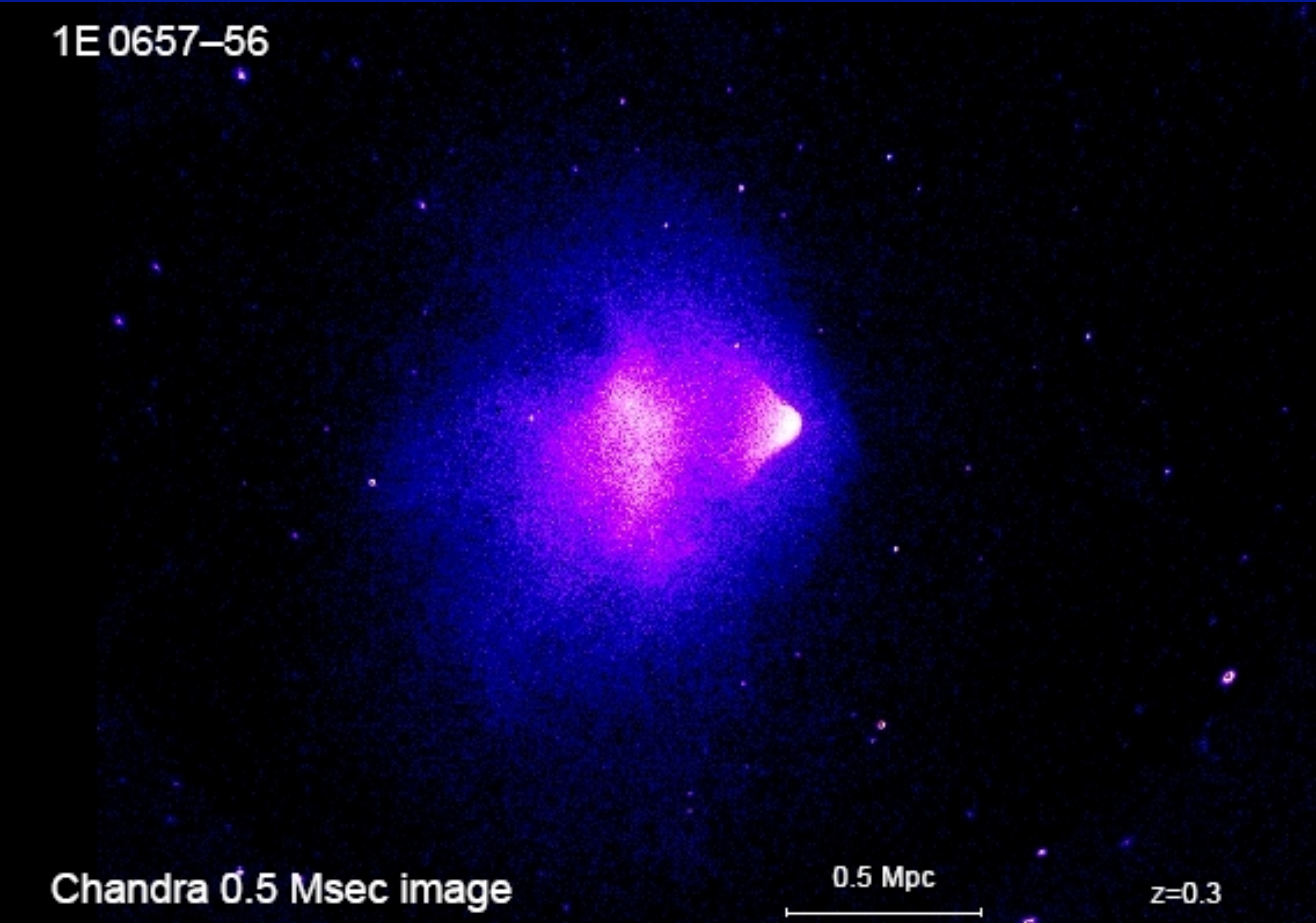

Modelling

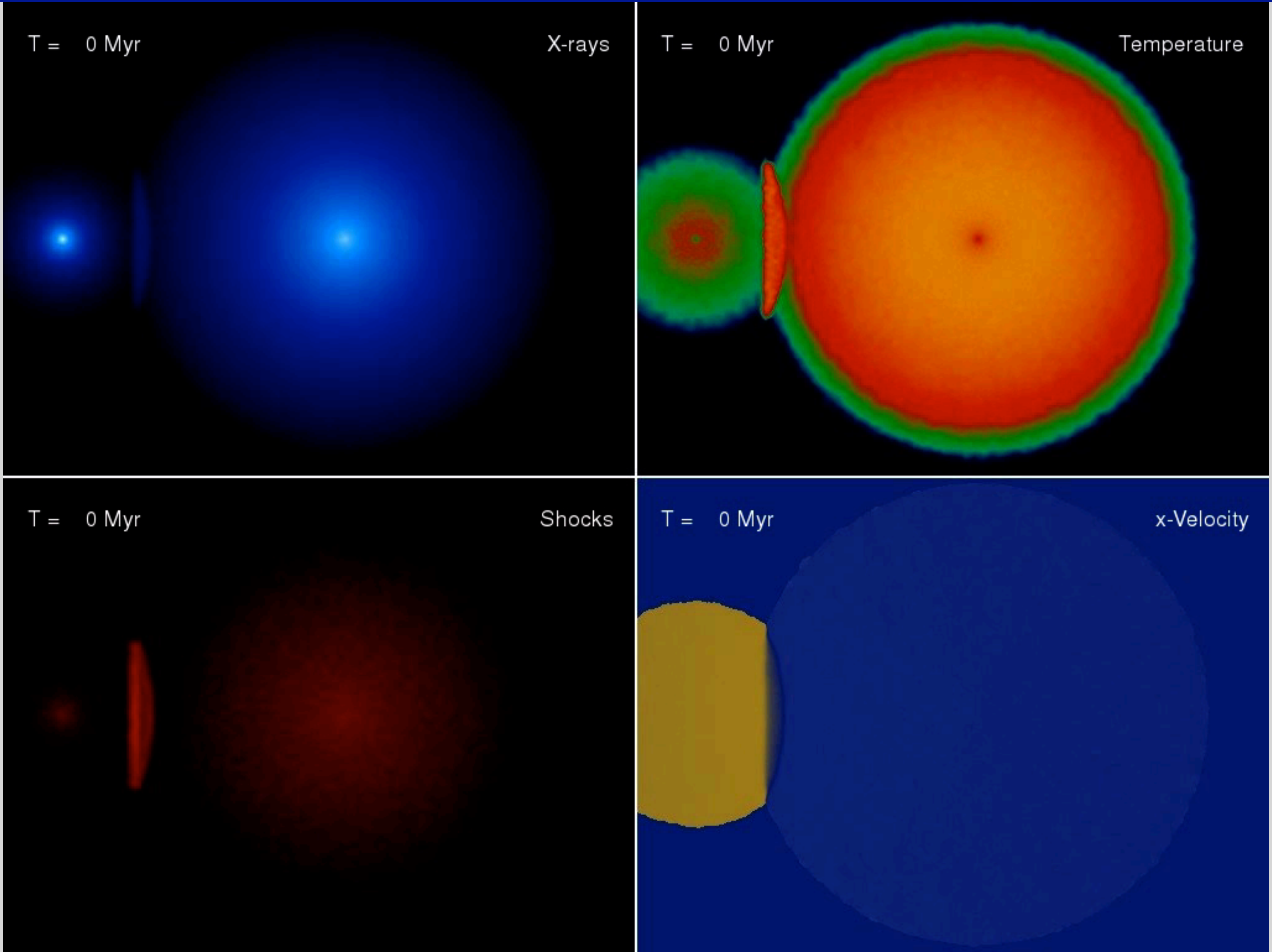

T = 0 Myr
X-rays
T = 0 Myr
Temperature
T = 0 Myr
Shocks
T = 0 Myr
x-Velocity

What happens in a cluster collision?

- Dark matter does not collide
- Hot gas collides and gets shock-heated
- Galaxies do not collide.

So, galaxies and dark matter should move through each other whereas gas should stay behind.

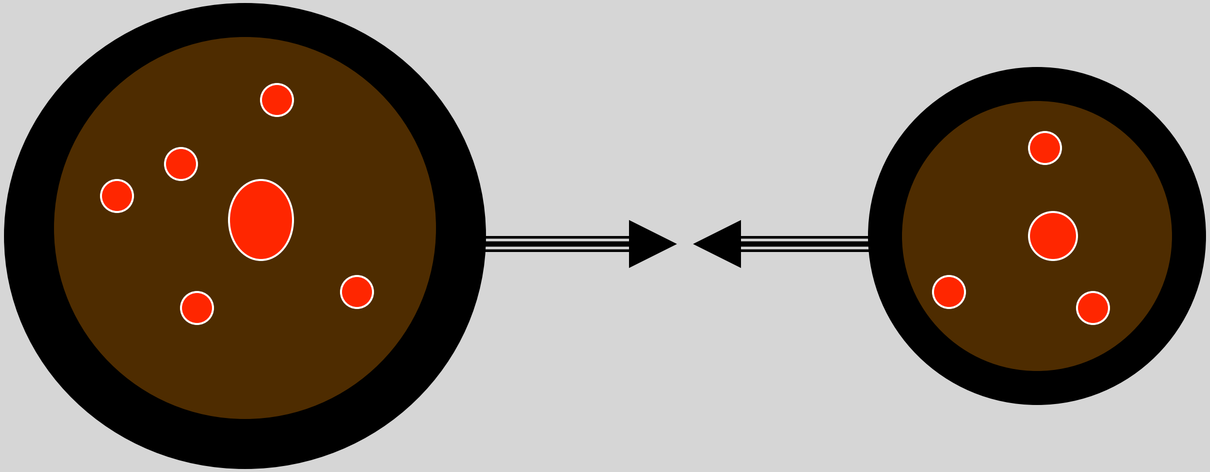

What happens in a cluster collision?

- Dark matter does not collide
- Hot gas collides and gets shock-heated
- Galaxies do not collide.

  So, galaxies and dark matter should move through each other whereas gas should stay behind.

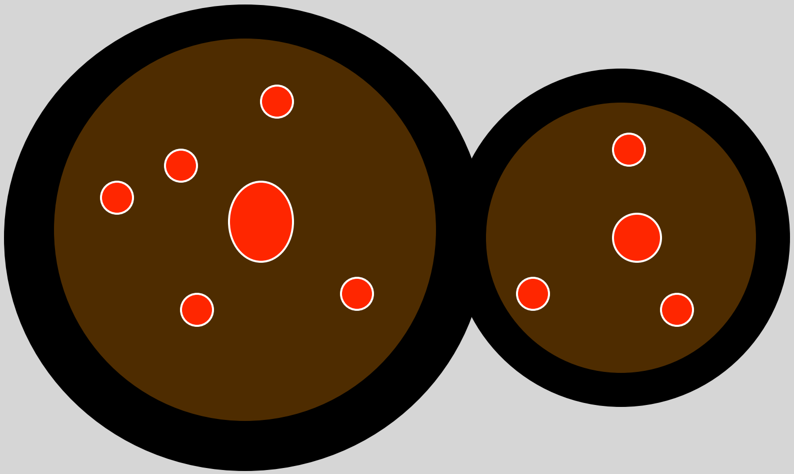

What happens in a cluster collision?

- Dark matter does not collide
- Hot gas collides and gets shock-heated
- Galaxies do not collide.

So, galaxies and dark matter should move through each other whereas gas should stay behind.

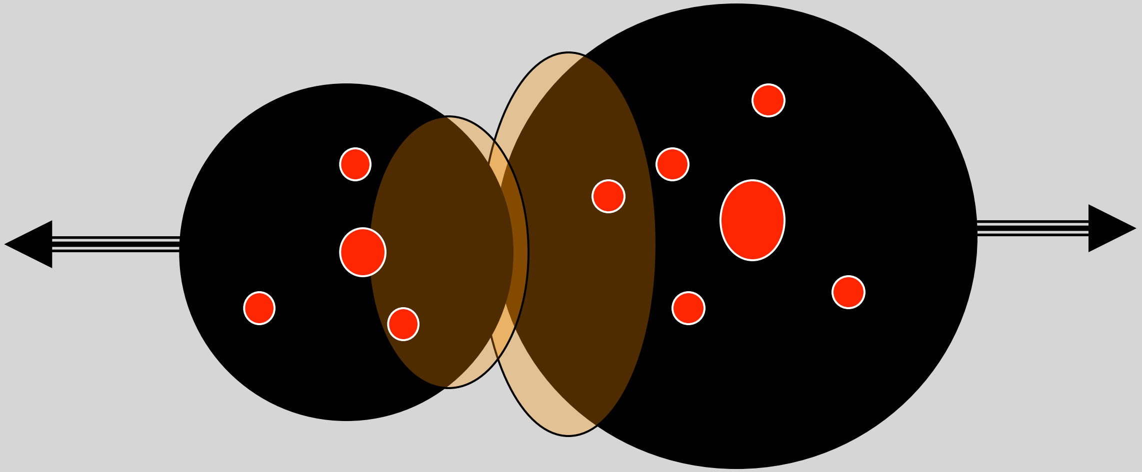

What happens in a cluster collision?

- Dark matter does not collide
- Hot gas collides and gets shock-heated
- Galaxies do not collide.

So, galaxies and dark matter should move through each other whereas gas should stay behind.

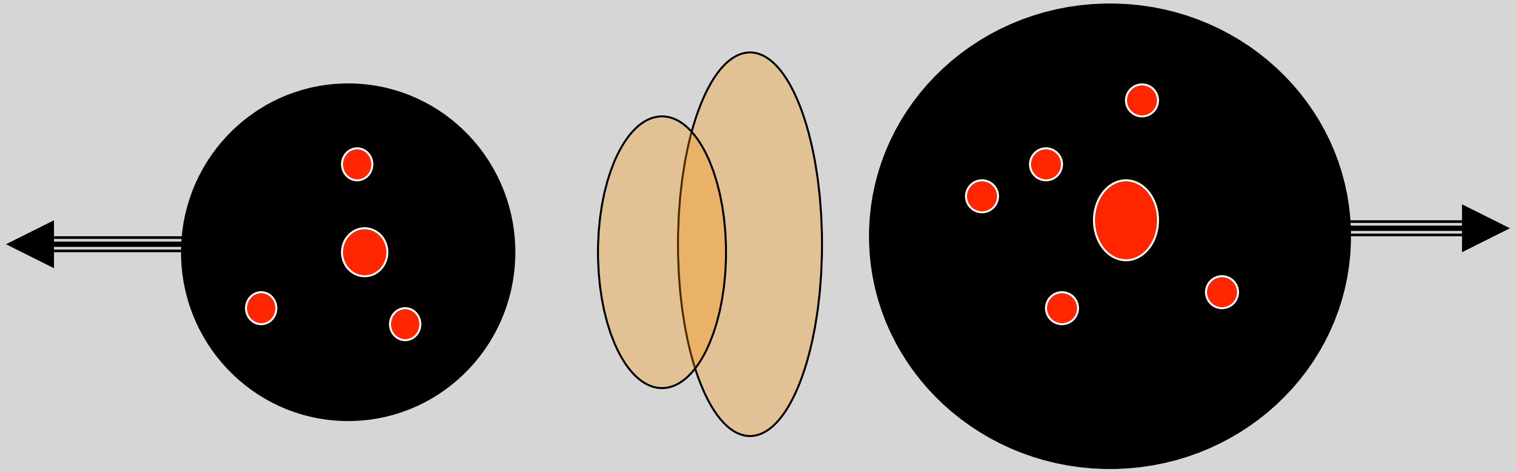

Modeling

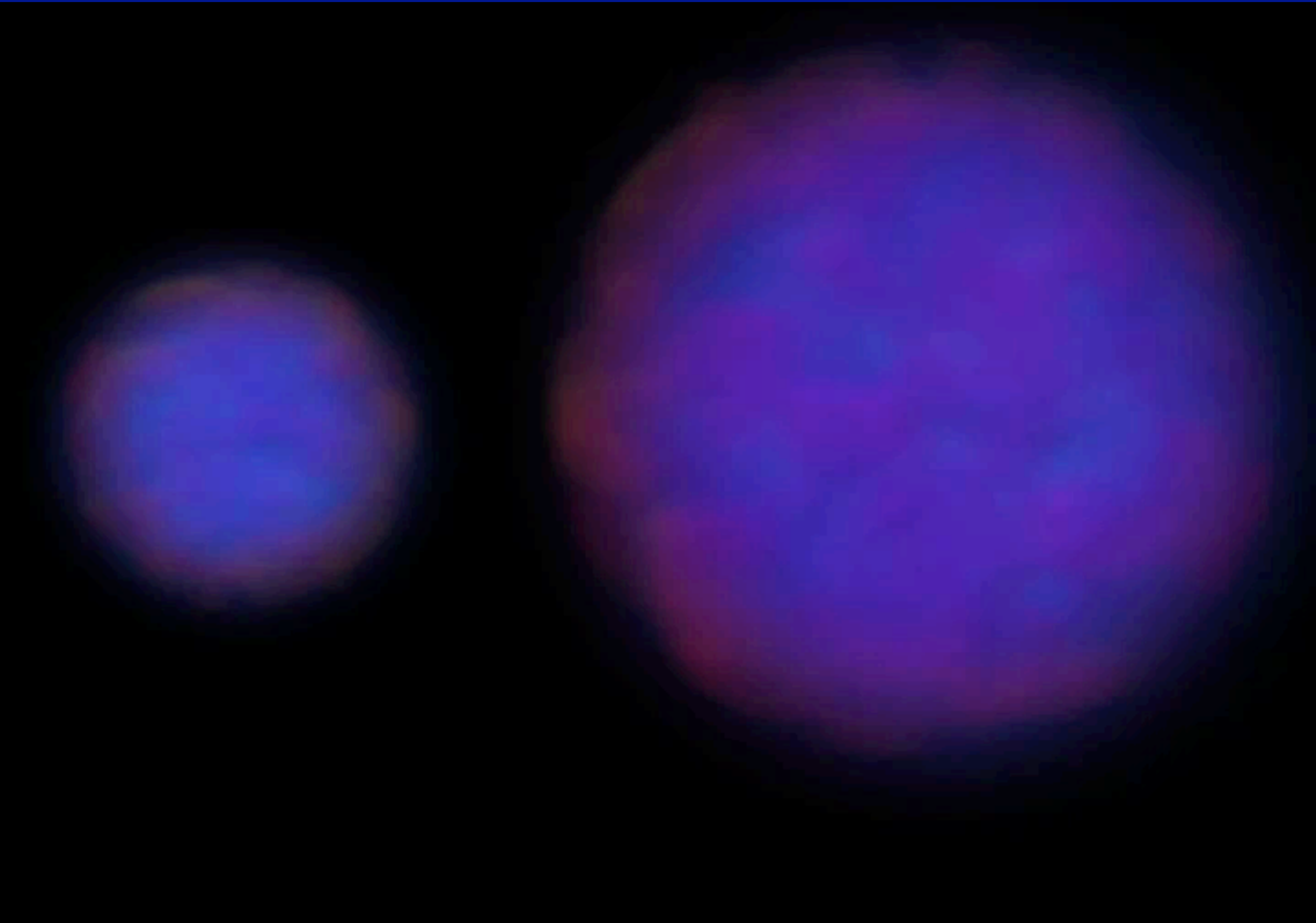

X-ray image

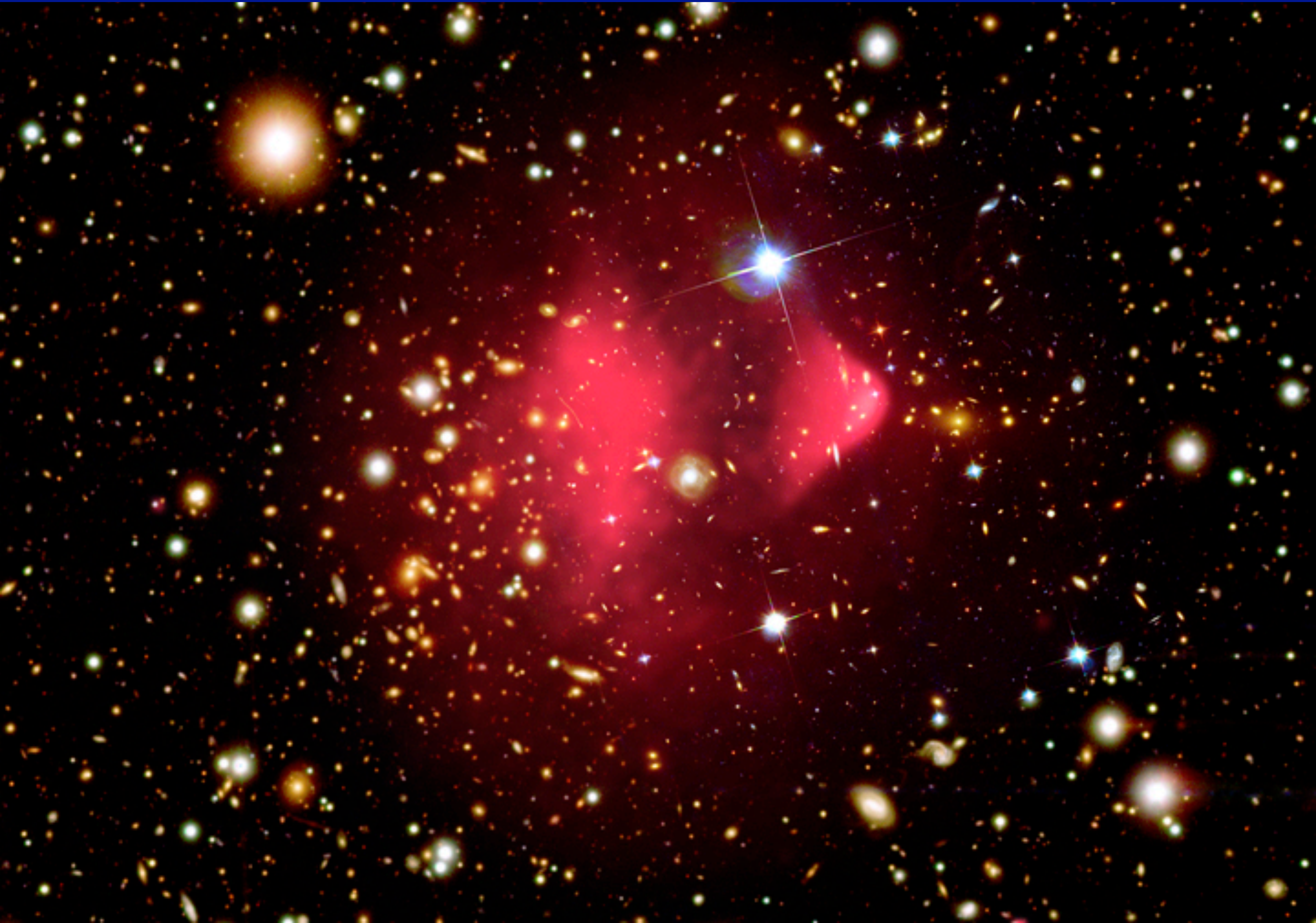

Lensing map

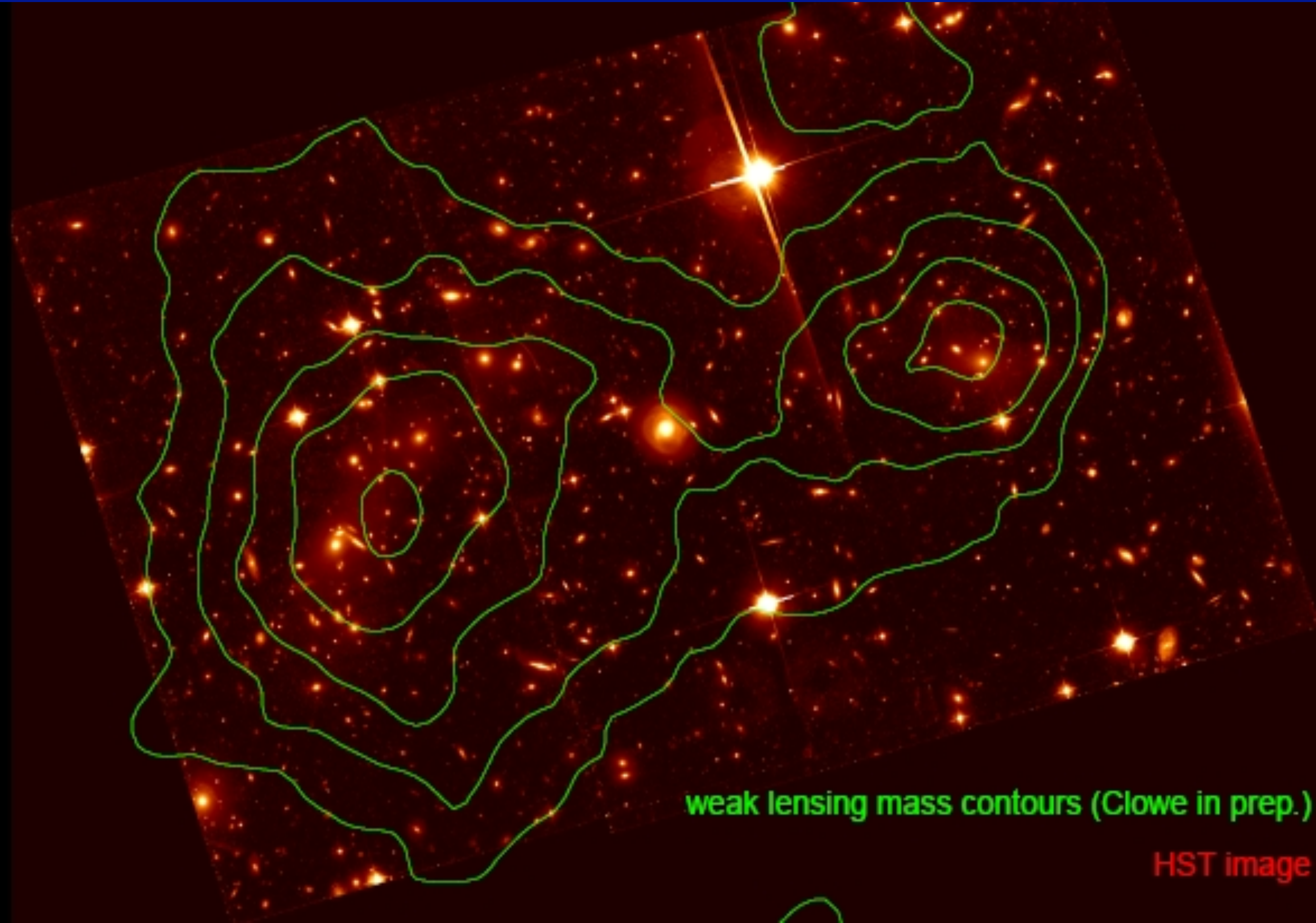

Lensing map

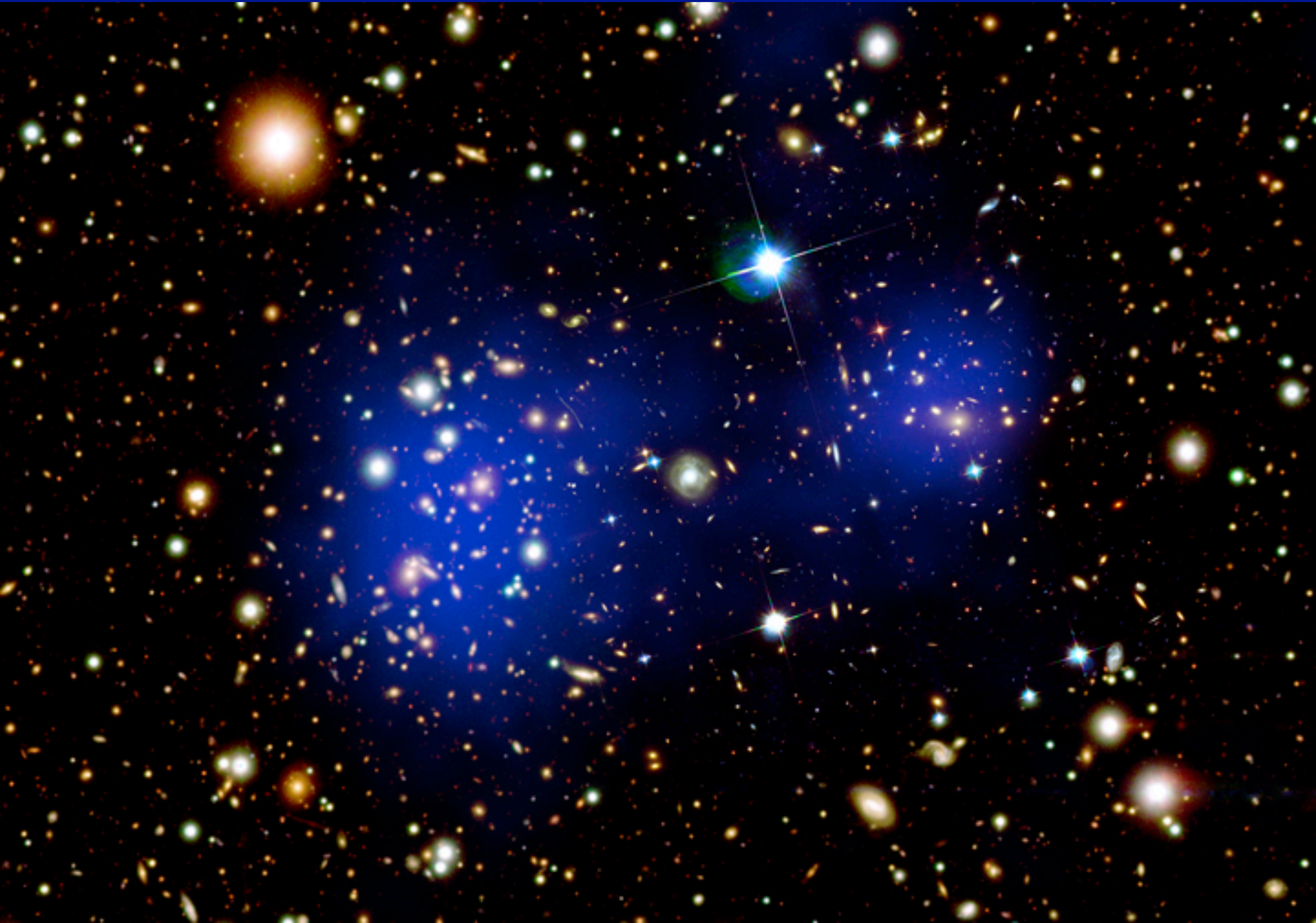

X-ray + Lensing map